Skin Cancer Detector

Project Team

Ahmed Abu Diak   **Ahmed Daraghma**

Supervisor

Eng. Ali Amro

Submitted to the College of Engineering

In partial fulfillment of the requirements for the degree of

Bachelor degree in Biomedical Engineering

Palestine Polytechnic University

Dec, 2019

Palestine Polytechnic University

Collage of Engineering

Electrical Engineering Department

Hebron- Palestine

Skin Cancer Detector

Project Team

Ahmed Abu Diak   **Ahmed Daraghma**

Submitted to the College of Engineering

in partial fulfillment of the requirements for the degree of

Bachelor degree in Biomedical Engineering

Supervisor Signature

……………………………………..

Testing Committee Signature

……………………………………..   ……………………………………..

Chair of the Department Signature

……………………………………..

Dec, 2019

الإهداء

إلى معلمنا وقائدنا وقدوتنا وحبيبنا وشفيعنا محمد ﷺ.

إلى من رسموا بدمائهم خارطة الوطن وطريق المستقبل وهندسوا بأجسادهم معاقل العزة والكرامة إلى من هم أكرم منا جميعا إلى شهداء الوطن الحبيب.

إلى الذين عشقوا الحرية التي تفوح منها رائحة الياسمين وتواروا خلف القضبان ليفسحوا لنا النور إلى أسرانا الأبطال.

إلى التي رآنا قلبها قبل عينيها واحتضنتنا أحشائها قبل يديها إلى التي تعجز الكلمات عن شكرها إلى منبع الحنان وتاج الرأس ومن تنحني لها جباهنا, كيف لا والجنة تحت إقدامها, أمهاتنا الفاضلات.

إلى من وصلوا النهار بالليل, و بذلوا الغالي والنفيس من أجلنا. إلى مصدر فخرنا و عزنا, آبائنا الكرام.

إلى من يحملون في قلوبهم ذكرياتنا ويتقاسمون معنا أفراحنا وهمومنا ومن ساندونا إخوتنا وأخواتنا الأعزاء.

إلى من ضاقت السطور لذكرهم فوسعتهم قلوبنا, أصدقائنا الأعزاء.

إلى من علمونا حروفا من ذهب وكلمات من درر. إلى من جعلوا أفكارهم منارة تنير لنا الطريق إلى محبي العلم والمعرفة, أساتذتنا الكرام.

إلى من رسم معنا خطوات هذا النجاح, إلى من بذل جهده ووقته وكان لنا مرشدا وناصحا وأخا إلى مشرفنا الحبيب المهندس علي أحمد عمرو.

إلى صرحنا العظيم ومكمن فخرنا وصانع مجدنا إلى بيتنا الثاني التي قضينا فيها أجمل أيامنا جامعتنا الحبيبة.

إلى محفزنا الأول والأخير إلى قبلتنا ومقصد بوصلتنا إلى من احتضنتنا كل هذه السنين رغم أوجاعها إلى دولتنا الفلسطينية وجوهرتها القدس الشريف.

إلى الزملاء وكوادر جامعة بوليتكنك فلسطين.

أحمد أبودياك

أحمد دراغمه

Acknowledgments

The project team expresses their thanks to all who made this

project a reality. Special thanks to the biomedical

engineering staff, including:

Dr. Ramzi Qawasmeh, Dr. Abdullah Arman,

Eng Fidaa Ja'afra and specially to

Eng. Ali Amro, our graduating project supervisor for his

support and encouragement.

Always, we have had enormous support and encouragement

from our families and friends and our gratitude for their

patience can never be fully expressed.

Ahmed Abu Diak

Ahmed Daraghma

Abstract

Skin cancer is on the rise. Despite the fact that melanoma is harmless if detected early, it still accounts for large percentage of all skin cancer related deaths. The problem lies in the fact that diagnosis is often left up to visual inspections of moles or time-consuming and expensive biopsies.

Cancer cells have higher temperature and oxygen levels because they have more blood vessels, higher blood flow rates and increased metabolism activity, thereby the temperature and oxygen saturation is above the normal range.

So a portable medical device was designed to detect melanoma in its early stages where its treatable, using a Temperature sensor and Oxygen levels sensor that can detect the thermal and oxygen levels changes in malignant or benign cells. Then the system analyzes the measured values and provides the patient with the diagnosis result on LCD screen. This process was applied on 20 sample and results were taken.

الملخص

سرطان الجلد في تزايد، على الرغم من حقيقة أن سرطان الجلد غير ضار إذا تم اكتشافه مبكراً، إلا أنه لا يزال يمثل نسبة كبيرة من جميع الوفيات المرتبطة بسرطان الجلد. تكمن المشكلة في حقيقة أن التشخيص غالبًا ما يتم تركه لعمليات الفحص البصري للشامات أو الخزعات المكلفة التي تستهلك كثيراً من الوقت.

تتمتع الخلايا السرطانية بارتفاع في درجة الحرارة ومستويات الأكسجين لأنها تحتوي على عدد أكبر من الأوعية الدموية، ومعدلات تدفق الدم المرتفعة وزيادة نشاط التمثيل الغذائي، وبالتالي تكون درجة الحرارة وتشبع الأكسجين فيها أعلى من المعدل الطبيعي.

لهذا تم تصميم جهاز طبي محمول لديه القدرة على اكتشاف سرطان الجلد في مراحله المبكرة ـحيث يمكن علاجهـ باستخدام مستشعر درجة الحرارة ومستشعر مستويات الأوكسجين اللذان يمكنهما اكتشاف التغيرات الحرارية ومستويات الأكسجين في الخلايا الخبيثة أو الحميدة. ثم يقوم النظام بتحليل القيم المقاسة ويزود المريض بنتيجة التشخيص على شاشة (LCD). هذه العملية تم تطبيقها على ٢٠ عينة وتم تسجيل النتائج.

List of Contents

Chapter One

ChapterTwo

ChapterThree

ChapterFour

ChapterFive

ChapterSix

ChapterSeven

List of Figures

List of Tables

List of Abbreviation

Abbreviation	Full Meaning
ABCDE	Asymmetry, Border, Color, Diameter, Evolving
GP	General practitioners
PCP	Primary care physicians
IR	Infrared radiation
NIR	Near infrared
MIR	Mid infrared
FIR	Far infrared
UFIR	Ultra-far infrared
SNR	Signal to noise ratio
BB	Black Body
GB	Gray Body
IDE	Integrated Development Environment
PPG	Photoplethysmogram

Introduction

1.1 Literature review

1.2 Project objectives

1.3 Project importance

1.4 Project block diagram

1.5 Project timeline

1.6 Project budget

Skin cancer is on the rise. Despite the fact that melanoma is harmless if detected early, it still accounts for large percentage of all skin cancer related deaths. The problem lies in the fact that diagnosis is often left up to visual inspections of moles or time-consuming and expensive biopsies.

Skin cancers, like all solid malignant tumors, require a blood supply in order to grow larger than a few millimeters in diameter. Tumors induce the growth of new capillary blood vessels by producing specific angiogenesis-promoting growth factors. New blood-vessel growth continues through the progression from precancerous skin lesions to full-blown skin cancer as depicted in. The presence of new blood vessels and the increased blood supply somehow change the thermal response of the tumor cells when a stimulus is applied. It is quite unacceptable that so many lives are lost annually from something could have been easily avoided if detected earlier.

The cancer cells use chemical substances known as growth factors to promote the formation blood vessels to supply the cells themselves with enough nutrition and oxygen [1].

Cancer cells have higher temperature and oxygen levels because they have more blood vessels, higher blood flow rates and increased metabolism activity, thereby the temperature and oxygen saturation is above the normal range.

1.1 Literature review

There is a higher incidence of skin cancer than the combined occurrence of breast, prostate, lung and colon cancers [2]. Melanoma, which accounts for an estimated 4% of skin cancer cases, is responsible for approximately 75% of all deaths from skin cancer. The total deaths in the United States due to melanomas and other types of skin cancer are estimated to be more than 12,000 for 2014 [3]. Currently, the detection of melanoma relies on a subjective ABCDE (Asymmetry, Border, Color, Diameter and Evolution) test performed visually by dermatologists, general practitioners (GP) or primary care physicians (PCP). However, the ABCDE test provides a qualitative guideline and it requires a trained specialist to actually distinguish malignant lesions from benign nevi. Moreover, the ABCDE approach has a relatively high false-alarm probability (0.35–0.44, i.e., a specificity in the range 56%

to 65%) and moderate detection probability (0.47–0.89) [4-6].Since a false negative (i.e., a patient with malignant condition that is declared to have benign condition) could lead to metastasis (spreading to other parts of the body) and death, excisional biopsies are routinely performed even on lesions that are non-cancerous. It was estimated that the number of biopsies undertaken in nine geographical areas of the US between 1986 and 2001 was close to 60 for every melanoma detected [7].

One of the critical barriers in early skin-cancer detection is the lack of reliable non-invasive techniques that can detect the cancer at an early stage with high detection probability (i.e., the probability of correctly detecting a malignant lesion) and low false-alarm probability (i.e., the probability of declaring a benign lesion as malignant).

1.2 Project objectives

The main objectives of the project were achieved by designing an IR sensor and oxygen levels sensor that can detect the thermal and oxygen levels changes in malignant or benign cells then process the output of the sensors by building a suitable conditioning circuit and display the output variation of the sensors using a microcontroller.

1.3 Project importance

The main importance of the project is to detect melanoma in its early stages where its treatable with portable low price detector that minimize the number of visual inspections of moles, time-consuming and expensive biopsies.

1.4 Project block diagram

The first step to detect the IR and oxygen levels from the cells with the sensors and convert this signal to the next step using suitable conditioning circuit and display the output variation of the sensors using a microcontroller on LCD as shown in Figure 1.1.

temperature sensor

oxygen sensor

Signal processing Circuit

controller

Display
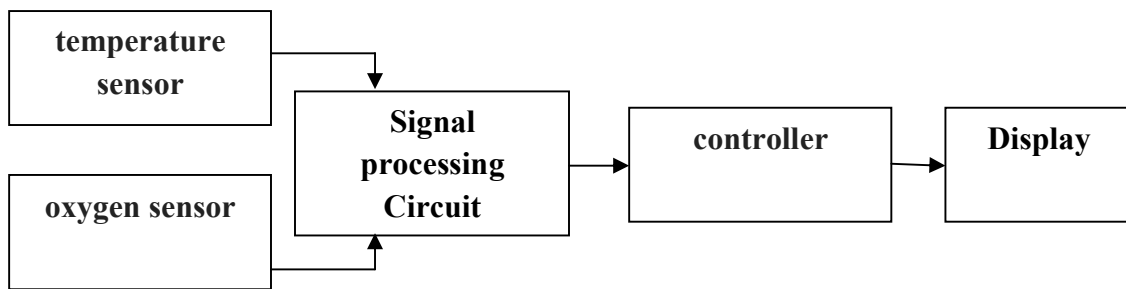
Figure 1.1 System block diagram

1.5 Project timeline

By following this timeline shown in Table 1.1 and Table 1.2 the project will be ready to be discussed on time.

Table 1.1 Time schedule of spring 2018-2019 semester

Week / Task	1	2	3	4	5	6	7	8	9	10	11	12	13	14	15
Project idea	■	■													
Proposal			■	■											
Searching for information				■	■	■	■	■	■	■					
Sorting the information and documentation				■	■	■	■	■	■	■	■	■	■	■	
First edition														■	
Print the final book															■

Table 1.2 Time schedule of winter 2019-2020 semester

Week / Task	1	2	3	4	5	6	7	8	9	10	11	12	13	14	15
Full designing	■	■	■	■											
Purchasing the components				■	■	■	■	■							
System implementation						■	■	■	■	■	■	■			
System analysis									■	■	■	■			
Documentation											■	■	■	■	

1.6 Project budget

The prices of the project as shown in Table 1.2 is estimated as the following :

Table 1.3 Project budget

Type	Price	Quantity
Temperature Sensor	25$	1
Arduino Uno	30$	1
LCD	10$	1
Photodiode	15$	1
The other components involves: amplifiers, capacitors, diodes, resistors, LEDs, logic dates, boards, transistors and switches.	100$	
Total Price=180$		

Skin

2.1 Skin Layers

2.2 Skin Cancer

2.3 Risk Factors for Skin Cancer

2.4 Methods of Melanoma Detection

2.5 Moles and Melanoma

2.6 Oxygen Saturation in the Blood

2.7 Normal Cells versus Melanoma Cells Temperature and Oxygen Levels

The skin is one of the largest organs of the body and is responsible for providing protection to the other systems of the body. Skin prevents water loss and dehydration, shields the internal organs in the event of injury, regulates body temperature, senses outside stimuli such as touch as well as heat and cold, and serves as a barrier to infection. As seen below, the skin is made up of three layers: the outer epidermis, the dermis and the deep subcutis layer.

Figure 2.1 The structure of the skin [9]

Other important elements of the skin include: hair follicles, sweat glands and nerve endings. Hair follicles protrude into the dermis layer and help regulate body

temperature. Microscopic pores on the surface of the skin are connected to sweat glands which also help maintain homeostasis [9].

2.1 Skin Layers

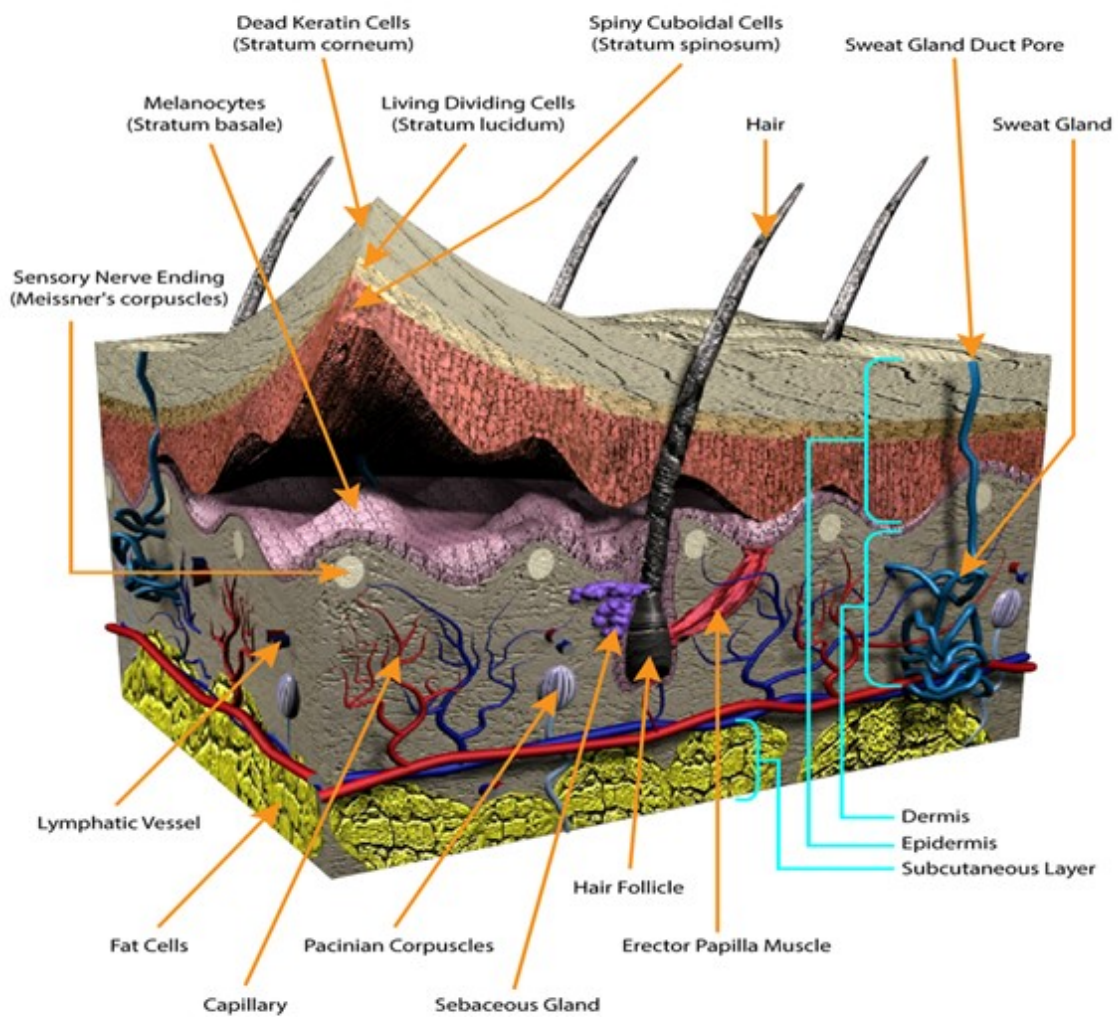The skin is a vital organ for the human body. Man cannot live comfortably without skin covering the whole body. It is also the largest organ of the body, which can make out one-third of a normal person's total body weight [10].

The skin is mainly divided into three layers: the epidermis, dermis, and hypodermis. The outermost layer is the epidermis. The innermost layer is the subcutaneous layer also called hypodermis. The dermis is the middle layer that is sandwiched between both the epidermis and hypodermis. All three layers take role in the functions performed by the skin according to their respective order and construction.

The epidermis is 0.1 mm (approximately) thick and contains no blood vessels [10]. It is subdivided into four parts that lie one beneath the other: the stratum basale (basal layer), the stratum spinosum (spinous or prickle-cell layer), the stratum granulosum (granular layer), and the uppermost stratum corneum (surface layer). This last layer is the one that is in direct contact with the environment.

The dermis is the thickest sub-layer of the skin. Thickness, however vary noticeably according to the area that skin covers and might also differ from male and female as well as thickness depends on age. This sub-layer exists under the epidermis directly. It supplies the epidermis and itself with nutrients and oxygen carried by the blood. The dermis many useful structures such as blood vessels, sensory nerve endings, hair follicles, and sweat glands. This sub layer also give the skin it strength and elasticity. It contains two distinct regions: the papillary dermis and the reticular dermis.

This sub-layer lies under the dermis in the skin. It contains fat-filled adipose cells. This layer exerts control on heat conservation for the human body and preserves fat which is one of the primary sources of energy to muscles.

2.2 Skin Cancer

Millions of skin cancer cases are recorded every year around the world [11]. since the skin is the largest organ, it is probably the most common cancer that can be developed in a human being. On the other hand, not all skin cancers are created equal. Skin cancer is a type of epithelial tissue cancer. It can be both benign and malignant. Since skin has access to both nearby lymphatic system as well as blood system, malignant types can produce metastasis to the whole body and become extremely lethal. Actually, it is these metastases that can cause most deaths from skin cancer. There are three main types of skin cancer: Basal cell carcinoma, Squamous cell carcinoma and Melanoma.

Melanoma is the most aggressive type of skin cancer and is considered to be highly malignant and can be extremely fatal. Naturally, cancerous cells suffer also from uncontrolled growth rate and frequently exceed that of normal tissue [11]. Moreover, the cancerous cells themselves develop non-regular shape that distinguishes them from normal skin cells. The cancer cells use chemical substances known as growth factors to promote the formation blood vessels to supply the cells themselves with enough nutrition and oxygen. This process is termed angiogenesis [11].

Figure 2.2 shows a tumor angiogenesis in cancer at different stages: (a) The tumor release growth factors that activate the growing cells generating blood vessel sprouts. (b) The blood vessels feed the tumor that growths thanks to cell proliferation. (c) The tumor becomes vascularized and it starts to metastasize through the blood stream [12].
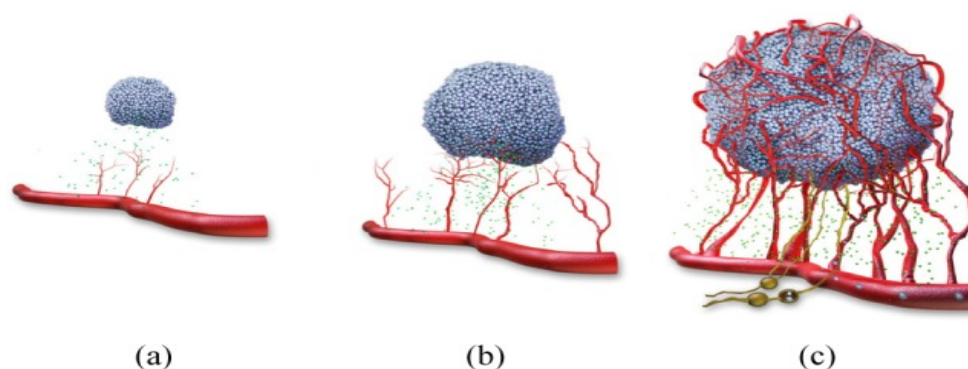

(a)   (b)   (c)

Figure 2.2 Tumor angiogenesis in skin cancer at different stages [12]

2.3 Risk Factors for Skin Cancer

This section outlines major factors that have been associated with patients having higher likelihood of developing skin cancer [13]:

1. Ultraviolet rays' exposure usually from the sun rays. It is largely thought to be main cause of skin cancer especially with the constant increase in skin cancer cases. It has been suggested that UVB causes BCC and SCC, while UVA is thought to cause melanoma. This is done mostly by harmful alteration in the DNA. X-rays can also increase a person's susceptibility to skin cancer as well as other types of ionizing radiation.

2. Ethnicity most risk for skin cancer has been recorded in Caucasians European descent persons. The color of a person's skin is therefore associated with likelihood of developing skin cancer and must be warned against.

3. Genetics inherited mutation in a gene that is especially if controlling cell division or cell death increases susceptible to developing cancer.

4. Geographical Location higher risk close to the equator for example of developing skin cancer is largely due to the higher UV radiation levels.

5. Personal Habits such as exposure to sunlight for long periods of time and smoking for example forms higher risk of developing skin cancer.

6. Age as young people have more sensitive skin than adults. This combined with other factors such as habits or location.

7. Immunosuppressive drugs used to prevent organ rejection in organ transplantation transplant recipients, are at a higher risk of developing skin cancer.

8. Virus infections, such as HPV is mentioned to increase risk for developing skin cancer.

2.4 Methods of Melanoma Detection

May be the most common method of melanoma detection is the visual and manual method. Therefore normally an oncologist will look for superficial skin characteristics that resemble know melanoma or non-melanoma forms. These characteristics are referred to as ABCDE method [12]:

1. Asymmetry: the mole does not match normal appearance.
2. Border: the mole has irregular outline or pigment.
3. Color: the mole develops an uneven color with shades of dark or light shades.
4. Diameter: the mole has larger size horizontal or vertical.
5. Evolving: the mole looks different from the rest or is changing in size, shape or color.

However some other technologies are developing for more accurate and automated detection of melanoma using skin temperature, impedance and blood oxygen saturation (SpO2) techniques [14,15].

2.5 Moles and Melanoma

Melanoma has also been associated with skin moles. These are gathering of melanocytes in the skin epidermis. These are benign in most cases. Due to exposure to UV radiation they can develop genetic mutation and from a melanoma focus. They start slowly to spread horizontally in the epidermis and continue to extend upwards often referred to as in-situ. After sufficient time they can spread vertically to lower layers of the skin and possibly metastasizes. Figure 2.3 shows a magnified view of a mole.

Figure 2.3 Magnified view of a small mole on the back skin [11]

Minimizing exposure to sources of ultraviolet radiation (the sun and sunbeds), following sun protection measures and wearing sun protective clothing (long-sleeved shirts, long trousers, and broad-brimmed hats) can offer protection. Using artificial light for tanning was once believed to help prevent skin cancers, but it can actually lead to an increased incidence of melanomas.

Figure 2.4 displays few shapes of normal moles 1a to 1e. Note that there are few differences among them that can be visually seen [11].
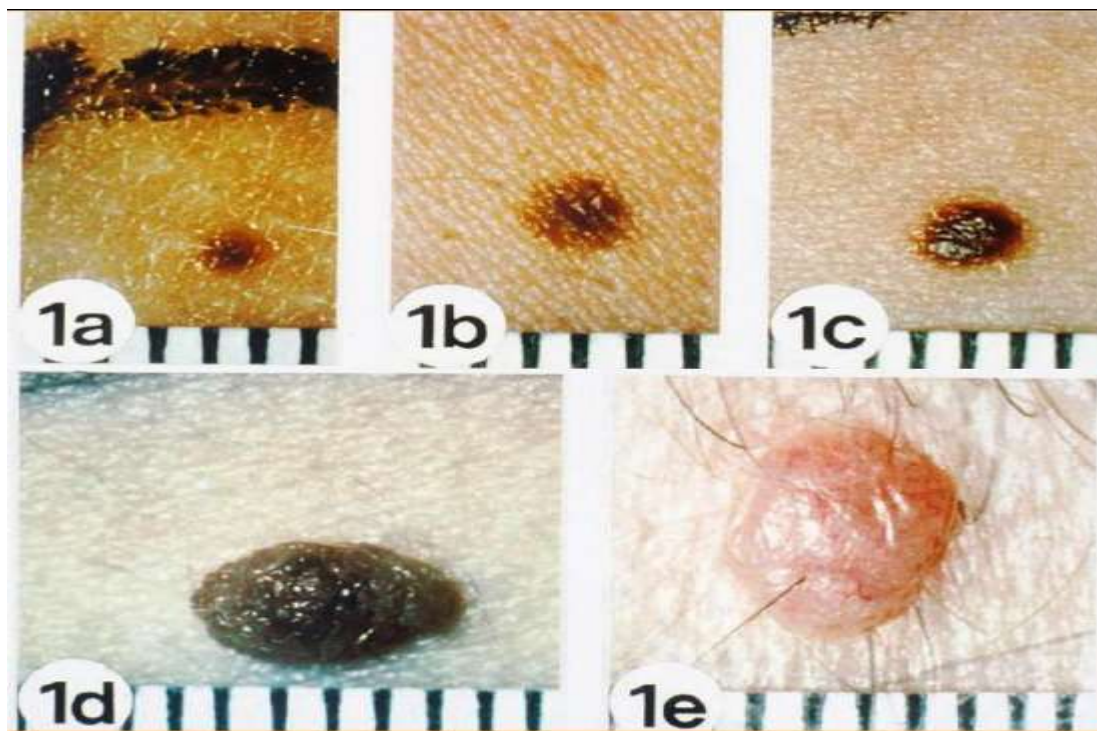
Figure 2.4 Illustration of normal moles in various shapes [11]

The depth of penetration of a melanoma into various skin layers is usually used as an indication of severity as well as treatment possibility. Breslow thickness and Clark levels are known measures that are used in this context. Level I to V are assigned to melanoma cases to indicate how did the cancer spreads and the likelihood of metastasis and its severity. Level I indicates confined melanoma to epidermis and limited spread horizontally is normally expected on the skin surface. It is also accompanied with high possibility of effective treatment. On the other hand, level V indicates significant invasion of melanoma to the subcutaneous sub-layer as well as very high likelihood of metastasis in other organs through blood stream or lymphatic

system. Level V is accompanied with significant reduction in survival rate even after the total removal of melanoma. The recurrence risk associated with level V is also very high. All levels in between obviously offer a combination of metastastic behavior, recurrence, and treatment success. Surface size of melanoma can extend from one millimeter up to few centimeters in most cases.

It is also known that skin cancer might not be inevitable and it can be preventable in many cases. Once the suitable technology is available, it is supposed be detected much easier than many other cancers since location is superficial and full accessibility is not a big problem.

2.6 Oxygen Saturation in the Blood

The average human adult has more than 5 liters (6 quarts) of blood in his or her body. Blood carries oxygen and nutrients to living cells and takes away their waste products. It also delivers immune cells to fight infections and contains platelets that can form a plug in a damaged blood vessel to prevent blood loss. Each year in the USA, 30 million units of blood components are transfused to patients who need them. Blood is deemed so precious that is sometimes called red gold [16].

If a test tube of blood is left to stand for half an hour, the blood separates into three layers as the denser components sink to the bottom of the tube and fluid remains at the top. The straw-colored fluid that forms the top layer is called plasma and forms about 60% of blood. The middle white layer is composed of white blood cells (WBCs) and platelets (PLTs), and the bottom red layer is the red blood cells (RBCs). These bottom two layers of cells form about 40% of the blood. Plasma is mainly water, but it also contains many important substances such as proteins (albumin, clotting factors, antibodies, enzymes, and hormones), sugars (glucose), and fat particles. All of the cells found in the blood come from bone marrow. They begin their life as stem cells, and they mature into three main types of cells— RBCs, WBCs, and PLTs [16].

Every second, 2-3 million RBCs are produced in the bone marrow and released into the circulation. Also known as erythrocytes, RBCs are the most

common type of cell found in the blood, with each cubic millimeter of blood containing 4-6 million cells. They circulate around the body for up to 120 days, at which point the old or damaged RBCs are removed from the circulation by the spleen and liver. If a patient has a low level of hemoglobin, a condition called anemia, they may appear pale because hemoglobin gives RBCs, and hence blood, their red color. They may also tire easily and feel short of breath because of the essential role of hemoglobin in transporting oxygen to the entire body from the lungs [16].

WBCs come in many different shapes and sizes. Despite their differences in appearance, all of the various types of WBCs have a role in the immune response. They circulate in the blood until they receive a signal that a part of the body is damaged. In response to these signals, the WBCs leave the blood vessel by squeezing through holes in the blood vessel wall. They migrate to the source of the signal and help begin the healing process.

Platelets are irregularly shaped fragments of cells that circulate in the blood until they are either activated to form a blood clot or are removed by the spleen after about 9 days [16].

The primary function of blood is to supply oxygen and nutrients as well as constitutional elements to tissues and to remove waste products. Blood also enables hormones and other substances to be transported between tissues and organs. Problems with blood composition or circulation can lead to downstream tissue malfunction. Blood is also involved in maintaining homeostasis by acting as a medium for transferring heat to the skin and by acting as a buffer system for bodily pH.

The blood is circulated through the lungs and body by the pumping action of the heart. The right ventricle pressurizes the blood to send it through the capillaries of the lungs, while the left ventricle re-pressurizes the blood to send it throughout the body. Pressure is essentially lost in the capillaries, hence gravity and especially the actions of skeletal muscles are needed to return the blood to the heart.

Oxygen saturation—sometimes referred to as O sats, or simply, sats—refers to the extent to which hemoglobin is saturated with oxygen. Hemoglobin is an element in the blood that binds with oxygen to carry it through the bloodstream to the organs,

tissues, and cells of the body. Normal oxygen saturation is usually between 96 percent and 98 percent [14,15].

Each of our red blood cells contains 4 molecules of hemoglobin. Iron, which is present in hemoglobin, is what oxygen binds to after diffusing from the alveoli in the lungs and into the capillaries of the lungs. Most of the time the hemoglobin is fully saturated.

2.7 Normal Cells versus Melanoma Cells Temperature and Oxygen Saturation

Cancer cells have higher temperature and oxygen saturation because they have more blood vessels, higher blood flow rates and increased metabolism activity, thereby the temperature and oxygen saturation is above the normal range.

Chapter Three

Technology Background

3.1 Fundamental Physics Concepts of Temperature Variation Analysis

    3.1.1 IR Radiometry

    3.1.2 IR Sensors

    3.1.3 Black body & Gray body

    3.1.4 Emissivity

3.2 Measuring Oxygen Saturation Using Red and IR Radiation

    3.2.1 Beer-Lambert Law

    3.2.2 Pulse Oximeter

In 1800 the extensive work of Sir Frederick William Herschel (1738 – 1822) has put IR radiation ability to produce thermal effect into the spot of light it deserves. Since that time infrared radiation received more attention in the physics and technology world. To shed some light on a few of Nobel Prize work done: may be one cannot miss the work of Wilhelm Wien (1864 – 1928) which led to Nobel Prize in physics in 1911. Recently it was John C. Mather and George F. Smoot who was awarded Nobel Prize in physics jointly in 2006 for their work on blackbody radiation in astrophysics that might help to understand the big bang. In this context Nobel Prize winner in 1918 Max Planck (1858 – 1947) whose work led to the description of black body radiation cannot go unnoticed also.

Infrared (IR) radiation is a part of the electromagnetic spectrum that lies directly after the visible range. IR wave length range extends, generally, from around 800 nm up to 1 mm as shown in Figure 3.1. It can enjoy naturally both the characteristics of electromagnetic wave nature as well as being formed out of photons. One more aspect that is almost always accompanying infrared is its association with thermal activity. Actually, all objects emit electromagnetic radiation once their temperature is above the absolute zero temperature 0 K (equivalent to -273 °C). Furthermore, the radiated electromagnetic objects cover a broad spectrum of wavelengths. The spectrum varies also in magnitude of radiated at each wavelength. Therefore it can be true that many objects emit visible electromagnetic radiation (λ = 380 - 780 nm) but it is extremely weak and human eye cannot detect it.
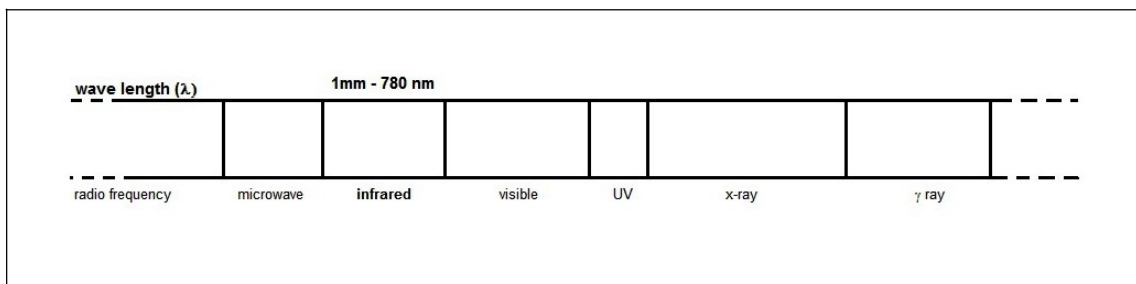

Figure 3.1 electromagnetic wave Spectrum [17, 18]

The IR radiation also enjoys the possibility of non-contact and non-invasive measurement techniques that allow remote sensing and monitoring. Although the atmosphere can absorb and attenuate severely IR radiation at certain wavelengths, it still offers trivial attenuation to other IR radiation wavelengths. Figure 3.2 shows a sample of the attenuation suffered by IR spectrum in the range of $\lambda = 1 - 15$ μm which is a favorable range in many applications. Note that 10 m and 100 m propagation path curves are included. The sole reason for this attenuation of IR radiation in atmosphere is water vapor (H_2O) and carbon dioxide (CO_2). Nevertheless, not all IR radiation wavelengths are classified equally. There exists a classification used to specify certain ranges of IR wavelengths.
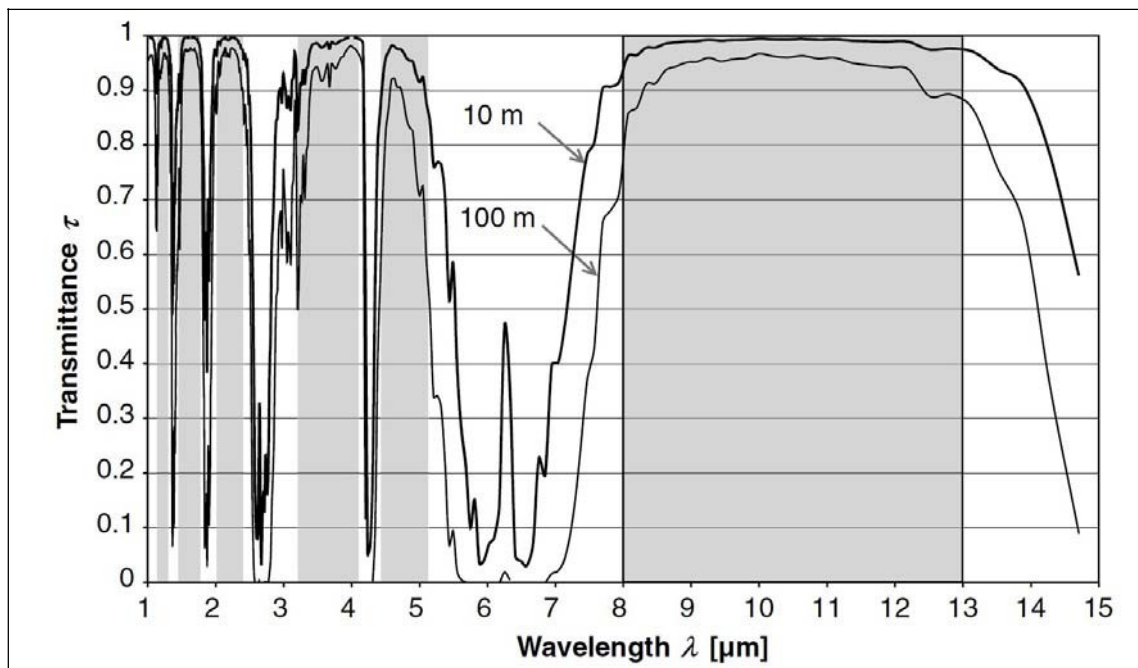

Figure 3.2 illustration of a typical transmission (τ) curves in atmosphere in summer of Central Europe [17]

Near infrared (NIR) extends from 0.78 to 3 μm, mid infrared (MIR) from 3 to 6 μm, far infrared (FIR) from 6 to 40 μm, and ultra-far infrared (UFIR) from 40 to 1000 μm [17, 19]. Hence an object can emit a spectrum that includes all these classes rather than a monochromatic radiation.

3.1 Fundamental Physics Concepts of Temperature Variation Analysis

3.1.1 IR Radiometry

An object that emits IR radiation to the surroundings can be characterized by the exitance (M) which is the flux (Φ) emitted by a unit area of the object surface (A):

$$M = \frac{d\Phi}{dA} \qquad (3\text{-}1)$$

This should include the entire spectrum and is measured as watt per square meter (W/m^2). On the other hand, if an IR radiation falls onto a sensor the amount received per unit area is called irradiance (E) as follows:

$$E = \frac{d\Phi}{dA} \qquad (3\text{-}2)$$

Where

dA is the normal surface area to the direction of IR radiation.

Both exitance (M) and irradiance (E) are measures of the total contribution of all IR flux that includes all wavelengths in that radiation. This clearly emphasizes the wide spectrum of IR radiation that usually contains a narrow or broad spectrum of wavelengths depending on the temperature of the object that is being tested. It is also worth mentioning that not all the power spectrum is uniformly distributed. The IR flux (Φ) peaks at certain wavelength where most of the power is concentrated. This is illustrated in figure 3.3. This reflects also the dependence of all radiometric parameters on temperature (T) and hence wavelength (λ) of the object.
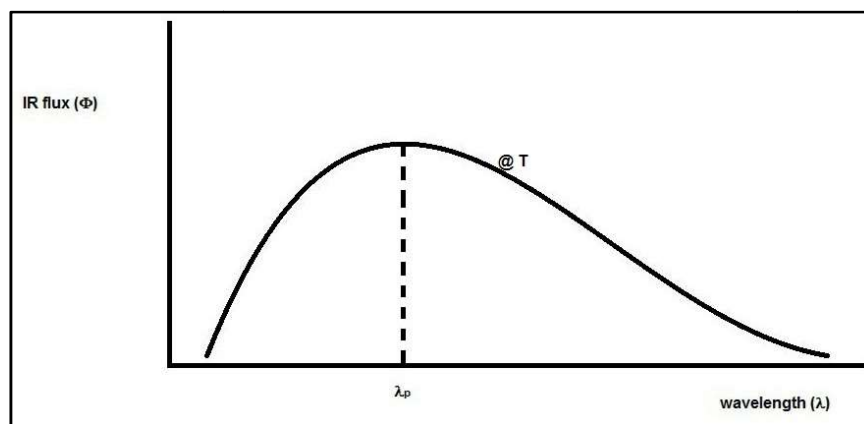

Figure 3.3 typical IR radiation spectrum from an object at an arbitrary temperature (T) [17]

3.1.2 IR sensors

IR radiation can be detected and quantified by either taking advantage of the thermal effect of the electromagnetic radiation flux itself or by using the quantum nature of IR radiation (i.e. IR photons). All IR sensors known today belong to either category. Figures 3.4 portrays both concepts, where (a) represents a simplified diagram for converting the IR radiation into electrical signal in IR thermal sensors and (b) represents IR quantum sensor.

If the sensor absorbs IR radiation and hence a change in temperature is developed in the sensor, then the sensor is often referred to as thermal sensor or radiation temperature sensor [17]. This change in temperature can in turn be converted to a change in output electrical signal. The output signal can be either current signal or voltage signal. If the output is a current signal then sensor responsivity (R_I) can be defined as:

$$R_I = \frac{\Delta I_S}{\Delta \Phi_S}$$
(3-3)

Where

ΔI_s is the change in current output from the sensor.
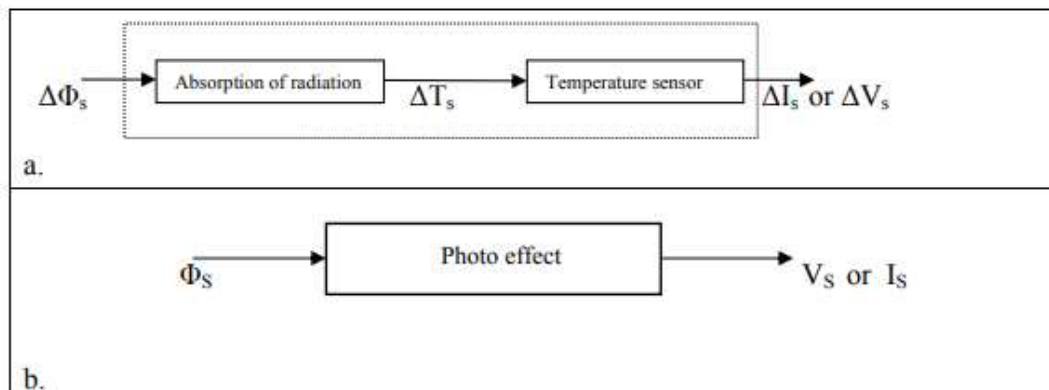
$\Delta \Phi_s$ is the change in the input flux.

Figure 3.4 IR sensors principles [17]

This type of sensors usually enjoys a rather constant responsivity (R_I) irrespective of the wavelength (λ). Furthermore, any change in the input flux ($\Delta \Phi$s)

causes a proportional change in sensor temperature (ΔTs) and hence a proportional output Absorption of radiation Temperature sensor affects the currents (ΔIs). This leads to simple detection and linear characteristics. On the other hand, the signal to noise ratio (SNR) of the sensor is expressed as a parameter called specific detectivity (D*) [17, 20]. It is also proportional to the sensor responsivity as follows:

$$\mathbf{D}^* = \mathbf{R_I} \cdot \frac{\sqrt{\mathbf{A_s}}}{\mathbf{i_n}} \qquad (3\text{-}4)$$

Where

A_S is the sensor surface area.

i_n is the effective noise current.

It is also worth mentioning that the frequency range extends up to several hundred Hz [17]. The most common types of thermal IR sensors are Thermocouple, Thermopile, Pyroelectrics and Bolometer.

Thermocouple is one of the classic and popular concepts in converting thermal radiation into electrical voltage. This is called the Seebeck effect. It is based on electrical potential that is generated when two different materials (metals or semiconductors) to form a junction at one end. When the junction suffers from thermal radiation, a voltage difference is generated at the open ends. It is robust, simple, inexpensive, and compact. Moreover, the dynamic range can be extremely large and extends to high temperatures. It also enjoy a rather fast response time also.

Thermopile is composed of several thermocouples connected together. The connection is in series to increase the output electric potential. All junctions of the thermocouples are oriented such that they are not far away from the measurement spot to reduce differences of thermal radiation received by each. The total output hence is a true indication of the amount of the IR thermal flux that falls on the thermopile. The modern technology has helped to fabricate extremely compact thermopiles from technologies such as CMOS. However the main concept is still the same i.e. based on Seebeck thermo-emf principle. Nevertheless, it offers a better responsivity. According lyresposivity increases as the number of thermocouples used increases.

Pyroelectrics uses spontaneous polarization that some materials exhibit due to their crystalline structure under the influence of thermal stress. The thermal stress affects the electric dipole moment generated in the sensor and renders it useful for measuring of the IR flux. Pyroelectric materials are, however, considered a subclass of piezoelectric dielectrics. Pyorelectic sensors can equally well operate in both current mode and voltage mode. They can easily be integrated with their corresponding signal amplifiers and readout electronic circuit into a single chip. Matrix of sensors can also be fabricated for IR imaging. Moreover, the main detection process depends on the change of flux over time (i.e. time derivative).

Bolometer which a change in the internal resistance is caused by a change in IR radiation flux that falls on it. This is due to the temperature coefficient of the bolometer resistance which determines how the resistance would change as result in the received IR radiation flux. Hence a change in the voltage drop across the bolometer can be converted to a signal representing the IR radiation flux. A bolometer is usually made of a metal or a semiconductor material. In metals an increase in temperature due to absorption of IR radiation flux causes an increase in the resistance. This leads to the fact that a metallic bolometer has a positive temperature coefficient. On the other hand, a semiconductor bolometer, usually, is based on a negative temperature coefficient. Therefore, an increase in temperature due to an incoming IR radiation flux causes a decrease in resistance. Bolometer IR radiation detector type enjoys stability and ease of integration. Bolometers, nonetheless, require electrical power continuously provided externally to them to perform their function. Microbolometer exists as an array for IR imaging purposes used in some industrial applications.

The other category IR sensors are photon detectors also called quantum detectors. This type is, normally, characterized by wavelength dependent parameters. The responsivity can be defined as [17]:

$$R_I = \frac{\Delta I_s}{\Delta \Phi_s} = \frac{\eta \cdot e}{h \cdot c} \cdot \lambda \qquad (3\text{-}5)$$

Where

η is the quantum efficiency of the sensor.

e is the electron charge.

h is Planck constant.

c is the speed of light.

This indicates a linear increase of responsivity with wavelength (λ). In reality, as wavelength (λ) increase the energy of the photon decreases leading to less signal detection. Therefore, the responsivity drops sharply after a certain peak and hence reaches almost zero at cutoff wavelength (λc).as shown in Figure 3.5. This leads to a restriction on the wavelength range for a quantum IR sensor. Nonetheless, this type is appealing to IR radiation detection since it relies on the quantum flux that is received. Therefore, the incident IR photons can be detected individually in a manner similar to photon counting. On the other hand, cooling to very low temperatures can significantly enhance signal to noise ratio (SNR) and hence the specific detectivity (D*) of this category of sensors. This category is mainly manufactured using semiconductor materials [18].
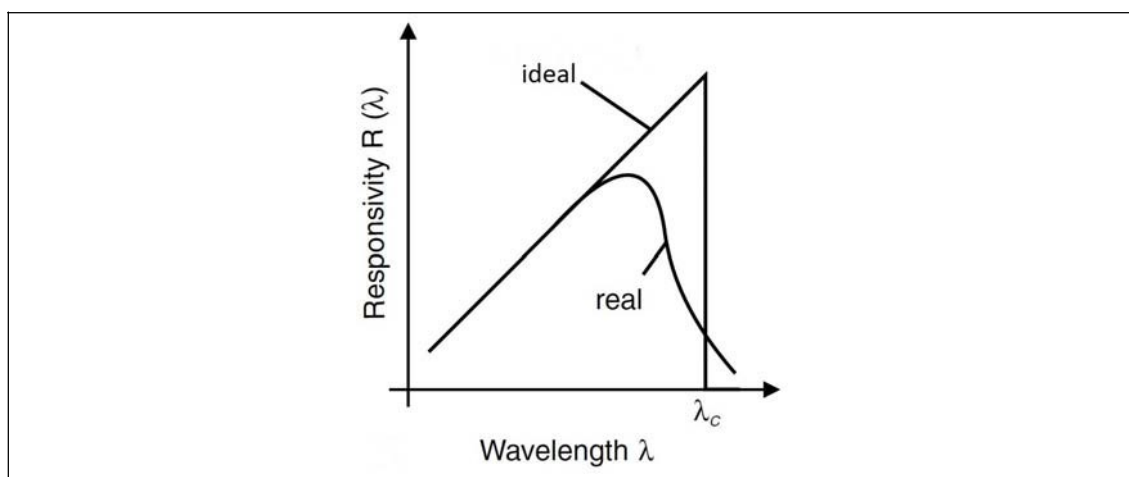

Figure 3.5 Dependence of quantum IR sensors on the wavelength (λ) [17]

3.1.3 Black body & Gray body

The black body (BB) is the ideal case of an object that emits IR radiation. Nevertheless, black body enjoys other properties that make it a perfect emitter as well as absorber for IR radiation. BB has several properties such as; it absorbs all IR radiation that hits its surface irrespective of the wavelength, it emits the maximum energy flux at any given temperature than any other object. This means that all objects

emit less energy than a BB at any temperature at any arbitrary wavelength and it emits omnidirectional regardless of its temperature.[18]

This makes BB as a standard when IR radiation is concerned. According to Max Planck equation the exitance at an arbitrary wavelength (λ) and temperature (T) is given by:

$$M_\lambda(T)d\lambda = \frac{2\pi hc^2}{\lambda^5}\left[\frac{1}{e^{\left(\frac{hc}{\lambda kT}\right)}-1}\right]d\lambda \qquad (3\text{-}6)$$

Where

k is Boltzman constant.

h is Planck's constant .

Therefore, the peak emission exitance will occur at λp satisfying the condition:

$$\frac{dM_{\lambda_p}}{d\lambda} = 0 \qquad (3\text{-}7)$$

Where

$T \cdot \lambda p = 2897.8 \ \mu m \ K$

This is also often referred to as Wein's displacement law(3-7). By using the above formulas it becomes possible to plot BB IR radiation spectrum at any arbitrary temperature. Figure 3.6 illustrates several plots of the exitance of a BB at corresponding temperatures. Note that as temperature increases λp shifts to lower values but the BB peak exitance value increase significantly in the mean while.
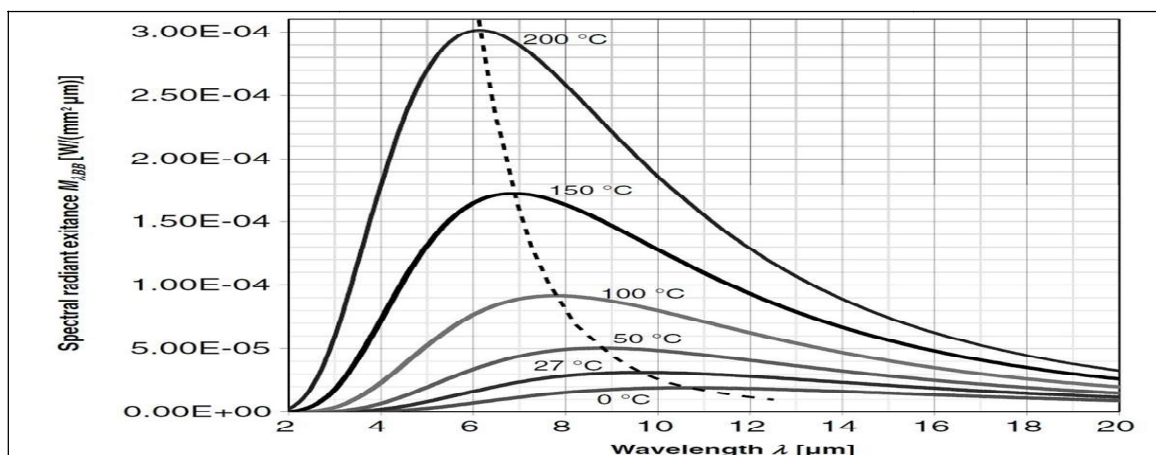

Figure 3.6 typical BB IR radiation spectrum at arbitrary temperatures [17]

It is worthwhile to mention that the Sun has a nominal temperature in the vicinity of 6000 °C and hence has a λp around 480 μm i.e. in the visible range of the electromagnetic spectrum. An even closer look to the figure 3.6 reveals that the λp values have a logarithmic relationship (note the dotted line). In figure 3.7 [18] another form of the IR radiation spectrum from a BB on a semi-log portrays this fact (λp values has a linear relation in this situation). Other objects that are not BB are usually referred to as gray bodies (GB). It follows very similar curves of IR spectral exitance depending on their characteristics but will be lower than those of BB as mentioned earlier. A gray body (GB) has an important parameter that measures this difference and it is called emissivity (will be dealt with later in this text). Therefore the emissivity of a BB is unity and any GB will have a lower than unity emissivity.

Another important law that governs BB radiation is the Stefan-Boltzman law. The formula relates the total exitance of a BB as related to temperature as follows:

$$M(T) = \sigma \cdot T^4 \qquad\qquad (3\text{-}8)$$

Where

σ is Stefan-Boltzman constant (5.67×10^{-12} W m^{-2} k^{-4}).

3.1.4 Emissivity

As mentioned earlier, a BB is an ideal case of an object used as a standard and for calibration purposes. The actual case is referred to as gray body (GB). The gray body (GB) usually follows the same emission criteria except that it is lower by a percentage called emissivity. The proper definition of emissivity (ε) is, therefore, the ratio of the amount of radiation from a GB to that of the BB at the same temperature. In other words is $0 \leq \varepsilon \leq 1$. Emissivity is also constant for most objects i.e. GBs. It is also sufficient to mention that emissivity holds true even for absorption of IR radiation.

There are however other parameters that can affect emissivity (other than the temperature and the wavelength). The material type is, nevertheless, the dominating

parameter in determining emissivity of the object. Some materials types such as metals are known to exhibit low emissivity values, while others have higher emissivity values such as glass. Object's surface structure can also affect emissivity for the same material type significantly. Metals, for example, can enjoy much higher values of emissivity if their surface is polished vs. those objects that exhibit roughened surface. Chemical modification of the surface can also enhance emissivity of the object noticeably [18]. Other parameters might also be of effect depending on the nature of the application.
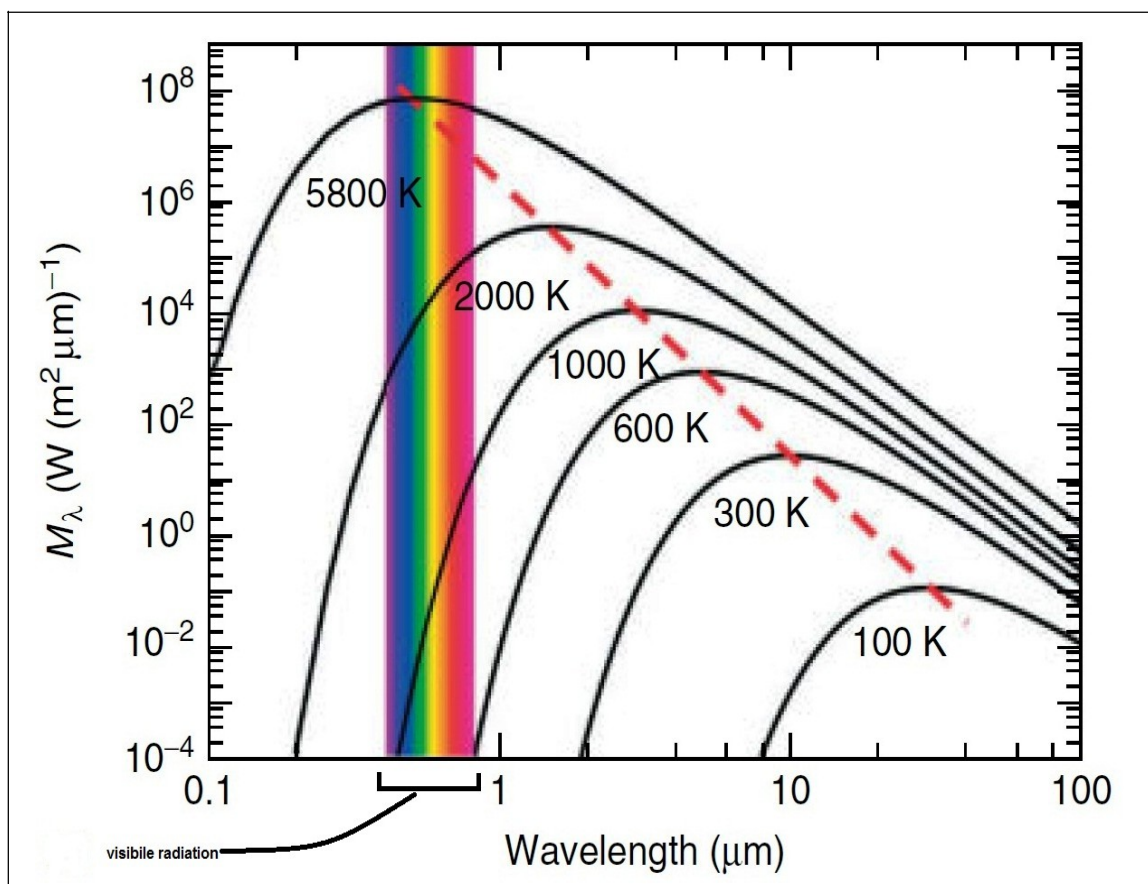
Figure 3.7 typical BB IR radiation spectrum at arbitrary temperatures on a semi-log scale [18]

3.2 Measuring Oxygen Saturation Using Red and IR Radiation

The measurement of the oxygen level in the skin is unremitting and noninvasive, this method usually allows detecting the oxygen levels which cannot be detected with subjective observations early. The measurement can be taken by placing the sensor above the tissue that consisting of a light source and light detector.

The basic aim of this measurement is to distinguish between oxygen and reduced hemoglobin. This distinction is the ratio of absorption of red and IR radiation, the red signal (660 nm wave-length) and IR signal (940 nm wave-length), sent by LEDs, then reflected to the photodiode which is in the same side as the source, then determining the degree of light absorption by the tissue, Red light is absorbed by hemoglobin, while IR light is absorbed by oxyhemoglobin. When the sensor is placed on the tissue touching the surface of the tissue, the photodiode measures the intensity of lights which are sent to the tissue by LEDs [14,15].
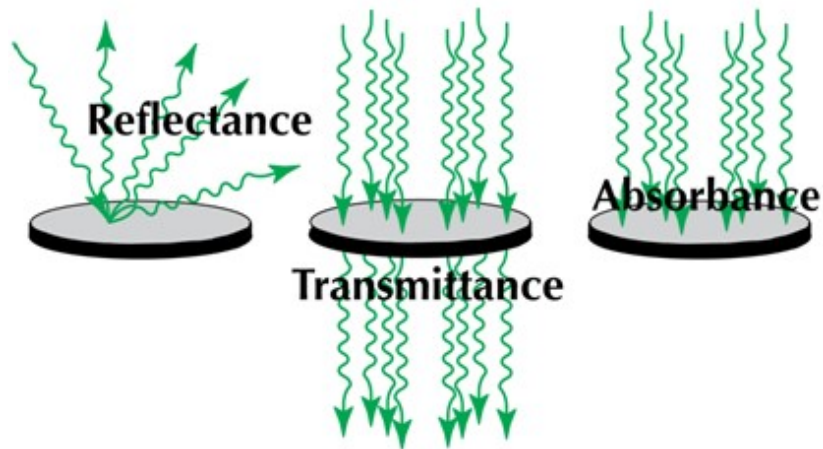

Figure 3.8 The difference between reflectance, transmittance and absorbance [15]

In this measurement the reflected radiation after the tissue absorbs a part of the radiation indicates the level of the oxygen level in the tissue.

3.2.1 Beer-Lambert Law

Beer-Lambert Law first developed by Pierre Bouguer before 1729. It was later attributed to Johann Heinrich Lambert who cited Bouguer's findings. The law included path length as a variable that affected absorbance. Later, Beer extended in 1852 the law to include the concentration of solutions, thus giving the law its name Beer-Lambert Law.

The Beer-Lambert law states that the quantity of light absorbed by a substance dissolved in a fully transmitting solvent is directly proportional to the concentration of the substance and the path length of the light through the solution [21].
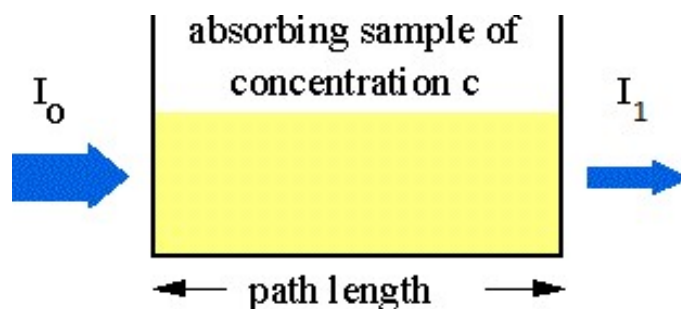
Figure 3.9 light absorption through the sample [21]

The transmission coefficient is given by the ratio of the transmitted intensity to the incident or initial intensity

$$T = \frac{I_1}{I_0} \qquad (3\text{-}9)$$

Where:

T : transmission coefficient.

I_1 : the light intensity after it passes through the sample.

I_0 : the initial light intensity before it passes through the sample.

The absorbance can be calculated through the Beer-Lambert Law:

$$A = \varepsilon C L \qquad (3\text{-}10)$$

Where:

A: the absorbance of radiation by the sample.

ε: the molar absorption coefficient (mol^{-1} cm^{-1}).

C: the concentration of the sample (mol L^{-1}).

L: length of solution the light passes through (cm).

Figure 3.10 depicts Beer-Lambert law relationships; Figure (a) shows the inverse relation between the path length of the sample and the transmission percentage, figure (b) shows the linear relation between the path length of the sample and the absorption and figure (c) shows the relation between the concentration and the absorption where at certain concentration the absorbance stops changing.

(a)   (b)   (c)
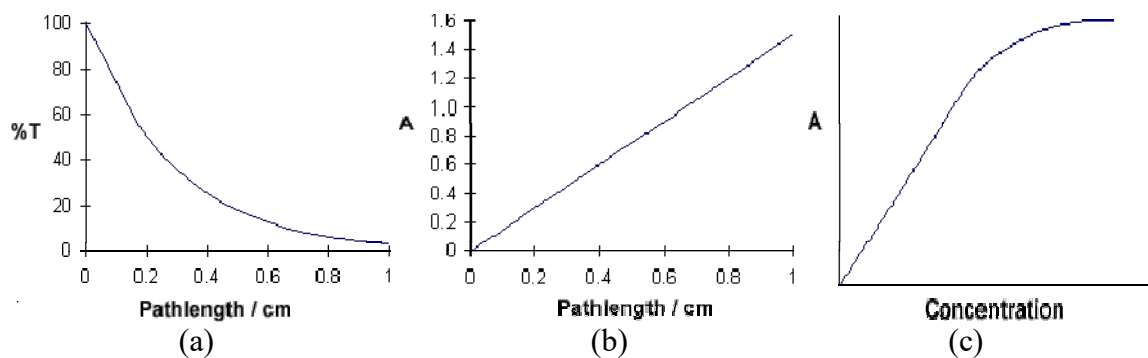
3.10 Beer-Lambert law relationships [21]

The choice of wavelengths of light mainly indicated the use of Red and Infrared wavelengths. Comparing light absorption characteristics of blood under Red and Infrared lights is said to provide a good basis for the measurement of blood oxygen saturation. Wavelengths of 660nm (Red) and 940nm (Infrared) were found to be most widely researched for this application, along with 890nm as an alternative Infrared wavelength.

The basis for using two different wavelengths of light is that oxygenated blood has different light absorption characteristics than deoxygenated blood. Thus, the two

wavelengths are chosen such that the contrast between oxygenated and deoxygenated blood is sharply visible. In this respect, 940nm is a better choice than 890nm for a wavelength in the Infrared spectrum, as the contrast between oxygenated and deoxygenated blood is more accentuated at 940nm than at 890nm as shown in Figure 3.11. Thus, when compared with the absorption due to 660nm light source for oxygen saturation calculation, the results will be less susceptible to noise [22].
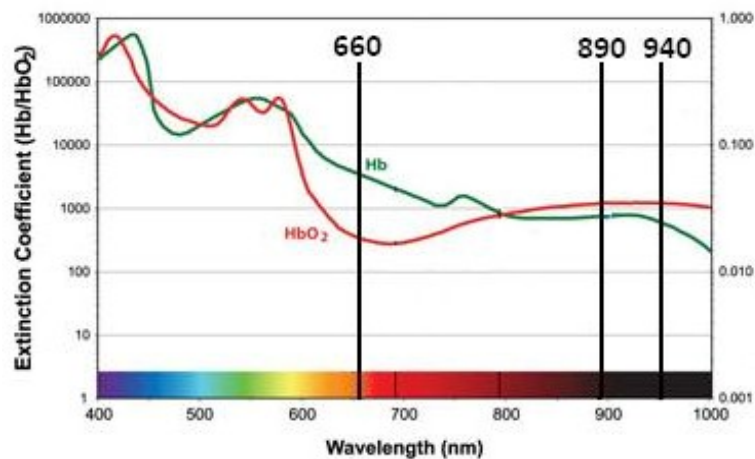

Figure 3.11 Light Absorption characteristics of HbO_2 and Hb at different wavelengths [22]

3.2.2 Pulse Oximeter

Pulse Oximeters in clinics have a finger clip type probe that has an LED on one side and a photo detector on the other side. The light emitted from one side of the finger travels through tissue, venous blood and arterial blood and is collected in the detector. Most of the light is absorbed or scattered before it reaches the photo detector in the other side of the finger. The flow of blood is heartbeat induced, or pulsatile in nature so the transmitted light changes with time. Red and infrared lights are used for pulse oximetry to estimate the true hemoglobin oxygen saturation of arterial blood. Oxyhemoglobin (HbO2) absorbs visible and infrared (IR) light differently than deoxyhemoglobin (Hb), and appears bright red as opposed to the darker brown Hb. Absorption in the arterial blood is represented by an AC signal which is superimposed on a DC signal representing absorptions in other substances like pigmentation in

tissue, venous, capillary, bone, and so forth. Cardiac-synchronized AC signal is approximately 1% of the DC level. This is referred to as the perfusion index %. The ratio of ratios 'R' is approximated in Equation (3-11). % SpO_2 is calculated as follows:

$$R = (ACrms\ of\ Red\ /\ DC\ of\ Red)\ /\ (ACrms\ of\ IR\ /\ DC\ of\ IR) \qquad (3\text{-}11)$$

The standard model of computing SpO_2 is defined as shown in Equation (3-12). This model is often used in the literature in the context of medical devices. However, accurate % SpO2 is computed based on the empirical calibration of the ratio of ratios for the specific device [23].

$$\%\ SpO2\ =110-25\times R \qquad (3\text{-}12)$$
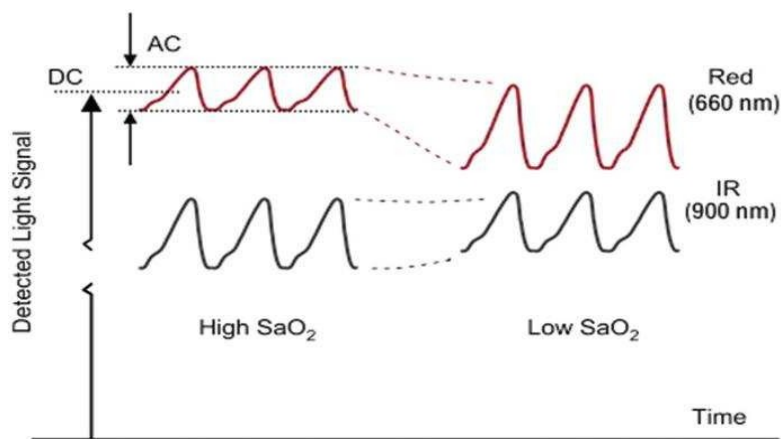
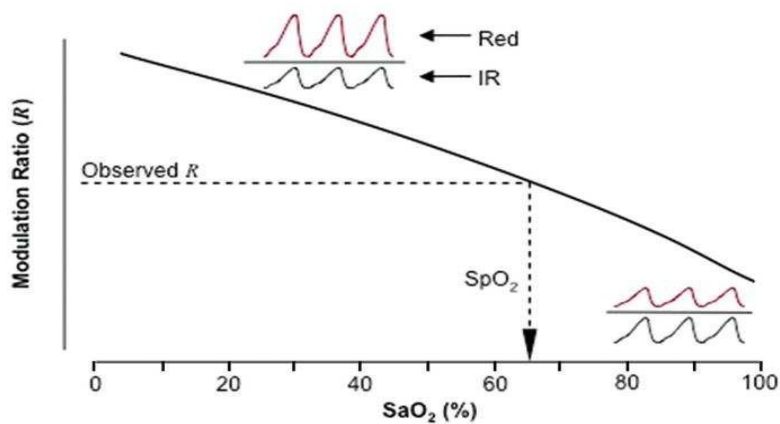Figure 3.12 Red and Infra Red Modulated by Cycling Blood [23]

Figure 3.13 Red/Infrared Modulation Ratio [23]

The optical system for SpO$_2$ measurement consists of LEDs that shine the light and a photodiode that receives the light. There are two types of optical arrangements – Transmissive and Reflective. In the transmissive case, the photodiode and the LED are placed on opposite sides of the human body part (most commonly the finger), with the photodiode collecting the residual light after absorption from the various components of the body part. In the reflective case, the photodiode and the LED are on the same side and the photodiode collects the light reflected from various depths underneath the skin. With the conventional finger clip type probes commonly seen in a clinic, one could simply imagine that the emitted light from the LED goes straight through the tissue, interacts with blood cells somehow and continues to travel in the same direction until it reaches the photodiode, or photo detector (PD). This is not the case. Photons in the light scatter in every direction when it hits an object, for example, blood cells. LED and PD separation in the finger clip probe is around 10 mm. However, most of the photons travel 20 cm to 10 cm before reaching the PD. Some travel as long as 200 mm. The photons could be described as walking randomly. This is why glow is seen in the skin of the finger tip in Figure 3.14. If the light traveled in the straight path, that is the shortest one, how could the surrounding skin of the finger glow so bright? Since we have gotten out of the old belief that the emitter and detector have to face each other, we can try placing them in easier directions like side-by-side or even at 90 degrees [23].

In this project the reflective case is used because the oxygen level will be measured at different part of the skin so the transmissive won't work because of the long distance between transmitters and receiver.
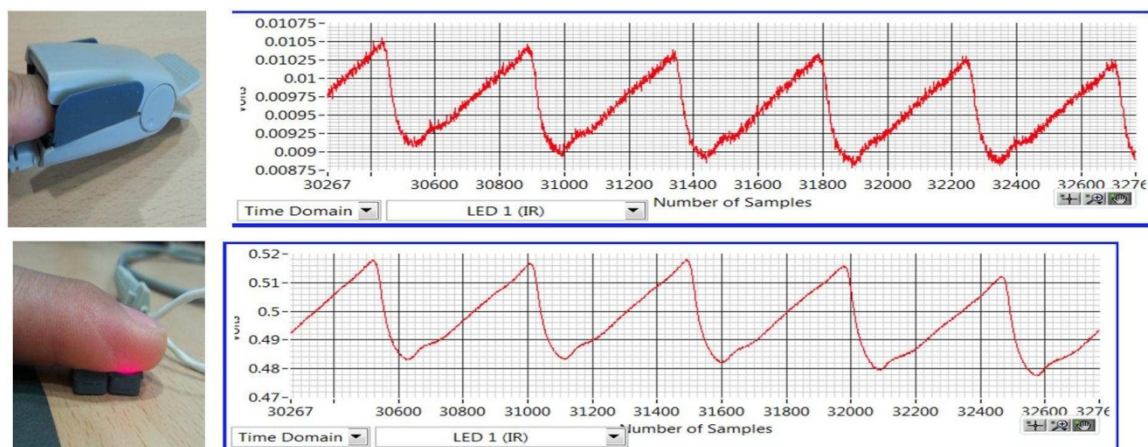

Figure 3.14 Signal Acquisition From Transmissive Versus Reflective Sensors [23]

System Design

4.1 Infrared Sensor Design

4.2 Oxygen Sensor Design

      4.2.1 Infrared and Red LEDs

      4.2.2 Phototransistor

      4.2.3 Band pass filter

      4.2.4 Low pass filter

4.3 Arduino Interfacing

4.4 Display Circuit

4.5 Power Supply

4.6 Flow Chart

This chapter talks about the system design including all the hardware and software components required. Each stage of the system will be explained in detail, the hardware components of each stage are chosen carefully to achieve the desired objectives.

The main system architecture is depicted in Figure 4.1, it is composed of two main parts, sensing and processing parts. The sensing part contains temperature IR sensor to measure skin temperature, oxygen sensor to measure the oxygen saturation in the skin. The main functions of the processing parts are receiving data from the sensing parts and process the output signal of each sensor, and send the results to the Microcontroller to analyze, compare with standard values, and display it using display device. The overall system is supplied by a rechargeable 14-V battery.
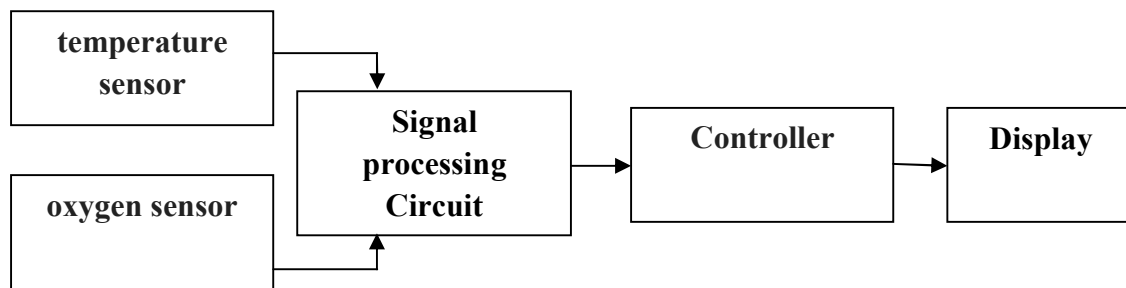
Figure 4.1 Main Block Diagram for the System

An explanation of each stage within the system is given in the following sections.

4.1 Infrared Sensor Design

IR sensor is required in the project to measure skin temperate. According to the preceding study regarding IR sensors,MLX90614 shown in Figure 4.2 is implemented in the system. This sensor was selected according to its medical

accuracy shown in Figure 4.3. Other characteristics were considered such as: small size, low cost and high accuracy ...etc [Appendix-A].

Other IR sensors could have been used such as CSmed LT sensor, but according to Table 4.1 MLX90614 sensor was the best choice for this project.
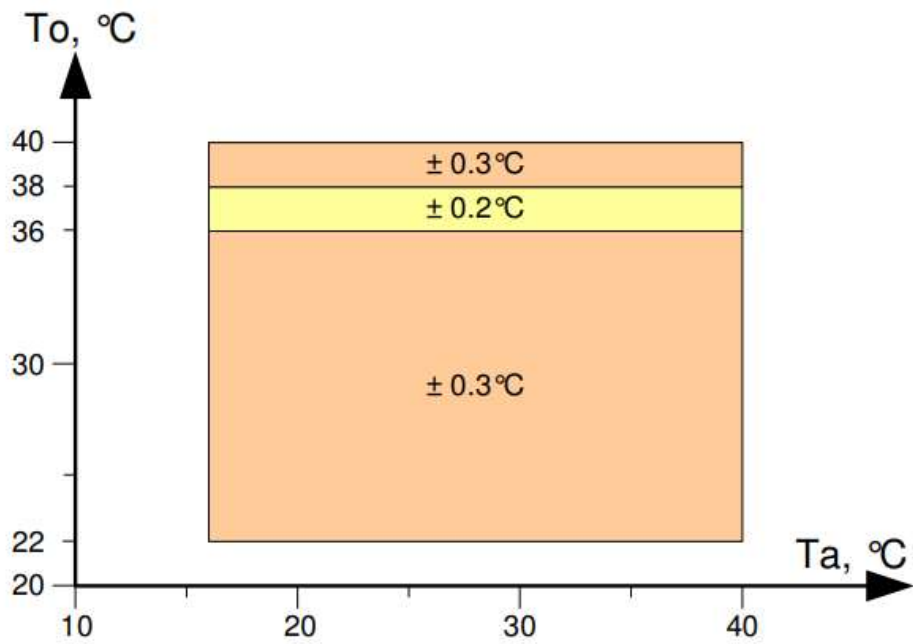

Figure 4.3 Accuracy of MLX90614 for medical applications [Appendix-A]

Table 4.1 MLX90614 and CSmed LT main features

Brand name	MLX90614	CSmed LT
Figure	 Figure 4.2 MLX90614 sensor	
Power Supply	3V DC	5−30 V DC
Current consumption	2 mA	10 mA

Temperature range	-70°C … +380°C	–40 °C … 1030 °C
medical accuracy	±0.5 °C	±1.5 % or ±1.5 °C
Measurement resolution	0.02°C	15:1°C
price	18.47$	107.49$

The following Figure 4.4 shows how to connect MLX90614 sensor in this system with the Microcontroller used where Signal processing also is done.
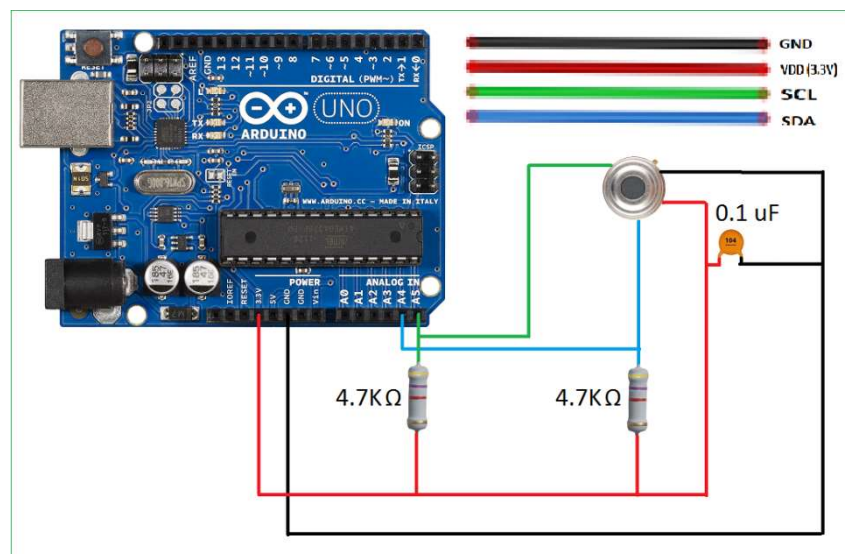

Figure 4.4 MLX90614 connection with Arduino

4.2 Oxygen Sensor Design

This section will present the design procedures that were implemented as per the methodology described in the previous chapter. The various hardware components that were used to acquire and extract the two photoplethysmogram (PPG) signals will be presented in detail, followed by the software infrastructure built for the purpose of parallel data processing on the processing centre. Finally, software data processing done to calculate the blood oxygen levels will be presented.
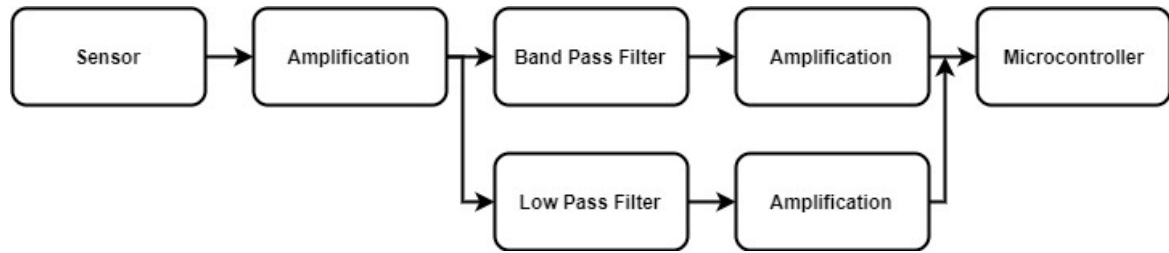
The system architecture is depicted in Figure 4.5.

Figure 4.5 Block Diagram for the O_2 sensor

4.2.1 Infrared and Red LEDs

The light signals sent from red and IR LEDs are received by phototransistor. Red LED is 660 nm and IR LED is 940 nm wave lengths.

To maintain the forward current 20mA and forward voltage 1.2V for Infrared LED [Appendix-B], the resistor R_2 is calculated by equation (4-1) and R_1 is the best choice from datasheet [Appendix-C].

$$R_2 = \frac{(7-1.2)V}{20mA} = 290\Omega \qquad (4\text{-}1)$$

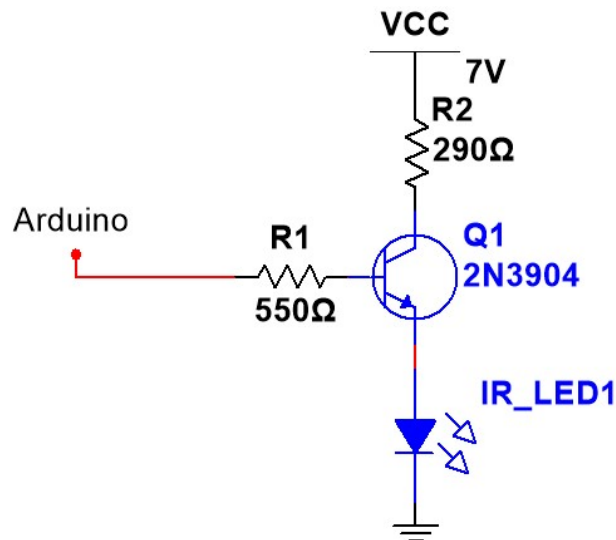Figure 4.6 shows the connection of Infrared LED with power supply.

Figure 4.6 Infrared LED connection

To maintain the forward current 20mA and forward voltage 1.7V for Red LED [Appendix-D], the resistor R_4 is calculated by equation (4-2) and R_3 is the best choice from datasheet [Appendix-C].

$$R_4 = \frac{(7-1.7)V}{20mA} = 265\Omega \qquad (4-2)$$

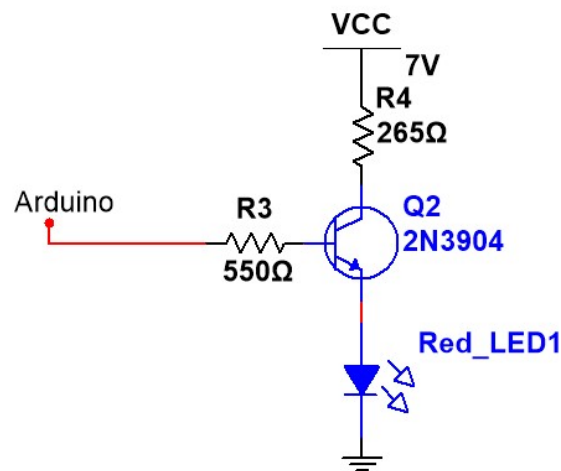Figure 4.7 shows the connection of Red LED with power supply.

Figure 4.7 Red LED connection

4.2.2 Phototransistor

The phototransistor in this project is implanted to receive the red and infrared light from the LEDs and produce waveform consisting of direct voltage (DC) and alternating voltage (AC) components. The DC component of the PPG waveform corresponds to the detected transmitted or reflected optical signal from the tissue, and depends on the structure of the tissue and the average blood volume of both arterial and venous blood. the DC component changes slowly with respiration. The AC component shows changes in the blood volume that occurs between the systolic and diastolic phases of the cardiac cycle; the fundamental frequency of the AC component depends on the heart rate and is superimposed onto the DC component [25].

voltage signal produced by the phototransistor [Appendix-E] was amplified to a voltage signal at the output node of the op-amp shown in Figure 4.8, with a

proportionality constant of R. Setting R=7k, the gain of the first stage was 8. Thus a voltage signal which was in the range of a few millivoltes was then in the range of several volts after this stage. The signal needed to be further amplified to be brought to the range of volts. However, it was deemed unwise to increase the feedback resistance of this stage to amplify the voltage signal further. This is because the gain of this stage was already high, and any further increase in gain would have deteriorated the signal in terms of its noise immunity. Furthermore, use of high values of resistance would not have been a good design decision.

The output of this stage using nodal analysis would be

$$Vo1=V_{photo}*(1+R15/R16) \tag{4-3}$$

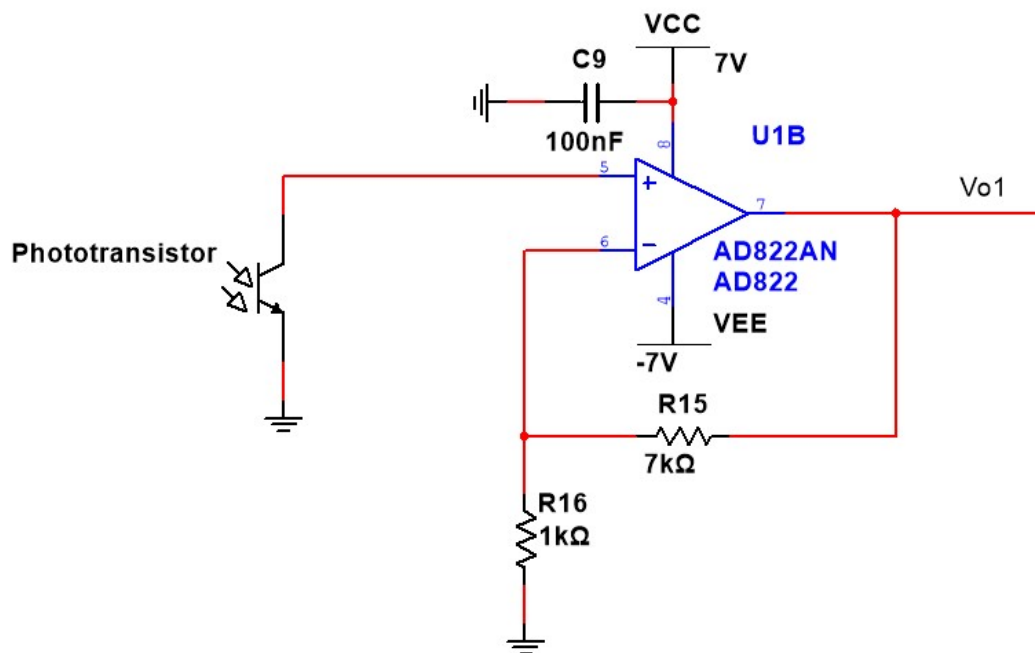Where the photo Voltage (V_{photo}) is from [Appendix-E].

Figure 4.8 Phototransistor connection with voltage amplifier circuit

Researches suggest that the spectral range of PPG is between 0.5–10 Hz [25]. Therefore a filter within this range was needed to extract out the PPG signal from the signal acquired.

4.2.3 Band pass filter

This stage consists of 2nd order active sallen key butterworth low pass filter (fc=10Hz) and passive high pass filter (fc=0.5Hz),LPF can filter fluctuating pulse wave (AC Component). The AC Component is through a band pass filter and a rail to rail amplifier. Circuit diagram of Band Pass filter (BPF) and amplifier is given in Figure 4.9. the BPF can filter the signal that is caused by light going through the body tissue and vein (DC Component) as well as high frequency noise such as interference from daylight lamp. As the AC component of the signal is low, an amplifier was needed to amplify it for further processing.

In first stage According to [Appendix-F] of the amplifier used and the equations (4-4), (4-5) [26], the values of resistors and capacitors shown in Figure 4.9 were found.
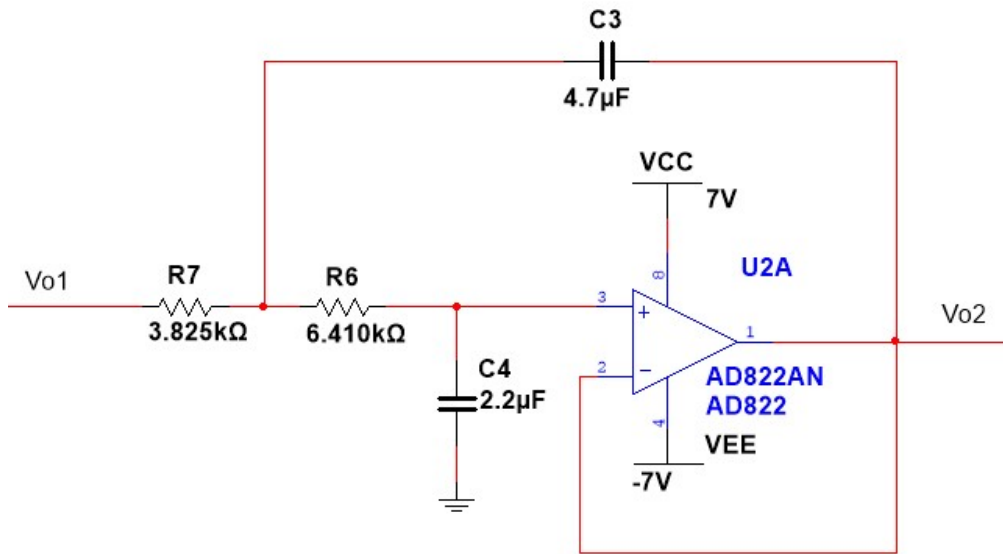

Figure 4.9 2nd Order Low Pass Filter Circuit

$$R_{7,6} = \frac{a_1 C_3 \mp \sqrt{a_1^2 C_3^2 - 4b_1 C_3 C_4}}{4\pi f_c C_3 C_4} \qquad (4\text{-}4)$$

$$C_3 \geq C_4 \frac{4b_1}{a_1^2} \qquad (4\text{-}5)$$

Specifying $C_4 = 2.2uF$

$C_3 = 4.7uF$

$R_7 = 3.825k\Omega$

$R_6 = 6.410k\Omega$

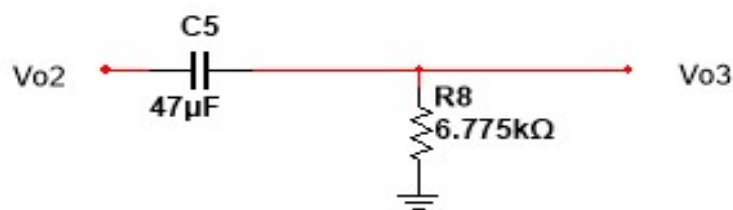In second stage a high pass filter was used with fc=0.5Hz as shown in figure 4.10.

Figure 4.10 High pass filter circuit

$$fc=0.5=\frac{1}{2\pi R_8 C_5} \qquad (4\text{-}6)$$

Specifying $C_5 = 47uF$

$R_8 = 6.775k\Omega$

4.2.4 Low pass filter

The DC Component is filtered by a 2nd order active sallen key butter worth low pass filter (LPF). The Circuit of low pass filter is shown in Figure 4.11. The Corner Frequency of low pass filter is 0.5 Hz. As a result, the LPF can filter fluctuating pulse wave (AC Component) and high frequency noise such as interference from daylight lamp.

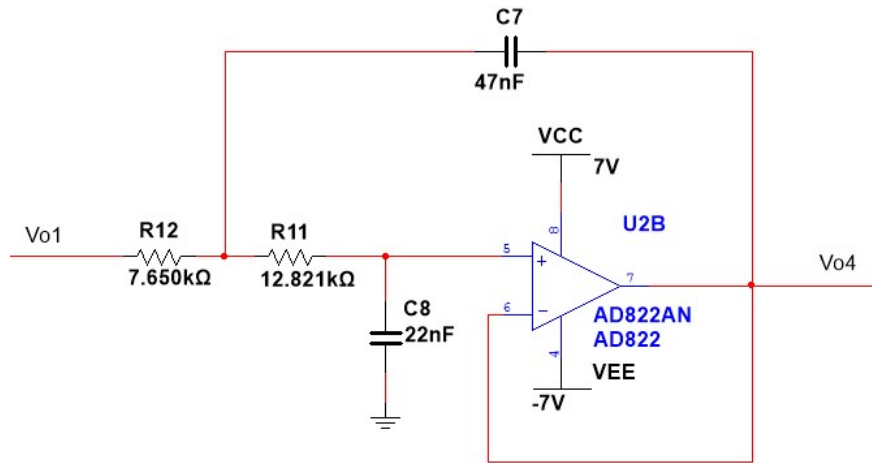According to equations (4-4), (4-5) the values of resistors and capacitors were found.

Figure 4.11 2nd Order Low Pass Filter Circuit

Specifying C_8= 22uF

C_7 = 47uF

R_{12} = 7.650kΩ

R_{11} = 12.821kΩ

4.3 Arduino Interfacing

Arduino Uno was selected in this project because it can handle the analog inputs of the sensors and the LCD connection. Arduino Uno is an open-source microcontroller board based on the Microchip ATmega328P microcontroller and developed by Arduino.cc. The board is equipped with sets of digital and analog input/output (I/O) pins that may be interfaced to various expansion boards (shields) and other circuits. The board has 14 Digital pins, 6 Analog pins, and programmable with the Arduino IDE (Integrated Development Environment) via a type B USB cable. It can be powered by a USB cable or by an external 9 volt battery, though it accepts voltages between 7 and 20 volts. It is also similar to the Arduino Nano and Leonardo [24].

4.4 Display Circuit

The display device that will be used in the project is LCD (4*16); it can display sixteen characters on four rows which is very good for the project. The data displayed on the LCD are temperature values, oxygen levels and the health condition (normal, abnormal case). Figure 4.12 shows the connection between LCD and Arduino .
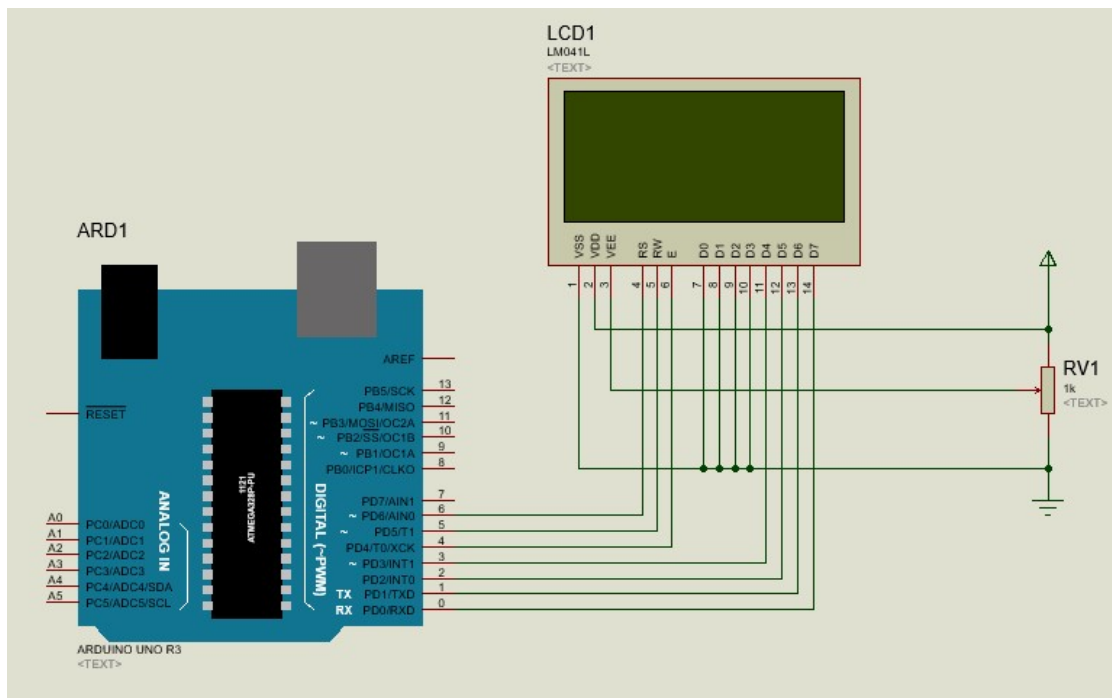

Figure 4.12 LCD Arduino connection

4.5 Power Supply

The hardware system needs power supply to provide its components with the required power. As the system is required to be portable a battery that has the following characteristics is required: light weight, provide required system power and has relatively long life.

Due to limitation of power supply in the system, choosing of system parts should fulfill the need for an optimal with minimum current consumption leading to increase the life time of the battery. The system intended to operate using a rechargeable (14volt) battery , but all stages need to operate within a voltage supply of (7) volt. This stage use voltage regulator (LM317) to obtain these voltage values from the battery keeping in mind the current consumption of all electrical parts used in the system. Table (4.2) explain the name of different parts used in the system with the power consumption relate to each one to find the overall system current consumption and verify that the power source able to give this desired value, also calculate the expected life time for the battery.

Table 4.2 current consumption of the internal system components

Part Name	Function	Quantity	Current consumption
MLX90614	Temperature sensor	1	2mA
AD822	Op-amp	4	0.75mA*4=3mA
IC-LQNP	Phototransistor	1	20mA
SSL-X5093SRC/DV	Red LED	1	20mA
LTE-5208A	Infrared LED	1	20mA
COM-09650	Green LED	1	20mA
2N3904	Transistor	2	150mA*2=300mA
Aruino Uno	Output Pins	1	20mA
LCD	Display	1	5mA
Total current consumption		410mA	

All data exist in the previous table obtained from the datasheet of each part [Appendix A-B-C-D-E-F-G] After this estimation about the expected current and voltage values of all system components, now it's important to choose the power supply parameters to meet these requirements reaching to optimal system operation, Polymer - Lithium 14v rechargeable battery with (2600mA/h) current capability, this battery is good enough to supply the portable system with its required power.

Figure 4.13 shows the schematic electrical connection of voltage regulator to obtain (+7) .
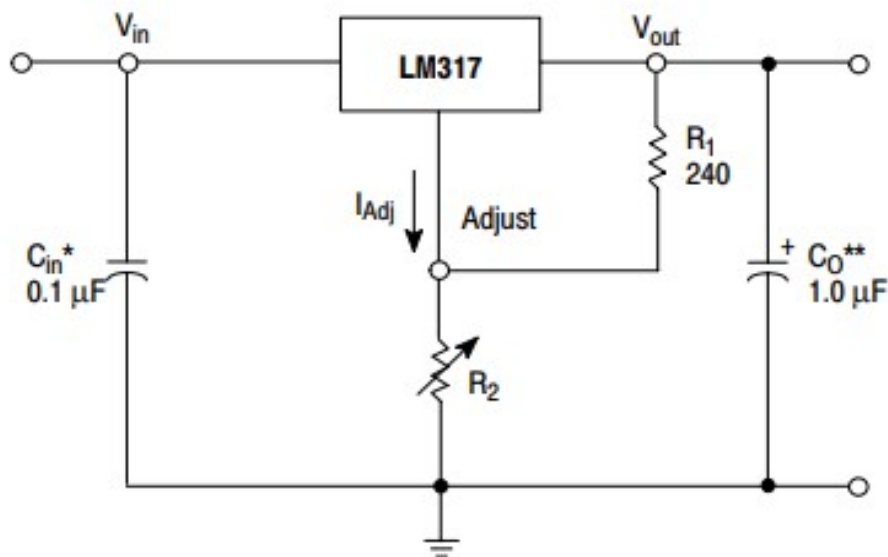

Figure 4.13 Circuit Diagram of Power Supply

LM317 (U1) was chosen as positive voltage regulator due to its relatively high output current capability (1.5A), adjustable output voltage, and low cost features. Desired output voltage can be computed according to the following formula :

$$V_{out} = 1.25V\left(1 + \frac{R_2}{R_1}\right) + I_{adj}R_2 \qquad (4\text{-}7)$$

According to U1, datasheet [Appendix-G], R1 ,C_{in} , and C_o equal 240Ω, 0.1uF and 1uF respectively. $R_2$was adjusted to obtain 7V output voltage, also I_{adj} is controlled to be less than 100 uA , and the error associated with this term is negligible

in most applications. Hence, substituting I_{adj} by 100 uA into equation (4-7) results in 7V output voltage as follows :

$$7 = 1.25V \left(1 + \frac{R_2}{R_1}\right) + I_{adj}R_2 \qquad (4\text{-}8)$$

Solving equation (4-8) for R_2 , obtaining R_2= 1083Ω.

4.6 Flow Chart

A controller is necessary in the project to acquire the data from the two sensors, analyze them and provide the display system with the result. The time required for measuring temperature for both normal and Suspicious skin is 1 minute and the time required for measuring oxygen level for both normal and Suspicious skin is 1 minute. Hence, the controller is programmed to activate the measurement sensor according to the stages shown in Table 4.3.

Table 4.3 Measurement Stages

Stage	Time	1st minute	2nd minute
1st stage	Temperature		
2nd stage	O$_2$ level		

After measuring the variables required for diagnosis and processing them including filtration and amplification circuits. Its necessary to analyze them to diagnose the patient. Arduino mega microcontroller is used in this project for this task. Its programmed to work according to the flowchart shown in figure 4.14.

In the first minute the two temperature readings for both normal (T_1) and Suspicious(T_2) skin is taken and in the second minute the two oxygen level reading for both normal ($SPO2_1$) and Suspicious ($SPO2_2$) skin is taken, then comparing these reading in the microcontroller to give the final result.
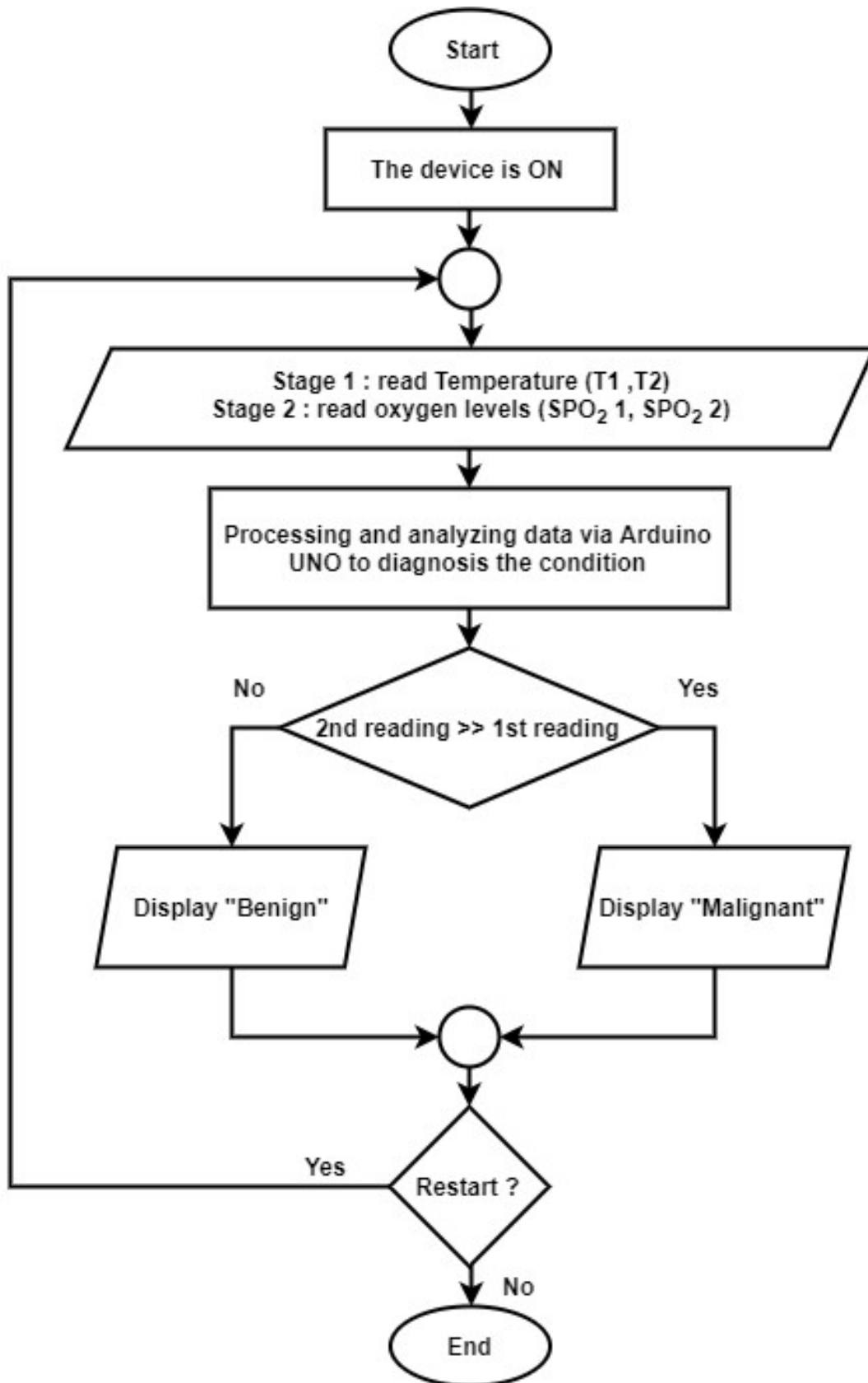
Figure 4.14 System Flow Chart

Chapter Five

O$_2$ levels Measurement System Simulation

5.1 Simulation

5.2 Results

5.3 Conclusions

5.1 Simulation

In this chapter an O_2 levels measurement system is simulated using NI Multisim 13.0 and after that results and conclusions will be taken according to the simulation.

Since any periodic signal can be represented by the sum of sin and cosine signals of different frequencies, multiplied by a different coefficient the PPG signal can be simulated.

In this project simulation, three function generators will be used for each AC signal generated from IR and red radiation. Figure 5.1 shows the function generators used to produce the IR Ac signal with deferent magnitudes and frequency range (1-10) Hz. Figure 5.2 shows the function generators used to produce the IR Ac signal with deferent magnitudes and frequency range (1-10) Hz.
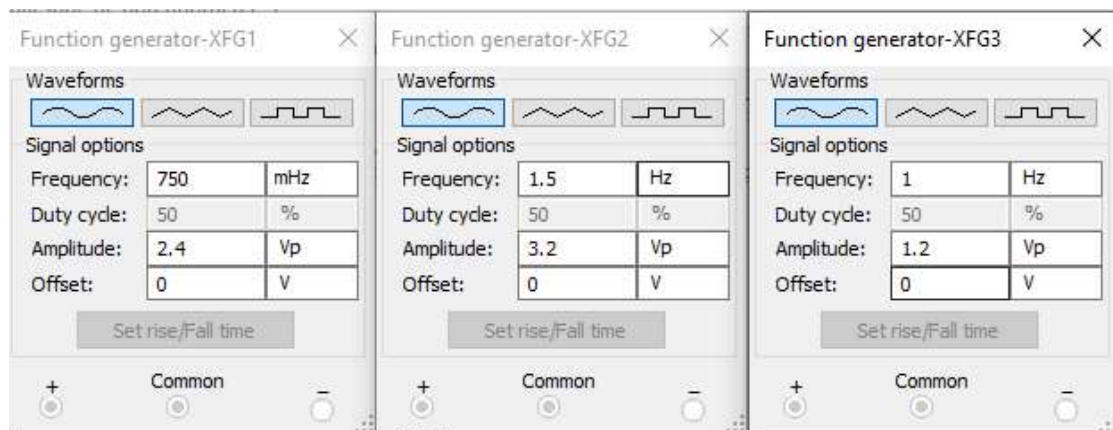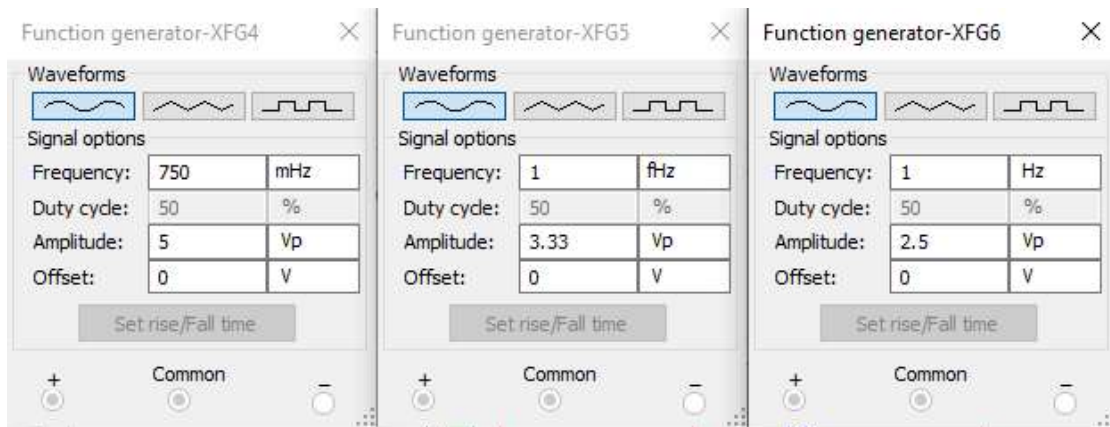

Figure 5.1 IR AC function generators

Figure 5.2 Red AC function generators

Note that a summing amplifier with gain = -1 was used in both cases to produce the PPG signal from the summing of sinusoidal signals. After that the DC component for each signal was represented as a voltage source controlled by a potentiometer .as motioned before the IR/RED signals consist of DC and AC components.

Figure 5.3 shows the circuit that controls the DC component for IR signal and Figure 5.4 shows the circuit that controls the DC component for Red signal.
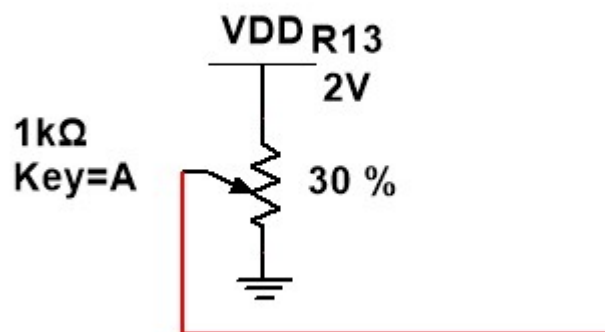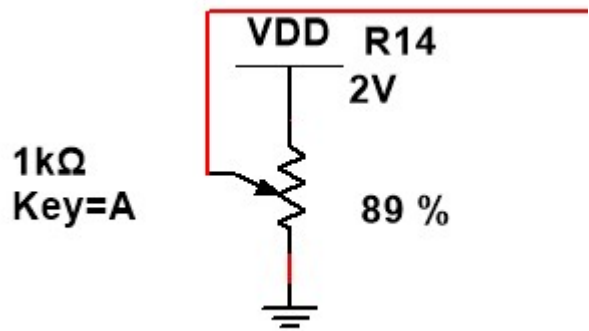

Figure 5.3 IR DC component circuit

Figure 5.4 Red DC component circuit

Since the ratio as mentioned before = $(AC/DC)_{red}/(AC/DC)_{IR}$ a dividing tool was used 3 times to get the ratio as showed in Figure 5.5.
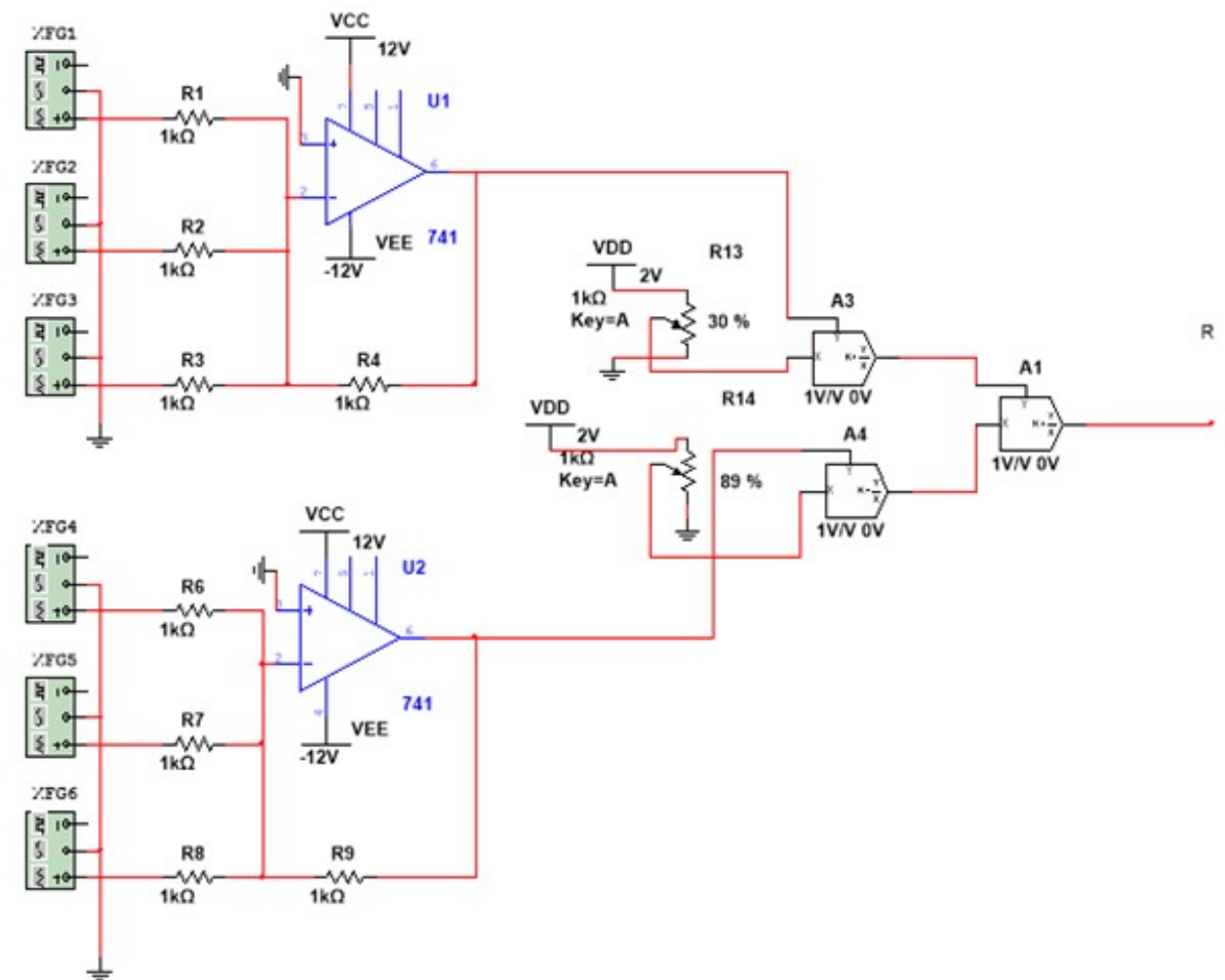

Figure 5.5 final ration circuit

After that a circuit that find the O_2 levels percentage was designed according to equation (3-12) % SpO2 $= 110 - 25 \times R$, so another summing amplifier was needed to design this circuit. Figure 5.6 shows the components that were used first a buffer then a summing amplifier with 2.5 gain for R and a $11V_{DC}$, to represent % SpO2 /10 so to get red of the 10 in the denominator a multiplier tool with gain $= 10$ was used so the final result will be the % SpO2.
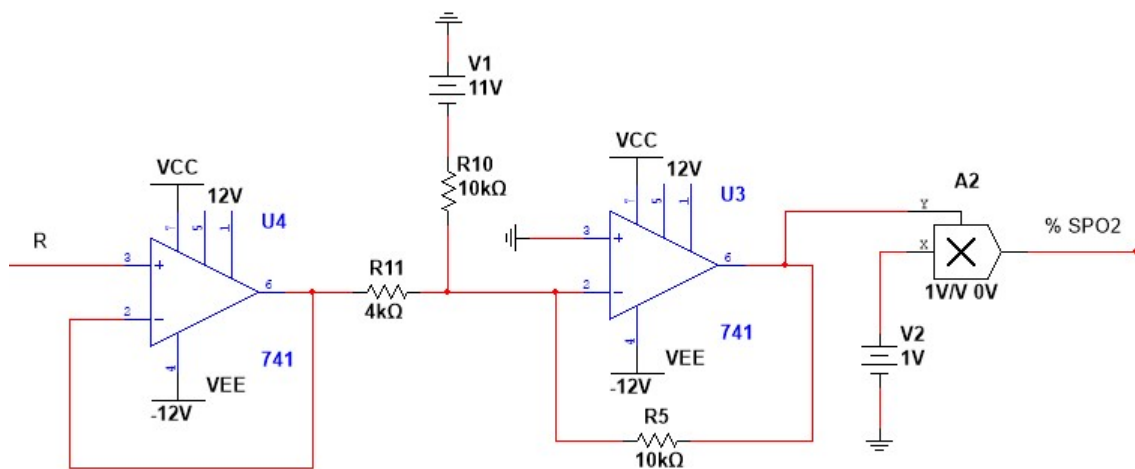

Figure 5.6 The final result of % SpO2

5.2 Results

The following table 5.1 shows the output of the simulation circuit at different AC/DC values for each Red/IR signals.

Table 5.1 The output of simulation at different ratio

Ratio	% SpO$_2$
0.6	95%
0.8	90%
1.2	80%
0.44	99%
0.5	97%
0.9	87%
1.1	82%

5.3 Conclusions

Note that if we substitute the values of R in equation (3-12) we get approximately the same values as the simulation values so we can say this simulation was successfully done.

Chapter Six

System Implementation and Testing

6.1 Project implementation

      6.1.1 Temperature Measurement Circuit

      6.1.2 O_2 Levels Measurement Circuit

      6.1.3 Controller Connections

      6.1.4 Power Supply Circuit

      6.1.5 Over All System Circuit

6.2 Project Testing

In this chapter the hardware system designed in the preceding chapter is implemented to accomplish the project as one unit which achieves the purpose of the project. In this section, subsystems circuit will be implemented before final implementations to the system.

6.1 Project Implementation

The temperate and O_2 level sensors have to be close enough to the patient's skin; therefore these sensors where located in two separated probes. The probes that used are made of a 3D printer materials which are suitable for the project. The probes used in the project are shown if Figure 6.1.

Figure 6.1 Probes of the temperatures and O_2 sensors

6.1.1 Temperature Measurement Circuit

The temperature sensor used in the temperature measurement circuit needs calibration in addition to software programming. It is calibrated, tested and programmed on the arduino as shown in the Figure 6.2.
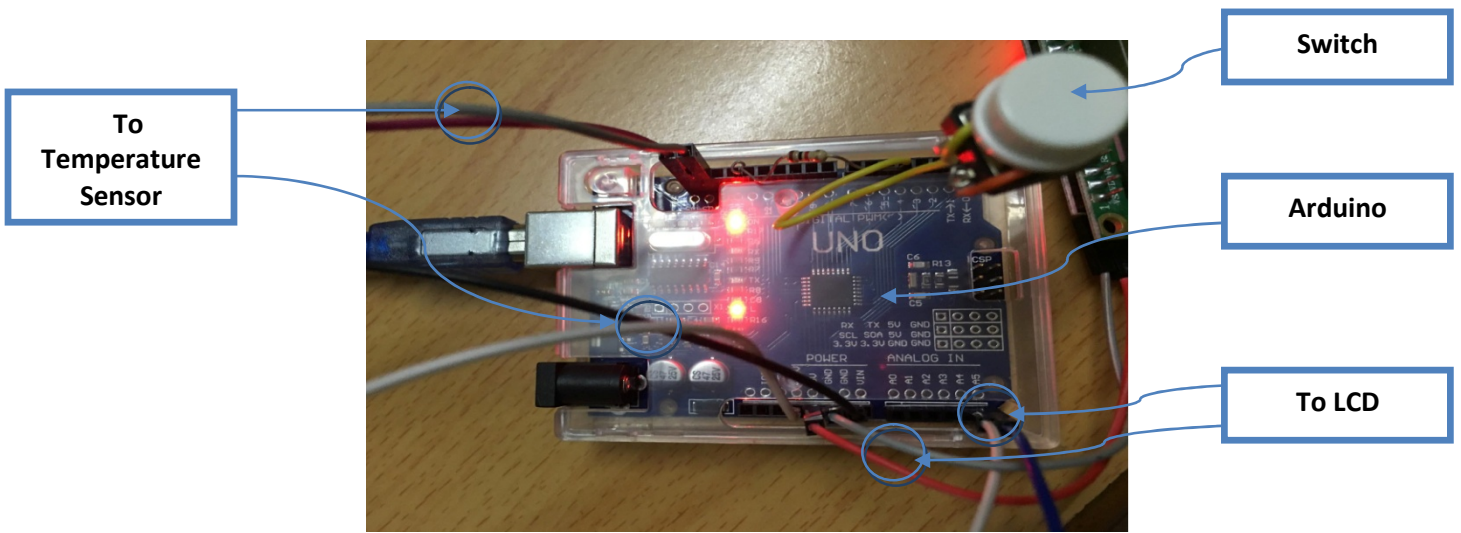
Figure 6.2 Temperature sensor connection

After programming the sensor, it is fixed on the probe and connected to the arduino Uno to measure the temperature of the patient's skin as discussed in chapter four.

6.1.2 O_2 Levels Measurement Circuit

The O_2 level measurement circuit consists of O_2 level sensor and processing circuit. The O_2 level sensor is located in one of the probes to be close to patient's skin, where the processing circuit is located in the system box. It composed of filtration and amplification circuits as shown in Figure 6.3.
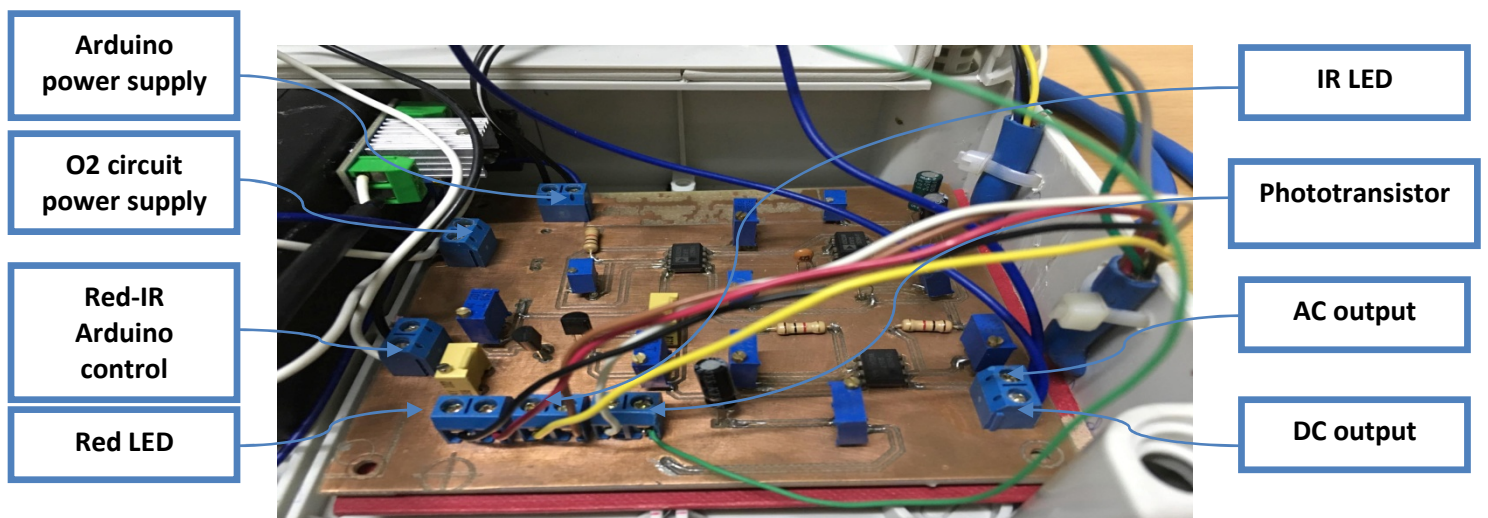

Figure 6.3 O_2 level sensor circuit

6.1.3 Controller Connections

As mentioned in chapter four, the arduino Uno is the brain of the project, so all of above circuits, LCD, LEDs and switches are connected to it. This section will show these connections in Figure 6.4.
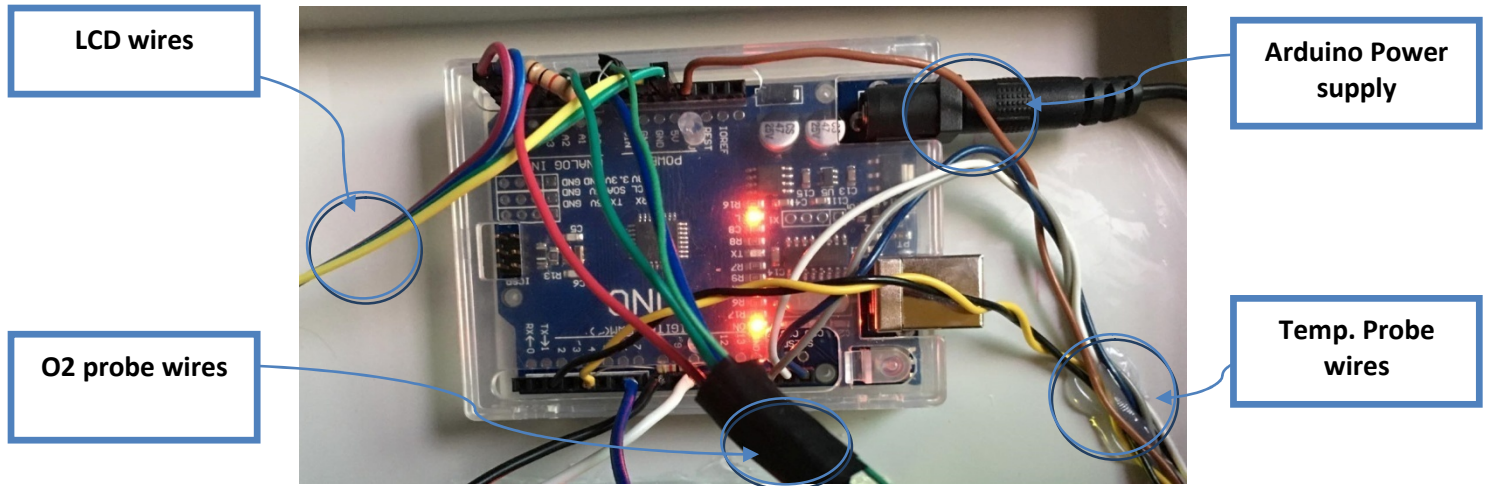

Figure 6.4 Controller connections

6.1.4 Power Supply Circuit

As mentioned in chapter four, the power supply circuit is used to provide the required voltage (7V) to the other circuits and subsystems. The power supply circuit and its components are shown in Figure 6.5.
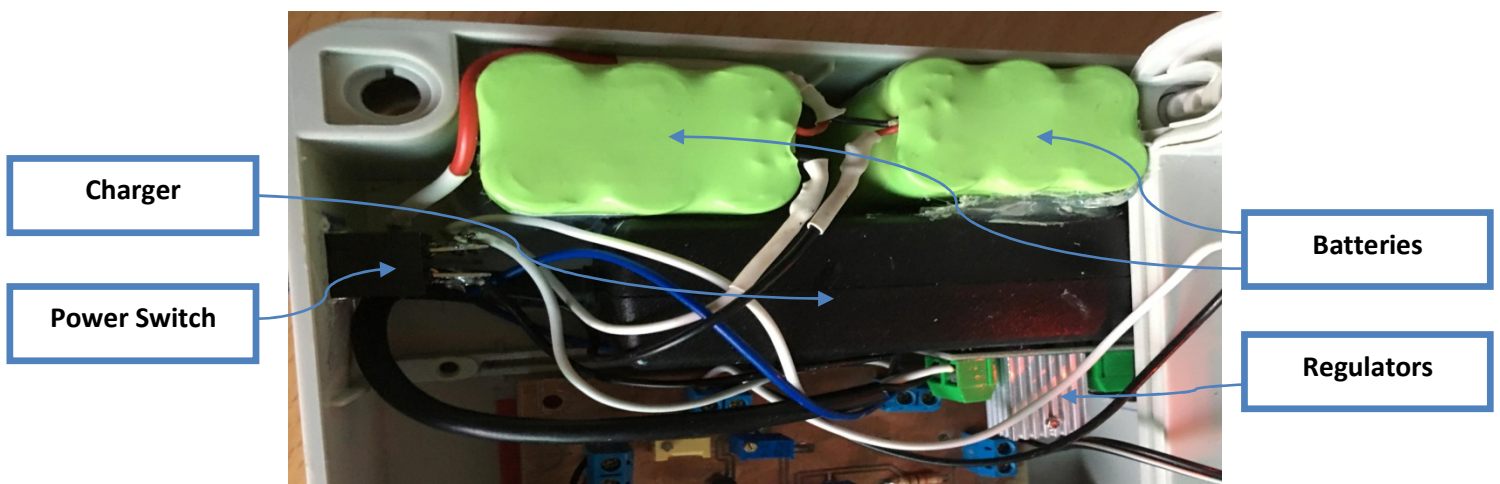

Figure 6.5 Power supply circuit

6.1.5 Over All System Circuit
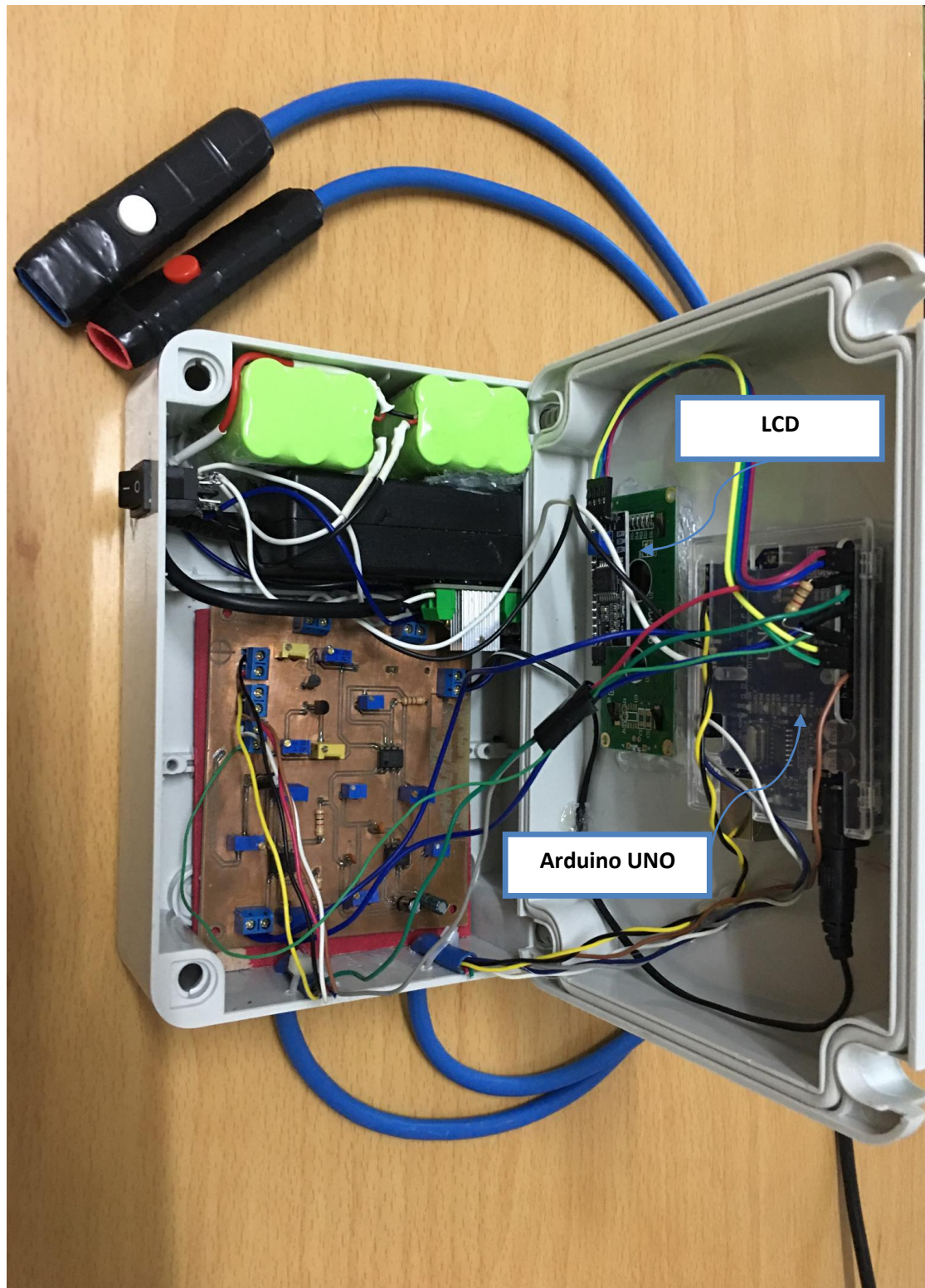
The overall circuit of the system is shown in Figure 6.6.

Figure 6.6 Overall system circuits

6.2 Project Testing

According to the project objectives, the system is supposed to presses the temperature values and oxygen levels values and then display the result on LCD screen whither the mole is malignant or benign as shown in Figure 6.7.
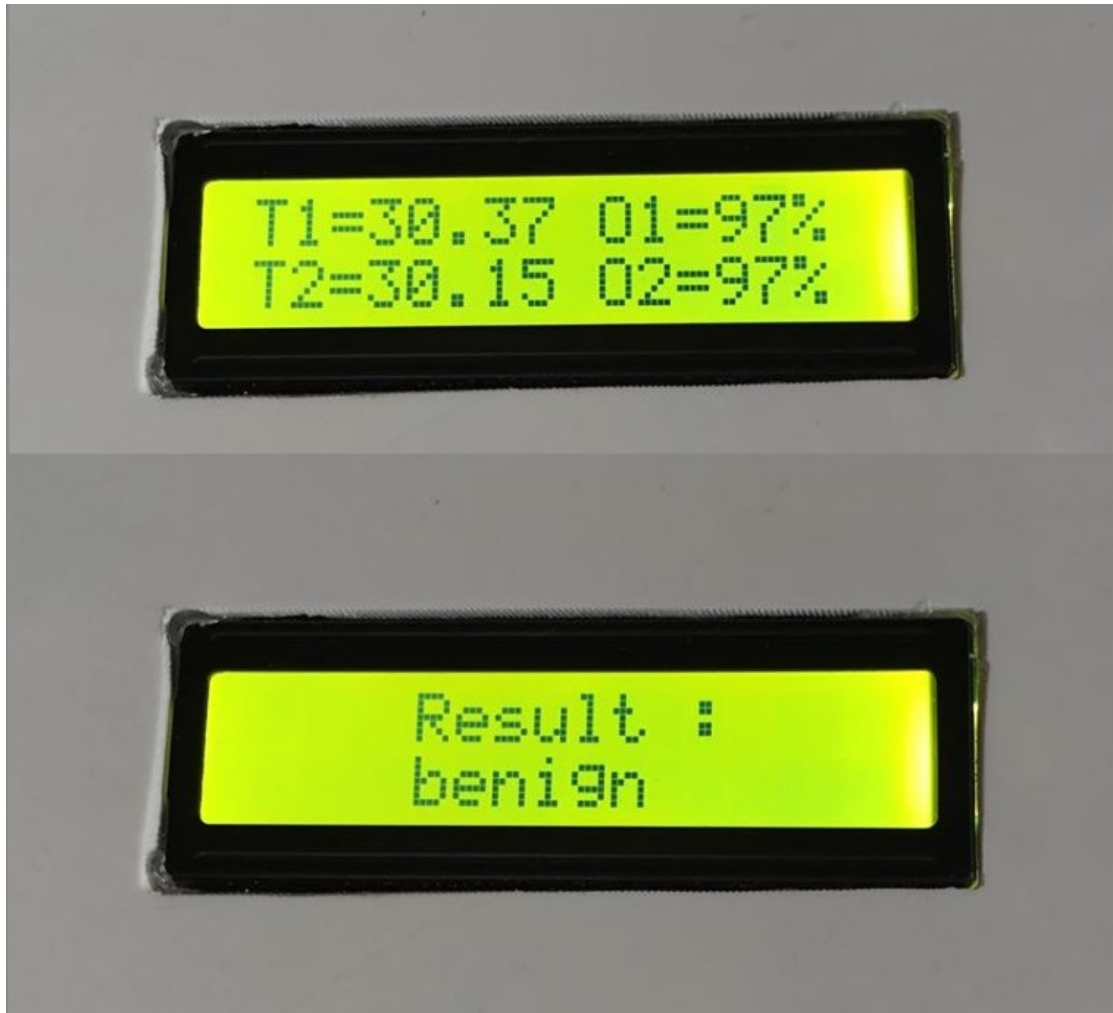

Figure 6.7 Output reading for benign mole

Results and Conclusions

7.1 Results

7.2 Challenges

7.3 Conclusions

7.4 Recommendations

7.1 Results

After the project is installed, the readings are examined on ten persons. The result of all readings is approximately close to the real readings. Table 6.1 shows this readings.

Table 7.1 Table of the results

#	Temperature values °C		Oxygen level values %		Status of the mole
	T1	T2	O1	O2	
1	37.4	37.4	97	97	Benign
2	36.8	36.7	96	96	Benign
3	38.0	38.1	99	99	Benign
4	37.8	37.8	97	97	Benign
5	37.4	37.5	96	96	Benign
6	37.1	37.2	98	98	Benign
7	36.0	35.9	99	99	Benign
8	36.8	36.9	97	97	Benign
9	37.0	37.1	98	98	Benign
10	36.9	36.8	96	96	Benign
11	37.5	37.3	97	97	Benign
12	36.9	37.2	98	98	Benign
13	38.1	37.9	99	99	Benign
14	37.6	38.0	96	96	Benign
15	36.9	37.0	98	98	Benign
16	37.8	38.0	97	97	Benign
17	37.9	37.7	96	96	Benign
18	36.7	37.9	96	96	Benign
19	38.0	37.7	99	99	Benign
20	37.2	37.3	98	98	Benign

7.2 Challenges

While designing the system, there are many challenges have been faced such as:

- High quality sensors are only available for researchable, and they are not allowed commercially.
- Not all required components are available in the Palestinian market.
- Some of the project components are expansive.
- The infrared sensor of the temperate is very sensitive for any motion.
- The arduino Uno couldn't be used for parallel data readings from the sensors.

7.3 Conclusions

The temperature and oxygen level sensor are used to indicate a very important physiological signs that help doctors to detect the skin melanoma early. After designing, processing, implementing and testing these sensors, the overall system can provide the following features:

- This system can detect melanoma using only two sensors.
- This system is portable and small size.
- The process of measuring the two parameter is very simple.
- The patient can use the devise without needing a doctor.
- The device is non-invasive.

7.4 Recommendations

In this project the system was designed to detect melanoma by detecting a various physiological signs such as temperature and oxygen level, but these signs are not sufficient to give the exact total diagnose, so this project needs more research time to improve its efficiency and some features could be added like image processing techniques.

References

[1] Keyvan Nouri, skin cancer. Mcgrawhill, 2008.

[2] Rogers H. W., Weinstock M. A., Harris A. R., Hinckley M. R., Feldman S. R., Fleischer A. B., Coldiron B. M., "Incidence estimate of nonmelanoma skin cancer in the United States, 2006," Arch. Dermatol. 146, 283–287 (2010).10.1001/archdermatol.2010.19

[3] "American Cancer Society Cancer Facts & Figures 2014," http://www.cancer.org/research/cancerfactsstatistics/cancerfactsfigures2014/. Last Accessed: Feb, 2019.

[4] Abbasi N. R., Shaw H. M., Rigel D. S., Friedman R. J., McCarthy W., Osman I., Kopf A. W., Polsky D., "Early diagnosis of cutaneous melanoma: Revisiting the ABCDE criteria," JAMA 292, 2771–2776 (2004).10.1001/jama.292.22.2771

[5] Thomas L., Tranchand P., Berard F., Secchi T., Colin C., Moulin G., "Semiological Value of ABCDE Criteria in the Diagnosis of Cutaneous Pigmented Tumors," Dermatology 197, 11–17 (1998).10.1159/000017969

[6] Benellii C., Roscetti E., Pozzo V. D., "The dermoscopic (7FFM) versus the clinical (ABCDE) diagnosis of small diameter melanoma," Eur. J. Dermatol. 10, 282–287 (2000).

[7] Welch H. G., Woloshin S., Schwartz L. M., "Skin biopsy rates and incidence of melanoma: population based ecological study," BMJ 331, 481 (2005).10.1136/bmj.38516.649537.E0

[8] Mayer J. E., Swetter S. M., Fu T., Geller A. C., "Screening, early detection, education, and trends for melanoma: Current status (2007–2013) andÂfuture directions: Part II. Screening, education, and future directions," Journal of the American Academy of Dermatology 71, 611 (2014).10.1016/j.jaad.2014.05.045

[9] Po-Lin So, Skin cancer, Infobase Publishing, 2008.

[10] Keyvan Nouri, skin cancer. Mcgrawhill, 2008.

[11] Dieter Marmé, Tumor Angiogenesis, 2008.

[12] Raymond W. Ruddon, CANCER BIOLOGY, Oxford University Press, Inc., 2007.

[13] R.F. Schmidt and G. Thews et al.,Human physiology, Springer-Verlag 1989.

[14] Kemal Polat & Gozde Cay, Measuring of Oxygen Saturation Using Pulse Oximeter Based on Fuzzy Logic, Abant İzzet Baysal University, 2012.

[15] Amal Jubran, Pulse oximetry, Loyola University of Chicago,2015.

[16] Debdatta Basu & Rajendra Kulkarni, Overview of blood components and their preparation , journal of anaesthesia, 2014.

[17] Helmut Budzier & Gerald Gerlach, Thermal infrared sensors: theory, optimization, and practice, John Wiley & Sons Ltd, 2011

[18] Michael Vollmer and Klaus-Peter Möllmann, Infrared Thermal Imaging: Fundamentals, Research and Applications, WILEY-VCH Verlag GmbH & Co. KGaA, 2010.

[19] Nicholas A. Diakides & Joseph D. Bronzino (eds), Medical infrared imaging, CRC press, 2008.

[20] R. A. Smith, F. E. Jones, and R. P. Chasmar, The detection and measurement of infra-red radiation, Oxford press, 1968.

[21] Du, H., et al., PhotochemCAD: A Computer-Aided Design and Research Tool in Photochemistry. Photochemistry and Photobiology, 1998.68(2): p. 141-142.

[22] Guowei Di, Xiaoying Tang and Weifeng Liu, "A Reflectance Pulse Oximeter Design Using the MSP430F149," *Complex Medical Engineering, 2007. CME 2007. IEEE/ICME International Conference on,* pp. 1081-1084, 2007.

[23] Oak SS, Aroul P. How to design peripheral oxygen saturation (spo2) and optical heart rate monitoring (ohrm) systems using the afe4403. Texas Instruments. 2015 Mar.

[24] "Adruino UNO for beginners - Progects, Programming and Parts". makerspaces.com

[25] R. C. Gupta, S. S. Ahluwalia and S. S. Randhawa, "Design and development of pulse oximeter," Engineering in Medicine and Biology Society, 1995 and 14th Conference of the Biomedical Engineering Society of India. an International Meeting, Proceedings of the First Regional Conference. , IEEE, pp. 1/13-1/16, 1995.

[26] Chen Y, Jaeger RC, Suhling JC. CMOS sensor arrays for high resolution die stress mapping in packaged integrated circuits. IEEE Sensors Journal. 2013 Jun;13(6):2066-76.

[Appendix-A]

Temperature Sensor (MLX9014)

MLX90614 family
Single and Dual Zone
Infra Red Thermometer in TO-39

Melexis
Microelectronic Integrated Systems

Features and Benefits

- ❑ Small size, low cost
- ❑ Easy to integrate
- ❑ Factory calibrated in wide temperature range:
  -40 to 125 ˚C for sensor temperature and
  -70 to 380 ˚C for object temperature.
- ❑ High accuracy of 0.5°C over wide temperature range (0..+50°C for both Ta and To)
- ❑ High (medical) accuracy calibration
- ❑ Measurement resolution of 0.02°C
- ❑ Single and dual zone versions
- ❑ SMBus compatible digital interface
- ❑ Customizable PWM output for continuous reading
- ❑ Available in 3V and 5V versions
- ❑ Simple adaptation for 8 to 16V applications
- ❑ Power saving mode
- ❑ Different package options for applications and measurements versatility
- ❑ Automotive grade

Applications Examples

- ❑ High precision non-contact temperature measurements;
- ❑ Thermal Comfort sensor for Mobile Air Conditioning control system;
- ❑ Temperature sensing element for residential, commercial and industrial building air conditioning;
- ❑ Windshield defogging;
- ❑ Automotive blind angle detection;
- ❑ Industrial temperature control of moving parts;
- ❑ Temperature control in printers and copiers;
- ❑ Home appliances with temperature control;
- ❑ Healthcare;
- ❑ Livestock monitoring;
- ❑ Movement detection;
- ❑ Multiple zone temperature control – up to 100 sensors can be read via common 2 wires
- ❑ Thermal relay/alert
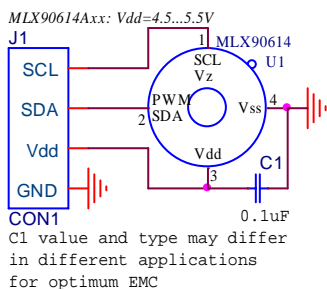- ❑ Body temperature measurement

Ordering Information

| Part No. MLX90614 | Temperature Code E (-40°C to 85°C) K (-40°C to 125°C) | Package Code SF (TO-39) | - Option Code - X X X (1) (2) (3) |

(1) Supply Voltage/ Acccuracy
 A - 5V
 B - 3V
 C - Reserved
 D - 3V medical accuracy

(2) Number of thermopiles:
 A – single zone
 B – dual zone

(3) Package options:
 A – Standard package
 B – Reserved
 C – 35° FOV

Example:
MLX90614ESF-BAA

1 Functional diagram

MLX90614Axx: Vdd=4.5...5.5V

C1 value and type may differ
in different applications
for optimum EMC

MLX90614 connection to SMBus

Figure 1 Typical application schematics

2 General Description

The MLX90614 is an Infra Red thermometer for non contact temperature measurements. Both the IR sensitive thermopile detector chip and the signal conditioning ASSP are integrated in the same TO-39 can.

Thanks to its low noise amplifier, 17-bit ADC and powerful DSP unit, a high accuracy and resolution of the thermometer is achieved.

The thermometer comes factory calibrated with a digital PWM and SMBus (System Management Bus) output.

As a standard, the 10-bit PWM is configured to continuously transmit the measured temperature in range of -20 to 120 ˚C, with an output resolution of 0.14 ˚C and the POR default is SMBus.

General description (continued)

The MLX90614 is built from 2 chips developed and manufactured by Melexis:
- The Infra Red thermopile detector MLX81101
- The signal conditioning ASSP MLX90302, specially designed to process the output of IR sensor.

The device is available in an industry standard TO-39 package.

Thanks to the low noise amplifier, high resolution 17-bit ADC and powerful DSP unit of MLX90302 high accuracy and resolution of the thermometer is achieved. The calculated object and ambient temperatures are available in RAM of MLX90302 with resolution of 0.01 ˚C. They are accessible by 2 wire serial SMBus compatible protocol (0.02°C resolution) or via 10-bit PWM (Pulse Width Modulated) output of the device.

The MLX90614 is factory calibrated in wide temperature ranges: -40 to 125 ˚C for the ambient temperature and -70 to 382.2 ˚C for the object temperature. The 10-bit PWM is as a standard configured to transmit continuously the measured object temperature for an object temperature range of -20 to 120 ˚C with an output resolution of 0.14 ˚C. The PWM can be easily customized for virtually any range desired by the customer by changing the content of 2 EEPROM cells. This has no effect on the factory calibration of the device.

The PWM pin can also be configured to act as a thermal relay (input is To), thus allowing for an easy and cost effective implementation in thermostats or temperature (freezing/boiling) alert applications. The temperature threshold is user programmable. In an SMBus system this feature can act as a processor interrupt that can trigger reading all slaves on the bus and to determine the precise condition.

As a standard, the MLX90614 is calibrated for an object emissivity of 1. It can be easily customized by the customer for any other emissivity in the range 0.1-1.0 without the need of recalibration with a black body.

The thermometer is available in 2 supply voltage options: 5V compatible or 3V (battery) compatible. The 5V can be easily adopted to operate from a higher supply voltage (8-16V, for example) by use of few external components (refer to "Applications information" section for details).

An optical filter (long-wave pass) that cuts off the visible and near infra-red radiant flux is integrated in the package to provide sunlight immunity.

3 Table of Contents

4 Glossary of Terms

PTAT	Proportional To Absolute Temperature sensor (package temperature)
PTC	Positive Temperature Coefficient sensor (package temperature)
POR	Power On Reset
HFO	High Frequency Oscillator (RC)
DSP	Digital Signal Processing
FIR	Finite Impulse Response. Digital filter
IIR	Infinite Impulse Response. Digital filter
IR	Infra-Red
PWM	Pulse With Modulation
DC	Duty Cycle (of the PWM) ; Direct Current (for settled conditions specifications)
FOV	Field Of View
SDA,SCL	Serial DAta, Serial CLock – SMBus compatible communication pins
Ta	Ambient Temperature measured from the chip – (the package temperature)
To	Object Temperature, 'seen' from IR sensor
ESD	Electro-Static Discharge
EMC	Electro-Magnetic Compatibility
TBD	To Be Defined

Note: sometimes the MLX90614xxx is referred to as "the module".

5 Maximum ratings

Parameter	MLX90614ESF-Axx	MLX90614ESF-Bxx MLX90614ESF-Dxx	MLX90614KSF-Axx
Supply Voltage, V_{DD} (over voltage)	7V	5V	7V
Supply Voltage, V_{DD} (operating)	5.5 V	3.6V	5.5V
Reverse Voltage	0.4 V		
Operating Temperature Range, T_A	-40…+85°C		-40…+125°C
Storage Temperature Range, T_S	-40…+125°C		-40…+125°C
ESD Sensitivity (AEC Q100 002)	2kV		
DC current into SCL/Vz (Vz mode)	2 mA		
DC sink current, SDA /PWM pin	25 mA		
DC source current, SDA/PWM pin	25 mA		
DC clamp current, SDA/PWM pin	25 mA		
DC clamp current, SCL pin	25 mA		

Table 1: Absolute maximum ratings for MLX90614

Exceeding the absolute maximum ratings may cause permanent damage. Exposure to absolute-maximum-rated conditions for extended periods may affect device reliability.
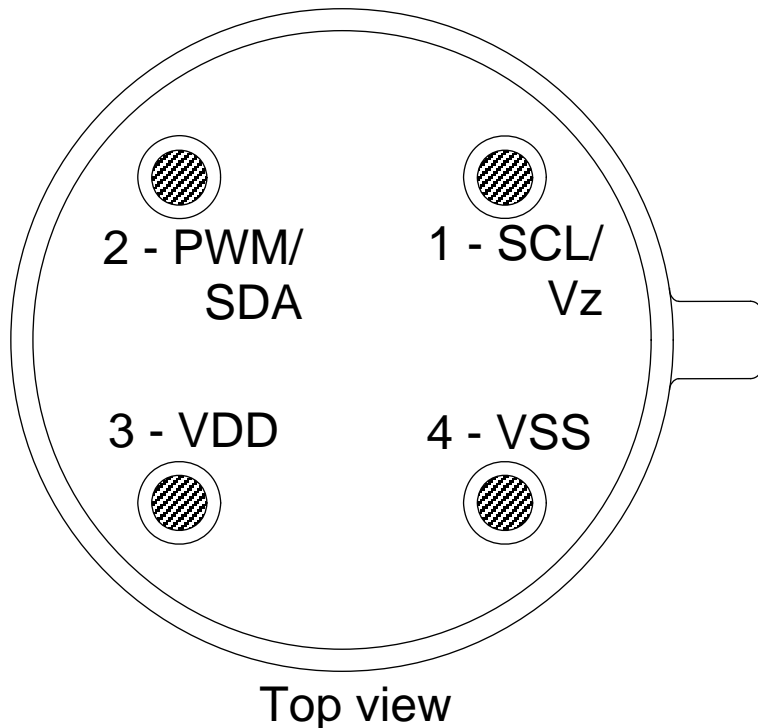
6 Pin definitions and descriptions

Figure 2: Pin description

Pin Name	Function
VSS	Ground. The metal can is also connected to this pin.
SCL / Vz	Serial clock input for 2 wire communications protocol. 5.7V zener is available at this pin for connection of external bipolar transistor to MLX90614A to supply the device from external 8 -16V source.
PWM / SDA	Digital input / output. In normal mode the measured object temperature is available at this pin Pulse Width Modulated. In SMBus compatible mode automatically configured as open drain NMOS.
VDD	External supply voltage.

Table 2: Pin description MLX90614

Note: for +12V (+8…+16V) powered operation refer to the Application information section. For EMC and isothermal conditions reasons it is highly recommended not to use any electrical connection to the metal can except by the Vss pin.
With the SCL/Vz and PWM/SDA pins operated in 2-wire interface mode, the input Schmidt trigger function is automatically enabled.

7 Electrical Specifications

7.1 MLX90614Axx

All parameters are preliminary for T_A = 25 ˚C, **V_{DD} =5V** (unless otherwise specified)

Parameter	Symbol	Test Conditions	Min	Typ	Max	Units
Supplies						
External supply	V_{DD}		4.5	5	5.5	V
Supply current	I_{DD}	No load		1	2	mA
Supply current (programming)	I_{DDpr}	No load, erase/write EEPROM operations		1.5	2.5	mA
Zener voltage	Vz	Iz = 75…400 uA	5.6	5.75	5.8	V
Zener voltage	Vz(Ta)	Iz=70…400uA, full temperature range	5.15	5.75	6.24	V
Power On Reset						
POR level	V_{POR}	Power-up, power-down and brown-out	2.7	3.0	3.3	V
V_{DD} rise time	T_{POR}	Ensure POR signal			3	ms
Output valid (result in RAM)	Tvalid	After POR		0.15		s
Pulse width modulation[1]						
PWM resolution	PWMres	Data band		10		bit
PWM output period	$PWM_{T,def}$	Factory default, internal oscillator factory calibrated		1.024		ms
PWM period stability	$dPWM_T$	Internal oscillator factory calibrated, over the entire operation range and supply voltage	-4		+4	%
Output high Level	PWM_{HI}	I_{source} = 2 mA	V_{DD}-0.2			V
Output low Level	PWM_{LO}	I_{sink} = 2 mA			V_{SS}+0.2	V
Output drive current	$Idrive_{PWM}$	Vout,H = V_{DD} - 0.8V		7		mA
Output sink current	$Isink_{PWM}$	Vout,L = 0.8V		13.5		mA
Output settling time	Tset	100 pF capacitive load, full operating Ta range		500		ns
Output settling time	$Tset_{RC}$	220 Ohm in series with 47nF load on the wire, full Ta operating range	20		50	us

Parameter	Symbol	Test Conditions	Min	Typ	Max	Units
SMBus compatible 2-wire interface[2]						
Input high voltage	V_{IH}		1.8	2	2.2	V
Input high voltage	$V_{IH}(Ta,V)$	Over temperature and supply	1.6		2.4	V
Input low voltage	V_{IL}		0.7	1.0	1.3	V
Input low voltage	$V_{IL}(Ta,V)$	Over temperature and supply	0.5		1.5	V
Output low voltage	V_{OL}	SDA pin in open drain mode, over temperature and supply, Isink = 2mA			0.2	V
SCL leakage	$I_{SCL},leak$	V_{SCL}=4V, Ta=+85°C			30	uA
SDA leakage	$I_{SDA},leak$	V_{SDA}=4V, Ta=+85°C			0.3	uA
SCL capacitance	C_{SCL}				10	pF
SDA capacitance	C_{SDA}				10	pF
Slave address	SA	Factory default		5Ah		hex
SMBus Request	t_{REQ}	SCL low	1.024			ms
Timeout, low	$T_{imeout,L}$	SCL low			30	ms
Timeout, high	$T_{imeout,H}$	SCL high			50	us
Acknowledge setup time	Tsuac(MD)	8-th SCL falling edge, Master	0.5		1.5	us
Acknowledge hold time	Thdac(MD)	9-th SCL falling edge, Master	1.5		2.5	us
Acknowledge setup time	Tsuac(SD)	8-th SCL falling edge, Slave	2.5			us
Acknowledge hold time	Thdac(SD)	9-th SCL falling edge, Slave	1.5			us
EEPROM						
Data retention		Ta = +85°C	10			years
Erase/write cycles		Ta = +25°C	100,000			Times
Erase/write cycles		Ta = +125°C	10,000			Times
Erase cell time	Terase			5		ms
Write cell time	Twrite			5		ms

Notes: All the communication and refresh rate timings are given for the nominal calibrated HFO frequency and will vary with this frequency's variations.

1. All PWM timing specifications are given for single PWM output (factory default for MLX90614xAx). For the extended PWM output (factory default for the MLX90614xBx) each period has twice the timing specifications (refer to the PWM detailed description section). With large capacitive load lower PWM frequency is recommended. Thermal relay output (when configured) has the PWM DC specification and can be programmed as push-pull, or NMOS open drain. PWM is free-running, power-up factory default is SMBus, refer to 7.6, "Switching between PWM and SMBus communication" for details..

2. For SMBus compatible interface on 12V application refer to Application information section. SMBus compatible interface is described in details in the SMBus detailed description section. Maximum number of MLX90614xxx devices on one bus is 127, higher pullup currents are recommended for higher number of devices, faster bus data transfer rates, and increased reactive loading of the bus.

MLX90614xxx is always a slave device on the bus. MLX90614xxx can work in both low-power and high-power SMBus communication.

All voltages are referred to the Vss (ground) unless otherwise noted.

Power saving mode is not available on the 5V version (MLX90614Axx).

7.2 MLX90614Bxx , MLX90614Dxx

All parameters are preliminary for T_A = 25 ˚C, **V_{DD} =3V** (unless otherwise specified)

Parameter	Symbol	Test Conditions	Min	Typ	Max	Units
Supplies						
External supply	V_{DD}		2.4	3	3.6	V
Supply current	I_{DD}	No load		1	2	mA
Supply current (programming)	I_{DDpr}	No load, erase/write EEPROM operations		1.5	2.5	mA
Power-down supply current	Isleep	no load	1	2.5	5	uA
Power-down supply current	Isleep	Full temperature range	1	2.5	6	uA
Power On Reset						
POR level	V_{POR}	Power-up, power-down and brown-out	1.6	1.85	2.1	V
V_{DD} rise time	T_{POR}	Ensure POR signal			1	ms
Output valid	Tvalid	After POR		0.15		s
Pulse width modulation[1]						
PWM resolution	PWMres	Data band		10		bit
PWM output period	$PWM_{T,def}$	Factory default, internal oscillator factory calibrated		1.024		ms
PWM period stability	$dPWM_T$	Internal oscillator factory calibrated, over the entire operation range and supply voltage	-4		+4	%
Output high Level	PWM_{HI}	I_{source} = 2 mA	V_{DD}-0.25			V
Output low Level	PWM_{LO}	I_{sink} = 2 mA			V_{SS}+0.25	V
Output drive current	$Idrive_{PWM}$	Vout,H = V_{DD} - 0.8V		4.5		mA
Output sink current	$Isink_{PWM}$	Vout,L = 0.8V		11		mA
Output settling time	Tset	100 pF capacitive load, full operating Ta range			150	ns
Output settling time	$Tset_{RC}$	220 Ohm in series with 47nF load on the wire, full Ta operating range		500		ns

Parameter	Symbol	Test Conditions	Min	Typ	Max	Units
SMBus compatible 2-wire interface[2]						
Input high voltage	V_{IH}		1.6	2	2.4	V
Input high voltage	$V_{IH}(Ta,V)$	Over temperature and supply	1.2	2	2.8	V
Input low voltage	V_{IL}		0.7	1.0	1.3	V
Input low voltage	$V_{IL}(Ta,V)$	Over temperature and supply	0.5	1.0	1.5	V
Output low voltage	V_{OL}	SDA pin in open drain mode, over temperature and supply, Isink = 2mA			0.25	V
SCL leakage	$I_{SCL},leak$	V_{SCL}=3V, Ta=+85°C			20	uA
SDA leakage	$I_{SDA},leak$	V_{SDA}=3V, Ta=+85°C			0.25	uA
SCL capacitance	C_{SCL}				10	pF
SDA capacitance	C_{SDA}				10	pF
Slave address	SA	Factory default		5Ah		hex
SMBus Request	t_{REQ}	SCL low	1.024			ms
Timeout,low	$T_{imeout,L}$	SCL low			30	ms
Timeout, high	$T_{imeout,H}$	SCL high			50	us
Acknowledge setup	Tsuac(MD)	8-th SCL falling edge, Master	0.5		1.5	us
Acknowledge hold	Thdac(MD)	9-th SCL falling edge, Master	1.5		2.5	us
Acknowledge setup	Tsuac(SD)	8-th SCL falling edge, Slave	2.5			us
Acknowledge hold	Thdac(SD)	9-th SCL falling edge, Slave	1.5			us
EEPROM						
Data retention		Ta = +85°C	10			years
Erase/write cycles		Ta = +25°C	100,000			Times
Erase/write cycles		Ta = +125°C	10,000			Times
Erase cell time	Terase			5		ms
Write cell time	Twrite			5		ms

Note: refer to MLX90614Axx notes.

8 Detailed description

8.1 Block diagram
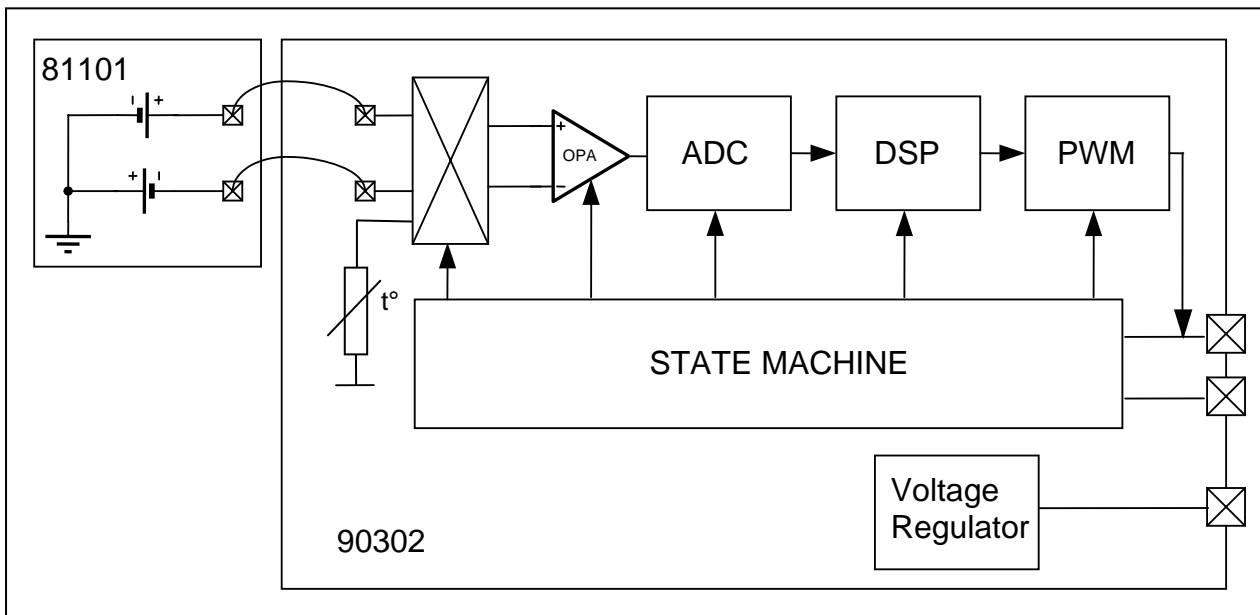
Figure 3: block diagram

8.2 Signal processing principle

The operation of the MLX90614 is controlled by an internal state machine, which controls the measurements and calculations of the object and ambient temperatures and does the post-processing of the temperatures to output them through the PWM output or the SMBus compatible interface.

The ASSP supports 2 IR sensors (second one not implemented in the MLX90614xAx).The output of the IR sensors is amplified by a low noise low offset chopper amplifier with programmable gain, converted by a Sigma Delta modulator to a single bit stream and fed to a powerful DSP for further processing. The signal is treated by programmable (by means of EEPROM contend) FIR and IIR low pass filters for further reduction of the band width of the input signal to achieve the desired noise performance and refresh rate. The output of the IIR filter is the measurement result and is available in the internal RAM. 3 different cells are available: One for the on-board temperature sensor (on chip PTAT or PTC) and 2 for the IR sensors.

Based on results of the above measurements, the corresponding ambient temperature Ta and object temperatures To are calculated. Both calculated temperatures have a resolution of 0.01 ˚C. The data for Ta and To can be read in two ways: Reading RAM cells dedicated for this purpose via the 2-wire interface (0.02°C resolution, fixed ranges), or through the PWM digital output (10 bit resolution, configurable range).

In the last step of the measurement cycle, the measured Ta and To are rescaled to the desired output resolution of the PWM) and the recalculated data is loaded in the registers of the PWM state machine, which creates a constant frequency with a duty cycle representing the measured data.

8.3 Block description

8.3.1 Amplifier

A low noise low offset amplifier with programmable gain is implemented for amplification of the IR sensor voltage. With a carefully designed input modulator and balanced input impedance, an offset as low as 0.5μV is achieved.

8.3.2 Supply regulator and POR

The module can operate from 2 different supplies:
VDD= 5V => MLX90614Axx
VDD=3.3V => MLX90614Bxx (battery or regulated supply)
Refer to "Applications information" section for information about adopting higher voltage supplies.

The Power On Reset (POR) is connected to Vdd supply. The on-chip POR circuit provides an active (high) level of the POR signal when the Vdd voltage rises above approximately 0.5V and holds the entire MLX90614xxx in reset until the Vdd is higher than the specified POR threshold V_{POR} (note that this level is different for MLX90614Axx and MLX90614Bxx). During the time POR is active, the POR signal is available as an open drain (active high) at the PWM/SDA pin. After the MLX90614xxx exits the POR condition, the function programmed in EEPROM takes precedence for that pin.

8.3.3 EEPROM

A limited number of addresses in the EEPROM memory can be changed by the customer. The whole EEPROM can be read via SMBus interface.

EEPROM (32X16)		
Name	Address	Write acces
To$_{max}$	000h	Yes
To$_{min}$	001h	Yes
PWMCTRL	002h	Yes
Ta range	003h	Yes
Emissivity correction coefficient	004h	Yes
Config Register1	005h	Yes
Melexis reserved	006h	No
…	…	…
Melexis reserved	00Dh	No
SMBus address	00Eh	Yes
Melexis reserved	00Fh	Yes
Melexis reserved	010h	No
…	…	…
Melexis reserved	018	No
Melexis reserved	019h	Yes
Melexis reserved	01Ah	No
Melexis reserved	01Bh	No
ID number	01Ch	No
ID number	01Dh	No
ID number	01Eh	No
ID number	01Fh	No

The addresses To$_{max}$, To$_{min}$ and Ta range are for customer dependent object and ambient temperature ranges. For details see point 8.5.3 below in this document
The address **Emissivity** contains the object emissivity (factory default 1.0 = 0xFFFF), 16 bit.

$$Emissivity = dec2hex[\ round(\ 65535 \times \varepsilon)\ ]$$

where dec2hex[round(X)] represents decimal to hexadecimal conversion with round-off to nearest value (not truncation). In this case the physical emissivity values are ε = 0.1…1.0.

The address **PWMCTRL** consists of control bits for configuring the PWM/SDA pin:

Bit 0	Select the type of PWM mode:	1 - Single PWM, factory default for MLX90614xAx	0 – Extended PWM, factory default for MLX90614xBx
Bit 1	Enable/disable the PWM:	1 - Enable PWM, disable SMBus	0 - Disable PWM (Enable SMBus), Factory default
Bit 2	Configuration of the pin PWM:	1 - Push-Pull,	0 – OpenDrain NMOS, factory default
Bit 3	Mode selection	1 - ThermoRelay,	0 - PWM, Factory default
Bits[8:4]	Extemded PWM definition	Number of repetitions divided by 2 of sensor 1 and 2 in Extended PWM mode. The number of repetitions can vary from 0 to 64 times.	
Bits[15:9]	PWM clock configuration	2MHz divided by the number written in this place. (128 in case the number is 0.) A single PWM period consists of 2048 clocks and extended PWM of 4096 clocks for each period (2T in figure 6). The 2 MHz clock is valid for the nominal HFO frequency.	

The address **ConfigRegister1** consists of control bits for configuring the analog and digital parts:

Bits[2:0]	– Configure coefficients of IIR digital filter:	Bit 2	Bit 1	Bit 0	a_1	b_1
		0	x	x	0.5	0.5
		1	1	1	0.571428571	0.428571428
		1	1	0	0.666(6)	0.333(3)
		1	0	1	0.8	0.2
		1	0	0	1	0 (IIR bypassed)

Bit 3	– Configure the type of ambient temperature sensor:	1 - PTC,	0 – PTAT.

Bits[5:4]	– Configure the type of data transmitted through PWM:	Bit 5	Bit 4	Data 1	Data 2
		0	0	Ta	IR 1
		0	1	Ta	IR 2
		1	1	IR 1	IR 2
		1	0	IR 2	Undefined*

Bit 6	– Define the number of IR sensors:	1 – 2 sensors,	0 -1 sensor.

Bit 7	– Define the sign Ks (Ks=dAlpha/dTobj) :	Factory calibration, do not alter	

Bits[10:8]	– Configure coefficient N of FIR digital filter:	Bit 10	Bit 9	Bit 8	N
		0	0	0	8**
		0	0	1	16**
		0	1	0	32**
		0	1	1	64**
		1	0	0	128
		1	0	1	256
		1	1	0	512
		1	1	1	1024

Bits[13:11]	– Configure the gain of amplifier:	Bit 13	Bit 12	Bit 11	Gain
		0	0	0	1 (preamplifier bypassed)
		0	0	1	3
		0	1	0	6
		0	1	1	12.5
		1	0	0	25
		1	0	1	50
		1	1	0	100
		1	1	1	100

Bit 14	Unused		
Bit 15	– Define the sign of thermo-shock compensation:	1 - negative,	0 – positive.

Note: The following bits/registers should not be altered (except with special tools – contact Melexis for such tools availability) in order to keep the factory calibration relevant:
Ke [15..0] ; Config Register1 [13..11;7;3] ; addresses 00Fh and 019h.
* not recommended for extended PWM mode
** note recommended values

8.3.4 RAM

It is not possible to write into the RAM memory. It can only be read and only a limited number of RAM registers are of interest to the customer.

RAM (32x17)		
Name	Address	Read access
Melexis reserved	000h	Yes
…	…	…
Melexis reserved	005h	Yes
T_A	006h	Yes
T_{OBJ1}	007h	Yes
T_{OBJ2}	008h	Yes
Melexis reserved	009h	Yes
…	…	…
Melexis reserved	01Fh	Yes

8.4 SMBus compatible 2-wire protocol

The chip supports a 2 wires serial protocol, build with pins PWM/SDA and SCL.

- SCL – digital input, used as the clock for SMBus compatible communication. This pin has the auxiliary function for building an external voltage regulator. When the external voltage regulator is used, the 2-wire protocol is available only if the power supply regulator is overdriven.
- PWM/SDA – Digital input/output, used for both the PWM output of the measured object temperature(s) or the digital input/output for the SMBus. The pin can be programmed in EEPROM to operate as Push/Pull or open drain NMOS (open drain NMOS is factory default). In SMBus mode SDA is forced to open drain NMOS I/O, push-pull selection bit defines PWM/Thermal relay operation.

8.4.1 Functional description

The SMBus interface is a 2-wire protocol, allowing communication between the Master Device (MD) and one or more Slave Devices (SD). In the system only one master can be presented at any given time [1]. The MLX90614 can only be used as a slave device.

Generally, the MD initiates the start of data transfer by selecting a SD through the Slave Address (SA).

The MD has read access to the RAM and EEPROM and write access to 9 EEPROM cells (at addresses 0x20h, 0x21h, 0x22h, 0x23h, 0x24h, 0x25h*, 0x2Eh, 0x2Fh, 0x39h). If the access to the MLX90614 is a read operation it will respond with 16 data bits and 8 bit PEC only if its own slave address, programmed in internal EEPROM, is equal to the SA, sent by the master. The SA feature allows connecting up to 127 devices with only 2 wires, unless the system has some of the specific features described in paragraph 5.2 of reference [1]. In order to provide access to any device or to assign an address to a SD before it is connected to the bus system, the communication must start with zero SA followed by low RWB bit. When this command is sent from the MD, the MLX90614 will always respond and will ignore the internal chip code information.
Special care must be taken not to put two MLX90614 devices with the same SD addresses on the same bus as MLX90614 does not support ARP[1].
The MD can force the MLX90614 into low consumption mode "sleep mode" (3V version only).
Read flags like "EEBUSY" (1 – EEPROM is busy with executing the previous write/erase), "EE_DEAD" (1 – there is fatal EEPROM error and this chip is not functional**).
Note*: This address is readable and writable. Bit 3 should not be altered as this will cancel the factory calibration.
Note**: EEPROM error signaling is implemented in automotive grade parts only.

8.4.2 Differences with the standard SMBus specification (reference [1])

There are eleven command protocols for standard SMBus interface. The MLX90614 supports only two of them. Not supported commands are:
- Quick Command
- Byte commands - Sent Byte, Receive Byte, Write Byte and Read Byte
- Process Call
- Block commands – Block Write and Write-Block Read Process Call

Supported commands are:
- Read Word
- Write Word

8.4.3 Detailed description

The PWM/SDA pin of MLX90614 can operate also as PWM output, depending on the EEPROM settings. If PWM is enabled, after POR the PWM/SDA pin is directly configured as PWM output. The PWM mode can be avoided and the pin can be restored to its Data function by a special command. That is why hereafter both modes are treated separately.

8.4.3.1 Bus Protocol

1	7	1	1	8	1	1
S	Slave Address	Wr	A	Data Byte	A	P

S   Start Condition

Sr   Repeated Start Condition

Rd   Read (bit value of 1)

Wr   Write (bit value of 0)

A   Acknowledge (this bit can be 0 for ACK and 1 for NACK)

S   Stop Condition

PEC   Packet Error Code

        Master-to-Slave

        Slave-to-Master
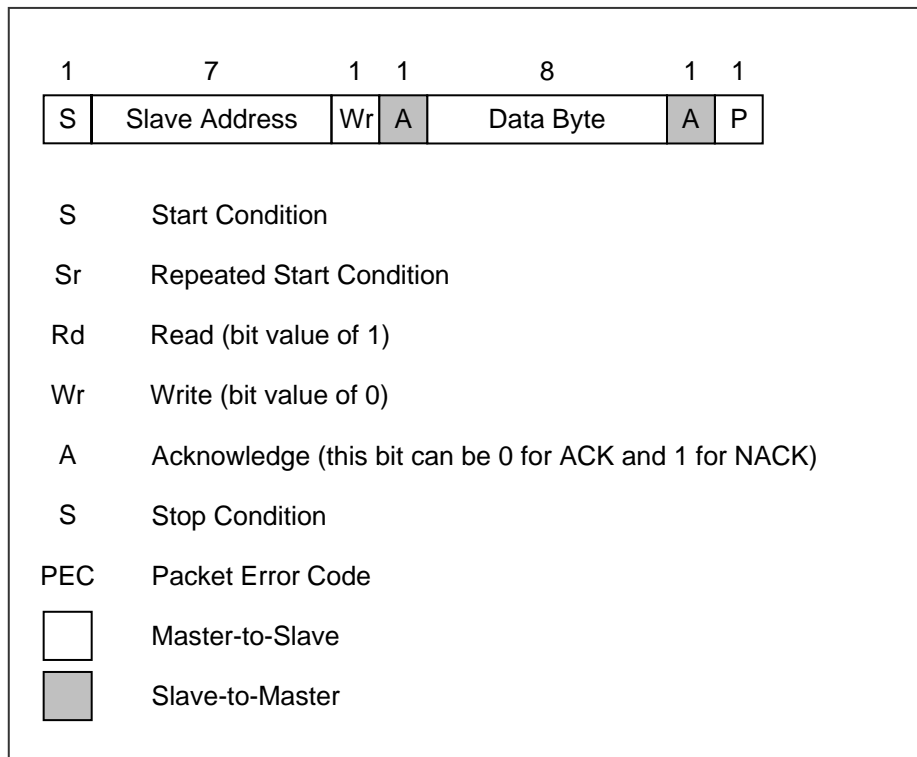
Figure 4: SMBus packet element key

After every 8 bits received by the SD an ACK/NACK takes place. When a MD initiates communication, it first sends the address of the slave and only the SD which recognizes the address will ACK, the rest will remain silent. In case the SD NACKs one of the bytes, the MD should stop the communication and repeat the message. A NACK could be received after the PEC. This means that there is an error in the received message and the MD should try sending the message again. The PEC calculation includes all bits except the START, REPEATED START, STOP, ACK, and NACK bits. The PEC is a CRC-8 with polynomial X8+X2+X1+1. The Most Significant Bit of every byte is transferred first.

8.4.3.1.1 Read Word (depending on the command – RAM or EEPROM)

1	7	1	1	8	1	1	7	1	1	
S	Slave Address	Wr	A	Command	A	Sr	Slave Address	Rd	A	………..

	8	1	8	1	8	1	1
………..	Data Byte Low	A	Data Byte High	A	PEC	A	P
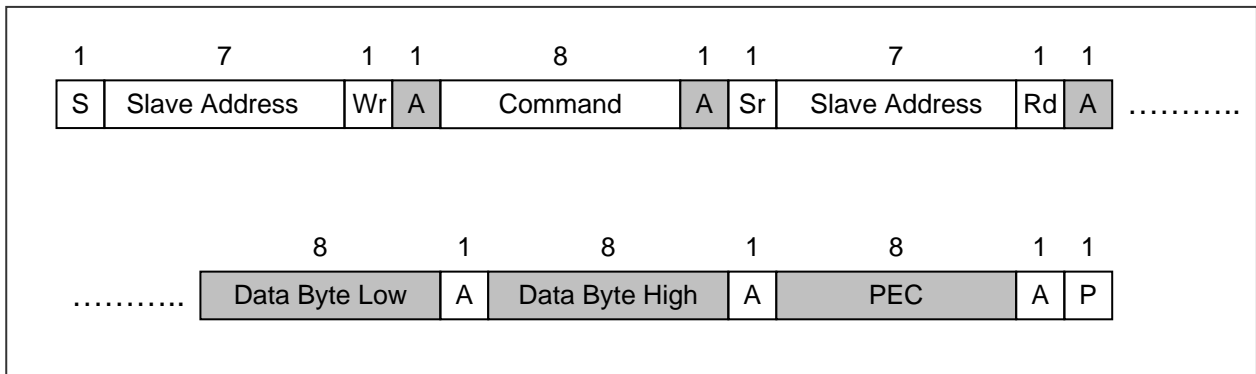
Figure 5: SMBus read word format

8.4.3.1.2 Write Word (depending on the command – RAM or EEPROM)

1	7	1	1	8	1	
S	Slave Address	Wr	A	Command	A	………..

	8	1	8	1	8	1	1
………..	Data Byte Low	A	Data Byte High	A	PEC	A	P
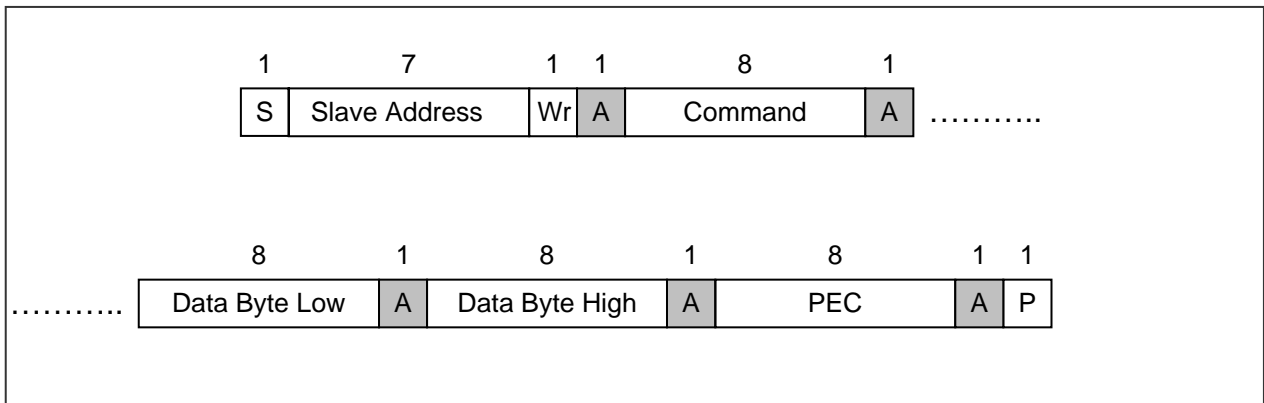
Figure 6: SMBus write word format

8.4.4 AC specification for SMBus

8.4.4.1 Timing

The MLX90614 meets all the timing specifications of the SMBus [1]. The maximum frequency of the MLX90614 SMBus is 100 KHz and the minimum is 10 KHz.
The specific timings in MLX90614's SMBus are:
<u>SMBus Request</u> (t_{REQ}) is the time that the SCL should be forced low in order to switch MLX90614 from PWM mode to SMBus mode;
<u>Timeout L</u> is the maximum allowed time for SCL to be low. After this time the MLX90614 will reset its communication block and will be ready for new communication;
<u>Timeout H</u> is the maximum time for which it is allowed for SCL to be high during communication. After this time MLX90614 will reset its communication block assuming that the bus is idle (according to the SMBus specification).
<u>Tsuac(SD)</u> is the time after the eighth falling edge of SCL that MLX90614 will force PWM/SDA low to acknowledge the last received byte.
<u>Thdac(SD)</u> is the time after the ninth falling edge of SCL that MLX90614 will release the PWM/SDA (so the MD can continue with the communication).
<u>Tsuac(MD)</u> is the time after the eighth falling edge of SCL that MLX90614 will release PWM/SDA (so that the MD can acknowledge the last received byte).
<u>Thdac(MD)</u> is the time after the ninth falling edge of SCL that MLX90614 will take control of the PWM/SDA (so it can continue with the next byte to transmit).

The indexes MD and SD for the latest timings are used – MD when the master device is making acknowledge; SD when the slave device is making acknowledge-. For other timings see [1].
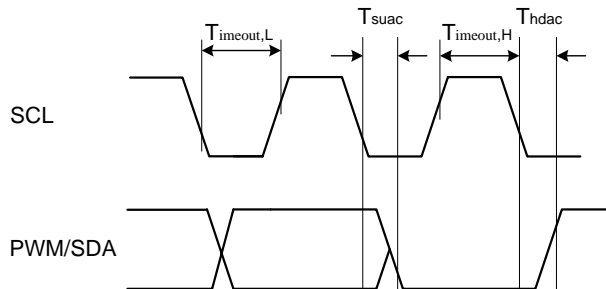
Figure 7: SMBus timing

8.4.5 Bit transfer
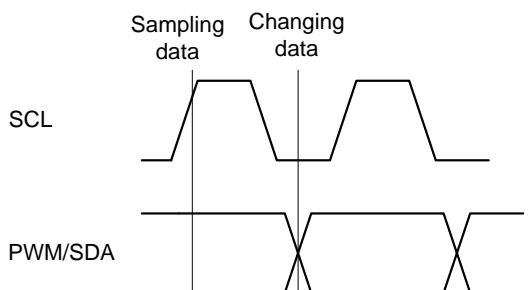
Figure 8: Bit transfer on SMBus

The data on PWM/SDA must be changed when SCL is low (min 300ns after the falling edge of SCL). The data is fetched by both MD and SDs on the rising edge of the SCL.

8.4.6 Commands

RAM and EEPROM can be read both with 32x16 sizes. If the RAM is read, the data are divided by two, due to a sign bit in RAM (for example, T_{OBJ1} - RAM address 0x07h will sweep between 0x27ADh to 0x7FFF as the object temperature rises from -70.01°C to +382.19°C). The MSB read from RAM is an error flag (active high) for the linearized temperatures (T_{OBJ1}, T_{OBJ2} and T_a). The MSB for the raw data (e.g. IR sensor1 data) is a sign bit (sign and magnitude format). A write of 0x0000 must be done prior to writing in EEPROM in order to erase the EEPROM cell content. Refer to EEPROM detailed description for factory calibration EEPROM locations that need to be kept unaltered.

Opcode	Command
000x xxxx*	RAM Access
001x xxxx*	EEPROM Access
1111_0000**	Read Flags
1111_1111	Enter SLEEP mode

Note*: The xxxxx represent the 5 LSBits of the memory map address to be read/written.
Note**: Behaves like read command. The MLX90614 returns PEC after 16 bits data of which only 4 are meaningful and if the MD wants it, it can stop the communication after the first byte. The difference between read and read flags is that the latter does not have a repeated start bit.
Flags read are:
Data[15] – EEBUSY – the previous write/erase EEPROM access is still in progress. High active.
Data[14] – Unused
Data[13] - EE_DEAD – EEPROM double error has occurred. High active.
Data[12] – INIT – POR initialization routine is still ongoing. Low active.
Data[11] – not implemented.
Data[10..0] – all zeros.
Flags read is a diagnostic feature. The MLX90614 can be used regardless of these flags.

8.4.7 Sleep Mode

The MLX90614 can enter in Sleep Mode via the command "Enter SLEEP mode" sent via the SMBus interface. This mode is not available for the 5V supply version. To limit the current consumption to 2.5uA (typical), the SCL pin should be kept low during sleep. MLX90614 goes back into power-up default mode (via POR reset) by setting SCL pin high and then PWM/SDA pin low for at least t_{DDq}=80ms. **If EEPROM is configured for PWM (EN_PWM is high), the PWM interface will be selected after awakening and if PWM control [2], PPODB is 1 the MLX90614 will output a PWM pulse train with push-pull output.**

8.4.7.1 Enter Sleep Mode
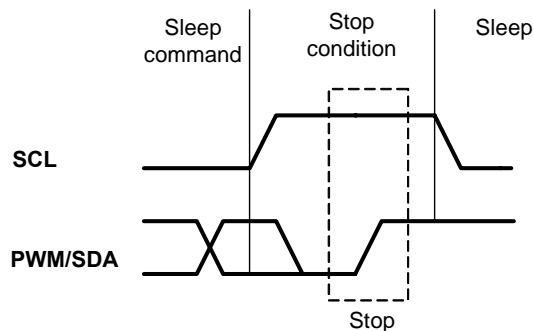
Figure 9: Enter sleep

8.4.7.2 Exit from Sleep Mode
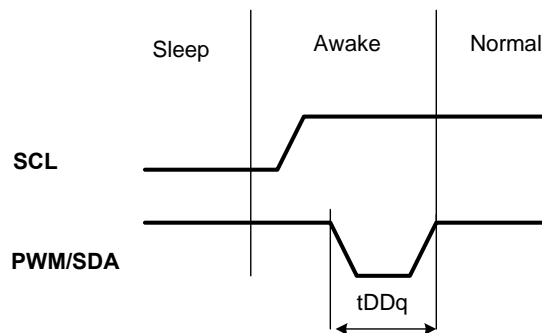
Figure 10: Exit Sleep Mode

8.5 PWM

The MLX90614 can be read via PWM or SMBus compatible interface. Selection of PWM output is done in EEPROM configuration (factory default is SMBus). PWM output has two programmable formats, single and dual data transmission, providing single wire reading of two temperatures (dual zone object or object and ambient). The PWM period is derived from the on-chip oscillator and is programmable.

Config Register[5:4]	PWM1 data	PWM2 data	$Tmin,1$	$Tmax,1$	$Tmin,2$	$Tmax,2$
00	Ta	T_{obj1}	Ta_{range},L	Ta_{range},H	To_{min}	To_{max}
01	Ta	T_{obj2}	Ta_{range},L	Ta_{range},H	To_{min}	To_{max}
11	T_{obj1}	T_{obj2}	To_{min}	To_{max}	To_{min}	To_{max}
10*	T_{obj2}	Undefined	To_{min}	To_{max}	N.A.	N.A.

Note: Serial data functions (2-wire / PWM) are multiplexed with a thermal relay function (described in the "Thermal relay" section).
* not recommended for extended PWM format operation
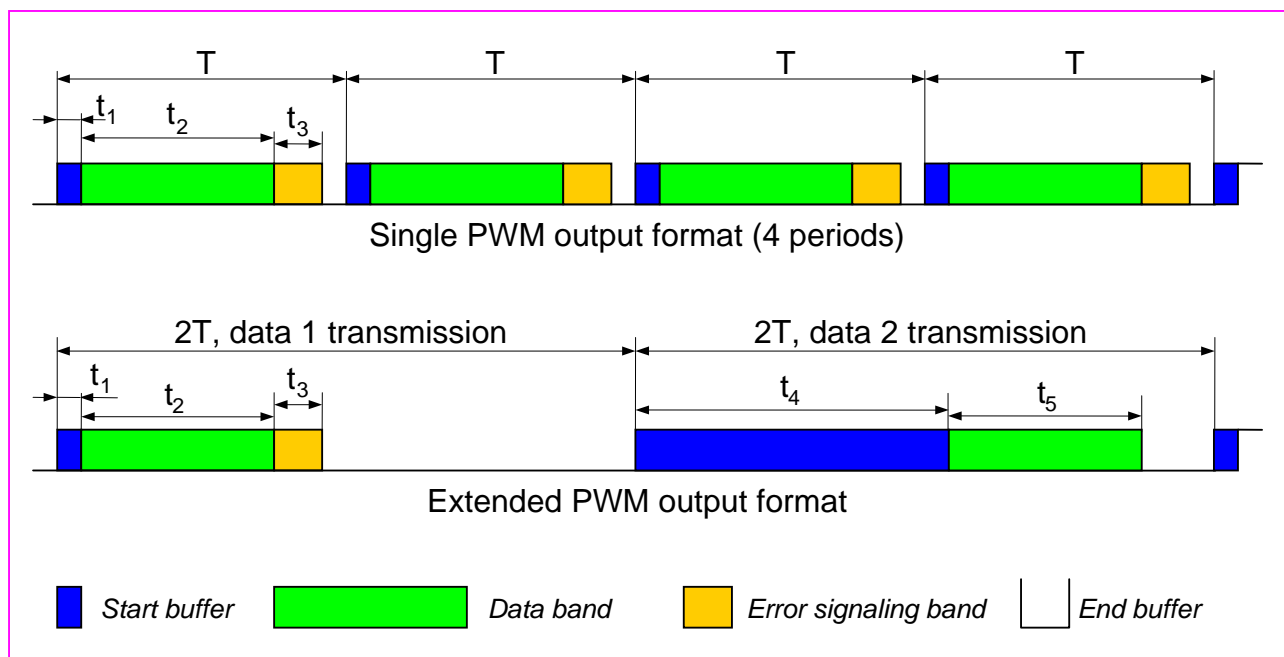
Figure 11: PWM timing

8.5.1 Single PWM format

In single PWM output mode the settings for PWM1 data only are used. The temperature reading can be calculated from the signal timing as:

$$Tout = \left[\frac{2t_2}{T} * (Tmax - Tmin) \right] + Tmin,$$

where Tmin and Tmax are the corresponding rescale coefficients in EEPROM for the selected temperature output (Ta, object temperature range is valid for both Tobj1 and Tobj2 as specified in the previous table) and T is the PWM period. Tout is T_{obj1}, T_{obj2} or T_a according to Config Register [5:4] settings.

The different time intervals t_1-t_3 have the following functions:

t_1: Start buffer. During this time the signal is always high. $t_1 = 0.125*T$ (T is the PWM period, refer to fig. 11).

t_2: Valid Data Output Band, 0 to 1/2T. PWM output data resolution is 10 bit.

t_3: Error band – information for fatal error in EEPROM (double error detected, not correctable). $t_3 = 0.25 * T$. Therefore a PWM pulse train with a duty cycle of 0.875 will indicate a fatal error in EEPROM (for single PWM format).

Example:

T_{obj1} => Config Reg[5:4] = 11'b

To_{min} = 0°C   => To_{min} [EEPROM] = 100 * (to_{min} + 273.15) = 6AB3h

To_{max} = +50°C   => To_{max} [EEPROM] = 100 * (to_{max} + 273.15) = 7E3Bh

Captured PWM high duration is 0.495*T => t_2=(0.495 – 0.125)*T=0.370*T =>
measured object temperature = 2X0.370* (50°C -0°C)+0°C = +37.0°C.

8.5.2 Extended PWM format

The PWM format for extended PWM is shown in Figure 11. Note that with bits DUAL[5:1]>00h each period will be outputted 2N+1 times, where N is the decimal value of the number written in DUAL[5:1] (*DUAL[5:1] =PWM control & clock [8:4]*), like shown on Figure 12.

2N+1=3 times Data1   *2N+1=3 times Data2*   *New Data 1*
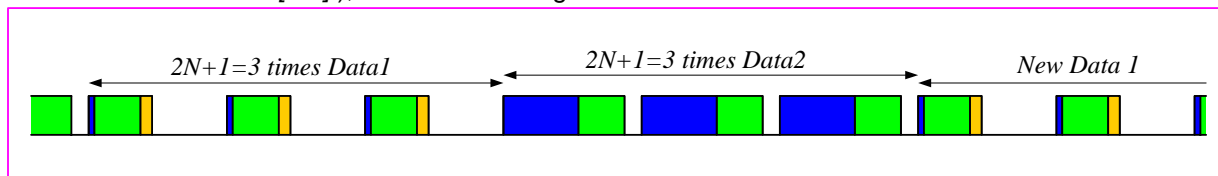
Figure 12: Extended PWM format with DUAL[5:1] = 01h (2 repetitions for each data)

The temperature transmitted in Data 1 field can be calculated using the following equation:

$$Tout_1 = \left[\frac{2t_2}{T} * (Tmax_1 - Tmin_1) \right] + Tmin_1$$

For Data 2 field the equation is:

$$Tout_2 = \left[\frac{2t_5}{T} * (Tmax_2 - Tmin_2) \right] + Tmin_2$$

Where $Tmin_1$, $Tmax_1$, $Tmin_2$ and $Tmax_2$ are given in Table 9, $t_2=t_{high1}-t_1$, and $t_5=t_{high2}-t_4$.

Time bands are: $t_1=0.125*T$, $t_3=0.25*T$ and $t_4=1.125*T$. As shown in Figure 11, in extended PWM format the period is twice the period for the single PWM format. All equations provided herein are given for the single PWM period T. The EEPROM Error band signaling will be 43.75% duty cycle for Data1 and 93.75% for Data2.

Note: EEPROM error signaling is implemented in automotive grade parts only.

Example:

Configuration: Ta : T_{obj1} @ Data1 : Data2 => Config Reg[5:4] = 00b,

Ta_{min} = -5°C   => Ta_{range}, L [EEPROM] = 100*(Ta_{min}+38.2)/64 = 34h,

Ta_{max} = +105°C   => Ta_{range},H [EEPROM] = 100*(Ta_{max}+38.2)/64 = E0h,

                Ta_{range} [EEPROM]=E034h

To_{min} = 0°C   => To_{min} [EEPROM] = 100 * (To_{min} + 273.15) = 6AB3h

To_{max} = +50°C   => To_{max} [EEPROM] = 100 * (To_{max} + 273.15) = 7E3Bh

Captured high durations are 0.13068*(2T) and 0.7475*(2T), where 2T is each captured PWM period. Time band t_4 is provided for reliable determination between Data1 and Data2 data fields. Thus Data1 is represented by 0.13068*(2T) and Data2 – by 0.7475*(2T), and the temperatures can be calculated as follows:

$t_2/T=(t_{high1}/T)-0.125=0.13636$ => Ta=+25.0°C,

$t_5/T=(t_{high2}/T)-1.125=0.370$ => T_{obj1}=+37.0°C.

8.5.3 Customizing the temperature range for PWM output

The calculated ambient and object temperatures are stored in RAM with a resolution of 0.01 °C (16 bit). The PWM operates with a 10-bit word so the transmitted temperature is rescaled in order to fit in the desired range.

For this goal 2 cells in EEPROM are foreseen to store the desired range for To (To_{min} and To_{max}) and one for Ta (Ta_{range}: the 8MSB are foreseen for Ta_{max} and the 8LSB for Ta_{min}).

Thus the output range for To can be programmed with an accuracy of 0.01 °C, while the corresponding Ta range can be programmed with an accuracy of 2.56 °C.

The **object** data for PWM is rescaled according to the following equation:

$$T_{PWM_{obj}} = \frac{T_{RAM} - T_{MIN_{EEPROM}}}{K_{PWM_{obj}}}, K_{PWM_{obj}} = \frac{T_{MAX_{EEPROM}} - T_{MIN_{EEPROM}}}{1023}$$

The T_{RAM} is the linearized Tobj, 16-bit (0000…FFFFh, 0000 for -273.15°C and FFFFh for +382.2°C) and the result is a 10-bit word, in which 000h corresponds to To_{MIN}[°C], 3FFh corresponds to To_{MAX}[°C] and 1LSB

corresponds to $\frac{To_{MAX} - To_{MIN}}{1023}$ [°C]

$$T_{MIN_{EEPORM}} = T_{MIN} * 100 \, \text{LSB}$$

$$T_{MAX_{EEPORM}} = T_{MAX} * 100 \, \text{LSB}$$

The **ambient** data for PWM is rescaled according to the following equation:

$$T_{PWM_{ambient}} = \frac{T_{RAM} - T_{MIN_{EEPROM}}}{K_{PWM_{ambient}}}, K_{PWM_{ambient}} = \frac{T_{MAX_{EEPROM}} - T_{MIN_{EEPROM}}}{1023}$$

The result is a 10-bit word, where 000h corresponds to -38.2 °C (lowest Ta that can be read via PWM), 3FFh

corresponds to 125 °C (highest Ta that can be read via PWM) and 1LSB corresponds to $\frac{T_{MAX} - T_{MIN}}{1023}$ [°C]

$$T_{MIN_{EEPORM}} = [T_{MIN} - (-38.2)] * \frac{100}{64} \, \text{LSB}$$

$$T_{MAX_{EEPORM}} = [T_{MAX} - (-38.2)] * \frac{100}{64} \, \text{LSB}$$

8.6 Switching Between PWM and SMBus communication

8.6.1 PWM is enabled

The diagram below illustrates the way of switching to SMBus if PWM is enabled (factory programmed POR default for MLX90614 is SMBus, PWM disabled). Note that the SCL pin needs to be kept high in order to use PWM.
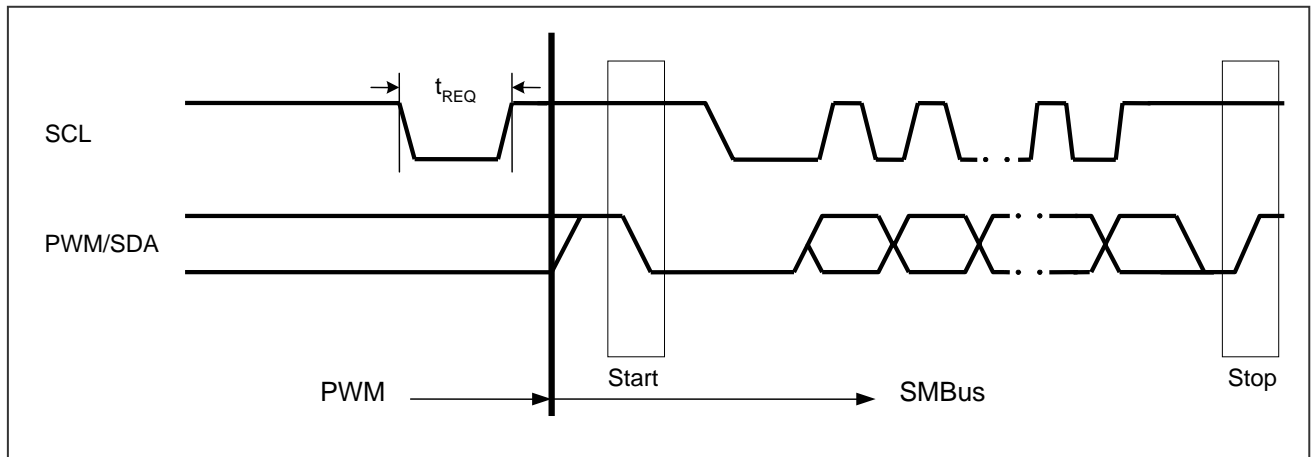
Figure 13: Switching from PWM mode to SMBus

8.6.2 Request condition
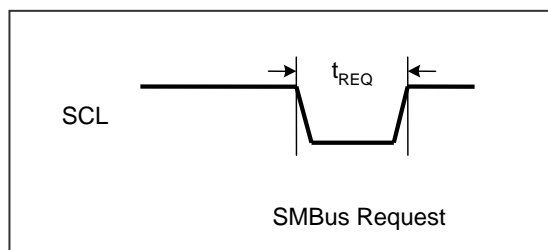
Figure 14: Request (switch to SMBus) condition

If PWM is enabled, the MLX90614's SMBus Request condition is needed to disable PWM and reconfigure PWM/SDA pin before starting SMBus communication. Once PWM is disabled, it can be only enabled by switching the supply Off-On or exit from Sleep Mode. The MLX90614's SMBus request condition requires forcing LOW the SCL pin for period longer than the request time (t_{REQ}). The SDA line value is ignored in this case.

8.6.3 PWM is disabled

If PWM is disabled by means of EEPROM the PWM/SDA pin is directly used for the SMBus purposes after POR. **Request condition should not be sent in this case**.

8.7 Computation of ambient and object temperatures

The IR sensor consists of serial connected thermo-couples with cold junctions placed at thick chip substrate and hot junctions, placed over thin membrane. The IR radiation absorbed from the membrane heats (or cools) it. The thermopile output signal is:

$$V_{ir}(Ta, To) = A.(To^4 - Ta^4),$$

Where To is the object temperature absolute (Kelvin) temperature, Ta is the sensor die absolute (Kelvin) temperature, and A is the overall sensitivity.
An on board temperature sensor is needed to measure the chip temperature. After measurement of the output of both sensors, the corresponding ambient and object temperatures can be calculated. These calculations are done by the internal DSP, which produces digital outputs, linearly proportional to measured temperatures.

8.7.1 Ambient temperature Ta

The Sensor die temperature is measured with a PTC or a PTAT element. All the sensors' conditioning and data processing is handled on-chip and the linearized sensor die temperature Ta is made available in memory.
The resolution of the calculated temperature is 0.02 ˚C. The sensor is factory calibrated for the full automotive range (-40 to 125 ˚C). In RAM cell 006h, 2DE4h corresponds to -38.2 ˚C (linearization output lower limit) and 4DC4h (19908d) corresponds to 125 ˚C. The conversions from RAM contend to real Ta is easy using the following relation:

$$Ta[°K] = Tareg \times 0.02 \text{ , or 0.02 °K / LSB.}$$

8.7.2 Object temperature To

The result has a resolution of 0.02 ˚C and is available in RAM. To is derived from RAM as:

$$To[°K] = Toreg \times 0.02 \text{ , or 0.02 °K / LSB.}$$

8.7.3 Calculation flow

The measurement, calculation and linearization are held by core, which executes a program form ROM.
After POR the chip is initialized with calibration data from EEPROM. During this phase the number of IR sensors is selected and it is decided which temperature sensor will be used. Measurements, compensation and linearization routines run in a closed loop afterwards.

Processing ambient temperature includes:
Offset measurement with fixed length FIR filter
Additional filtering with fixed length IIR filter. The result is stored into RAM as T_{OS}
Temperature sensor measurement using programmable length FIR *.
Offset compensation
Additional processing with programmable length IIR **. The result is stored into RAM as T_D.
Calculation of the ambient temperature. The result is stored into RAM as T_A
Processing of the object temperature consists of three parts. The first one is common for both IR sensors, the third part can be skipped if only one IR sensor is used.
IR offset:
Offset measurement with a fixed length FIR
Additional filtering with a fixed length IIR. The result is stored into RAM as IR_{OS}.

Gain measurement with fixed length FIR filter

Offset compensation

Additional gain filtering with fixed length IIR, storing the result into RAM as IR_G.

Gain compensation calculation, the result is stored into RAM as K_G

Object temperature:

IR1 sensor:

IR sensor measurement with programmable length FIR filter *.

Offset compensation

Gain compensation

Filtering with programmable length IIR filter**, storing the result into RAM as $IR1_D$.

Calculation of the object temperature. The result is available in RAM as T_{OBJ1}.

IR2 sensor:

IR sensor measurement with programmable length FIR filter *.

Offset compensation

Gain compensation

Filtering with programmable length IIR filter**, storing the result into RAM as $IR2_D$

Calculation of the object temperature. The result is available in RAM as T_{OBJ2}.

PWM calculation:

Recalculate the data for PWM with 10 bit resolution

Load data into PWM module

Note*: The measurements with programmable filter length for FIR filter use the same EEPROM cells for N.
Note**: The IIR filter with programmable filter length uses the same EEPROM cells for L.
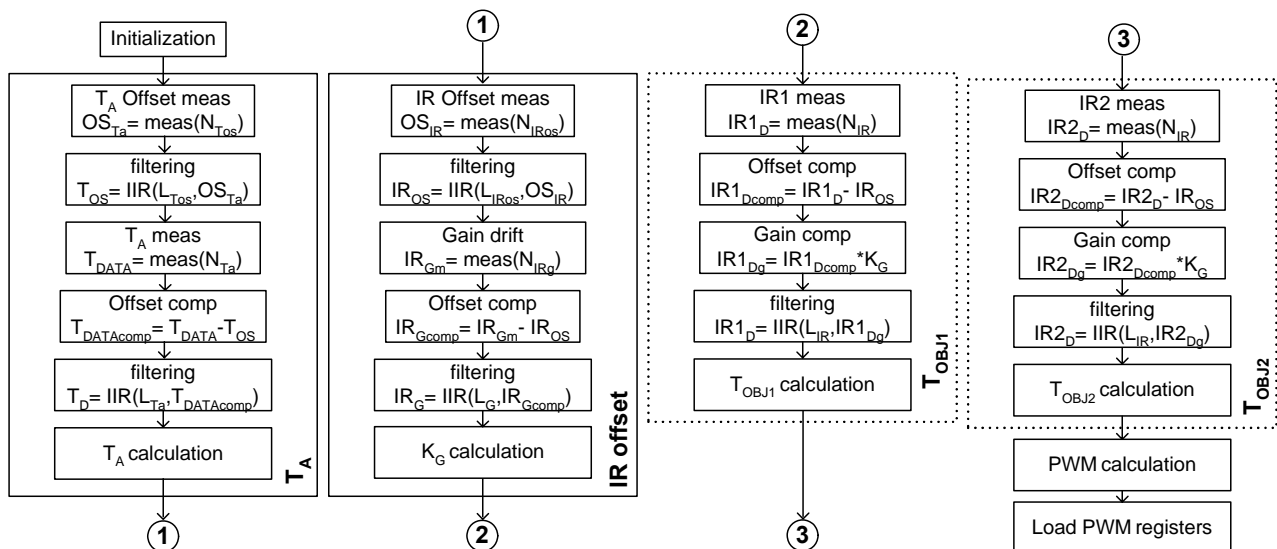
Figure 15: Software flow

8.8 Thermal relay

The MLX90614 can be configured to behave as a thermo relay with programmable threshold and hysteresis on the PWM/SDA pin. The input for the comparator unit of the relay is the object temperature from sensor 1 **The output of the MLX90614 is NOT a relay driver but a logical output which should be connected to a relay driver if necessary.**
In order to configure the MLX90614 to work as thermal relay two conditions must be met:
- o   Set bit TRPWMB high at address 002h in EEPROM
- o   Enable PWM output i.e. EN_PWM is set high

The PWM/SDA pin can be programmed as a push-pull or open drain NMOS (via bit PPODB in EEPROM PWMCTRL), which can trigger an external device. The temperature threshold data is determined by EEPROM at address 021h (Tomin) and the hysteresis at address 020h (To$_{max}$).
The logical state of the PWM/SDA pin is as follows:

PWM/SDA pin is high if $T_{obj}1 \geq threshold + hysteresis$

PWM/SDA pin is low if $T_{obj}1 \leq threshold - hysteresis$
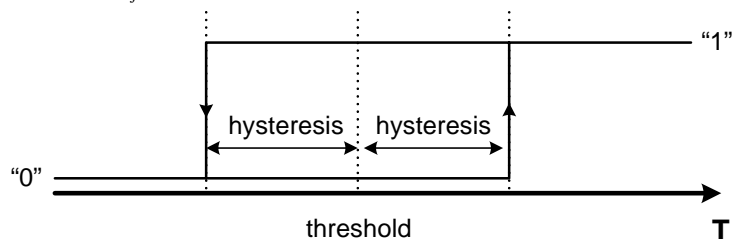
Figure 16: Thermal relay : "PWM" pin versus Tobj

The MLX90614 preserves its normal operation when configured as a thermal relay (PWM configuration and specification applies as a general rule also for the thermal relay) and therefore it can be read using the SMBus (entering the SMBus mode from both PWM and thermal relay configuration is the same).
For example, the MLX90614 can generate a wake-up alert for a system upon reaching a certain temperature and then be read as a thermometer. A reset condition (enter-and exit Sleep, for example) will be needed in order to return to the thermal relay configuration.

Example: threshold 5 °C => (5 + 273.15)*100 = 27815 = 6CA7h
        hysteresis is 1°C => 1 * 100 = 100 = 64h
        PWM/SDA pin will be low at object temperature below 4 °C
        PWM/SDA pin will be high at object temperature higher that 6 °C

9 Unique Features

The MLX90614 is a ready-to use low-cost non contact thermometer provided from Melexis with output data linearly dependent on the object temperature with high accuracy and extended resolution.

It supports versatile customization to a very wide range of temperatures, power supplies and refresh rates. The user can program the internal object emissivity correction for objects with a low emissivity. An embedded error checking and correction mechanism provides high memory reliability.

The sensors are housed in an industry standard TO39 package for both single- and dual-zone IR thermometers. The thermometer is available in automotive grade and can use two different packages for wider applications' coverage.

The low power consumption and sleep mode make the thermometer ideally suited for handheld mobile applications.

The digital sensor interface can be either a power-up-and-measure PWM or an enhanced access SMBus compatible protocol. Systems with more than 100 devices can be built with only two signal lines. Dual zone non contact temperature measurements are available via a single line (extended PWM).

A built-in thermal relay function further extends the easy implementation of wide variety of freezing/boiling prevention and alert systems, as well as thermostats (no MCU is needed).

10 Performance Graphs

10.1 Temperature accuracy of the MLX90614
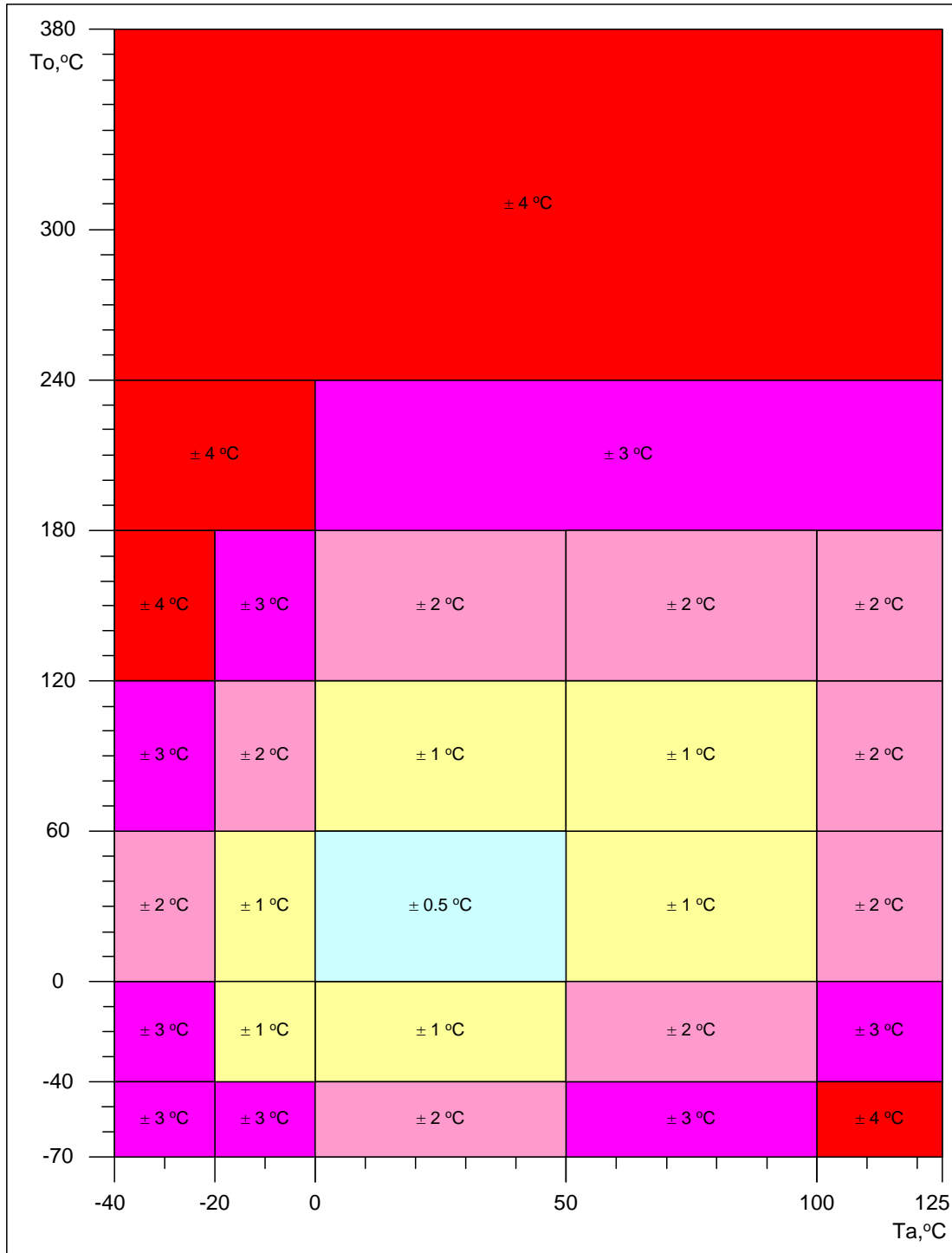
Figure 17: Preliminary accuracy of MLX90614 (Ta,To)

All accuracy specifications apply under settled isothermal conditions only.

A version of the MLX90614 with accuracy suited for medical applications is available. The accuracy in the range Ta 10ºC - 40ºC and To 32ºC - 42ºC is shown in diagram below. The accuracy for the rest of the temperature ranges is the same as in previous diagram. Medical accuracy specification is only available for the MLX90614DAA version.
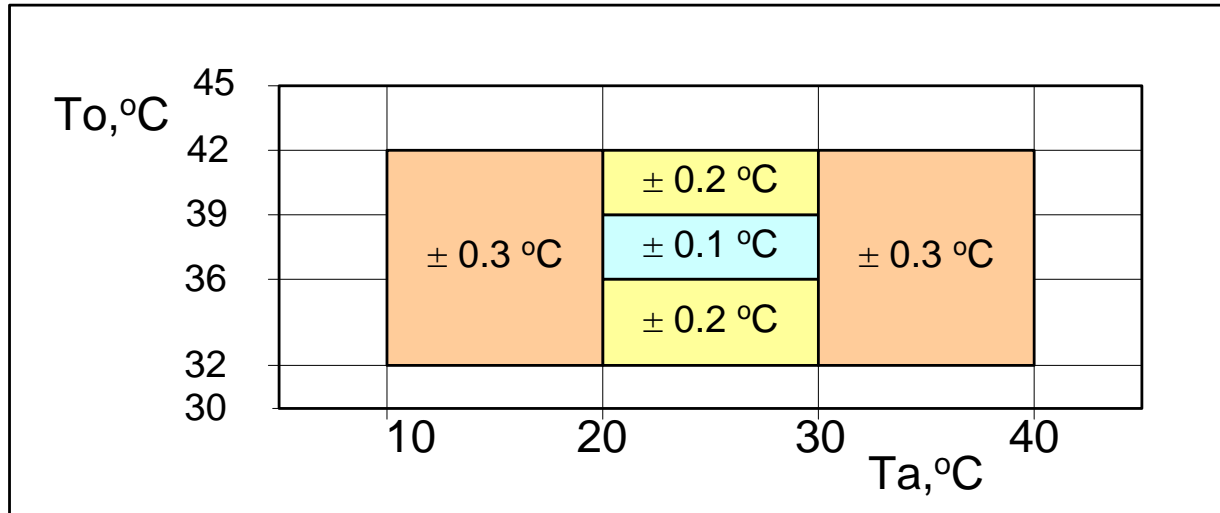
Figure 18: Preliminary accuracy of MLX90614DAA (Ta,To) for medical applications.

10.2 Field Of View (FOV)

Field of view is determined at 50% thermopile signal and with respect to the sensor main axis.

Parameter	MLX90614xAA	MLX90614xBA	MLX90614xAC
Peak zone 1	±0°	-25°	±0°
Width zone 1	90°	70°	35°
Peak zone 2	Not applicable	-25°	Not applicable
Width zone 2		70°	
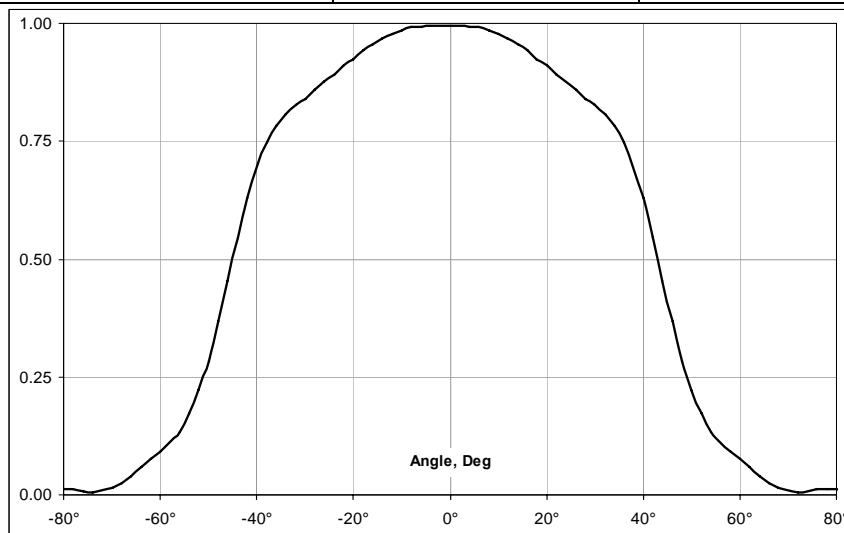
Figure 19: FOV of MLX90614xAA
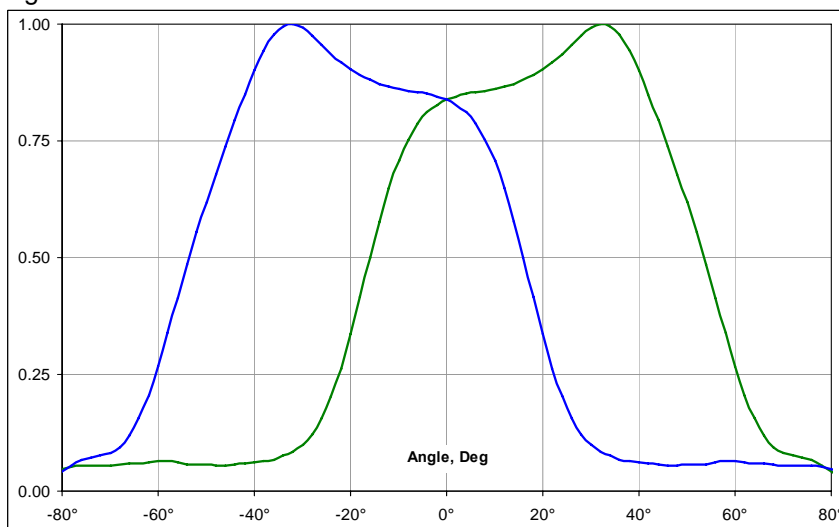
Figure 20: FOV of MLX90614xBA

Figure 21: identification of zone 1&2 relative to alignment tab.
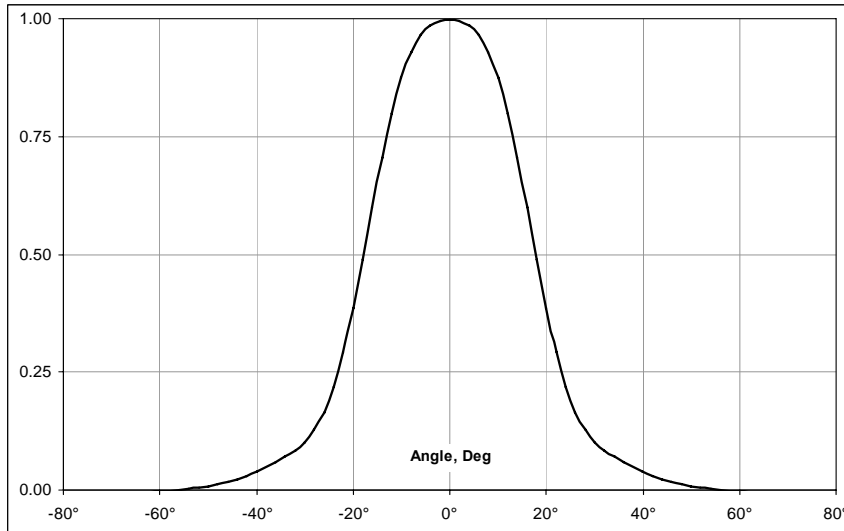
Figure 21: FOV of MLX90614xAC

11 Applications Information

11.1 Use of the MLX90614 thermometer in SMBus configuration
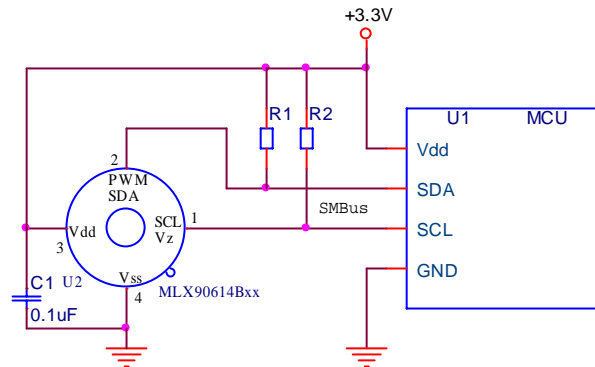
Figure 22: MLX90614 SMBus connection

Connection of the MLX90614 to SMBus with 3.3V power supply. The MLX90614 has diode clamps SDA/SCL to Vdd so it is necessary to provide MLX90614 with power in order not to load the SMBus lines.

11.2 Use of multiple MLX90614s in SMBus configuration
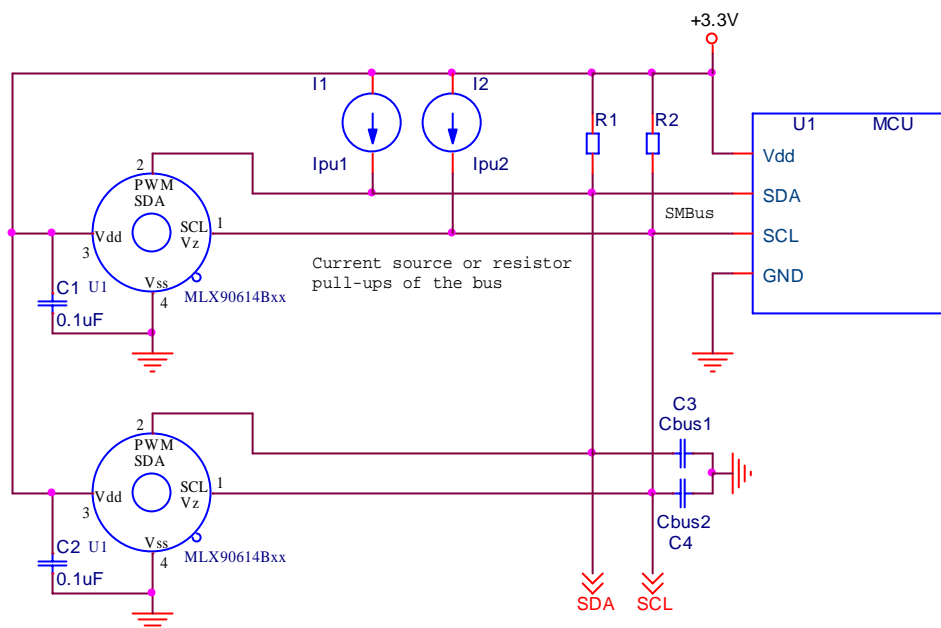
Figure 23: Use of multiple MLX90614 devices in SMBus network

The MLX90614 supports a 7-bit slave address in EEPROM, thus allowing up to 127 devices to be read via two common wires. With the MLX90614BBx this results in 254 object temperatures measured remotely and an additional 127 ambient temperatures which are also available. Current source pull-ups may be preferred with higher capacitive loading on the bus (C3 and C4 represent the lines' parasitics), while simple resistive pull-ups provide the obvious low cost advantage.

11.3 PWM output operation

Using the PWM output mode of the MLX90614 is very simple, as shown on Figure 24.
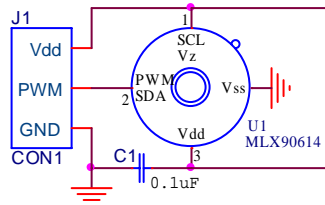
Figure 24: Connection of MLX90614 for PWM output mode

The PWM mode is free-running after POR when configured in EEPROM. The SCL pin must be forced high (can be shorted to Vdd pin) for PWM mode operation.
A pull-up resistor can be used to preserve the option for SMBus operation while having PWM as a default as is shown on Figure 25.
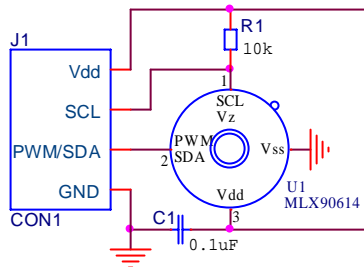
Figure 25: PWM output with SMBus available

Again, the PWM mode needs to be written as the POR default in EEPROM. Then for PWM operation the SCL line can be high impedance, forced high, or even not connected. The pull-up resistor R1 will ensure there is a high level on the SCL pin and the PWM POR default will be active. SMBus is still available (for example – for further reconfiguration of the MLX90614, or sleep mode power management) as there are pull-up resistors on the SMBus lines anyway.
PWM can be configured as open drain NMOS or a push-pull output. In the case of open drain external pull-up will be needed. This allows cheap level conversion to lower logic high voltage. Internal pull-ups present in many MCUs can also be used.

11.4 Thermal alert / thermostat
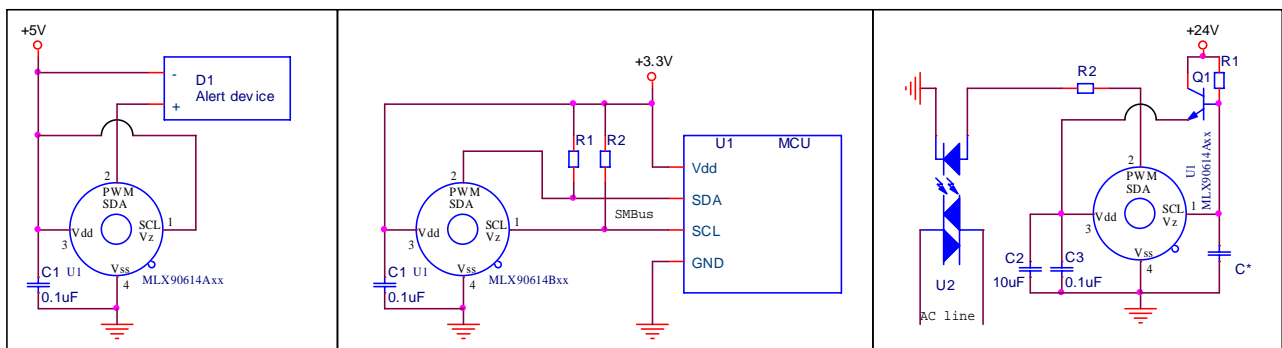
Figure 26: Thermal alert/thermostat applications of MLX90614

The MLX90614 can be configured in EEPROM to operate as a thermal relay. A non contact freezing or boiling prevention with 1 mA quiescent current can be built with two components only – the MLX90614 and a

capacitor. The PWM/SDA pin can be programmed as a push-pull or open drain NMOS, which can trigger an external device, such as a relay (refer to electrical specifications for load capability), buzzer, RF transmitter or a LED. This feature allows very simple thermostats to be built without the need of any MCU and zero design overhead required for firmware development. In conjunction with a MCU, this function can operate as a system alert that wakes up the MCU. Both object temperature and sensor die temperature can also be read in this configuration.

11.5 High voltage source operation

As a standard, the module MLX90614Axx works with a supply voltage of 5Volt. In addition, thanks to the integrated internal reference regulator available at pin SCL/Vz, this module can easily be powered from higher voltage source (like VDD=8…16V). Only a few external components as depicted in the diagram below are required to achieve this.
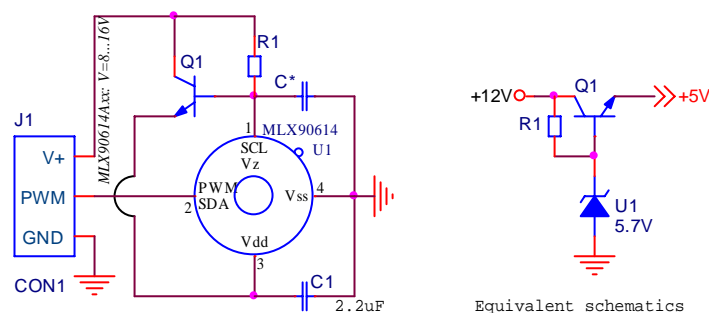
Figure 27: 12V regulator implementation

With the second (synthesized Zener diode) function of the SCL/Vz pin used, the 2-wire interface function is available only if the voltage regulator is overdriven (5V regulated power is forced to Vdd pin).

12 Application Comments

Significant **contamination** at the optical input side (sensor filter) might cause unknown additional filtering/distortion of the optical signal and therefore result in unspecified errors.

IR sensors are inherently susceptible to errors caused by **thermal gradients**. There are physical reasons for these phenomena and, in spite of the careful design of the MLX90614xxx, it is recommended not to subject the MLX90614 to heat transfer and especially transient conditions.

Upon **power-up** the MLX90614 passes embedded checking and calibration routines. During these routines the output is not defined and it is recommended to wait for the specified POR time before reading the module. Very slow power-up may cause the embedded POR circuitry to trigger on inappropriate levels, resulting in unspecified operation and this is not recommended.

The MLX90614xxx is designed and calibrated to operate as a non contact thermometer in **settled conditions**. Using the thermometer in a very different way will result in unknown results.

Capacitive loading on a SMBus can degrade the communication. Some improvement is possible with use of current sources compared to resistors in pull-up circuitry. Further improvement is possible with specialized commercially available bus accelerators. With the MLX90614xxx additional improvement is possible by increasing the pull-up current (decreasing the pull-up resistor values). Input levels for SMBus compatible mode have higher overall tolerance than the SMBus specification, but the output low level is rather low even with the high-power SMBus specification for pull-up currents. Another option might be to go for a slower communication (clock speed), as the MLX90614xxx implements Schmidt triggers on its inputs in SMBus compatible mode and is therefore not really sensitive to rise time of the bus (it is more likely the rise time to be an issue than the fall time, as far as the SMBus systems are open drain with pull-up).

For **ESD protection** there are clamp diodes between the Vss and Vdd and each of the other pins. This means that the MLX90614 might draw current from a bus in case the SCL and/or SDA is connected and the Vdd is lower than the bus pull-ups' voltage.

In **12V powered systems SMBus usage is constrained** because the SCL pin is used for the Zener diode function. Applications where the supply is higher than 5V should use the PWM output or an external regulator. Nevertheless, in the 12V powered applications MLX90614 can be programmed (configured and customized) by forcing the Vdd to 5V externally and running the SMBus communication.

Sleep mode is available in MLX90614Bxx. This mode is entered and exited via the SMBus compatible 2-wire communication. On the other hand, the extended functionality of the SCL pin yields in increased leakage current through that pin. As a result, this pin needs to be forced low in power-down mode and the pull-up on the SCL line needs to be disabled in order to keep the overall power drain in power-down really small.

The **PWM pin is not designed for direct drive of inductive loads** (such as electro-magnetic relays). Some drivers need to be implemented for higher load, and auxiliary protection might be necessary even for light but inductive loading.

It is possible to use the MLX90614xxx in applications, powered directly from the AC line (transformer less). In such cases it is very important not to forget that **the metal package of the sensor is not isolated** and therefore may occur to be connected to that line, too. Melexis can not be responsible for any application like this and highly recommends not to use the MLX90614xxx in that way.

Power dissipation within the package may affect performance in two ways: by heating the "ambient" sensitive element significantly beyond the actual ambient temperature, as well as by causing gradients over the package that will inherently cause thermal gradient over the cap. Loading the outputs also causes increased

power dissipation. In case of using the MLX90614Axx internal zener voltage feature, the regulating external transistor should also not cause heating of the TO39 package.

High capacitive load on a PWM line will result in significant charging currents from the power supply, bypassing the capacitor and therefore causing EMC, noise, level degradation and power dissipation problems. A simple option is adding a series resistor between the PWM/SDA pin and the capacitive loaded line, in which case timing specifications have to be carefully reviewed. For example, with a PWM output that is set to 1.024 ms and the output format that is 11 bit, the time step is 0.5 μs and a settling time of 2 μs would introduce a 4 LSBs error.

Power supply decoupling capacitor is needed as with most integrated circuits. MLX90614 is a mixed-signal device with sensors, small signal analog part, digital part and I/O circuitry. In order to keep the noise low power supply switching noise needs to be decoupled. High noise from external circuitry can also affect noise performance of the device. In many applications a 100nF SMD ceramic capacitor close to the Vdd and Vss pins would be a good choice. It should be noted that not only the trace to the Vdd pin needs to be short, but also the one to the Vss pin. Using MLX90614 with short pins improves the effect of the power supply decoupling.
Severe noise can also be coupled within the package from the SCL (in worst cases also from the SDA) pin. This issue can be solved by using PWM output. Also the PWM output can pass additional filtering (at lower PWM frequency settings). With a simple LPF RC network added also increase of the ESD rating is possible.

Check www.melexis.com for most recent application notes about MLX90614.

13 Standard information regarding manufacturability of Melexis products with different soldering processes

Our products are classified and qualified regarding soldering technology, solderability and moisture sensitivity level according to following test methods:

Wave Soldering THD's (Through Hole Devices)

- EIA/JEDEC JESD22-B106 and EN60749-15
  Resistance to soldering temperature for through-hole mounted devices

Iron Soldering THD's (Through Hole Devices)

- EN60749-15
  Resistance to soldering temperature for through-hole mounted devices

Solderability THD's (Through Hole Devices)

- EIA/JEDEC JESD22-B102 and EN60749-21
  Solderability

For all soldering technologies deviating from above mentioned standard conditions (regarding peak temperature, temperature gradient, temperature profile etc) additional classification and qualification tests have to be agreed upon with Melexis.

Melexis is contributing to global environmental conservation by promoting **lead free** solutions. For more information on qualifications of **RoHS** compliant products (RoHS = European directive on the Restriction Of the use of certain Hazardous Substances) please visit the quality page on our website: http://www.melexis.com/quality.aspx
The MLX90614 is RoHS compliant

14 ESD Precautions

Electronic semiconductor products are sensitive to Electro Static Discharge (ESD).
Always observe Electro Static Discharge control procedures whenever handling semiconductor products.

15 FAQ

When I measure aluminum and plastic parts settled at the same conditions I get significant errors on aluminum. Why?

Different materials have different **emissivity**. A typical value for aluminum (roughly polished) is 0.18 and for plastics values of 0.84…0.95 are typical. IR thermometers use the radiation flux between the sensitive element in the sensor and the object of interest, given by the equation

$$q = \varepsilon_1 . \alpha_1 . \left(T_1^{\,4} \right) \sigma . A_1 . F_{a-b} - \varepsilon_2 . \left(T_2^{\,4} \right) \sigma . A_2 \,,$$

Where:
ε_1 and ε_2 are the emissivities of the two objects,
α_1 is the absorptivity of the sensor (in this case),
σ is the Stefan-Boltzmann constant,
A_1 and A_2 are the surface areas involved in the radiation heat transfer,
F_{a-b} is the shape factor,
T_1 and T_2 are known temperature of the sensor die (measured with specially integrated and calibrated element) and the object temperature that we need.
Note that these are all in Kelvin, heat exchange knows only physics.
When a body with low emissivity (such as aluminum) is involved in this heat transfer, the portion of the radiation incident to the sensor element that really comes from the object of interest decreases – and the reflected environmental IR emissions take place. (This is all for bodies with zero transparency in the IR band.)
The IR thermometer is calibrated to stay within specified accuracy – but it has no way to separate the incoming IR radiation into real object and reflected environmental part. Therefore, measuring objects with low emissivity is a very sophisticated issue and infra-red measurements of such materials is a specialized field.
What can be done to solve that problem? Look at paintings – for example, oil paints are likely to have emissivity of 0.85…0.95 – but keep in mind that the stability of the paint emissivity has inevitable impact on measurements.
It is also a good point to keep in mind that not everything that looks black is "black" also for IR. For example, even heavily oxidized aluminum has still emissivity as low as 0.30.
How high is enough? Not an easy question – but, in all cases the closer you need to get to the real object temperature the higher the needed emissivity will be, of course.
With the real life emissivity values the environmental IR comes into play via the reflectivity of the object (the sum of Emissivity, Reflectivity and Absorptivity gives 1.00 for any material). The larger the difference between environmental and object temperature is at given reflectivity (*with an opaque for IR material reflectivity equals 1.00 minus emissivity*) the bigger errors it produces.

After I put the MLX90614 in the dashboard I start getting errors larger than specified in spite that the module was working properly before that. Why?

Any object present in the FOV of the module provides IR signal. It is actually possible to introduce error in the measurements if the module is attached to the dashboard with an opening that enters the FOV. In that case portion of the dashboard opening will introduce IR signal in conjunction with constraining the effective FOV and thus compromising specified accuracy. Relevant opening that takes in account the FOV is a must for accurate measurements. Note that the basic FOV specification takes 50% of IR signal as threshold (in order to define the area, where the measurements are relevant), while the entire FOV at lower level is capable of introducing lateral IR signal under many conditions.

When a hot (cold) air stream hits my MLX90614 some error adds to the measured temperature I read. What is it?

IR sensors are inherently sensitive to difference in temperatures between the sensitive element and everything incident to that element. As a matter of fact, this element is not the sensor package, but the sensor die inside. Therefore, a thermal gradient over the sensor package will inevitably result in additional IR flux

between the sensor package and the sensor die. This is real optical signal that can not be segregated from the target IR signal and will add errors to the measured temperature.

Thermal gradients with impact of that kind are likely to appear during transient conditions. The sensor used is developed with care about sensitivity to this kind of lateral phenomena, but their nature demands some care when choosing place to use the MLX90614 in order to make them negligible.

I measure human body temperature and I often get measurements that significantly differ from the +37°C I expect.

IR measurements are true surface temperature measurements. In many applications this means that the actual temperature measured by an IR thermometer will be temperature of the clothing and not the skin temperature. Emissivity (explained first in this section) is another issue with clothes that has to be considered. There is also the simple chance that the measured temperature is adequate – for example, in a cold winter human hand can appear at temperatures not too close to the well known +37°C.

I consider using MLX90614AAA to measure temperature within car compartment, but I am embarrassed about the Sun light that may hit the module. Is it a significant issue?

Special care is taken to cut off the visible light spectra as well as the NIR (near IR) before it reaches the sensitive sensor die. Even more, the glass (in most cases) is not transparent to the IR radiation used by the MLX90614. Glass has temperature and really high emissivity in most cases – it is "black" for IR of interest. Overall, Sun behind a window is most likely to introduce relatively small errors. Why is it not completely eliminated after all? Even visible light partially absorbed in the filter of the sensor has some heating potential and there is no way that the sensor die will be "blind" for that heating right in front of it.

16 Package Information

16.1 MLX90614XXA

The MLX90614 is packaged in an industry standard TO – 39 can.
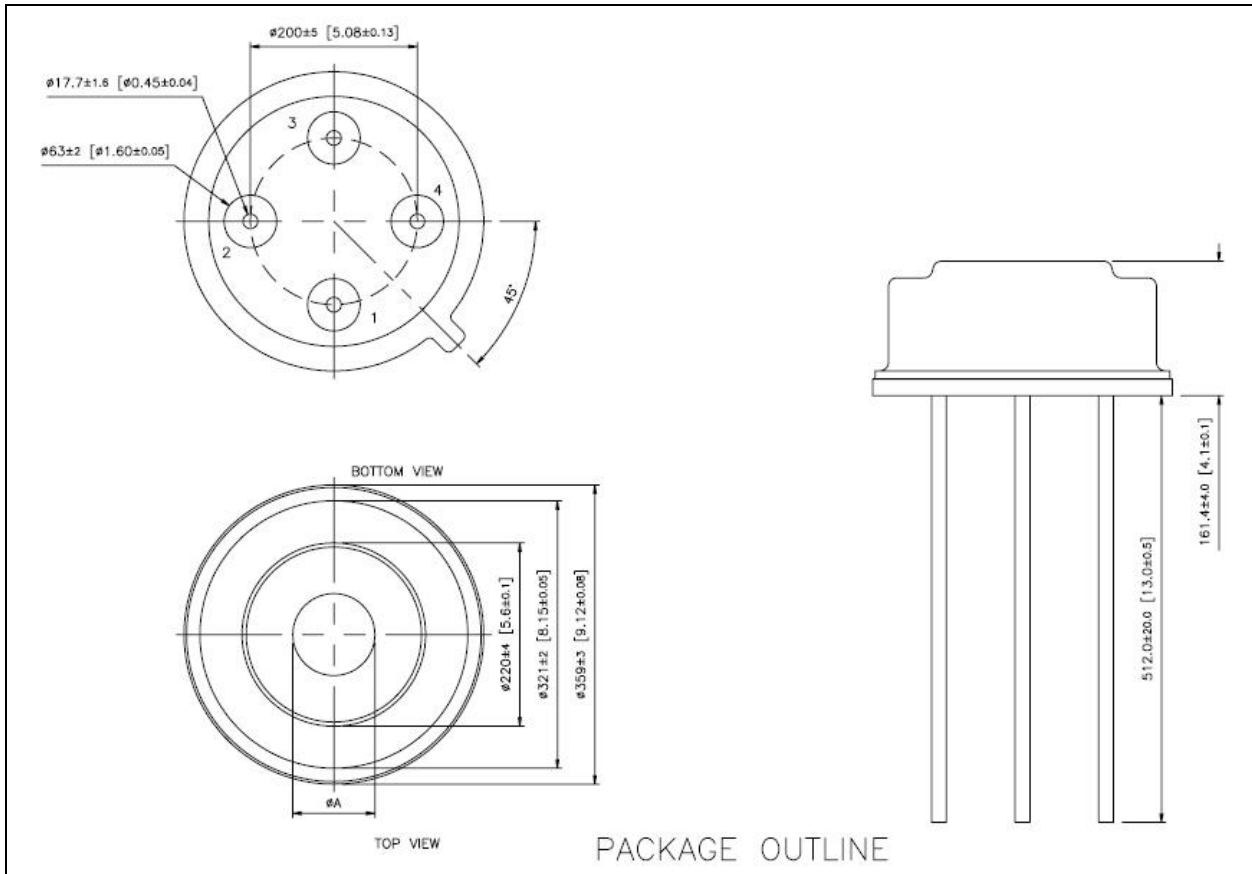
Figure 28: MLX90614XXA package

Note:
1. All dimensions are in mils [mm]
2. ØA = 3.5 mm

16.2 MLX90614XXC
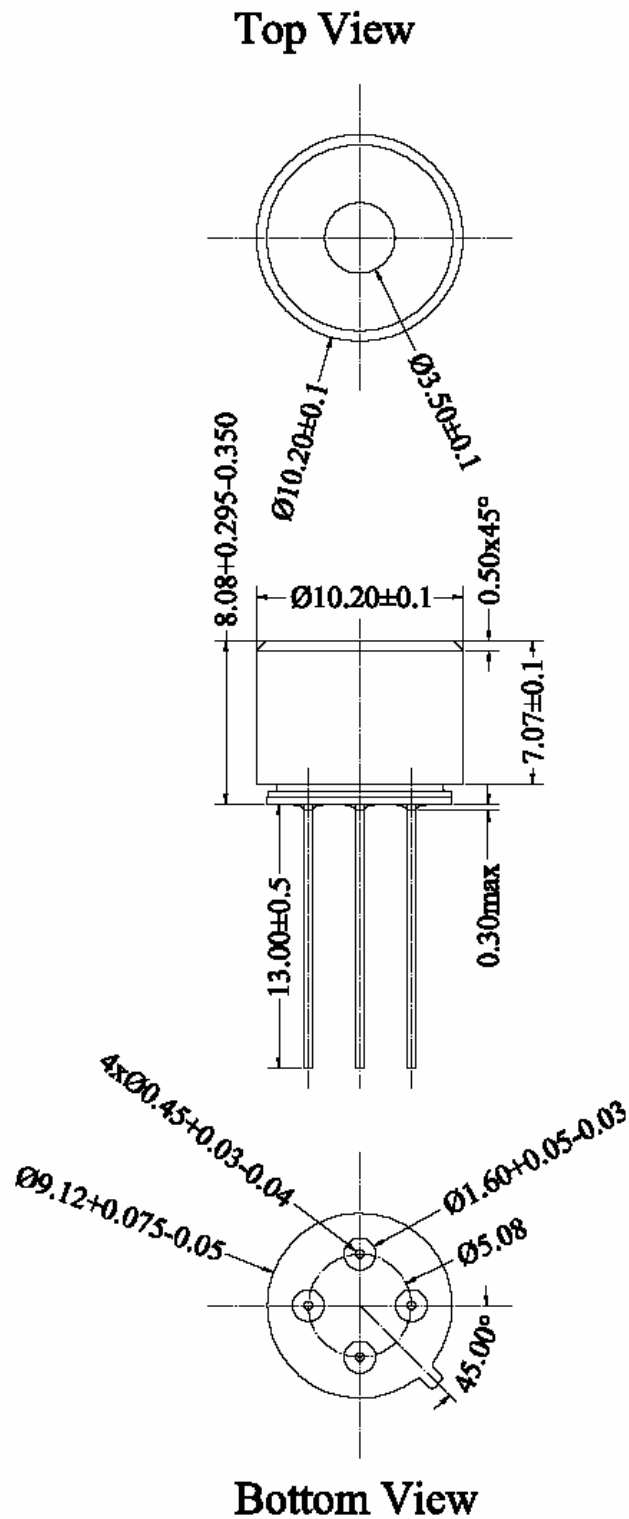
Figure 29: MLX90614XXC package

17 References

[1] **System Management Bus (SMBus) Specification** Version 2.0 August 3, 2000
SBS Implementers Forum Copyright . 1994, 1995, 1998, 2000
Duracell, Inc., Energizer Power Systems, Inc., Fujitsu, Ltd., Intel Corporation, Linear Technology
Inc., Maxim Integrated Products, Mitsubishi Electric Semiconductor Company, PowerSmart, Inc.,
Toshiba Battery Co. Ltd., Unitrode Corporation, USAR Systems, Inc.

18 Disclaimer

Devices sold by Melexis are covered by the warranty and patent indemnification provisions appearing in its Term of Sale. Melexis makes no warranty, express, statutory, implied, or by description regarding the information set forth herein or regarding the freedom of the described devices from patent infringement. Melexis reserves the right to change specifications and prices at any time and without notice. Therefore, prior to designing this product into a system, it is necessary to check with Melexis for current information. This product is intended for use in normal commercial applications. Applications requiring extended temperature range, unusual environmental requirements, or high reliability applications, such as military, medical life-support or life-sustaining equipment are specifically not recommended without additional processing by Melexis for each application.
The information furnished by Melexis is believed to be correct and accurate. However, Melexis shall not be liable to recipient or any third party for any damages, including but not limited to personal injury, property damage, loss of profits, loss of use, interrupt of business or indirect, special incidental or consequential damages, of any kind, in connection with or arising out of the furnishing, performance or use of the technical data herein. No obligation or liability to recipient or any third party shall arise or flow out of Melexis' rendering of technical or other services.

For the latest version of this document, go to our website at
www.melexis.com

Or for additional information contact Melexis Direct:

Europe, Africa, Asia:	America:
Phone: +32 1367 0495	Phone: +1 603 223 2362
E-mail: sales_europe@melexis.com	E-mail: sales_usa@melexis.com

ISO/TS 16949 and ISO14001 Certified

[Appendix-B]

Infrared LED (LTE-5208A)

LITEON

LITE-ON ELECTRONICS, INC.

Property of Lite-On Only

FEATURES

* SELECTED TO SPECIFIC ON-LINE INTENSITY AND RADIANT INTENSITY RANGES
* LOW COST MINIATURE PLASTIC END LOOKING PACKAGE
* MECHANICALLY AND SPECTRALLY MATCHED TO THE LTR-3208 SERIES OF PHOTOTRANSISTOR
* CLEAR TRANSPARENT COLOR PACKAGE

PACKAGE DIMENSIONS

5.0 (.197)

8.6 (.34)

1.0 (.04)

SEE NOTE 3

3 DIA. (.118)

5.85 (.23)

22.0MIN. (.866)

□0.5 TYP. (.02)

1.0 MON. (.04)

2.54NOM. (.1) (SEE NOTE 4)

DOT DENOTES CATHODE

A ──▷|── K
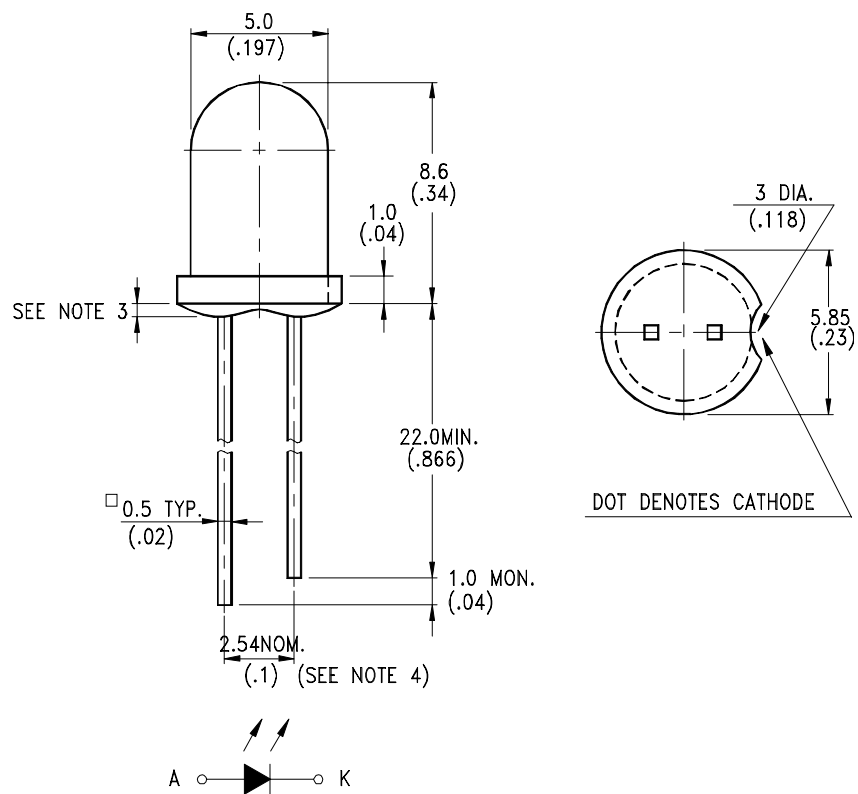
NOTES:
1. All dimensions are in millimeters (inches).
2. Tolerance is ± 0.25mm(.010") unless otherwise noted.
3. Protruded resin under flange is 1.5mm(.059") max.
4. Lead spacing is measured where the leads emerge from the package.
5. Specifications are subject to change without notice.

ABSOLUTE MAXIMUM RATINGS AT TA=25℃

PARAMETER	MAXIMUM RATING	UNIT
Power Dissipation	150	mW
Peak Forward Current (300pps, 10 μ s pulse)	2	A
Continuous Forward Current	100	mA
Reverse Voltage	5	V
Operating Temperature Range	-40℃ to + 85℃	
Storage Temperature Range	-55℃ to + 100℃	
Lead Soldering Temperature [1.6mm(.063") From Body]	260℃ for 5 Seconds	

ELECTRICAL OPTICAL CHARACTERISTICS AT TA=25℃

PARAMETER	SYMBOL	MIN.	TYP.	MAX.	UNIT	TEST CONDITION	BIN NO.
Aperture Radiant Incidence	Ee	0.44		0.96	mW/cm²	$I_F = 20mA$	BIN A
		0.64		1.20			BIN B
		0.80		1.68			BIN C
		1.12					BIN D
Radiant Intensity	I_E	3.31		7.22	mW/sr	$I_F = 20mA$	BIN A
		4.81		9.02			BIN B
		6.02		12.63			BIN C
		8.42					BIN D
Peak Emission Wavelength	λ_{Peak}		940		nm	$I_F = 20mA$	
Spectral Line Half-Width	$\Delta \lambda$		50		nm	$I_F = 20mA$	
Forward Voltage	V_F		1.2	1.6	V	$I_F = 20mA$	
Reverse Current	I_R			100	μ A	$V_R = 5V$	
Viewing Angle (See FIG.6)	$2\theta_{1/2}$		40		deg.		

TYPICAL ELECTRICAL / OPTICAL CHARACTERISTICS CURVES

(25℃ Ambient Temperature Unless Otherwise Noted)
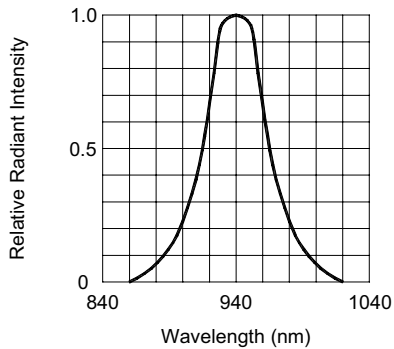
FIG.1 SPECTRAL DISTRIBUTION
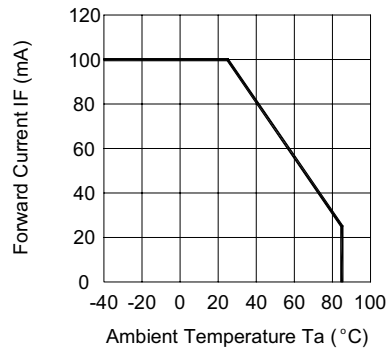
FIG.2 FORWARD CURRENT VS. AMBIENT TEMPERATURE
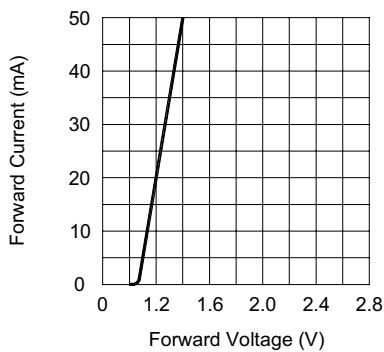
FIG.3 FORWARD CURRENT VS. FORWARD VOLTAGE
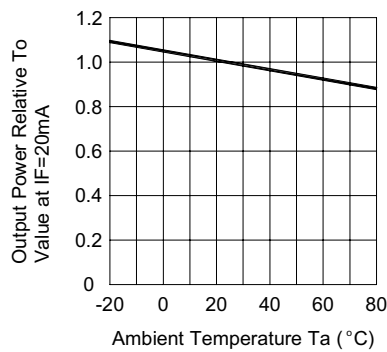
FIG.4 RELATIVE RADIANT INTENSITY VS. AMBIENT TEMPERATURE
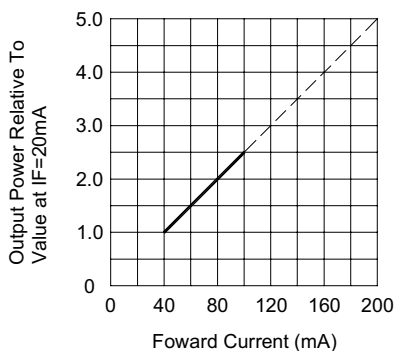
FIG.5 RELATIVE RADIANT INTENSITY VS. FORWARD CURRENT

FIG.6 RADIATION DIAGRAM

Part No. : LTE-5208A DATA SHEET   Page :   3   of   3

BNS-OD-C131/A4
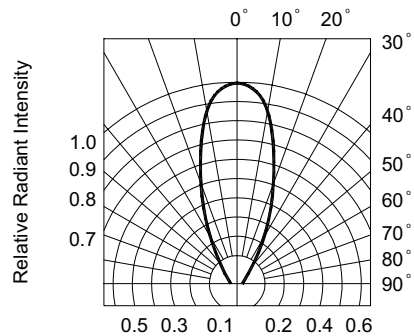
[Appendix-c]

Transistors (2N3904)

2N3903, 2N3904

2N3903 is a Preferred Device

General Purpose Transistors

NPN Silicon

ON Semiconductor™

http://onsemi.com

COLLECTOR
3

2
BASE

1
EMITTER

STYLE 1

TO–92
CASE 29
STYLE 1

MAXIMUM RATINGS

Rating	Symbol	Value	Unit
Collector–Emitter Voltage	V_{CEO}	40	Vdc
Collector–Base Voltage	V_{CBO}	60	Vdc
Emitter–Base Voltage	V_{EBO}	6.0	Vdc
Collector Current – Continuous	I_C	200	mAdc
Total Device Dissipation @ $T_A = 25°C$ Derate above 25°C	P_D	625 5.0	mW mW/°C
Total Device Dissipation @ $T_C = 25°C$ Derate above 25°C	P_D	1.5 12	Watts mW/°C
Operating and Storage Junction Temperature Range	T_J, T_{stg}	−55 to +150	°C

THERMAL CHARACTERISTICS (Note 1.)

Characteristic	Symbol	Max	Unit
Thermal Resistance, Junction to Ambient	$R_{\theta JA}$	200	°C/W
Thermal Resistance, Junction to Case	$R_{\theta JC}$	83.3	°C/W

1. Indicates Data in addition to JEDEC Requirements.

MARKING DIAGRAMS

2N
3903
YWW

2N
3904
YWW
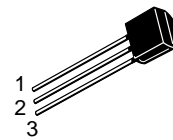
Y = Year
WW = Work Week

ORDERING INFORMATION

Device	Package	Shipping
2N3903	TO–92	5000 Units/Box
2N3903RLRM	TO–92	2000/Ammo Pack
2N3904	TO–92	5000 Units/Box
2N3904RLRA	TO–92	2000/Tape & Reel
2N3904RLRE	TO–92	2000/Tape & Reel
2N3904RLRM	TO–92	2000/Ammo Pack
2N3904RLRP	TO–92	2000/Ammo Pack
2N3904RL1	TO–92	2000/Tape & Reel
2N3904ZL1	TO–92	2000/Ammo Pack

Preferred devices are recommended choices for future use and best overall value.

ELECTRICAL CHARACTERISTICS (T_A = 25°C unless otherwise noted)

Characteristic		Symbol	Min	Max	Unit
OFF CHARACTERISTICS					
Collector–Emitter Breakdown Voltage (Note 2.) (I_C = 1.0 mAdc, I_B = 0)		$V_{(BR)CEO}$	40	–	Vdc
Collector–Base Breakdown Voltage (I_C = 10 μAdc, I_E = 0)		$V_{(BR)CBO}$	60	–	Vdc
Emitter–Base Breakdown Voltage (I_E = 10 μAdc, I_C = 0)		$V_{(BR)EBO}$	6.0	–	Vdc
Base Cutoff Current (V_{CE} = 30 Vdc, V_{EB} = 3.0 Vdc)		I_{BL}	–	50	nAdc
Collector Cutoff Current (V_{CE} = 30 Vdc, V_{EB} = 3.0 Vdc)		I_{CEX}	–	50	nAdc
ON CHARACTERISTICS					
DC Current Gain (Note 2.)		h_{FE}			–
(I_C = 0.1 mAdc, V_{CE} = 1.0 Vdc)	2N3903		20	–	
	2N3904		40	–	
(I_C = 1.0 mAdc, V_{CE} = 1.0 Vdc)	2N3903		35	–	
	2N3904		70	–	
(I_C = 10 mAdc, V_{CE} = 1.0 Vdc)	2N3903		50	150	
	2N3904		100	300	
(I_C = 50 mAdc, V_{CE} = 1.0 Vdc)	2N3903		30	–	
	2N3904		60	–	
(I_C = 100 mAdc, V_{CE} = 1.0 Vdc)	2N3903		15	–	
	2N3904		30	–	
Collector–Emitter Saturation Voltage (Note 2.)		$V_{CE(sat)}$			Vdc
(I_C = 10 mAdc, I_B = 1.0 mAdc)			–	0.2	
(I_C = 50 mAdc, I_B = 5.0 mAdc			–	0.3	
Base–Emitter Saturation Voltage (Note 2.)		$V_{BE(sat)}$			Vdc
(I_C = 10 mAdc, I_B = 1.0 mAdc)			0.65	0.85	
(I_C = 50 mAdc, I_B = 5.0 mAdc)			–	0.95	
SMALL–SIGNAL CHARACTERISTICS					
Current–Gain – Bandwidth Product		f_T			MHz
(I_C = 10 mAdc, V_{CE} = 20 Vdc, f = 100 MHz)	2N3903		250	–	
	2N3904		300	–	
Output Capacitance (V_{CB} = 5.0 Vdc, I_E = 0, f = 1.0 MHz)		C_{obo}	–	4.0	pF
Input Capacitance (V_{EB} = 0.5 Vdc, I_C = 0, f = 1.0 MHz)		C_{ibo}	–	8.0	pF
Input Impedance		h_{ie}			k Ω
(I_C = 1.0 mAdc, V_{CE} = 10 Vdc, f = 1.0 kHz)	2N3903		1.0	8.0	
	2N3904		1.0	10	
Voltage Feedback Ratio		h_{re}			X 10^{-4}
(I_C = 1.0 mAdc, V_{CE} = 10 Vdc, f = 1.0 kHz)	2N3903		0.1	5.0	
	2N3904		0.5	8.0	
Small–Signal Current Gain		h_{fe}			–
(I_C = 1.0 mAdc, V_{CE} = 10 Vdc, f = 1.0 kHz)	2N3903		50	200	
	2N3904		100	400	
Output Admittance (I_C = 1.0 mAdc, V_{CE} = 10 Vdc, f = 1.0 kHz)		h_{oe}	1.0	40	μmhos
Noise Figure		NF			dB
(I_C = 100 μAdc, V_{CE} = 5.0 Vdc, R_S = 1.0 k Ω, f = 1.0 kHz)	2N3903		–	6.0	
	2N3904		–	5.0	

SWITCHING CHARACTERISTICS

		Symbol	Min	Max	Unit
Delay Time	(V_{CC} = 3.0 Vdc, V_{BE} = 0.5 Vdc, I_C = 10 mAdc, I_{B1} = 1.0 mAdc)	t_d	–	35	ns
Rise Time		t_r	–	35	ns
Storage Time	(V_{CC} = 3.0 Vdc, I_C = 10 mAdc, I_{B1} = I_{B2} = 1.0 mAdc) — 2N3903	t_s	–	175	ns
	2N3904		–	200	
Fall Time		t_f	–	50	ns

2. Pulse Test: Pulse Width ≤ 300 μs; Duty Cycle ≤ 2%.

2N3903, 2N3904
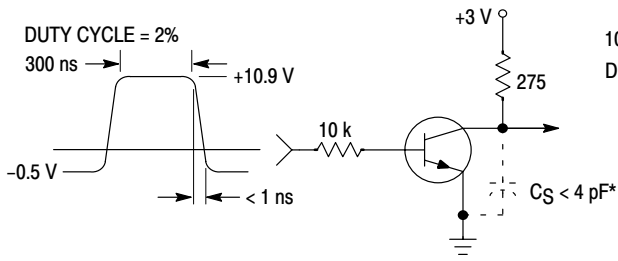
Figure 1. Delay and Rise Time Equivalent Test Circuit

* Total shunt capacitance of test jig and connectors
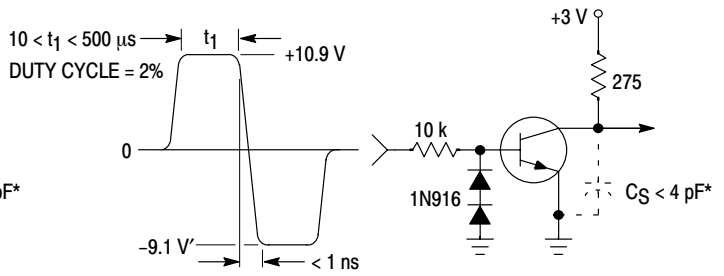
Figure 2. Storage and Fall Time Equivalent Test Circuit

TYPICAL TRANSIENT CHARACTERISTICS
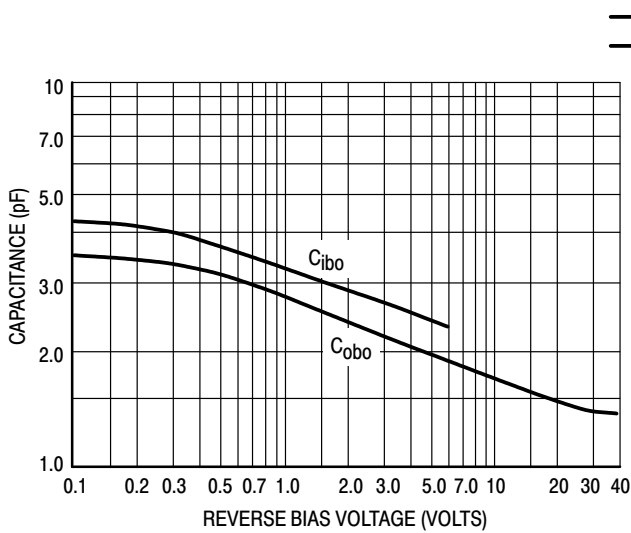
$T_J = 25°C$
$T_J = 125°C$

Figure 3. Capacitance
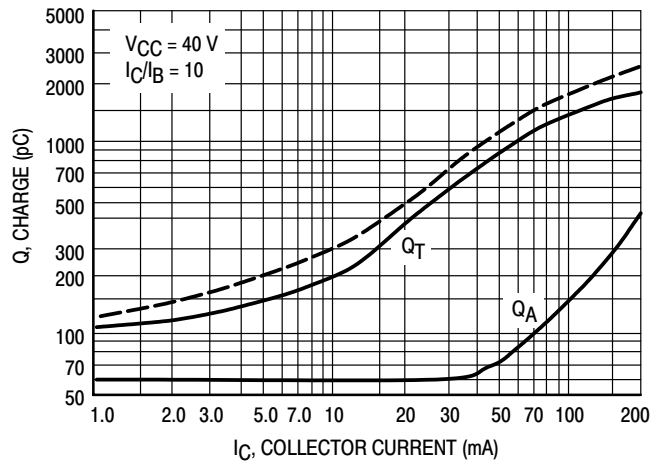
Figure 4. Charge Data
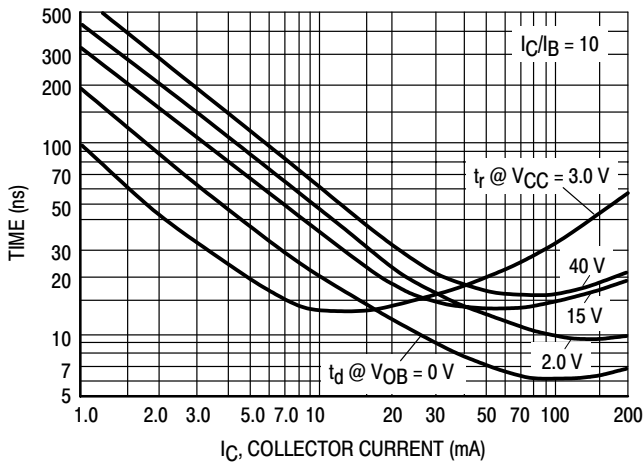
Figure 5. Turn−On Time
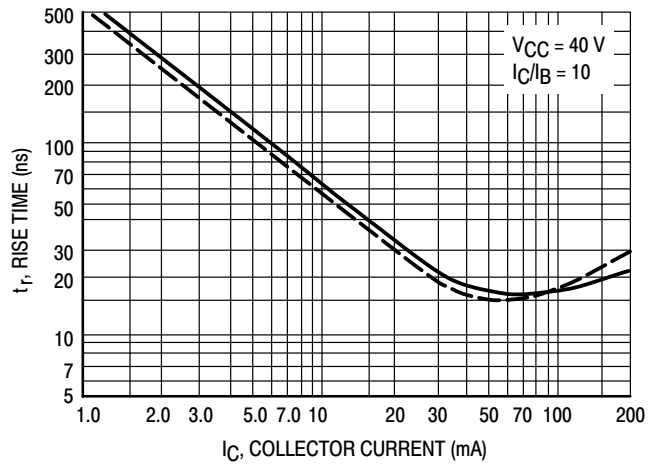
Figure 6. Rise Time
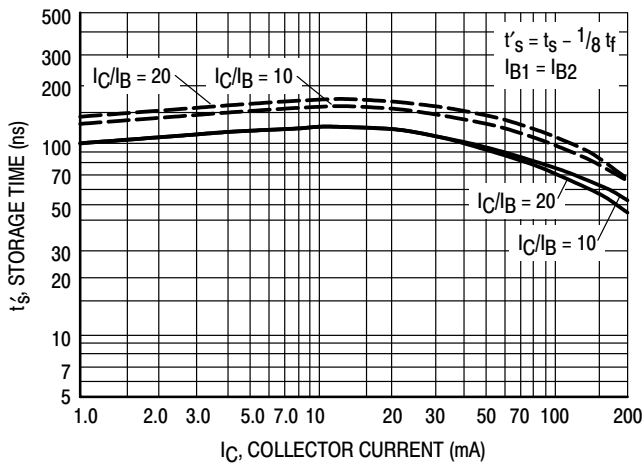
Figure 7. Storage Time
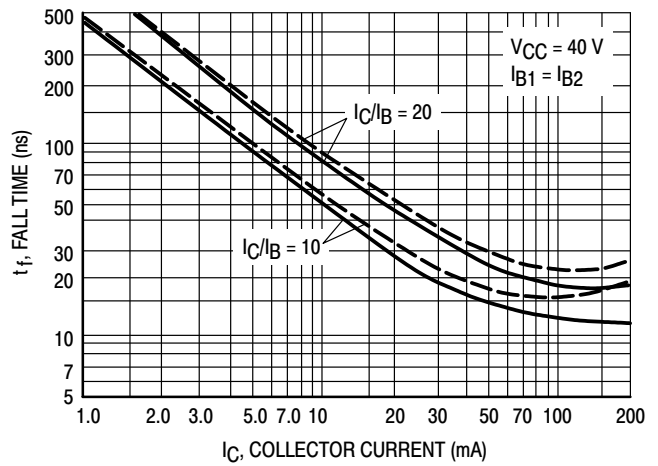
Figure 8. Fall Time

TYPICAL AUDIO SMALL−SIGNAL CHARACTERISTICS
NOISE FIGURE VARIATIONS

(V_{CE} = 5.0 Vdc, T_A = 25°C, Bandwidth = 1.0 Hz)
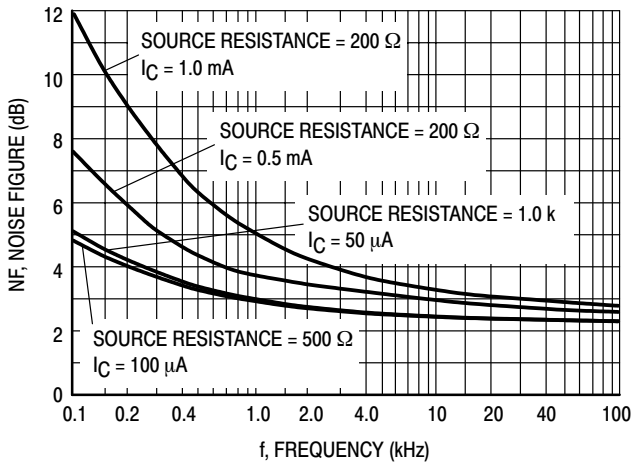
Figure 9.
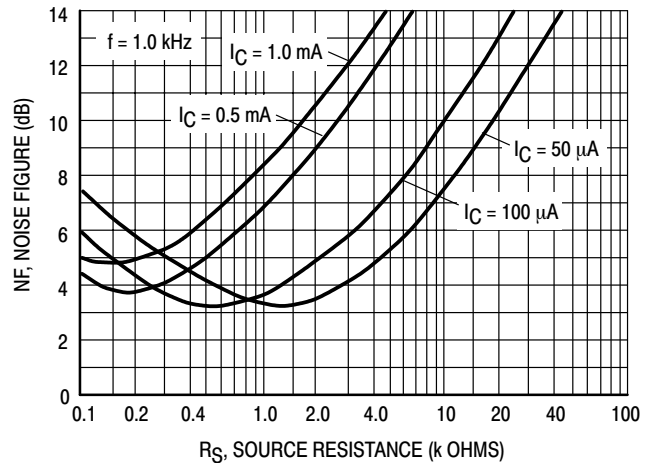
Figure 10.

h PARAMETERS

(V_{CE} = 10 Vdc, f = 1.0 kHz, T_A = 25°C)
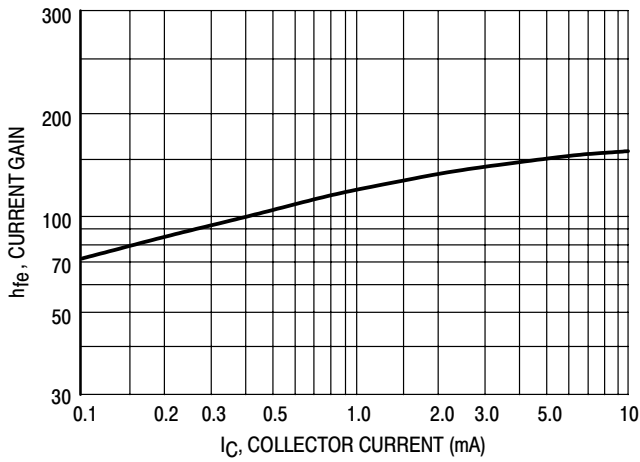
Figure 11. Current Gain
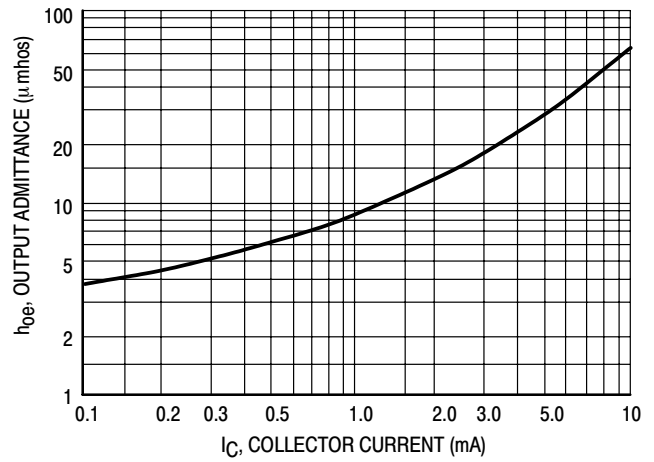
Figure 12. Output Admittance
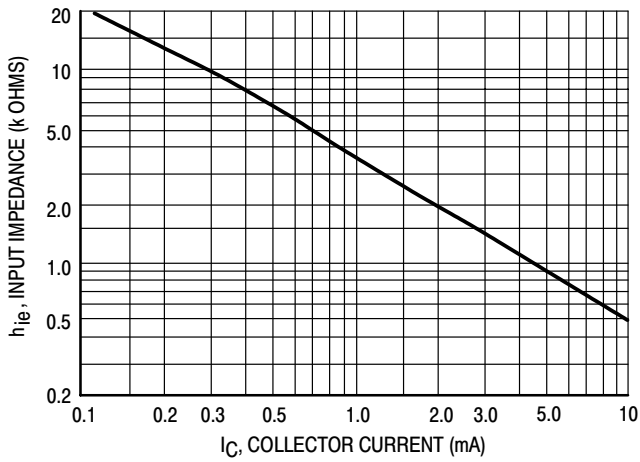
Figure 13. Input Impedance
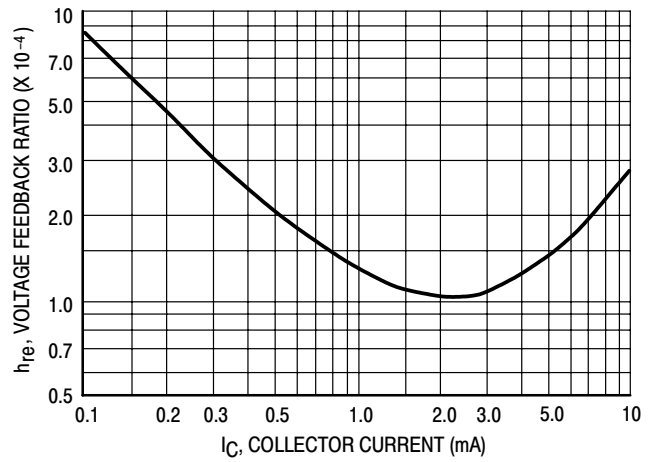
Figure 14. Voltage Feedback Ratio

2N3903, 2N3904

TYPICAL STATIC CHARACTERISTICS
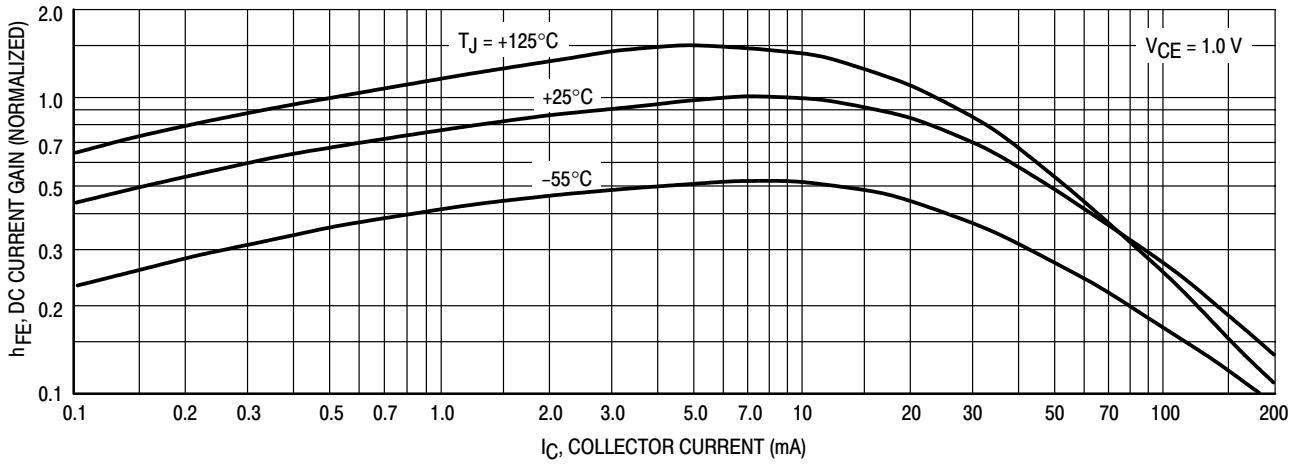
Figure 15. DC Current Gain
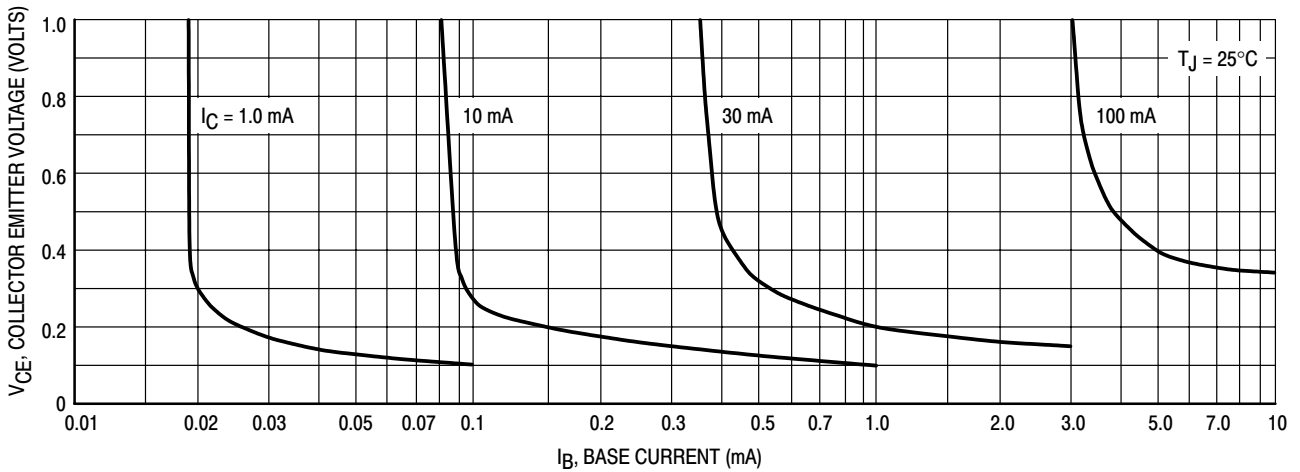
Figure 16. Collector Saturation Region
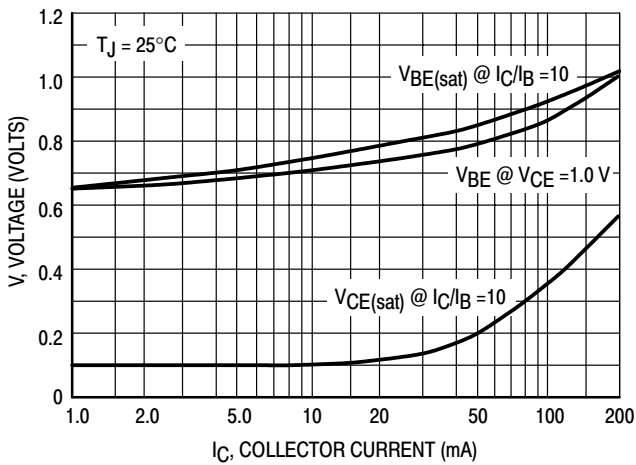
Figure 17. "ON" Voltages
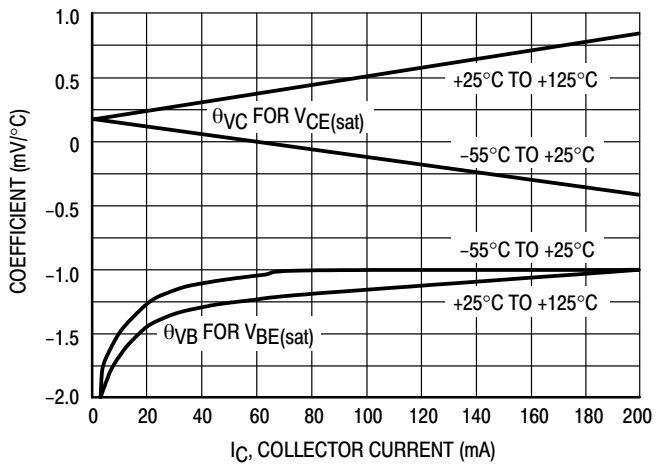
Figure 18. Temperature Coefficients

PACKAGE DIMENSIONS

TO–92
TO–226AA
CASE 29–11
ISSUE AL

SECTION X–X
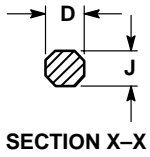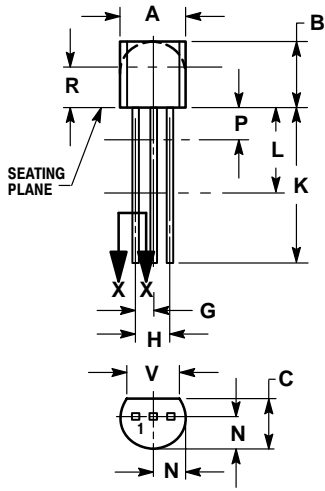
NOTES:
1. DIMENSIONING AND TOLERANCING PER ANSI Y14.5M, 1982.
2. CONTROLLING DIMENSION: INCH.
3. CONTOUR OF PACKAGE BEYOND DIMENSION R IS UNCONTROLLED.
4. LEAD DIMENSION IS UNCONTROLLED IN P AND BEYOND DIMENSION K MINIMUM.

DIM	INCHES		MILLIMETERS	
	MIN	MAX	MIN	MAX
A	0.175	0.205	4.45	5.20
B	0.170	0.210	4.32	5.33
C	0.125	0.165	3.18	4.19
D	0.016	0.021	0.407	0.533
G	0.045	0.055	1.15	1.39
H	0.095	0.105	2.42	2.66
J	0.015	0.020	0.39	0.50
K	0.500	---	12.70	---
L	0.250	---	6.35	---
N	0.080	0.105	2.04	2.66
P	---	0.100	---	2.54
R	0.115	---	2.93	---
V	0.135	---	3.43	---

STYLE 1:
PIN 1. EMITTER
    2. BASE
    3. COLLECTOR

STYLE 14:
PIN 1. EMITTER
    2. COLLECTOR
    3. BASE

[Appendix-D]

Red LED (SSL-X5093SRC)

UNCONTROLLED DOCUMENT

PART NUMBER | REV.
SSL-LX5093SRC/X | D

REV.	E.C.N. NUMBER AND REVISION COMMENTS	DATE
A	UPDATED SPECS.	1.5.95
B	E.C.N. #10251.	9.30.96
C	E.C.N. #10BRDR. & REDRAWN IN 3D.	5.31.01
D	E.C.N. #10788.	9.13.01
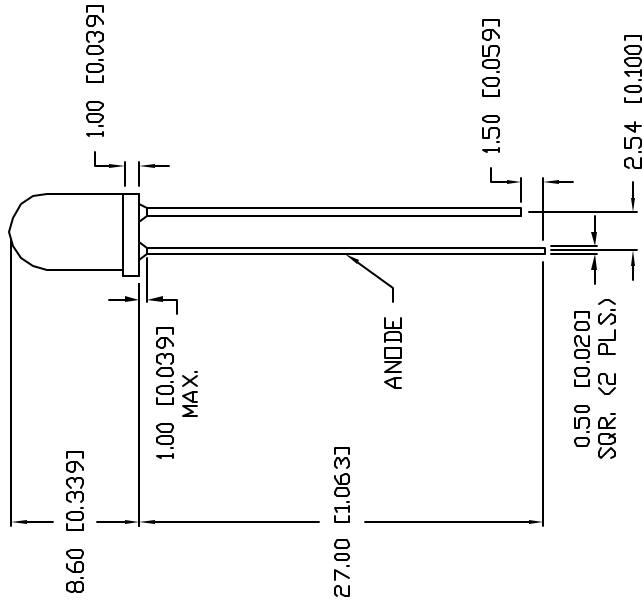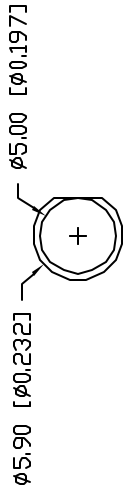
ELECTRO-OPTICAL CHARACTERISTICS $T_A=25°C$ $I_f=20mA$

PARAMETER		MIN	TYP	MAX	UNITS	TEST COND
PEAK WAVELENGTH			660		nm	$I_f=20mA$
FORWARD VOLTAGE			1.7	2.2	Vf	$I_f=20mA$
REVERSE VOLTAGE		4.0			Vr	$I_r=100\mu A$
AXIAL INTENSITY	/DU	1000	1200		mcd	$I_f=20mA$
	/DV	1300	1500		mcd	$I_f=20mA$
	/DW	1600	1800		mcd	$I_f=20mA$
	/E	2000	2800		mcd	$I_f=20mA$
	/F	3500	4000		mcd	$I_f=20mA$
VIEWING ANGLE			30		2x theta	

EMITTED COLOR: RED
EPOXY LENS FINISH: WATER CLEAR

LIMITS OF SAFE OPERATION AT 25°C

PARAMETER	MAX	UNITS
PEAK FORWARD CURRENT*	150	mA
STEADY CURRENT	30	mA
POWER DISSIPATION	100	mW
DERATE FROM 25°C	-1.2	mW/°C
OPERATING, STORAGE TEMP.	-40 TO +85	°C
SOLDERING TEMP.	+260	°C
2.0mm FROM BODY		3 SEC. MAX

* t<10µS

ø5.90 [ø0.232]
ø5.00 [ø0.197]
+
1.00 [0.039]
8.60 [0.339]
1.00 [0.039] MAX.
27.00 [1.063]
ANODE
1.50 [0.059]
2.54 [0.100]
0.50 [0.020] SQR. (2 PLS.)

REPLACES PART #: SSL-LX5093SRC(/B-/E)

*UNLESS OTHERWISE SPECIFIED TOLERANCES PER DECIMAL PRECISION ARE: X=±1 (±0.039), X.X=±0.5 (±0.020), X.XX=±0.25 (±0.010), X.XXX=±0.127 (±0.005). LEAD SIZE=±0.05 (±0.002), LEAD LENGTH=±0.75 (±0.030). MIN=+0.00 DECIMAL PRECISION MAX.=-0.00

DRAWN BY:	CHECKED BY:	APPROVED BY:	DATE:	2.9.93
	BC		PAGE:	1 OF 1
			SCALE:	N/A

UNCONTROLLED DOCUMENT

REV.	PART NUMBER	
D	SSL-LX5093SRC/X	

T-5mm (T-1 3/4) 660nm SUPER RED LED, WATER CLEAR LENS.

[Appendix-E]

Phototransistor (IC-LQNP)

iC-LQNP
PULSE AND AC LIGHT SENSOR

FEATURES

♦ Fast response amplifier with on-chip photodiode

♦ High interference immunity due to monolithic design

♦ Active photodiode area of ca. 1 mm²

♦ Suitable for visible light and near infrared

♦ Integrated band-pass filter with 140 kHz center frequency

♦ Maximum gain obtained for pulse light of 1.4 µs and upwards

♦ High LF and DC (ambient) light suppression

♦ Transfer characteristics irrespective of ambient light level

♦ Soft signal and noise limiter with excess ambient light

♦ Fast recovery from flashes

♦ Complementary analogue current source outputs, transimpedance can be set by external resistor

♦ Single 5 to 12 V supply, low power consumption also with bright ambient light

♦ **Options:** customised COB versions

APPLICATIONS

♦ Receiver for through beam and reflection light barriers with background suppression (sunlight) e.g. for presence detection in power operated gates, doors and windows etc.

PACKAGES
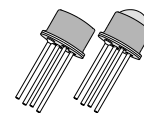
TO18-4F/L   cDFN6

oBGA LQ1C

BLOCK DIAGRAM
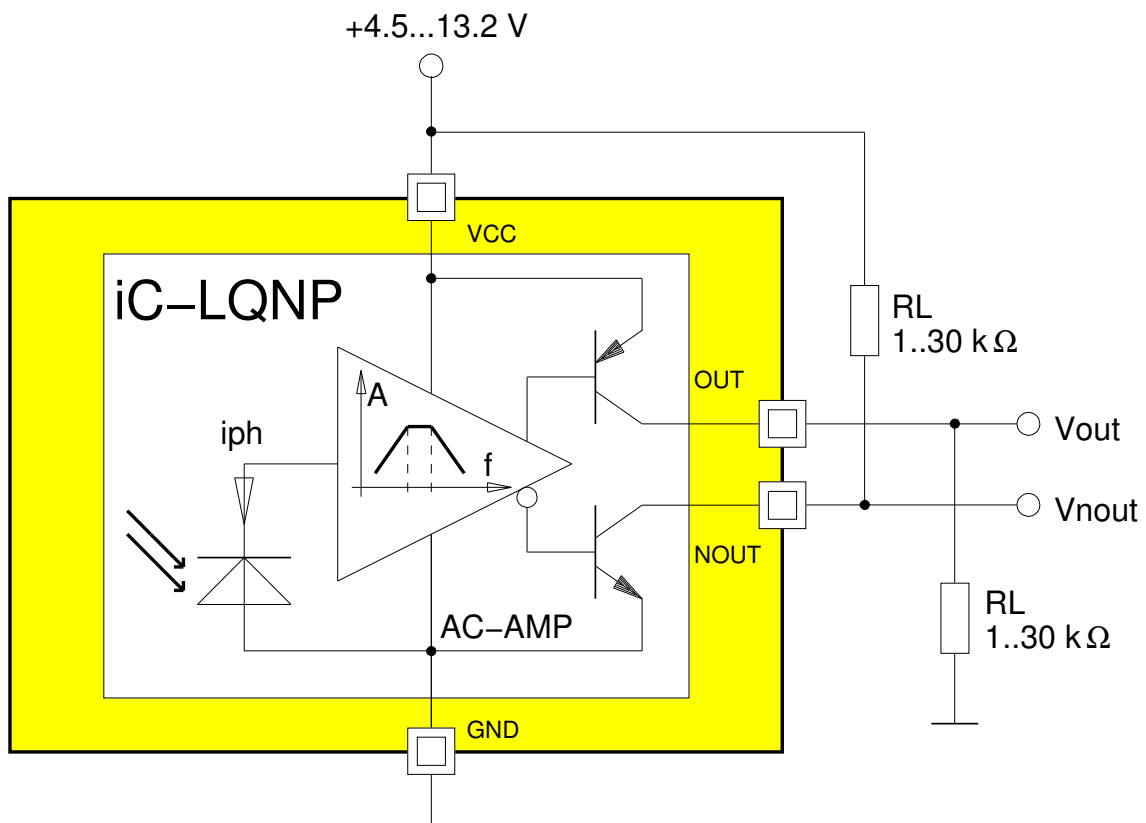
iC-LQNP
PULSE AND AC LIGHT SENSOR

DESCRIPTION

iC-LQNP is a sensor for pulse and alternating light with a monolithically integrated photodiode. The device supersedes conventional photoreceivers, such as those in light barriers, for example.

Changes in the photocurrent are amplified whereas the photocurrents caused by background light are electronically suppressed with over 60 dB (at 100 Hz).

The integrated amplifier forms a band-pass characteristic without using any external components. The high pass filter suppresses ambient light and low frequency alternating light and the low pass filter reduces high frequency noise.

For visible light or near infrared the highest sensitivity for alternating light signals is reached at approximately 140 kHz; for pulse light this is reached at 1.4 µs and upwards.

The transimpedance can be selected within a range of approximately 1 to 10 MΩ via the external load resistor.

iC-LQNP is available as a 4-lead TO18 metal can package with a glass lens or flat window. Customised COB versions are also possible.

iC-LQNP
PULSE AND AC LIGHT SENSOR

PACKAGES TO18-4F/L, cDFN6, oBGA LQ1C

PIN CONFIGURATION TO18-4F/L

photosensitive
area
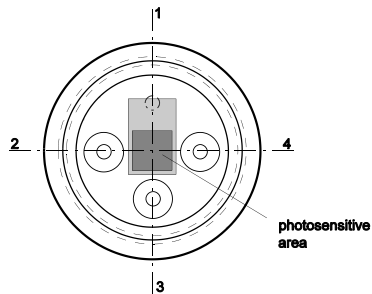
PIN FUNCTIONS

No.	Name	Function
1	GND	Ground
2	OUT	High-Side Current Output
3	VCC	+4.5 to +13.2 V Supply Voltage
4	NOUT	Low-Side Current Output

PIN CONFIGURATION cDFN6 3 mm x 3 mm
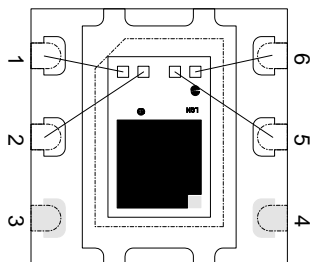
PIN FUNCTIONS

No.	Name	Function
1	GND	Ground
2	OUT	High-Side Current Output
3	n.c.	
4	n.c.	
5	NOUT	Low-Side Current Output
6	VCC	+4.5 to +13.2 V Supply Voltage

PIN CONFIGURATION oBGA LQ1C
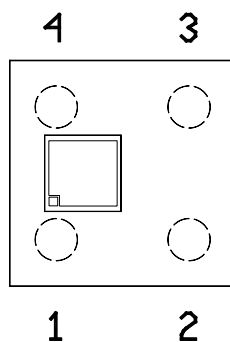
PIN FUNCTIONS

No.	Name	Function
1	GND	Ground
2	VCC	+4.5 to +13.2 V Supply Voltage
3	OUT	High-Side Current Output
4	GND	Ground

iC-LQNP
PULSE AND AC LIGHT SENSOR

ABSOLUTE MAXIMUM RATINGS

Beyond these values damage may occur; device operation is not guaranteed.

Item No.	Symbol	Parameter	Conditions	Min.	Max.	Unit
G001	VCC	Supply Voltage		0	15	V
G002	I()	Output Current		-4	4	mA
G003	Vd()	ESD susceptibility at all pins	HBM, 100 pF discharged through 1.5 kΩ		1.5	kV
G004	Tj	Junction Temperature		-40	150	°C
G005	Ts	Storage Temperature	see package specifications			

THERMAL DATA

Operating Conditions: VCC = 4.5...13.2 V

Item No.	Symbol	Parameter	Conditions	Min.	Typ.	Max.	Unit
T01	Ta	Operating Ambient Temperature Range	cDFN6 for other packages, see relevant package specifications	-20		85	°C
T02	Tpk	Peak Temperature cDFN6	tpk < 10 s, convection reflow MSL6, TOL (max. floor life 8 h at 30 °C and 60% RH) See Customer Information #7 for detailed information.			245	°C

All voltages are referenced to ground unless otherwise stated.
All currents into the device pins are positive; all currents out of the device pins are negative.

iC-LQNP
PULSE AND AC LIGHT SENSOR

ELECTRICAL CHARACTERISTICS

Operating Conditions: VCC = 4.5...13.2 V, R1 = 10 kΩ, CL = 20 pF, λ = 875 nm, Tj = -25...125 °C, if not otherwise stated.

Item No.	Symbol	Parameter	Conditions	Min.	Typ.	Max.	Unit
Total Device							
001	VCC	Permissible Supply Voltage		4.5		13.2	V
002	I(VCC)	Supply Current	E(PD) = 0 E(PD)ac = 0, E(PD)pk = 0, E(PD)cw = 30 mW/cm², no load	0.4	0.8	1.4 2	mA mA
003	Vs(OUT)	Output Saturation Voltage at OUT	I() = -1 mA, Vs(OUT) = VCC − V(OUT)			0.5	V
004	Vs(NOUT)	Output Saturation Voltage at NOUT	I() = 1 mA			0.5	V
005	I()	Permissible Output Current in NOUT, OUT	I(NOUT) I(OUT)	0 -2		2 0	mA mA
006	I0()	Output Bias Current in OUT	E(PD) = 0 E(PD) = 0, VCC = 5 V, Tj = 27 °C	-235	-145	-105	µA µA
007	I0()	Output Bias Current in NOUT	E(PD) = 0 E(PD) = 0, VCC = 5 V, Tj = 27 °C	105	145	235	µA µA
008	Vc()hi	Output Clamp Voltage hi	Vc()hi = V(OUT) − VCC, VCC = 0V, I() = 4 mA	0.25	0.5	1.4	V
009	Vc()lo	Output Clamp Voltage lo	I() = -4 mA	-1.4	-0.5	-0.25	V
Photodiode							
101	Aph()	Radiant Sensitive Area			1		mm²
102	S(λ)max	Spectral Sensitivity			0.5		A/W
103	λ_{ar}	Spectral Application Range	Se(λ_{ar}) = 0.1 × S(λ)max	500		1050	nm
Photocurrent Amplifier							
201	E()cw	Permissible DC Irradiance	λ_{LED} für S(λ)max, iC-LQNP Chip			30	mW/cm²
202	Ev()cw	Ambient Light Susceptibility	standard illuminant A, T = 2856 K; TO18-4F TO18-4L		50 7		mW/cm² mW/cm²
203	Ev()cw	Ambient Light Susceptibility	standard illuminant A, T = 2856 K; TO18-4F TO18-4L		70 10		klx klx
204	E()pk	Permissible Peak Irradiance	|I((N)OUT)| increases or remains constant as E()pk increases; chip, TO18-4F TO18-4L			100 15	mW/cm² mW/cm²
205	Gpk	Pulse Light Amplification 875 nm	VCC = 5 V, E(PD)pk = 35 µW/cm², tr = tf = 0.1 µs, twpk = 1.4 µs; chip, TO18-4F TO18-4L	100 700	220 1540	350 2500	A/W A/W
206	Gpk	Pulse Light Amplification 850 nm	see 205; chip, TO18-4F TO18-4L		250 1800		A/W A/W
207	Δt()	Output Current Delay	see 205, |I((N)OUT)|: 0 → 50% peak value			1.5	µs
208	trec	Recovery Time	see 205, settled better 10% to initial quiescent point			15	µs
209	trec	Power Flash Recovery Time	E(PD)pk = 35 mW/cm², twpk = 100 µs			60	µs
210	Gac	AC Light Amplification	f = fc, E(PD)ac = 35 µW/cm²; Chip, TO18-4F TO18-4L		400 2800		A/W A/W
211	fc	Bandpass Center Frequency	Rl = 1 kΩ, CL = 20 pF Rl = 10 kΩ, CL = 20 pF		140 120		kHz kHz
212	fhc	Upper Cut-off Frequency (-3 dB)	R1 = 1 kΩ, CL = 20 pF R1= 10 kΩ, CL = 20 pF		400 360		kHz kHz

iC-LQNP
PULSE AND AC LIGHT SENSOR

ELECTRICAL CHARACTERISTICS

Operating Conditions: VCC = 4.5...13.2 V, R1 = 10 kΩ, CL = 20 pF, λ = 875 nm, Tj = -25...125 °C, if not otherwise stated.

Item No.	Symbol	Parameter	Conditions	Min.	Typ.	Max.	Unit
213	flc	Lower Cut-off Frequency (-3 dB)	R1 = 1 kΩ, CL = 20 pF R1 = 10 kΩ, CL = 20 pF		40 35		kHz kHz
214	Q	Filter Q-Factor	Q = fc / (fhc - flc); R1 = 1 kΩ, CL = 20 pF R1 = 10 kΩ, CL = 20 pF		0.65 0.65		
215	G100	LF Suppression	f = 100 Hz		60		dB
216	Vn()	Output Noise Voltage (RMS)	VCC = 5 V, E(PD) = 0 VCC = 5 V, Ev(PD)dc ca. 15.000 lx, standard illuminant A, T = 2856 K, chip		7 20		mV mV
217	ton(VCC)	Power-On Setup Time	Tj = -25...70 °C			450	µs

iC-LQNP
PULSE AND AC LIGHT SENSOR

CHARACTERISTICS: Diagrams
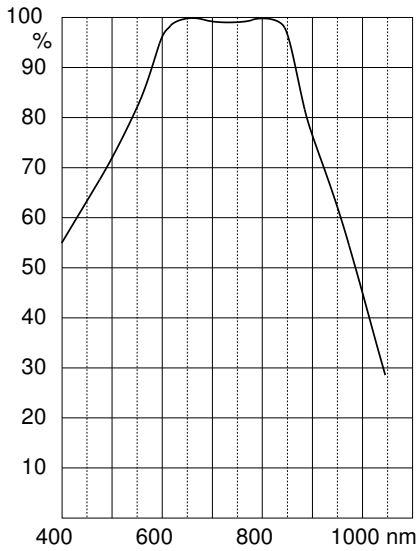
Figure 1: Typical relative spectral sensitivity
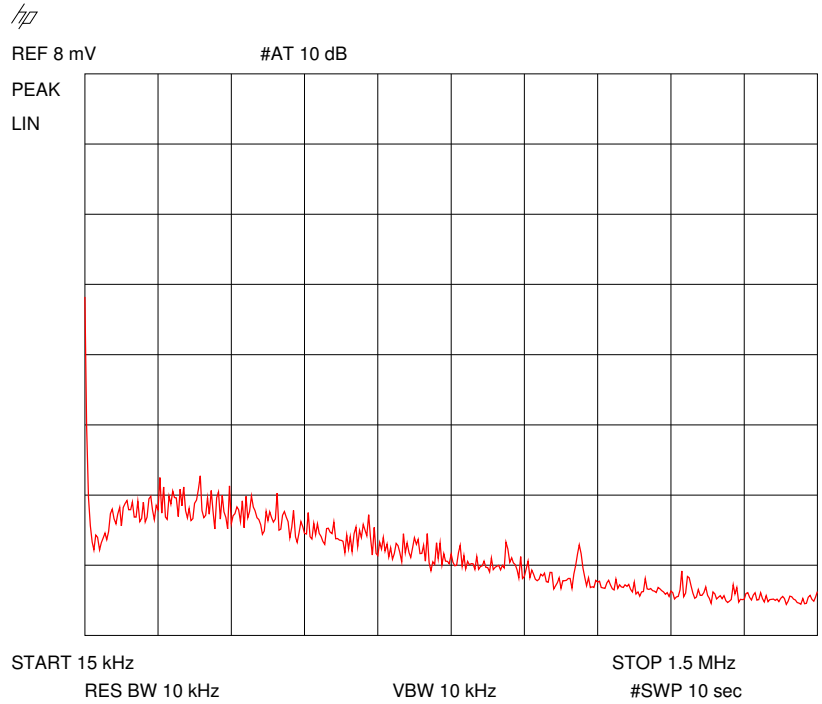
Figure 2: Output voltage noise [mV/$\sqrt{10\,\text{kHz}}$] to 10 kΩ/20 pF load with Ev()dc < 500 lx
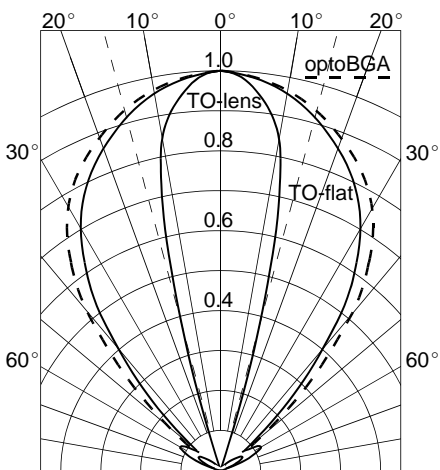
Figure 3: Typical directional characteristics for TO18 and opto-BGA™ packages
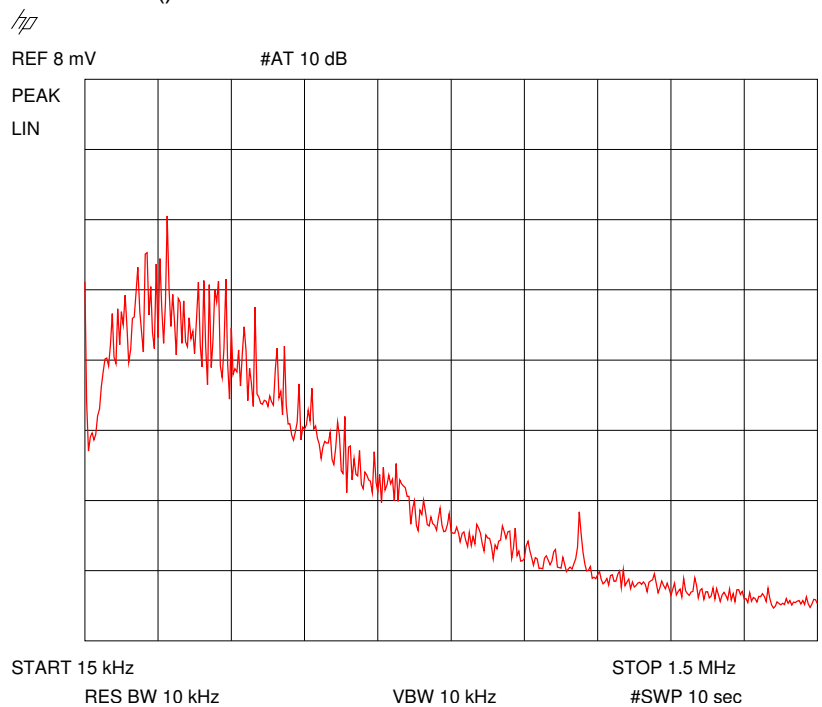
Figure 4: Output voltage noise [mV/$\sqrt{10\,\text{kHz}}$] to 10 kΩ/20 pF load with Ev()dc ca. 15.000 lx (standard illuminant A, T = 2856 K)

iC-LQNP
PULSE AND AC LIGHT SENSOR

APPLICATION HINTS

Example Output Signals
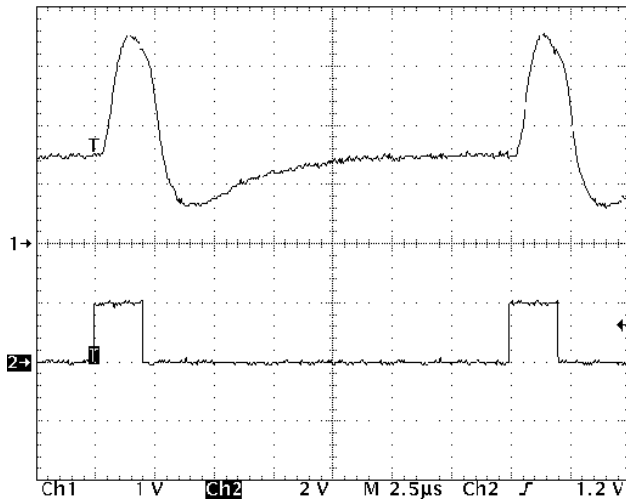
Figure 5: Output signal for 2 μs pulse light.
Transmitter: LED 875 nm with tr = tf = 0.1 μs;
VCC = 5 V, R1 = 10 kΩ, CL = 20 pF;
Chan 1: V(OUT), 1 V/DIV vertically,
Chan 2: I(LED), 20 mA/DIV vertically
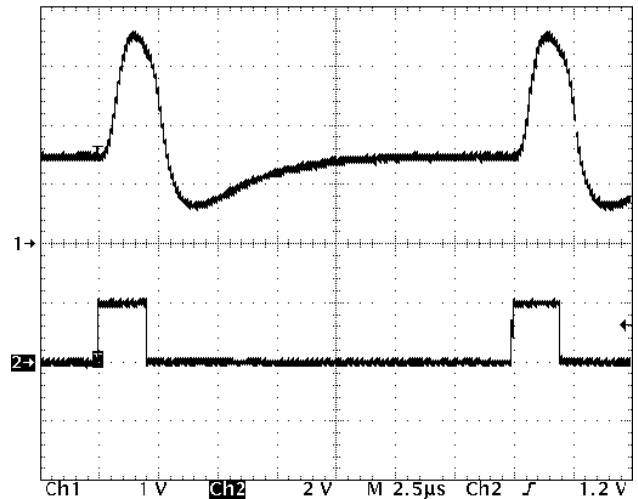
Figure 6: Output signal for 2 μs pulse light with noise
(accumulated over 256 samples)
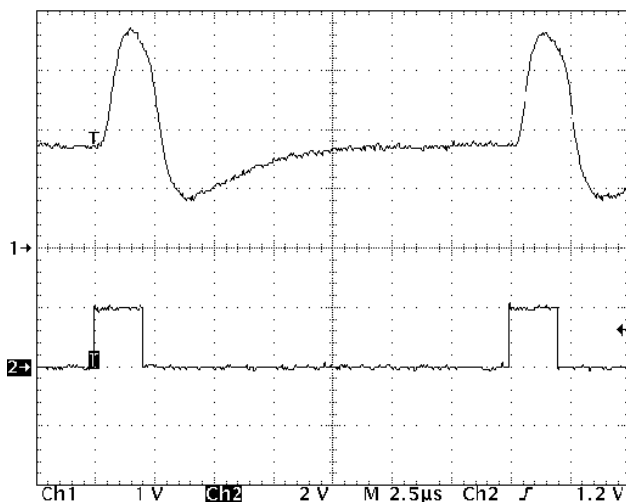
Figure 7: Output signal for 2 μs pulse light, superimposed by ambient light of approx. 15000 Lux
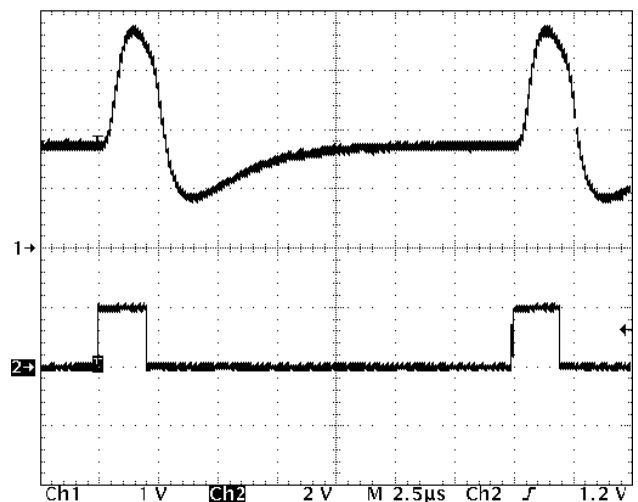
Figure 8: As in Fig. 7, accumulated for visibility over 256 samples. Despite of bright ambient light condition noise remains low level.
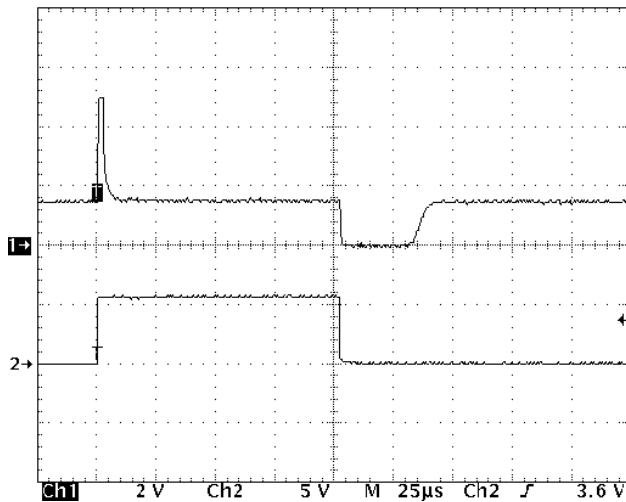
Figure 9: Recovery after 100 µs power pulse; back to ready-to-receive state after approx. 35 µs; Chan 1: V(OUT), 2 V/DIV vertically

ORDERING INFORMATION

Type	Package	Order Designation
iC-LQNP	TO18-4L	iC-LQNP TO18-4L
	TO18-4F	iC-LQNP TO18-4F
	cDFN6	iC-LQNP cDFN6
	oBGA LQ1C	iC-LQ oBGA LQ1C
	-	iC-LQNP chip

For technical support, information about prices and terms of delivery please contact:

iC-Haus GmbH   **Tel.: +49 (61 35) 92 92-0**
Am Kuemmerling 18   **Fax: +49 (61 35) 92 92-192**
D-55294 Bodenheim   **Web: http://www.ichaus.com**
GERMANY   **E-Mail: sales@ichaus.com**

Appointed local distributors: http://www.ichaus.de/support_distributors.php

[Appendix-F]

Amplifier (AD822)

ANALOG DEVICES

Single Supply, Rail-to-Rail
Low Power FET-Input Op Amp

AD822

FEATURES
TRUE SINGLE SUPPLY OPERATION
  Output Swings Rail to Rail
  Input Voltage Range Extends Below Ground
  Single Supply Capability from +3 V to +36 V
  Dual Supply Capability from ±1.5 V to ±18 V
HIGH LOAD DRIVE
  Capacitive Load Drive of 350 pF, G = 1
  Minimum Output Current of 15 mA
EXCELLENT AC PERFORMANCE FOR LOW POWER
  800 μA Max Quiescent Current per Amplifier
  Unity Gain Bandwidth: 1.8 MHz
  Slew Rate of 3.0 V/μs
GOOD DC PERFORMANCE
  800 μV Max Input Offset Voltage
  2 μV/°C Typ Offset Voltage Drift
  25 pA Max Input Bias Current
LOW NOISE
  13 nV/√Hz @ 10 kHz
NO PHASE INVERSION

APPLICATIONS
Battery Powered Precision Instrumentation
Photodiode Preamps
Active Filters
12- to 14-Bit Data Acquisition Systems
Medical Instrumentation
Low Power References and Regulators

PRODUCT DESCRIPTION
The AD822 is a dual precision, low power FET input op
amp that can operate from a single supply of +3.0 V to 36 V,
or dual supplies of ±1.5 V to ±18 V. It has true single supply
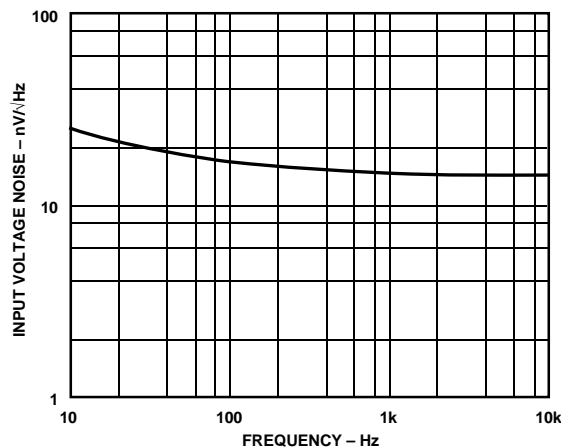
CONNECTION DIAGRAM
8-Pin Plastic DIP, Cerdip and SOIC

OUT1	1	8 V+
–IN1	2	7 OUT2
+IN1	3	6 –IN2
V–	4	5 +IN2
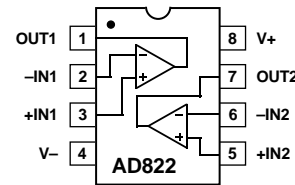
AD822

capability with an input voltage range extending below the
negative rail, allowing the AD822 to accommodate input signals
below ground in the single supply mode. Output voltage swing
extends to within 10 mV of each rail providing the maximum
output dynamic range.

Offset voltage of 800 μV max, offset voltage drift of 2 μV/°C,
input bias currents below 25 pA and low input voltage noise
provide dc precision with source impedances up to a Gigaohm.
1.8 MHz unity gain bandwidth, –93 dB THD at 10 kHz and
3 V/μs slew rate are provided with a low supply current of
800 μA per amplifier. The AD822 drives up to 350 pF of direct
capacitive load as a follower, and provides a minimum output
current of 15 mA. This allows the amplifier to handle a wide
range of load conditions. This combination of ac and dc
performance, plus the outstanding load drive capability, results
in an exceptionally versatile amplifier for the single supply user.

The AD822 is available in four performance grades. The A and
B grades are rated over the industrial temperature range of
–40°C to +85°C. There is also a 3 volt grade—the AD822A-3V,
rated over the industrial temperature range. The mil grade is
rated over the military temperature range of –55°C to +125°C
and is available processed on standard military drawing.

The AD822 is offered in three varieties of 8-pin package: plastic
DIP, hermetic cerdip and surface mount (SOIC) as well as die
form.

Input Voltage Noise vs. Frequency
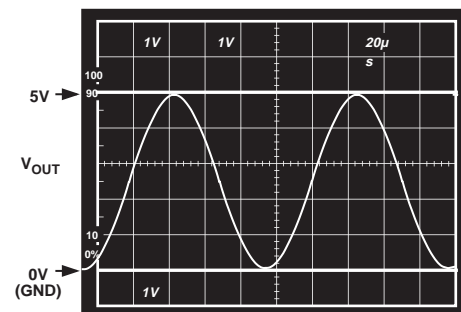
*Gain of +2 Amplifier; V_S = +5, 0, V_{IN} = 2.5 V Sine Centered
at 1.25 Volts, R_L = 100 kΩ*

REV. A

Parameter	Conditions	AD822A Min	Typ	Max	AD822B Min	Typ	Max	AD822S[1] Min	Typ	Max	Units
DC PERFORMANCE											
Initial Offset			0.1	0.8		0.1	0.4		0.1	0.8	mV
Max Offset over Temperature			0.5	1.2		0.5	0.9		0.5		mV
Offset Drift			2			2			2		µV/°C
Input Bias Current	V_{CM} = 0 V to 4 V		2	25		2	10		2	25	pA
at T_{MAX}			0.5	5		0.5	2.5		0.5		nA
Input Offset Current			2	20		2	10		2	20	pA
at T_{MAX}			0.5			0.5			1.5		nA
Open-Loop Gain	V_O = 0.2 V to 4 V										
	R_L = 100 k	500	1000		500	1000		500	1000		V/mV
T_{MIN} to T_{MAX}		400			400						V/mV
	R_L = 10 k	80	150		80	150		80	150		V/mV
T_{MIN} to T_{MAX}		80			80						V/mV
	R_L = 1 k	15	30		15	30		15	30		V/mV
T_{MIN} to T_{MAX}		10			10						V/mV
NOISE/HARMONIC PERFORMANCE											
Input Voltage Noise											
0.1 Hz to 10 Hz			2			2			2		µV p-p
f = 10 Hz			25			25			25		nV/$\sqrt{\text{Hz}}$
f = 100 Hz			21			21			21		nV/$\sqrt{\text{Hz}}$
f = 1 kHz			16			16			16		nV/$\sqrt{\text{Hz}}$
f = 10 kHz			13			13			13		nV/$\sqrt{\text{Hz}}$
Input Current Noise											
0.1 Hz to 10 Hz			18			18			18		fA p-p
f = 1 kHz			0.8			0.8			0.8		fA/$\sqrt{\text{Hz}}$
Harmonic Distortion	R_L = 10 k to 2.5 V										
f = 10 kHz	V_O = 0.25 V to 4.75 V		–93			–93			–93		dB
DYNAMIC PERFORMANCE											
Unity Gain Frequency			1.8			1.8			1.8		MHz
Full Power Response	V_O p-p = 4.5 V		210			210			210		kHz
Slew Rate			3			3			3		V/µs
Settling Time											
to 0.1%	V_O = 0.2 V to 4.5 V		1.4			1.4			1.4		µs
to 0.01%			1.8			1.8			1.8		µs
MATCHING CHARACTERISTICS											
Initial Offset				1.0			0.5			1.6	mV
Max Offset Over Temperature				1.6			1.3				mV
Offset Drift		3			3						µV/°C
Input Bias Current				20			10			20	pA
Crosstalk @ f = 1 kHz	R_L = 5 kΩ		–130			–130			–130		dB
f = 100 kHz			–93			–93			–93		dB
INPUT CHARACTERISTICS											
Common-Mode Voltage Range[2]		–0.2		4	–0.2		4	–0.2		4	V
T_{MIN} to T_{MAX}		–0.2		4	–0.2		4				V
CMRR	V_{CM} = 0 V to +2 V	66	80		69	80		66	80		dB
T_{MIN} to T_{MAX}		66			66						dB
Input Impedance											
Differential			10^{13}‖0.5			10^{13}‖0.5			10^{13}‖0.5		Ω‖pF
Common Mode			10^{13}‖2.8			10^{13}‖2.8			10^{13}‖2.8		Ω‖pF
OUTPUT CHARACTERISTICS											
Output Saturation Voltage[3]											
V_{OL}–V_{EE}	I_{SINK} = 20 µA		5	7		5	7		5	7	mV
T_{MIN} to T_{MAX}				10			10				mV
V_{CC}–V_{OH}	I_{SOURCE} = 20 µA		10	14		10	14		10	14	mV
T_{MIN} to T_{MAX}				20			20				mV
V_{OL}–V_{EE}	I_{SINK} = 2 mA		40	55		40	55		40	55	mV
T_{MIN} to T_{MAX}				80			80				mV
V_{CC}–V_{OH}	I_{SOURCE} = 2 mA		80	110		80	110		80	110	mV
T_{MIN} to T_{MAX}				160			160				mV
V_{OL}–V_{EE}	I_{SINK} = 15 mA		300	500		300	500		300	500	mV
T_{MIN} to T_{MAX}				1000			1000				mV
V_{CC}–V_{OH}	I_{SOURCE} = 15 mA		800	1500		800	1500		800	1500	mV
T_{MIN} to T_{MAX}				1900			1900				mV
Operating Output Current		15			15			15			mA
T_{MIN} to T_{MAX}		12			12						mA
Capacitive Load Drive			350			350			350		pF
POWER SUPPLY											
Quiescent Current T_{MIN} to T_{MAX}			1.24	1.6		1.24	1.6		1.24		mA
Power Supply Rejection	V_{S}+ = 5 V to 15 V	70	80		66	80		70	80		dB
T_{MIN} to T_{MAX}		70			66						dB

(V$_S$ = ±5 volts @ T$_A$ = +25°C, V$_{CM}$ = 0 V, V$_{OUT}$ = 0 V unless otherwise noted)

Parameter	Conditions	AD822A Min	AD822A Typ	AD822A Max	AD822B Min	AD822B Typ	AD822B Max	AD822S[1] Min	AD822S[1] Typ	AD822S[1] Max	Units
DC PERFORMANCE											
Initial Offset			0.1	0.8		0.1	0.4		0.1		mV
Max Offset over Temperature			0.5	1.5		0.5	1		0.5		mV
Offset Drift			2			2			2		µV/°C
Input Bias Current	V$_{CM}$ = –5 V to 4 V		2	25		2	10		2	25	pA
at T$_{MAX}$			0.5	5		0.5	2.5		0.5		nA
Input Offset Current			2	20		2	10		2		pA
at T$_{MAX}$			0.5			0.5			1.5		nA
Open-Loop Gain	V$_O$ = –4 V to 4 V										
	R$_L$ = 100 k	400	1000		400	1000		400	1000		V/mV
T$_{MIN}$ to T$_{MAX}$		400			400						V/mV
	R$_L$ = 10 k	80	150		80	150		80	150		V/mV
T$_{MIN}$ to T$_{MAX}$		80			80						V/mV
	R$_L$ = 1 k	20	30		20	30		20	30		V/mV
T$_{MIN}$ to T$_{MAX}$		10			10						V/mV
NOISE/HARMONIC PERFORMANCE											
Input Voltage Noise											
0.1 Hz to 10 Hz			2			2			2		µV p-p
f = 10 Hz			25			25			25		nV/√Hz
f = 100 Hz			21			21			21		nV/√Hz
f = 1 kHz			16			16			16		nV/√Hz
f = 10 kHz			13			13			13		nV/√Hz
Input Current Noise											
0.1 Hz to 10 Hz			18			18			18		fA p-p
f = 1 kHz			0.8			0.8			0.8		fA/√Hz
Harmonic Distortion	R$_L$ = 10 k										
f = 10 kHz	V$_O$ = ±4.5 V		–93			–93			–93		dB
DYNAMIC PERFORMANCE											
Unity Gain Frequency			1.9			1.9			1.9		MHz
Full Power Response	V$_O$ p-p = 9 V		105			105			105		kHz
Slew Rate			3			3			3		V/µs
Settling Time											
to 0.1%	V$_O$ = 0 V to ±4.5 V		1.4			1.4			1.4		µs
to 0.01%			1.8			1.8			1.8		µs
MATCHING CHARACTERISTICS											
Initial Offset				1.0			0.5			1.6	mV
Max Offset Over Temperature				3			2			2	mV
Offset Drift			3			3					µV/°C
Input Bias Current				25			10			25	pA
Crosstalk @ f = 1 kHz	R$_L$ = 5 kΩ		–130			–130			–130		dB
f = 100 kHz			–93			–93			–93		dB
INPUT CHARACTERISTICS											
Common-Mode Voltage Range[2]		–5.2		4	–5.2		4	–5.2		4	V
T$_{MIN}$ to T$_{MAX}$		–5.2		4	–5.2		4				V
CMRR	V$_{CM}$ = –5 V to +2 V	66	80		69	80		66	80		dB
T$_{MIN}$ to T$_{MAX}$		66			66						dB
Input Impedance											
Differential			10^{13}‖0.5			10^{13}‖0.5			10^{13}‖0.5		Ω‖pF
Common Mode			10^{13}‖2.8			10^{13}‖2.8			10^{13}‖2.8		Ω‖pF
OUTPUT CHARACTERISTICS											
Output Saturation Voltage[3]											
V$_{OL}$–V$_{EE}$	I$_{SINK}$ = 20 µA		5	7		5	7		5	7	mV
T$_{MIN}$ to T$_{MAX}$				10			10				mV
V$_{CC}$–V$_{OH}$	I$_{SOURCE}$ = 20 µA		10	14		10	14		10	14	mV
T$_{MIN}$ to T$_{MAX}$				20			20				mV
V$_{OL}$–V$_{EE}$	I$_{SINK}$ = 2 mA		40	55		40	55		40	55	mV
T$_{MIN}$ to T$_{MAX}$				80			80				mV
V$_{CC}$–V$_{OH}$	I$_{SOURCE}$ = 2 mA		80	110		80	110		80	110	mV
T$_{MIN}$ to T$_{MAX}$				160			160				mV
V$_{OL}$–V$_{EE}$	I$_{SINK}$ = 15 mA		300	500		300	500		300	500	mV
T$_{MIN}$ to T$_{MAX}$				1000			1000				mV
V$_{CC}$–V$_{OH}$	I$_{SOURCE}$ = 15 mA		800	1500		800	1500		800	1500	mV
T$_{MIN}$ to T$_{MAX}$				1900			1900				mV
Operating Output Current		15			15			15			mA
T$_{MIN}$ to T$_{MAX}$		12			12						mA
Capacitive Load Drive			350			350			350		pF
POWER SUPPLY											
Quiescent Current T$_{MIN}$ to T$_{MAX}$			1.3	1.6		1.3	1.6		1.3		mA
Power Supply Rejection	V$_S$+ = 5 V to 15 V	70	80		66	80		70	80		dB
T$_{MIN}$ to T$_{MAX}$		70			66						dB

(V$_S$ = ± 15 volts @ T$_A$ = +25°C, V$_{CM}$ = 0 V, V$_{OUT}$ = 0 V unless otherwise noted)

Parameter	Conditions	AD822A			AD822B			AD822S[1]			Units
		Min	Typ	Max	Min	Typ	Max	Min	Typ	Max	
DC PERFORMANCE											
Initial Offset			0.4	2		0.3	1.5		0.4	2.0	mV
Max Offset over Temperature			0.5	3		0.5	2.5		0.5		mV
Offset Drift			2			2			2		μV/°C
Input Bias Current	V$_{CM}$ = 0 V		2	25		2	12		2	25	pA
	V$_{CM}$ = –10 V		40			40			40		pA
at T$_{MAX}$	V$_{CM}$ = 0 V		0.5	5		0.5	2.5		0.5		nA
Input Offset Current			2	20		2	12		2	20	pA
at T$_{MAX}$			0.5			0.5			1.5		nA
Open-Loop Gain	V$_O$ = +10 V to –10 V										
	R$_L$ = 100 k	500	2000		500	2000		500	2000		V/mV
T$_{MIN}$ to T$_{MAX}$		500			500						V/mV
	R$_L$ = 10 k	100	500		100	500		150	400		V/mV
T$_{MIN}$ to T$_{MAX}$		100			100						V/mV
	R$_L$ = 1 k	30	45		30	45		30	45		V/mV
T$_{MIN}$ to T$_{MAX}$		20			20						V/mV
NOISE/HARMONIC PERFORMANCE											
Input Voltage Noise											
0.1 Hz to 10 Hz			2			2			2		μV p-p
f = 10 Hz			25			25			25		nV/$\sqrt{Hz}$
f = 100 Hz			21			21			21		nV/$\sqrt{Hz}$
f = 1 kHz			16			16			16		nV/$\sqrt{Hz}$
f = 10 kHz			13			13			13		nV/$\sqrt{Hz}$
Input Current Noise											
0.1 Hz to 10 Hz			18			18			18		fA p-p
f = 1 kHz			0.8			0.8			0.8		fA/$\sqrt{Hz}$
Harmonic Distortion	R$_L$ = 10 k										
f = 10 kHz	V$_O$ = ±10 V		–85			–85			–85		dB
DYNAMIC PERFORMANCE											
Unity Gain Frequency			1.9			1.9			1.9		MHz
Full Power Response	V$_O$ p-p = 20 V		45			45			45		kHz
Slew Rate			3			3			3		V/μs
Settling Time											
to 0.1%	V$_O$ = 0 V to ±10 V		4.1			4.1			4.1		μs
to 0.01%			4.5			4.5			4.5		μs
MATCHING CHARACTERISTICS											
Initial Offset				3			2			0.8	mV
Max Offset Over Temperature				4			2.5			1.0	mV
Offset Drift			3			3					μV/°C
Input Bias Current				25			12			25	pA
Crosstalk @ f = 1 kHz	R$_L$ = 5 kΩ		–130			–130			–130		dB
f = 100 kHz			–93			–93			–93		dB
INPUT CHARACTERISTICS											
Common-Mode Voltage Range[2]		–15.2		14	–15.2		14	–15.2		14	V
T$_{MIN}$ to T$_{MAX}$		–15.2		14	–15.2		14				V
CMRR	V$_{CM}$ = –15 V to 12 V	70	80		74	90		70	90		dB
T$_{MIN}$ to T$_{MAX}$		70			74						dB
Input Impedance											
Differential			10^{13}‖0.5			10^{13}‖0.5			10^{13}‖0.5		Ω‖pF
Common Mode			10^{13}‖2.8			10^{13}‖2.8			10^{13}‖2.8		Ω‖pF
OUTPUT CHARACTERISTICS											
Output Saturation Voltage[3]											
V$_{OL}$–V$_{EE}$	I$_{SINK}$ = 20 μA		5	7		5	7		5	7	mV
T$_{MIN}$ to T$_{MAX}$				10			10				mV
V$_{CC}$–V$_{OH}$	I$_{SOURCE}$ = 20 μA		10	14		10	14		10	14	mV
T$_{MIN}$ to T$_{MAX}$				20			20				mV
V$_{OL}$–V$_{EE}$	I$_{SINK}$ = 2 mA		40	55		40	55		40	55	mV
T$_{MIN}$ to T$_{MAX}$				80			80				mV
V$_{CC}$–V$_{OH}$	I$_{SOURCE}$ = 2 mA		80	110		80	110		80	110	mV
T$_{MIN}$ to T$_{MAX}$				160			160				mV
V$_{OL}$–V$_{EE}$	I$_{SINK}$ = 15 mA		300	500		300	500		300	500	mV
T$_{MIN}$ to T$_{MAX}$				1000			1000				mV
V$_{CC}$–V$_{OH}$	I$_{SOURCE}$ = 15 mA		800	1500		800	1500		800	1500	mV
T$_{MIN}$ to T$_{MAX}$				1900			1900				mV
Operating Output Current		20			20			20			mA
T$_{MIN}$ to T$_{MAX}$		15			15						mA
Capacitive Load Drive			350			350			350		pF
POWER SUPPLY											
Quiescent Current T$_{MIN}$ to T$_{MAX}$			1.4	1.8		1.4	1.8		1.4		mA
Power Supply Rejection	V$_S$+ = 5 V to 15 V	70	80		70	80		70	80		dB
T$_{MIN}$ to T$_{MAX}$		70			70						dB

REV. A

(V$_S$ = 0, 3 volts @ T$_A$ = +25°C, V$_{CM}$ = 0 V, V$_{OUT}$ = 0.2 V unless otherwise noted)

Parameter	Conditions	Min	Typ	Max	Units
			AD822A-3 V		
DC PERFORMANCE					
Initial Offset			0.2	1	mV
Max Offset over Temperature			0.5	1.5	mV
Offset Drift			1		μV/°C
Input Bias Current	V$_{CM}$ = 0 V to +2 V		2	25	pA
at T$_{MAX}$			0.5	5	nA
Input Offset Current			2	20	pA
at T$_{MAX}$			0.5		nA
Open-Loop Gain	V$_O$ = 0.2 V to 2 V				
	R$_L$ = 100 k	300	1000		V/mV
T$_{MIN}$ to T$_{MAX}$		300			V/mV
	R$_L$ = 10 k	60	150		V/mV
T$_{MIN}$ to T$_{MAX}$		60			V/mV
	R$_L$ = 1 k	10	30		V/mV
T$_{MIN}$ to T$_{MAX}$		8			V/mV
NOISE/HARMONIC PERFORMANCE					
Input Voltage Noise					
0.1 Hz to 10 Hz			2		μV p-p
f = 10 Hz			25		nV/√Hz
f = 100 Hz			21		nV/√Hz
f = 1 kHz			16		nV/√Hz
f = 10 kHz			13		nV/√Hz
Input Current Noise					
0.1 Hz to 10 Hz			18		fA p-p
f = 1 kHz			0.8		fA/√Hz
Harmonic Distortion	R$_L$ = 10 k to 1.5 V				
f = 10 kHz	V$_O$ = ±1.25 V		−92		dB
DYNAMIC PERFORMANCE					
Unity Gain Frequency			1.5		MHz
Full Power Response	V$_O$ p-p = 2.5 V		240		kHz
Slew Rate			3		V/μs
Settling Time					
to 0.1%	V$_O$ = 0.2 V to 2.5 V		1		μs
to 0.01%			1.4		μs
MATCHING CHARACTERISTICS					
Initial Offset				1	mV
Max Offset Over Temperature				2	mV
Offset Drift			2		μV/°C
Input Bias Current				10	pA
Crosstalk @ f = 1 kHz	R$_L$ = 5 kΩ		−130		dB
f = 100 kHz			−93		dB
INPUT CHARACTERISTICS					
Common-Mode Voltage Range[2]		−0.2		2	V
T$_{MIN}$ to T$_{MAX}$		−0.2		2	V
CMRR	V$_{CM}$ = 0 V to +1 V	60	74		dB
T$_{MIN}$ to T$_{MAX}$		60			dB
Input Impedance					
Differential			10^{13}‖0.5		Ω‖pF
Common Mode			10^{13}‖2.8		Ω‖pF
OUTPUT CHARACTERISTICS					
Output Saturation Voltage[3]					
V$_{OL}$–V$_{EE}$	I$_{SINK}$ = 20 μA		5	7	mV
T$_{MIN}$ to T$_{MAX}$				10	mV
V$_{CC}$–V$_{OH}$	I$_{SOURCE}$ = 20 μA		10	14	mV
T$_{MIN}$ to T$_{MAX}$				20	mV
V$_{OL}$–V$_{EE}$	I$_{SINK}$ = 2 mA		40	55	mV
T$_{MIN}$ to T$_{MAX}$				80	mV
V$_{CC}$–V$_{OH}$	I$_{SOURCE}$ = 2 mA		80	110	mV
T$_{MIN}$ to T$_{MAX}$				160	mV
V$_{OL}$–V$_{EE}$	I$_{SINK}$ = 10 mA		200	400	mV
T$_{MIN}$ to T$_{MAX}$				400	mV
V$_{CC}$–V$_{OH}$	I$_{SOURCE}$ = 10 mA		500	1000	mV
T$_{MIN}$ to T$_{MAX}$				1000	mV
Operating Output Current		15			mA
T$_{MIN}$ to T$_{MAX}$		12			mA
Capacitive Load Drive			350		pF
POWER SUPPLY					
Quiescent Current T$_{MIN}$ to T$_{MAX}$			1.24	1.6	mA
Power Supply Rejection	V$_S$+ = 3 V to 15 V	70	80		dB
T$_{MIN}$ to T$_{MAX}$		70			dB

AD822–SPECIFICATIONS

NOTES
[1]See standard military drawing for 883B specifications.
[2]This is a functional specification. Amplifier bandwidth decreases when the input common-mode voltage is driven in the range $(+V_S - 1 V)$ to $+V_S$.
  Common-mode error voltage is typically less than 5 mV with the common-mode voltage set at 1 volt below the positive supply.
[3]$V_{OL}-V_{EE}$ is defined as the difference between the lowest possible output voltage (V_{OL}) and the minus voltage supply rail (V_{EE}).
  $V_{CC}-V_{OH}$ is defined as the difference between the highest possible output voltage (V_{OH}) and the positive supply voltage (V_{CC}).

Specifications subject to change without notice.

CAUTION

ESD (electrostatic discharge) sensitive device. Electrostatic charges as high as 4000 V readily accumulate on the human body and test equipment and can discharge without detection. Although the AD822 features proprietary ESD protection circuitry, permanent damage may occur on devices subjected to high energy electrostatic discharges. Therefore, proper ESD precautions are recommended to avoid performance degradation or loss of functionality.

WARNING!

ESD SENSITIVE DEVICE

ABSOLUTE MAXIMUM RATINGS[1]

Supply Voltage . . . . ±18 V
Internal Power Dissipation
   Plastic DIP (N) . . . . Observe Derating Curves
   Cerdip (Q) . . . . Observe Derating Curves
   SOIC (R) . . . . Observe Derating Curves
Input Voltage . . . . $(+V_S + 0.2 V)$ to $-(20 V + V_S)$
Output Short Circuit Duration . . . . Indefinite
Differential Input Voltage . . . . ±30 V
Storage Temperature Range (N) . . . . −65°C to +125°C
Storage Temperature Range (Q) . . . . −65°C to +150°C
Storage Temperature Range (R) . . . . −65°C to +150°C
Operating Temperature Range
   AD822A/B . . . . −40°C to +85°C
   AD822S . . . . −55°C to +125°C
Lead Temperature Range (Soldering 60 sec) . . . . +260°C

NOTES
[1]Stresses above those listed under "Absolute Maximum Ratings" may cause permanent damage to the device. This is a stress rating only and functional operation of the device at these or any other conditions above those indicated in the operational section of this specification is not implied. Exposure to absolute maximum rating conditions for extended periods may affect device reliability.
[2]8-Pin Plastic DIP Package: $\theta_{JA} = 90°C/Watt$
  8-Pin Cerdip Package: $\theta_{JA} = 110°C/Watt$
  8-Pin SOIC Package: $\theta_{JA} = 160°C/Watt$

MAXIMUM POWER DISSIPATION

The maximum power that can be safely dissipated by the AD822 is limited by the associated rise in junction temperature. For plastic packages, the maximum safe junction temperature is 145°C. For the cerdip packages, the maximum junction temperature is 175°C. If these maximums are exceeded momentarily, proper circuit operation will be restored as soon as the die temperature is reduced. Leaving the device in the "overheated" condition for an extended period can result in device burnout. To ensure proper operation, it is important to observe the derating curves shown in Figure 24.

While the AD822 is internally short circuit protected, this may not be sufficient to guarantee that the maximum junction temperature is not exceeded under all conditions. With power supplies ±12 volts (or less) at an ambient temperature of +25°C or less, if the output node is shorted to a supply rail, then the amplifier will not be destroyed, even if this condition persists for an extended period.

ORDERING GUIDE

Model[1]	Temperature Range	Package Description	Package Option
AD822AN	−40°C to +85°C	8-Pin Plastic Mini-DIP	N-8
AD822BN	−40°C to +85°C	8-Pin Plastic Mini-DIP	N-8
AD822AR	−40°C to +85°C	8-Pin SOIC	R-8
AD822BR	−40°C to +85°C	8-Pin SOIC	R-8
AD822AR-3V	−40°C to +85°C	8-Pin SOIC	R-8
AD822AN-3V	−40°C to +85°C	8-Pin Plastic Mini-DIP	N-8
AD822A Chips	−40°C to +85°C	Die	
Standard Military Drawing[2]	−55°C to +125°C	8-Pin Cerdip	Q-8

NOTES
[1]Spice model is available on ADI Model Disc.
[2]Contact factory for availability.

METALIZATION PHOTOGRAPH

Contact factory for latest dimensions.
Dimensions shown in inches and (mm).
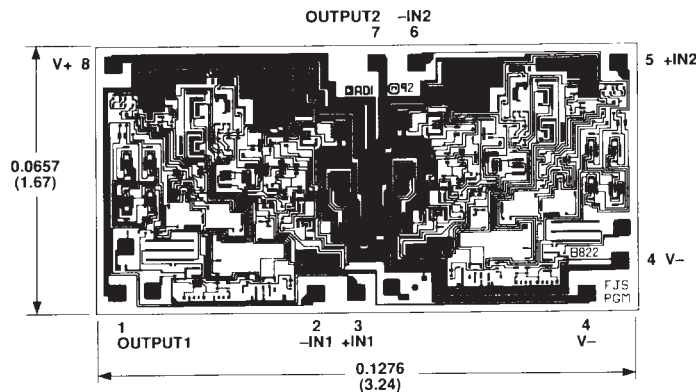
NOTE: BACK OF DIE IS AT $+V_S$ POTENTIAL.

REV. A
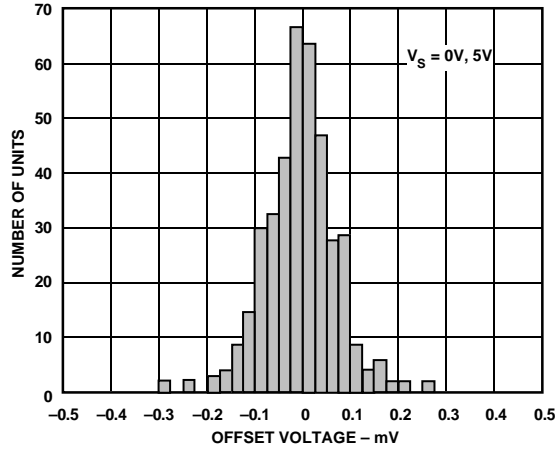
Figure 1. Typical Distribution of Offset Voltage (390 Units)

Figure 2. Typical Distribution of Offset Voltage Drift (100 Units)

Figure 3. Typical Distribution of Input Bias Current (213 Units)

Figure 4. Input Bias Current vs. Common-Mode Voltage; $V_S = +5$ V, 0 V and $V_S = \pm5$ V
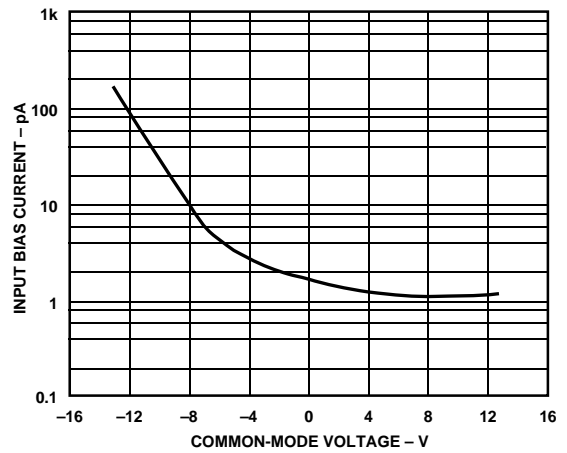
Figure 5. Input Bias Current vs. Common-Mode Voltage; $V_S = \pm15$ V
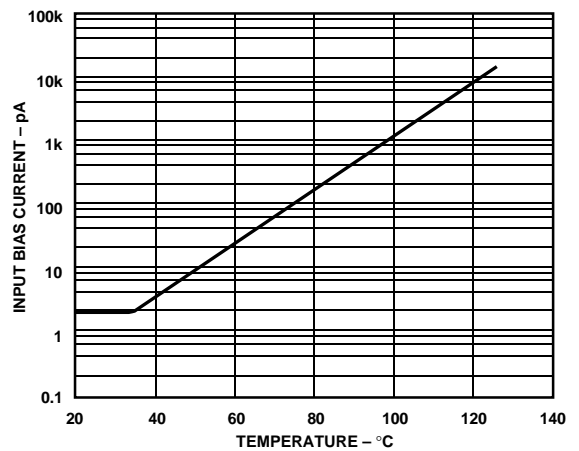
Figure 6. Input Bias Current vs. Temperature; $V_S = 5$ V, $V_{CM} = 0$

Figure 7. Open-Loop Gain vs. Load Resistance
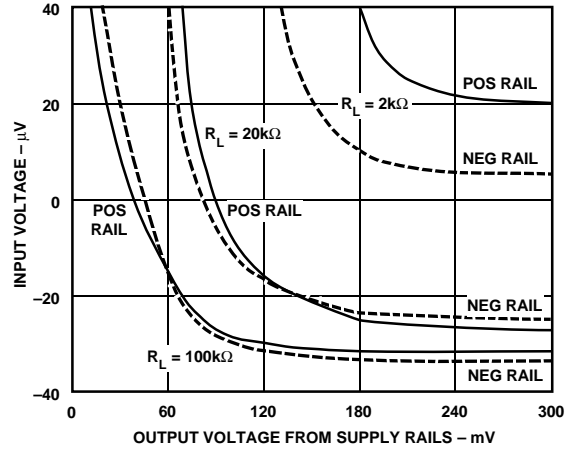
Figure 10. Input Error Voltage with Output Voltage within 300 mV of Either Supply Rail for Various Resistive Loads; $V_S = \pm5\ V$
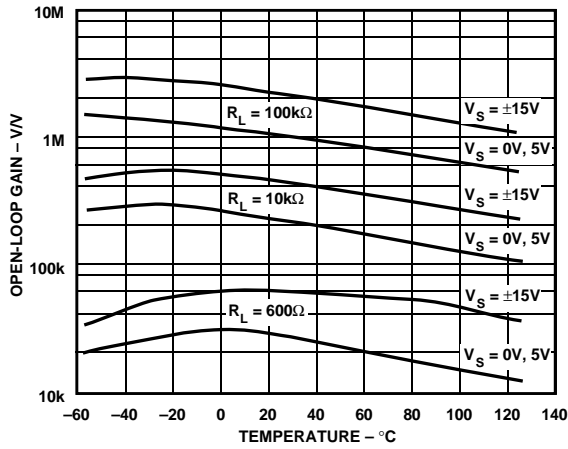
Figure 8. Open-Loop Gain vs. Temperature
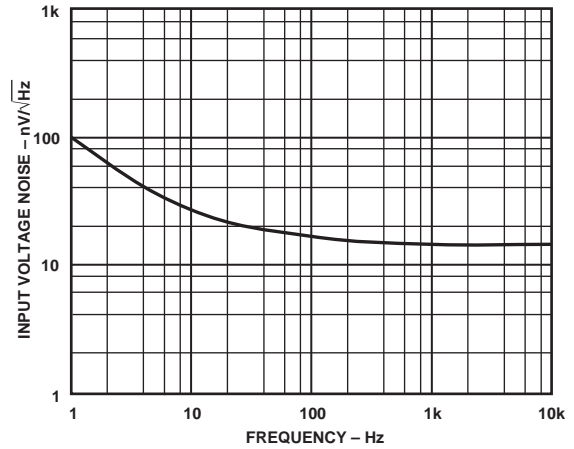
Figure 11. Input Voltage Noise vs. Frequency
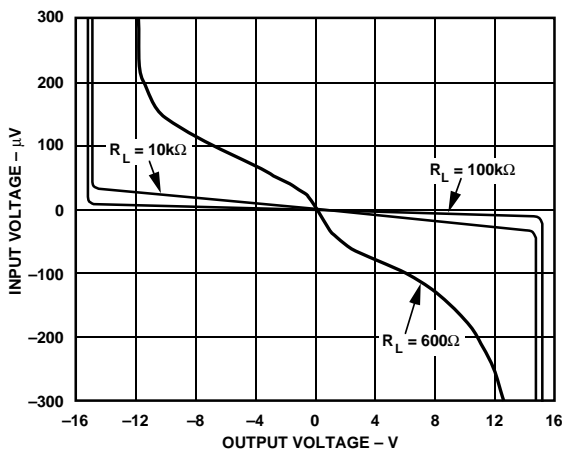
Figure 9. Input Error Voltage vs. Output Voltage for Resistive Loads
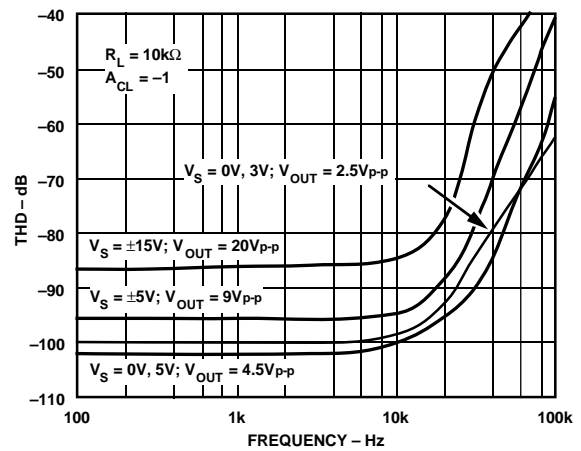
Figure 12. Total Harmonic Distortion vs. Frequency

REV. A
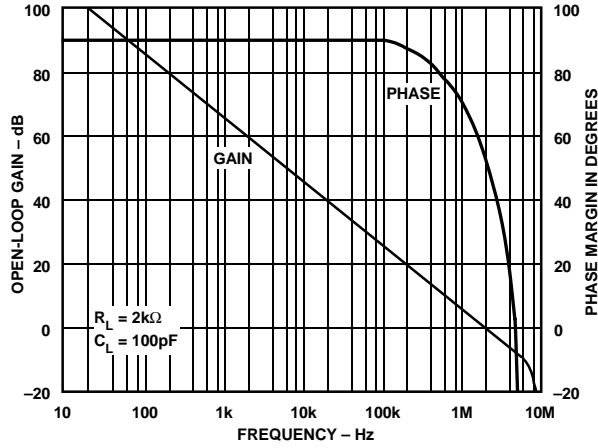
Figure 13. Open-Loop Gain and Phase Margin vs. Frequency
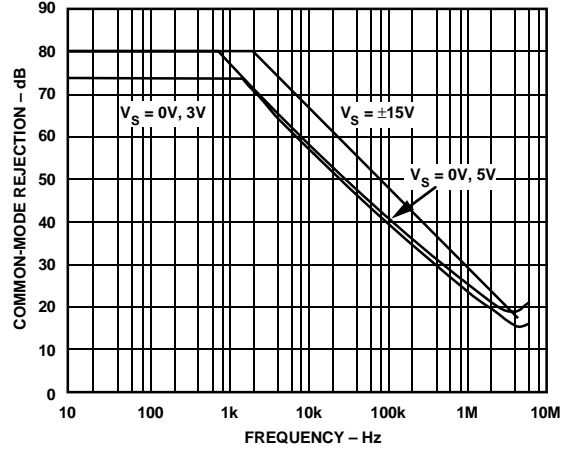
Figure 16. Common-Mode Rejection vs. Frequency
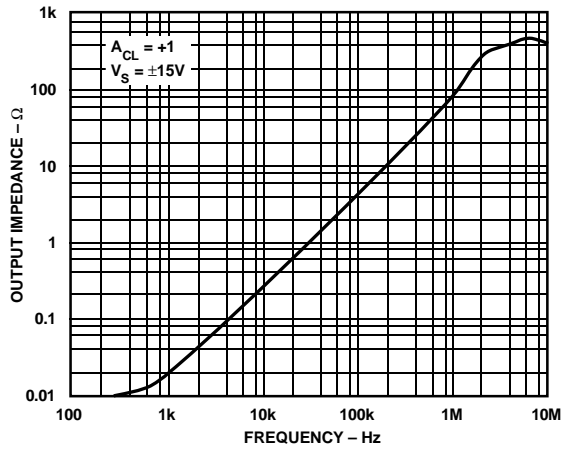
Figure 14. Output Impedance vs. Frequency
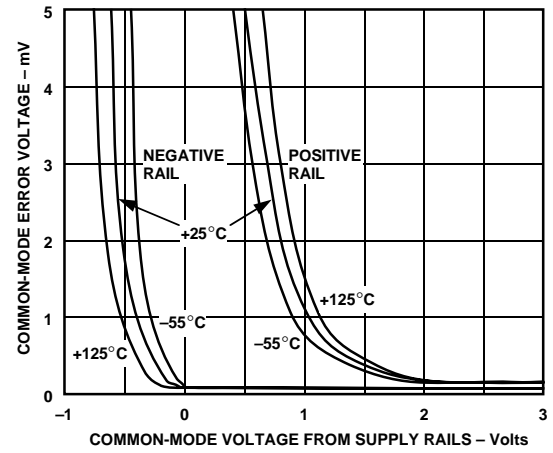
Figure 17. Absolute Common-Mode Error vs. Common-Mode Voltage from Supply Rails ($V_S − V_{CM}$)
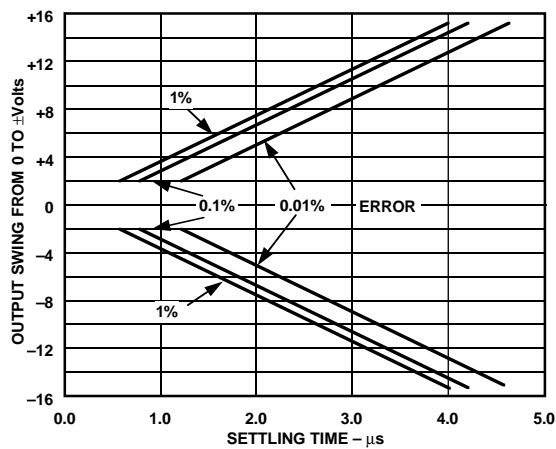
Figure 15. Output Swing and Error vs. Settling Time
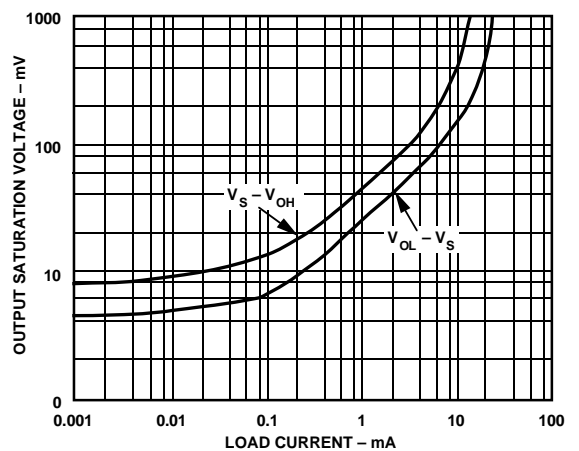
Figure 18. Output Saturation Voltage vs. Load Current

AD822–Typical Characteristics
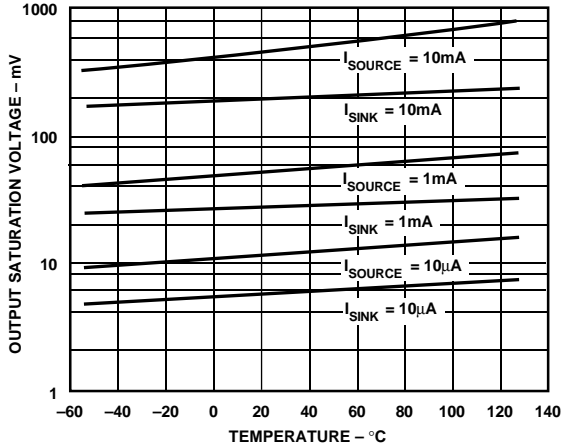
Figure 19. Output Saturation Voltage vs. Temperature
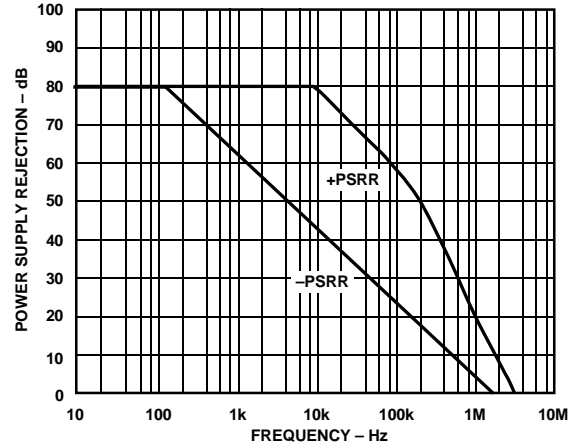
Figure 22. Power Supply Rejection vs. Frequency
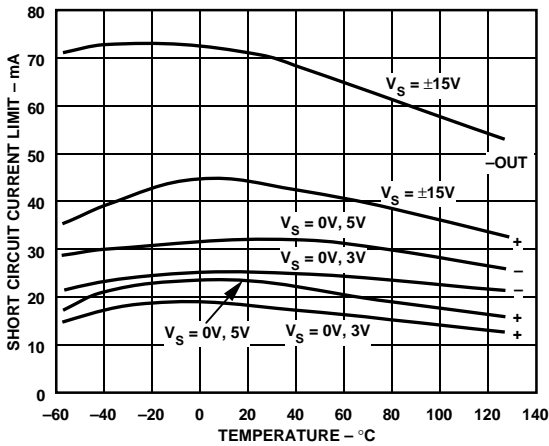
Figure 20. Short Circuit Current Limit vs. Temperature
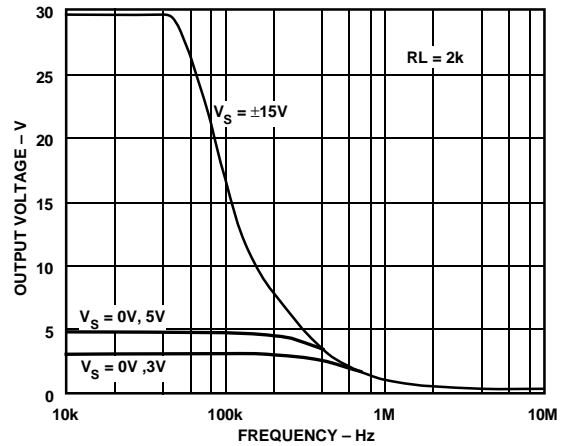
Figure 23. Large Signal Frequency Response
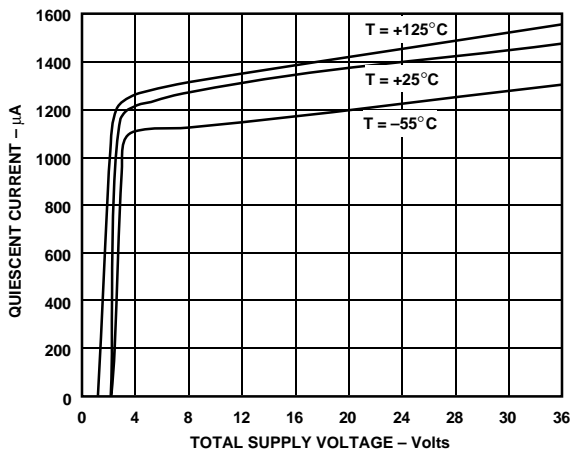
Figure 21. Quiescent Current vs. Supply Voltage vs. Temperature
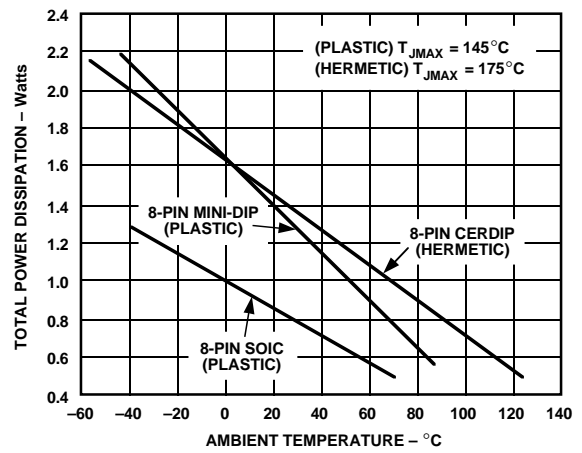
Figure 24. Maximum Power Dissipation vs. Temperature for Plastic and Hermetic Packages

REV. A
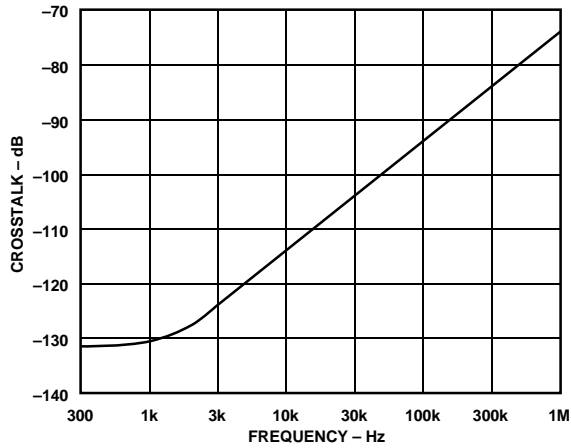
Figure 25. Crosstalk vs. Frequency

$$CROSSTALK = 20\ LOG\ \frac{V_{OUT}}{10V_{IN}}$$
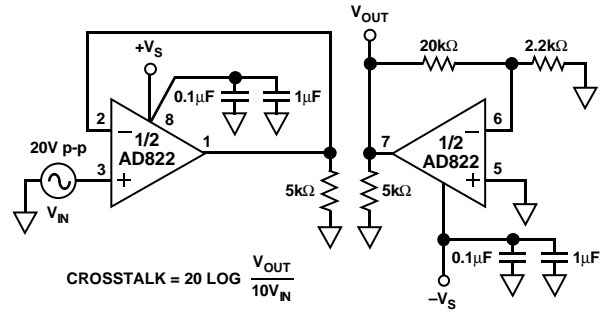
Figure 28. Crosstalk Test Circuit
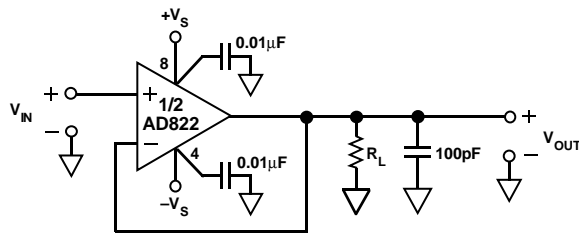
Figure 26. Unity-Gain Follower
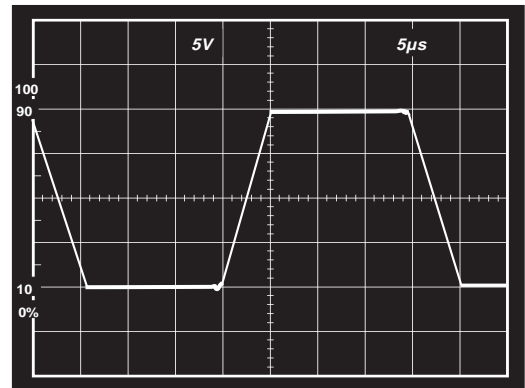
Figure 29. Large Signal Response Unity Gain Follower; $V_S = \pm15\ V$, $R_L = 10\ k\Omega$
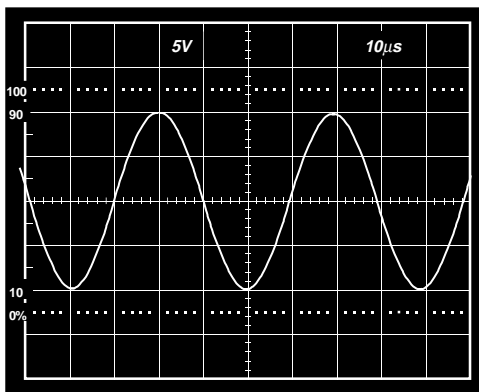
Figure 27. 20 V p-p, 25 kHz Sine Wave Input; Unity Gain Follower; $R_L = 600\ \Omega$, $V_S = \pm15\ V$
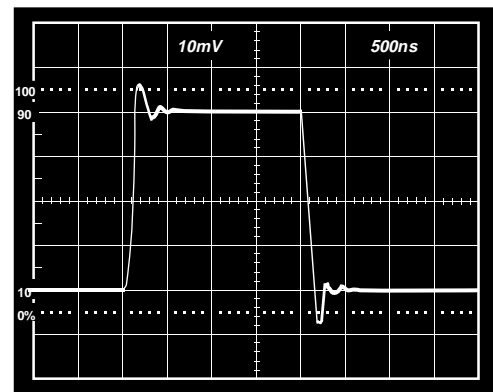
Figure 30. Small Signal Response Unity Gain Follower; $V_S = \pm15\ V$, $R_L = 10\ k\Omega$

AD822
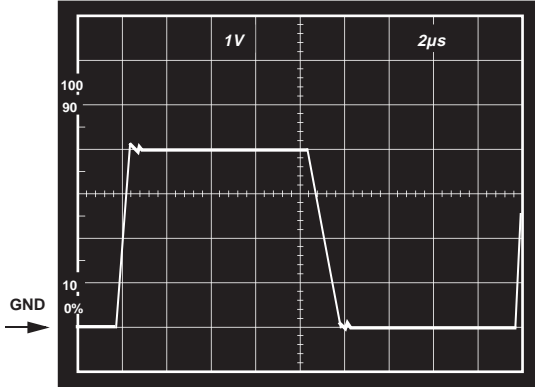
Figure 31. V_S = +5 V, 0 V; Unity Gain Follower Response to 0 V to 4 V Step
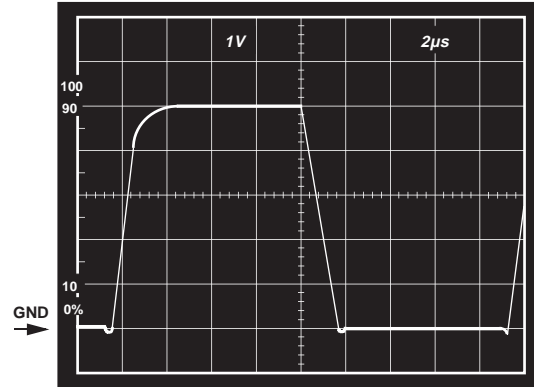
Figure 34. V_S = +5 V, 0 V; Unity Gain Follower Response to 0 V to 5 V Step
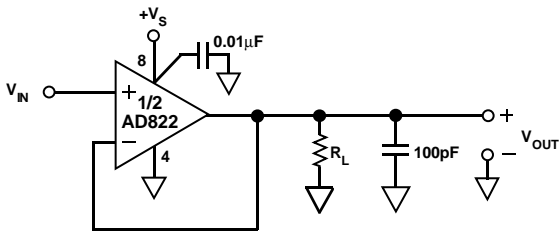
Figure 32. Unity Gain Follower
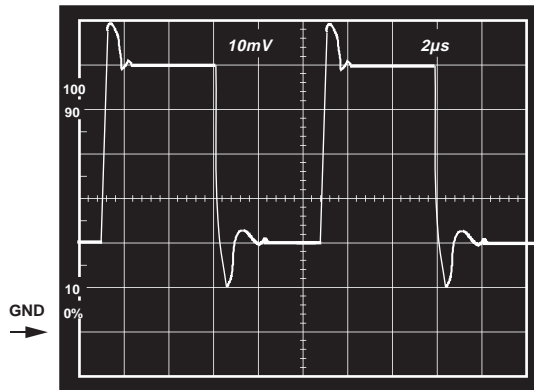
Figure 35. V_S = +5 V, 0 V; Unity Gain Follower Response, to 40 mV Step Centered 40 mV Above Ground, R_L = 10 kΩ
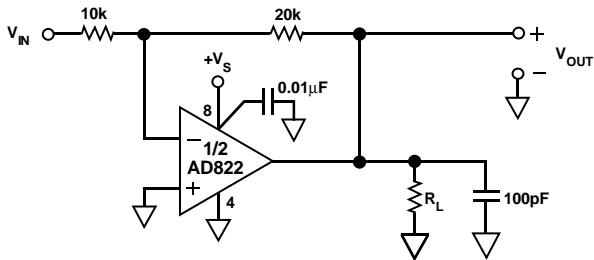
Figure 33. Gain of Two Inverter
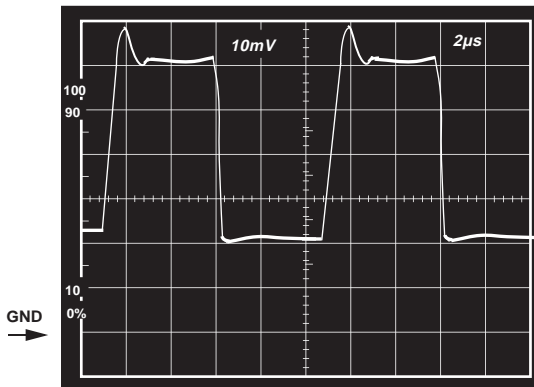
Figure 36. V_S = +5 V, 0 V; Gain of Two Inverter Response to 20 mV Step, Centered 20 mV Below Ground, R_L = 10 kΩ

REV. A
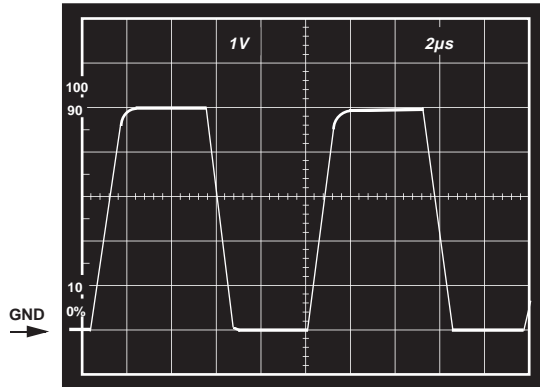
Figure 37. V_S = +5 V, 0 V; Gain of Two Inverter Response to 2.5 V Step Centered –1.25 V Below Ground, R_L = 10 kΩ
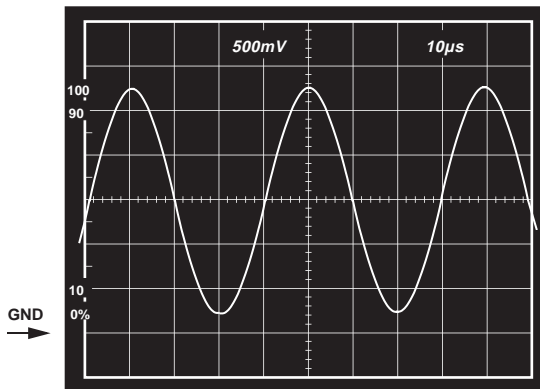
Figure 38. V_S = 3 V, 0 V; Gain of Two Inverter, V_{IN} = 1.25 V, 25 kHz, Sine Wave Centered at –0.75 V, R_L = 600 Ω
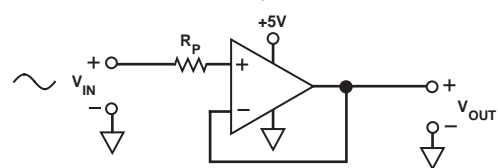

a

b.

Figure 39. (a) Response with R_P = 0; V_{IN} from 0 to +V_S
(b) V_{IN} = 0 to +V_S + 200 mV
V_{OUT} = 0 to +V_S
R_P = 49.9 kΩ

APPLICATION NOTES
INPUT CHARACTERISTICS

In the AD822, n-channel JFETs are used to provide a low offset, low noise, high impedance input stage. Minimum input common-mode voltage extends from 0.2 V below –V_S to 1 V less than +V_S. Driving the input voltage closer to the positive rail will cause a loss of amplifier bandwidth (as can be seen by comparing the large signal responses shown in Figures 31 and 34) and increased common-mode voltage error as illustrated in Figure 17.

The AD822 does not exhibit phase reversal for input voltages up to and including +V_S. Figure 39a shows the response of an AD822 voltage follower to a 0 V to +5 V (+V_S) square wave input. The input and output arc superimposed. The output tracks the input up to +V_S without phase reversal. The reduced bandwidth above a 4 V input causes the rounding of the output wave form. For input voltages greater than +V_S, a resistor in series with the AD822's noninverting input will prevent phase reversal, at the expense of greater input voltage noise. This is illustrated in Figure 39b.

Since the input stage uses n-channel JFETs, input current during normal operation is negative; the current flows out from the input terminals. If the input voltage is driven more positive than +V_S – 0.4 V, the input current will reverse direction as internal device junctions become forward biased. This is illustrated in Figure 4.

A current limiting resistor should be used in series with the input of the AD822 if there is a possibility of the input voltage exceeding the positive supply by more than 300 mV, or if an input voltage will be applied to the AD822 when ±V_S = 0. The amplifier will be damaged if left in that condition for more than 10 seconds. A 1 kΩ resistor allows the amplifier to withstand up to 10 volts of continuous overvoltage, and increases the input voltage noise by a negligible amount.

Input voltages less than –V_S are a completely different story. The amplifier can safely withstand input voltages 20 volts below the minus supply voltage as long as the total voltage from the positive supply to the input terminal is less than 36 volts. In addition, the input stage typically maintains picoamp level input currents across that input voltage range.

AD822

The AD822 is designed for 13 nV/√Hz wideband input voltage noise and maintains low noise performance to low frequencies (refer to Figure 11). This noise performance, along with the AD822's low input current and current noise means that the AD822 contributes negligible noise for applications with source resistances greater than 10 kΩ and signal bandwidths greater than 1 kHz. This is illustrated in Figure 40.
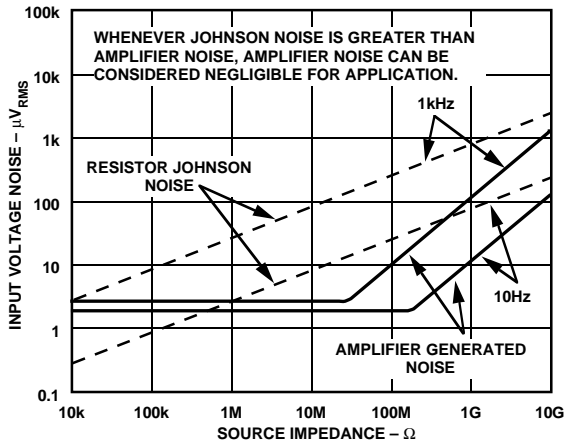

Figure 40. Total Noise vs. Source Impedance

OUTPUT CHARACTERISTICS

The AD822 s unique bipolar rail-to-rail output stage swings within 5 mV of the minus supply and 10 mV of the positive supply with no external resistive load. The AD822's approximate output saturation resistance is 40 Ω sourcing and 20 Ω sinking. This can be used to estimate output saturation voltage when driving heavier current loads. For instance, when sourcing 5 mA, the saturation voltage to the positive supply rail will be 200 mV, when sinking 5 mA, the saturation voltage to the minus rail will be 100 mV.

The amplifier's open-loop gain characteristic will change as a function of resistive load, as shown in Figures 7 through 10. For load resistances over 20 kΩ, the AD822's input error voltage is virtually unchanged until the output voltage is driven to 180 mV of either supply.

If the AD822's output is overdriven so as to saturate either of the output devices, the amplifier will recover within 2 μs of its input returning to the amplifier's linear operating region.

Direct capacitive loads will interact with the amplifier's effective output impedance to form an additional pole in the amplifier's feedback loop, which can cause excessive peaking on the pulse response or loss of stability. Worst case is when the amplifier is used as a unity gain follower. Figure 41 shows the AD822's pulse response as a unity gain follower driving 350 pF. This amount of overshoot indicates approximately 20 degrees of phase margin—the system is stable, but is nearing the edge. Configurations with less loop gain, and as a result less loop bandwidth, will be much less sensitive to capacitance load effects. Figure 42 is a plot of capacitive load that will result in a 20 degree phase margin versus noise gain for the AD822. Noise gain is the inverse of the feedback attenuation factor provided by the feedback network in use.
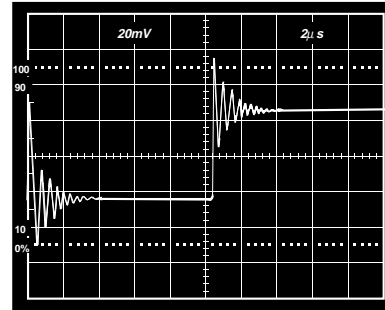

Figure 41. Small Signal Response of AD822 as Unity Gain Follower Driving 350 pF Capacitive Load
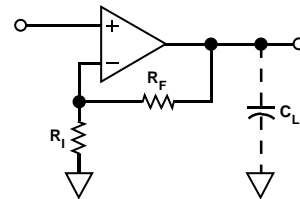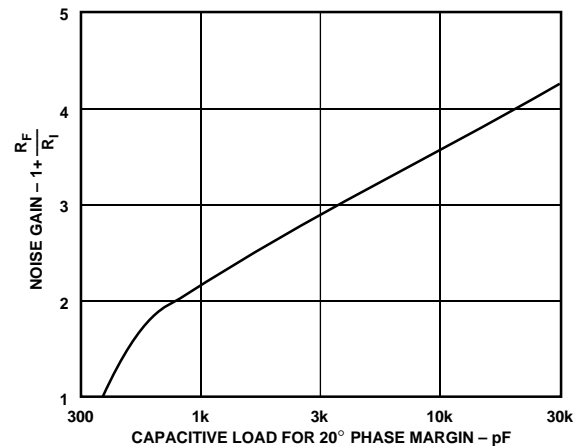

Figure 42. Capacitive Load Tolerance vs. Noise Gain

Figure 43 shows a method for extending capacitance load drive capability for a unity gain follower. With these component values, the circuit will drive 5,000 pF with a 10% overshoot.
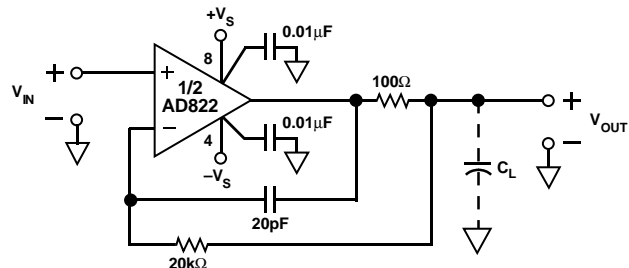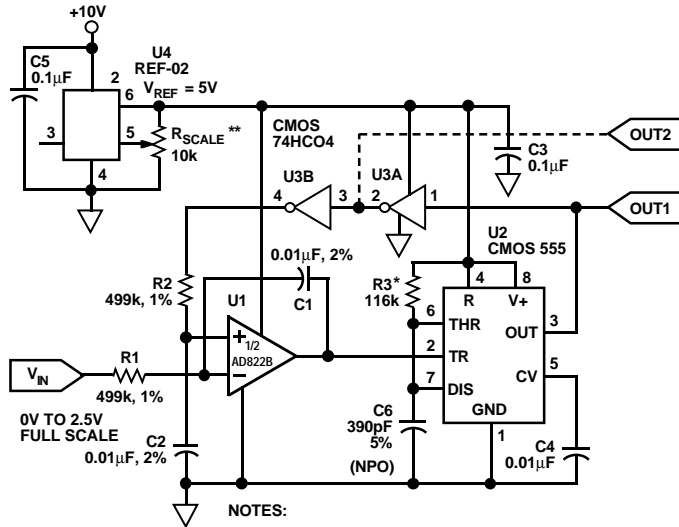

Figure 43. Extending Unity Gain Follower Capacitive Load Capability Beyond 350 pF

REV. A

APPLICATIONS

Single Supply Voltage-to-Frequency Converter

The circuit shown in Figure 44 uses the AD822 to drive a low power timer, which produces a stable pulse of width t_1. The positive going output pulse is integrated by R1-C1 and used as one input to the AD822, which is connected as a differential integrator. The other input (nonloading) is the unknown voltage, V_{IN}. The AD822 output drives the timer trigger input, closing the overall feedback loop.

Table I. AD822 In Amp Performance

Parameters	V_S = 3 V, 0 V	V_S = ±5 V
CMRR	74 dB	80 dB
Common-Mode		
Voltage Range	–0.2 V to +2 V	–5.2 V to +4 V
3 dB BW, G = 10	180 kHz	180 kHz
G = 100	18 kHz	18 kHz
$t_{SETTLING}$		
2 V Step (V_S = 0 V, 3 V)	2 µs	
5 V (V_S = ±5 V)		5 µs
Noise @ f = 1 kHz, G = 10	270 nV/$\sqrt{Hz}$	270 nV/$\sqrt{Hz}$
G = 100	2.2 µV/$\sqrt{Hz}$	2.2 µV/$\sqrt{Hz}$
I_{SUPPLY} (Total)	1.10 mA	1.15 mA

Figure 44. Single Supply Voltage-to-Frequency Converter
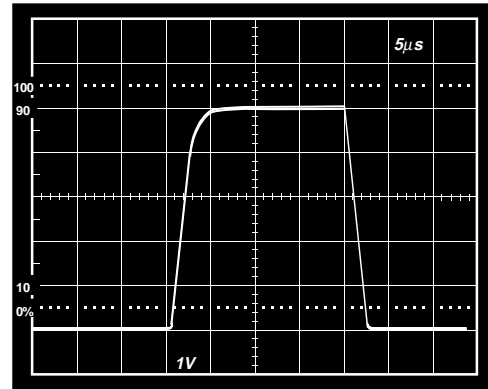
Figure 45a. Pulse Response of In Amp to a 500 mV p-p Input Signal; V_S = +5 V, 0 V; Gain = 10

Typical AD822 bias currents of 2 pA allow megaohm-range source impedances with negligible dc errors. Linearity errors on the order of 0.01% full scale can be achieved with this circuit. This performance is obtained with a 5 volt single supply which delivers less than 1 mA to the entire circuit.

Single Supply Programmable Gain Instrumentation Amplifier

The AD822 can be configured as a single supply instrumentation amplifier that is able to operate from single supplies down to 3 V, or dual supplies up to ±15 V. Using only one AD822 rather than three separate op amps, this circuit is cost and power efficient. AD822 FET inputs' 2 pA bias currents minimize offset errors caused by high unbalanced source impedances.

An array of precision thin-film resistors sets the in amp gain to be either 10 or 100. These resistors are laser-trimmed to ratio match to 0.01%, and have a maximum differential TC of 5 ppm/°C.

Figure 45b. A Single Supply Programmable Instrumentation Amplifier
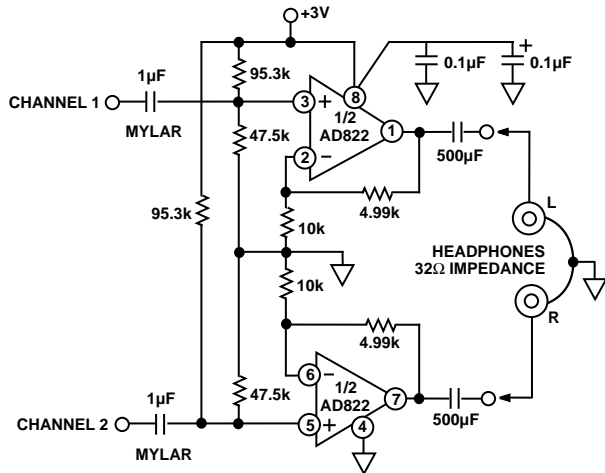
REV. A –15–

AD822

Figure 46. 3 Volt Single Supply Stereo Headphone Driver

3 Volt, Single Supply Stereo Headphone Driver

The AD822 exhibits good current drive and THD+N performance, even at 3 V single supplies. At 1 kHz, total harmonic distortion plus noise (THD+N) equals –62 dB (0.079%) for a 300 mV p-p output signal. This is comparable to other single supply op amps which consume more power and cannot run on 3 V power supplies.

In Figure 46, each channel s input signal is coupled via a 1 μF Mylar capacitor. Resistor dividers set the dc voltage at the non-inverting inputs so that the output voltage is midway between the power supplies (+1.5 V). The gain is 1.5. Each half of the AD822 can then be used to drive a headphone channel. A 5 Hz high-pass filter is realized by the 500 μF capacitors and the headphones, which can be modeled as 32 ohm load resistors to ground. This ensures that all signals in the audio frequency range (20 Hz–20 kHz) are delivered to the headphones.

Low Dropout Bipolar Bridge Driver

The AD822 can be used for driving a 350 ohm Wheatstone bridge. Figure 47 shows one half of the AD822 being used to buffer the AD589—a 1.235 V low power reference. The output of +4.5 V can be used to drive an A/D converter front end. The other half of the AD822 is configured as a unity-gain inverter, and generates the other bridge input of –4.5 V. Resistors R1 and R2 provide a constant current for bridge excitation. The AD620 low power instrumentation amplifier is used to condition the differential output voltage of the bridge. The gain of the AD620 is programmed using an external resistor R_G, and determined by:
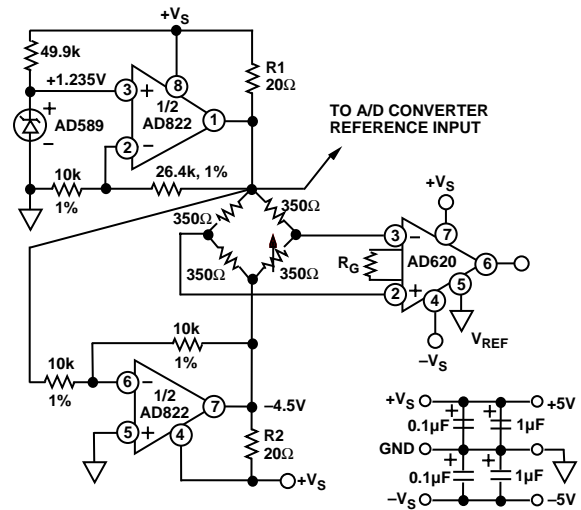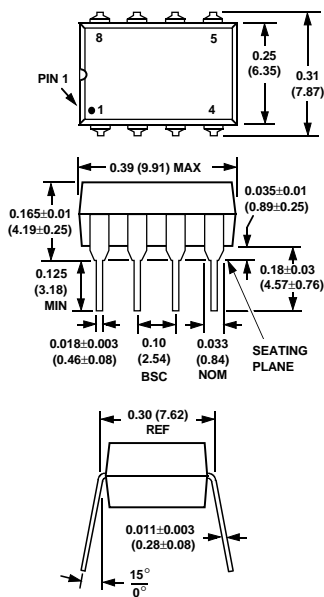
$$G = \frac{49.4 \ k\Omega}{R_G} + 1$$
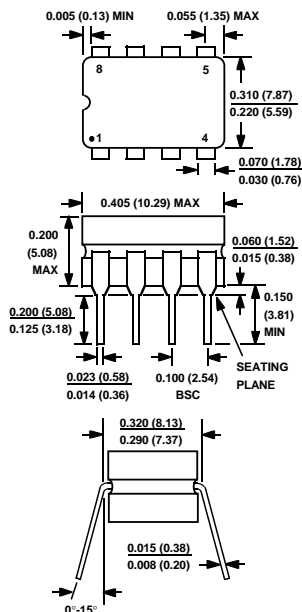

Figure 47. Low Dropout Bipolar Bridge Driver

OUTLINE DIMENSIONS

Dimensions shown in inches and (mm).

Mini-DIP (N) Package

Cerdip (Q) Package

SOIC (R) Package

–16–

REV. A
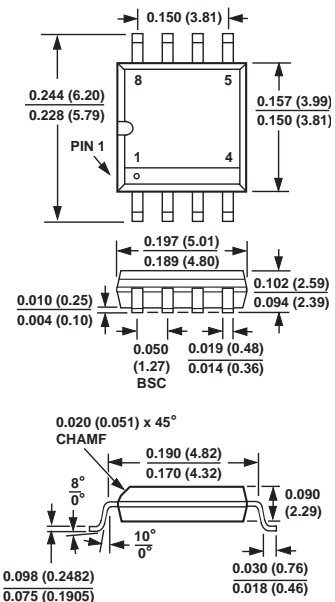
[Appendix-G]

## Regulator (LM317)

ON Semiconductor ™

1.5 A Adjustable Output, Positive Voltage Regulator

The LM317 is an adjustable 3–terminal positive voltage regulator capable of supplying in excess of 1.5 A over an output voltage range of 1.2 V to 37 V. This voltage regulator is exceptionally easy to use and requires only two external resistors to set the output voltage. Further, it employs internal current limiting, thermal shutdown and safe area compensation, making it essentially blow–out proof.

The LM317 serves a wide variety of applications including local, on card regulation. This device can also be used to make a programmable output regulator, or by connecting a fixed resistor between the adjustment and output, the LM317 can be used as a precision current regulator.

- Output Current in Excess of 1.5 A
- Output Adjustable between 1.2 V and 37 V
- Internal Thermal Overload Protection
- Internal Short Circuit Current Limiting Constant with Temperature
- Output Transistor Safe–Area Compensation
- Floating Operation for High Voltage Applications
- Available in Surface Mount D^2PAK, and Standard 3–Lead Transistor Package
- Eliminates Stocking many Fixed Voltages

Standard Application
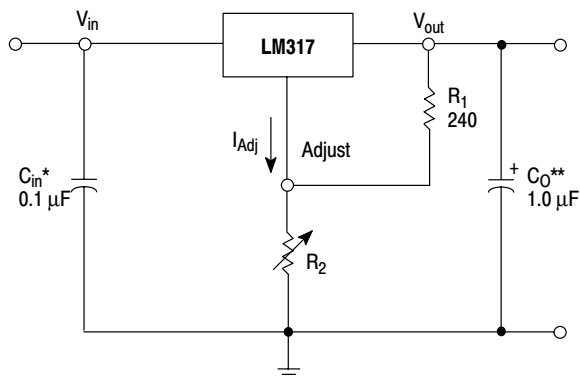
 * C_{in} is required if regulator is located an appreciable distance from power supply filter.
** C_O is not needed for stability, however, it does improve transient response.

$$V_{out} = 1.25 \, V \left(1 + \frac{R_2}{R_1} \right) + I_{Adj} \, R_2$$

Since I_{Adj} is controlled to less than 100 μA, the error associated with this term is negligible in most applications.
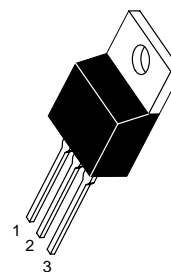
LM317

THREE–TERMINAL ADJUSTABLE POSITIVE VOLTAGE REGULATOR

SEMICONDUCTOR TECHNICAL DATA
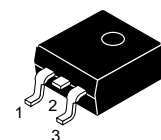

T SUFFIX
PLASTIC PACKAGE
CASE 221A

Heatsink surface
connected to Pin 2.

Pin 1. Adjust
2. V_{out}
3. V_{in}

D2T SUFFIX
PLASTIC PACKAGE
CASE 936
(D^2PAK)

Heatsink surface (shown as terminal 4 in
case outline drawing) is connected to Pin 2.

ORDERING INFORMATION

Device	Operating Temperature Range	Package
LM317BD2T	$T_J = -40°$ to $+125°C$	Surface Mount
LM317BT		Insertion Mount
LM317D2T	$T_J = 0°$ to $+125°C$	Surface Mount
LM317T		Insertion Mount

MAXIMUM RATINGS

Rating	Symbol	Value	Unit
Input–Output Voltage Differential	V_I–V_O	40	Vdc

Power Dissipation
Case 221A
    T_A = +25°C
    Thermal Resistance, Junction–to–Ambient
    Thermal Resistance, Junction–to–Case
Case 936 (D^{2}PAK)
    T_A = +25°C
    Thermal Resistance, Junction–to–Ambient
    Thermal Resistance, Junction–to–Case
	
	P_D
	θ_{JA}
	θ_{JC}
	
	P_D
	θ_{JA}
	θ_{JC}
		
		Internally Limited
		65
		5.0
		
		Internally Limited
		70
		5.0
			
			W
			°C/W
			°C/W
			
			W
			°C/W
			°C/W

Operating Junction Temperature Range	T_J	−40 to +125	°C
Storage Temperature Range	T_{stg}	−65 to +150	°C

ELECTRICAL CHARACTERISTICS (V_I–V_O = 5.0 V; I_O = 0.5 A for D2T and T packages; T_J = T_{low} to T_{high} [Note 1]; I_{max} and P_{max} [Note 2]; unless otherwise noted.)

Characteristics	Figure	Symbol	Min	Typ	Max	Unit
Line Regulation (Note 3), T_A = +25°C, 3.0 V ≤ V_I–V_O ≤ 40 V	1	Reg$_{line}$	–	0.01	0.04	%/V

Load Regulation (Note 3), T_A = +25°C, 10 mA ≤ I_O ≤ I_{max}
    V_O ≤ 5.0 V
    V_O ≥ 5.0 V
	2	Reg$_{load}$
		
			–
			–
				
				5.0
				0.1
					
					25
					0.5
						
						mV
						% V_O

Thermal Regulation, T_A = +25°C (Note 6), 20 ms Pulse		Reg$_{therm}$	–	0.03	0.07	% V_O/W
Adjustment Pin Current	3	I_{Adj}	–	50	100	μA
Adjustment Pin Current Change, 2.5 V ≤ V_I–V_O ≤ 40 V, 10 mA ≤ I_L ≤ I_{max}, P_D ≤ P_{max}	1, 2	ΔI_{Adj}	–	0.2	5.0	μA
Reference Voltage, 3.0 V ≤ V_I–V_O ≤ 40 V, 10 mA ≤ I_O ≤ I_{max}, P_D ≤ P_{max}	3	V_{ref}	1.2	1.25	1.3	V
Line Regulation (Note 3), 3.0 V ≤ V_I–V_O ≤ 40 V	1	Reg$_{line}$	–	0.02	0.07	% V

Load Regulation (Note 3), 10 mA ≤ I_O ≤ I_{max}
    V_O ≤ 5.0 V
    V_O ≥ 5.0 V
	2	Reg$_{load}$
		
			–
			–
				
				20
				0.3
					
					70
					1.5
						
						mV
						% V_O

Temperature Stability (T_{low} ≤ T_J ≤ T_{high})	3	T_S	–	0.7	–	% V_O
Minimum Load Current to Maintain Regulation (V_I–V_O = 40 V)	3	I_{Lmin}	–	3.5	10	mA

Maximum Output Current
    V_I–V_O ≤ 15 V, P_D ≤ P_{max}, T Package
    V_I–V_O = 40 V, P_D ≤ P_{max}, T_A = +25°C, T Package
	3	I_{max}	
			1.5
			0.15
				
				2.2
				0.4
					
					–
					–
						A

RMS Noise, % of V_O, T_A = +25°C, 10 Hz ≤ f ≤ 10 kHz		N	–	0.003	–	% V_O

Ripple Rejection, V_O = 10 V, f = 120 Hz (Note 4)
    Without C_{Adj}
    C_{Adj} = 10 μF
	4	RR	
			–
			66
				
				65
				80
					
					–
					–
						dB

Long–Term Stability, T_J = T_{high} (Note 5), T_A = +25°C for Endpoint Measurements	3	S	–	0.3	1.0	%/1.0 k Hrs.
Thermal Resistance Junction to Case, T Package		$R_{\theta JC}$	–	5.0	–	°C/W

NOTES: 1. T_{low} to T_{high} = 0° to +125°C, for LM317T, D2T. T_{low} to T_{high} = −40° to +125°C, for LM317BT, BD2T.
2. I_{max} = 1.5 A, P_{max} = 20 W
3. Load and line regulation are specified at constant junction temperature. Changes in V_O due to heating effects must be taken into account separately. Pulse testing with low duty cycle is used.
4. C_{Adj}, when used, is connected between the adjustment pin and ground.
5. Since Long–Term Stability cannot be measured on each device before shipment, this specification is an engineering estimate of average stability from lot to lot.
6. Power dissipation within an IC voltage regulator produces a temperature gradient on the die, affecting individual IC components on the die. These effects can be minimized by proper integrated circuit design and layout techniques. Thermal Regulation is the effect of these temperature gradients on the output voltage and is expressed in percentage of output change per watt of power change in a specified time.

LM317

Representative Schematic Diagram
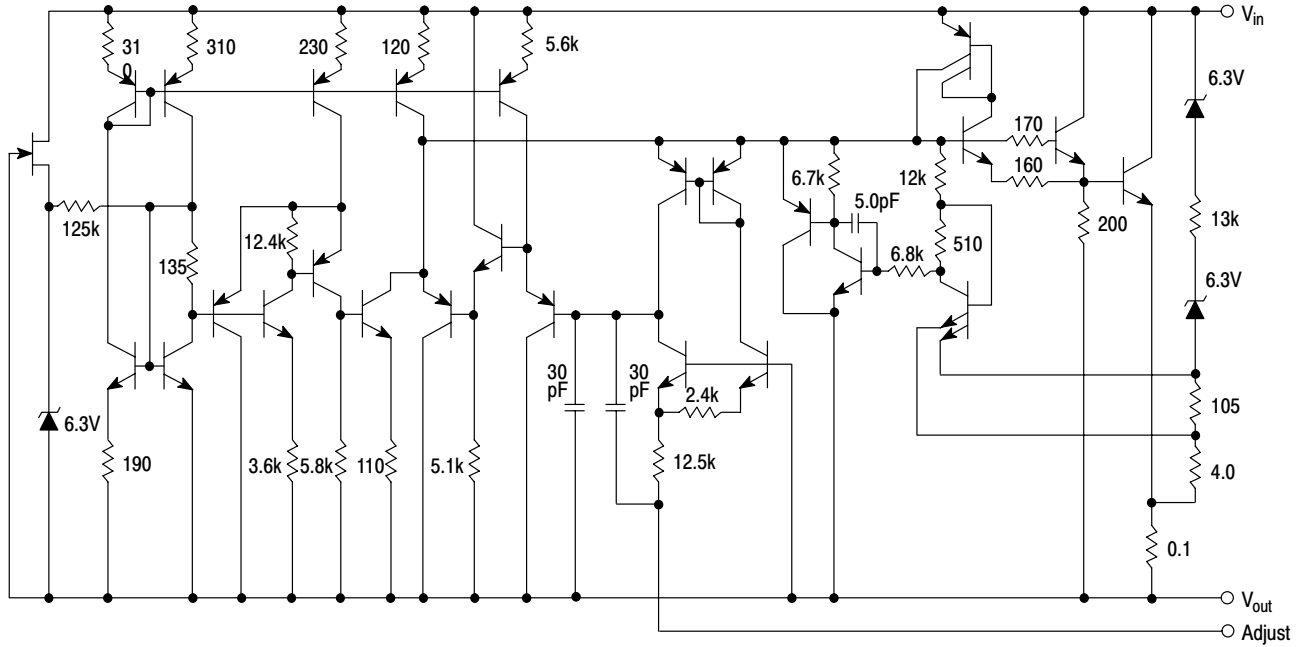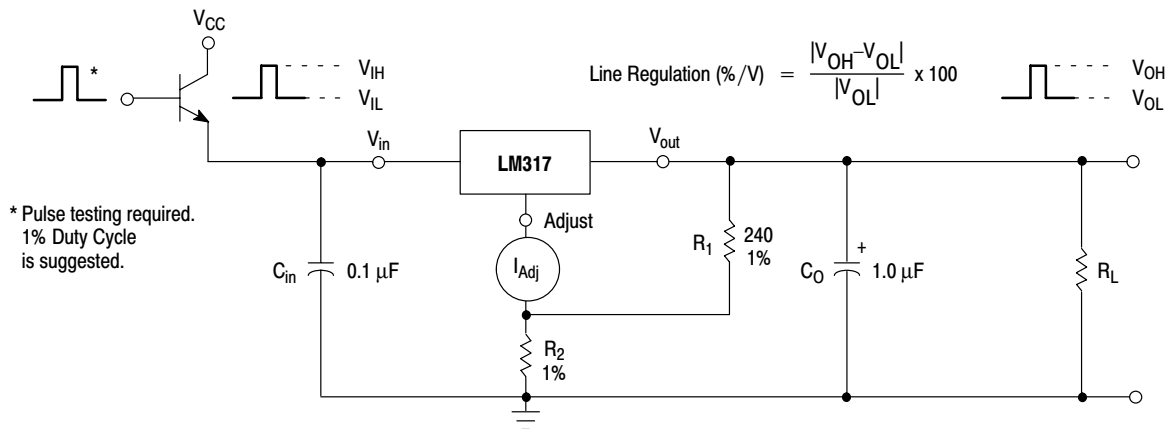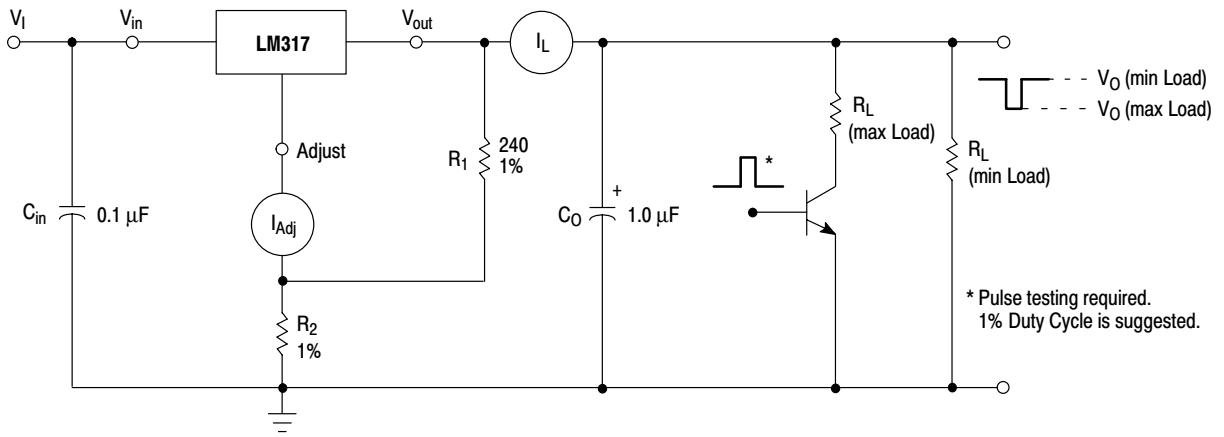

This device contains 29 active transistors.

$$\text{Line Regulation (\%/V)} = \frac{|V_{OH} - V_{OL}|}{|V_{OL}|} \times 100$$

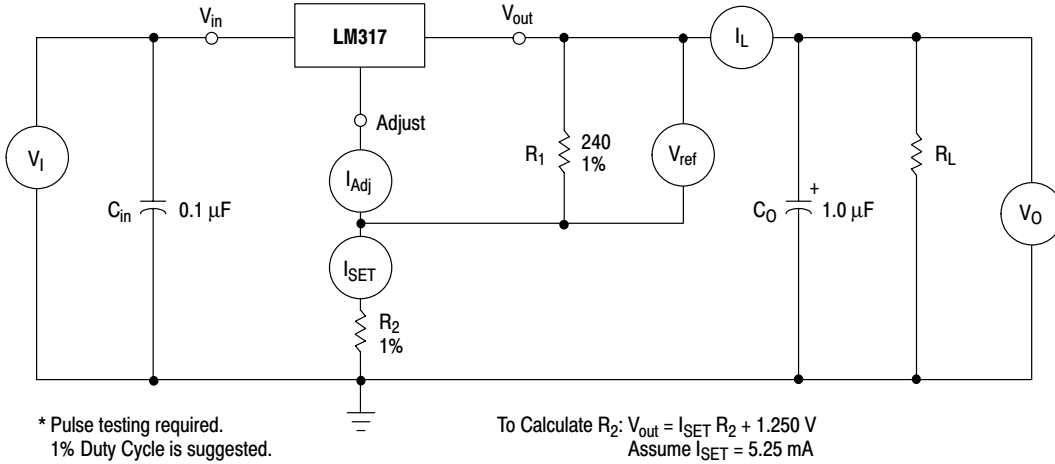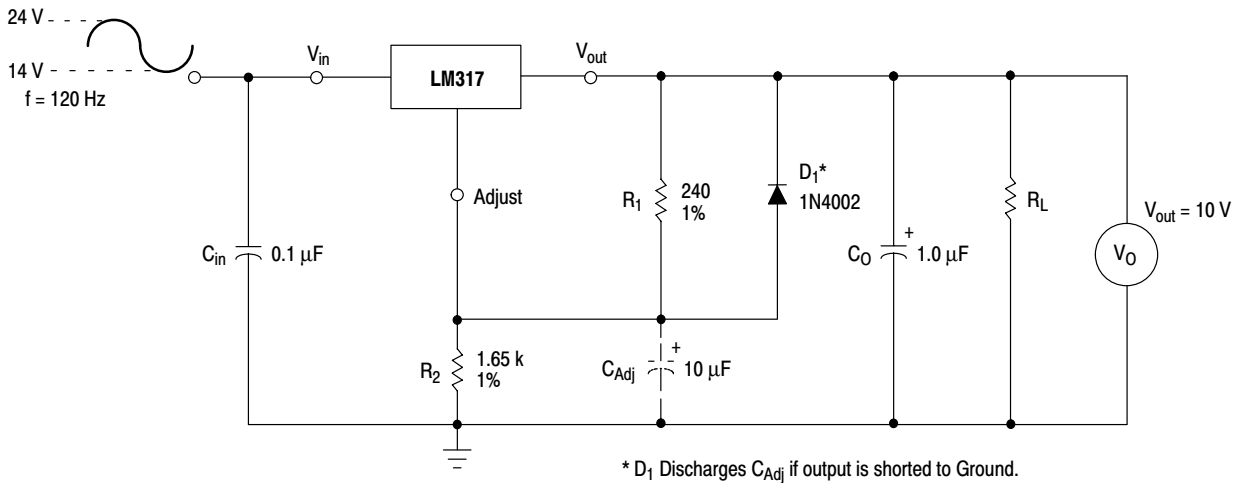**Figure 1. Line Regulation and ΔI_{Adj}/Line Test Circuit**

LM317

Load Regulation (mV) = V_O (min Load) − V_O (max Load)

Load Regulation (% V_O) = $\dfrac{V_O \text{ (min Load)} - V_O \text{ (max Load)}}{V_O \text{ (min Load)}}$ x 100

Figure 2. Load Regulation and ΔI_{Adj}/Load Test Circuit

* Pulse testing required.
  1% Duty Cycle is suggested.

To Calculate R_2: $V_{out} = I_{SET} R_2 + 1.250$ V
Assume $I_{SET} = 5.25$ mA

Figure 3. Standard Test Circuit

* D_1 Discharges C_{Adj} if output is shorted to Ground.

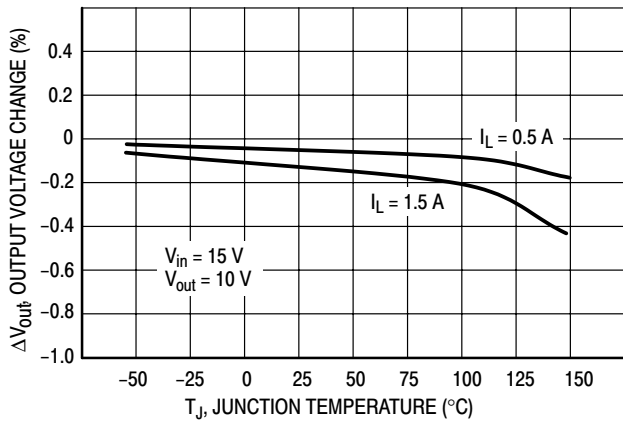**Figure 4. Ripple Rejection Test Circuit**

LM317

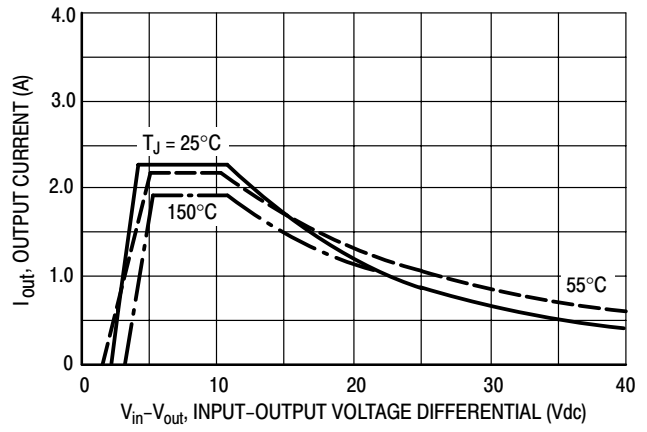**Figure 5. Load Regulation**
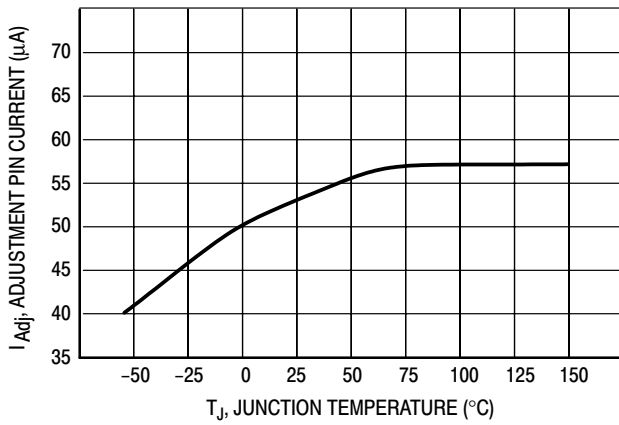

Figure 6. Current Limit

Figure 7. Adjustment Pin Current
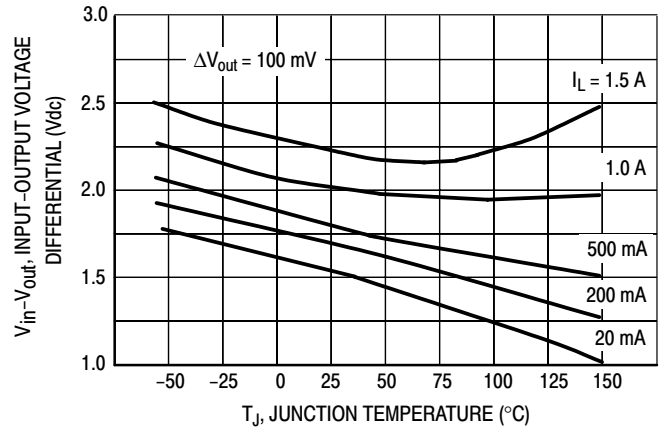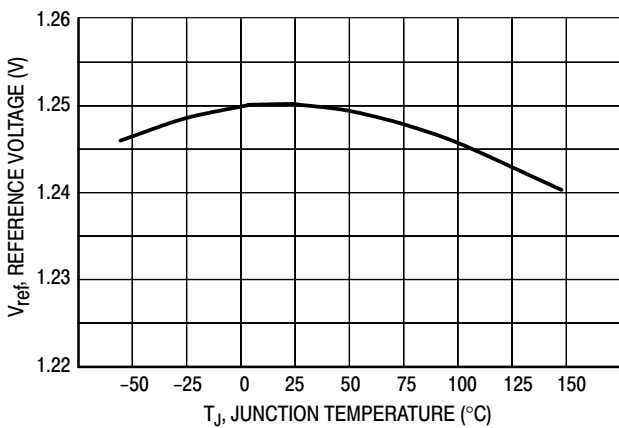

Figure 8. Dropout Voltage

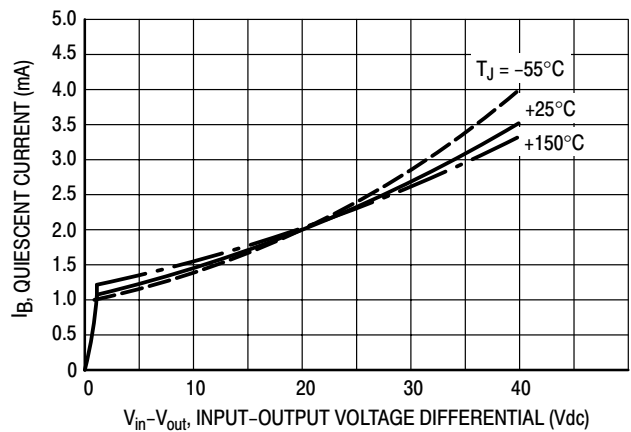**Figure 9. Temperature Stability**

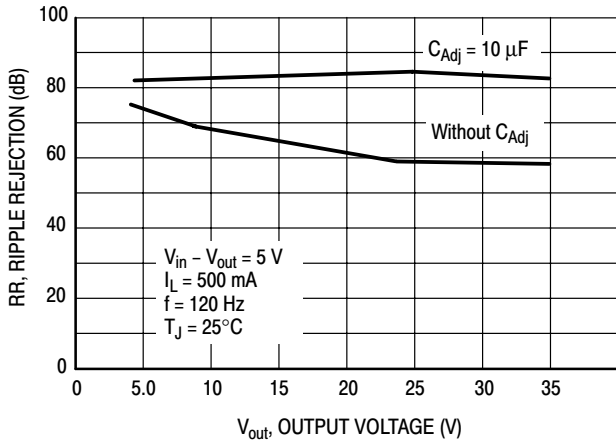**Figure 10. Minimum Operating Current**

LM317

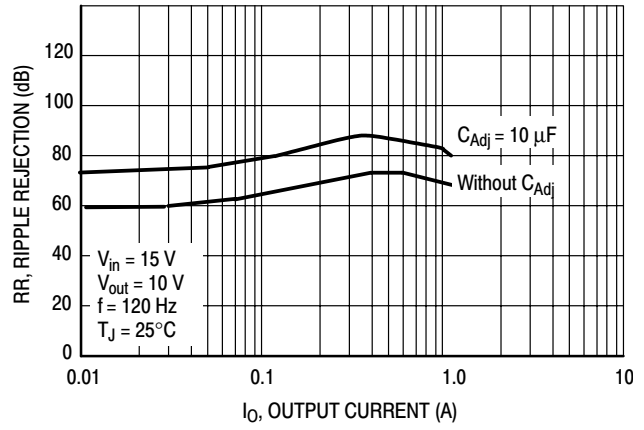Figure 11. Ripple Rejection versus Output Voltage

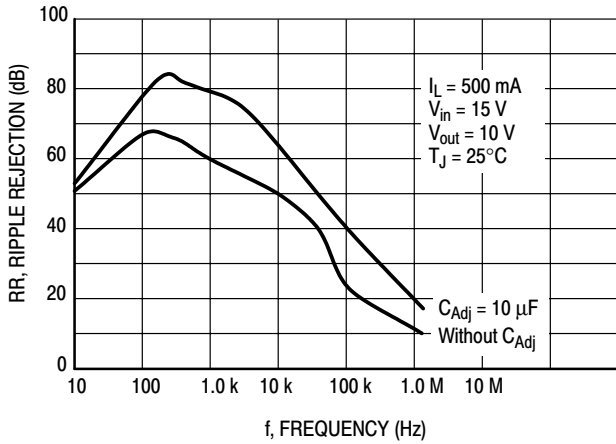Figure 12. Ripple Rejection versus Output Current
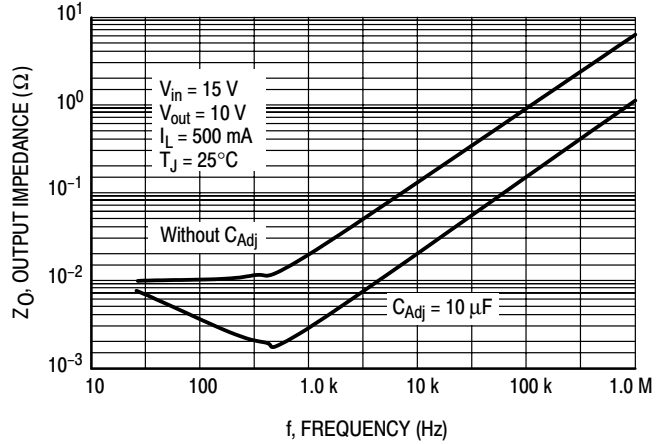

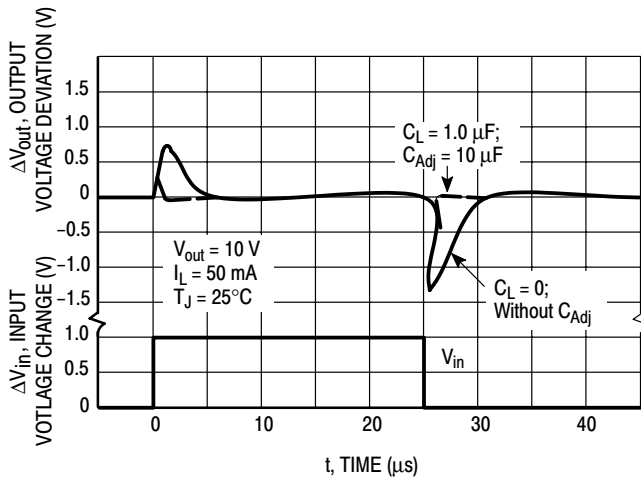Figure 13. Ripple Rejection versus Frequency

Figure 14. Output Impedance

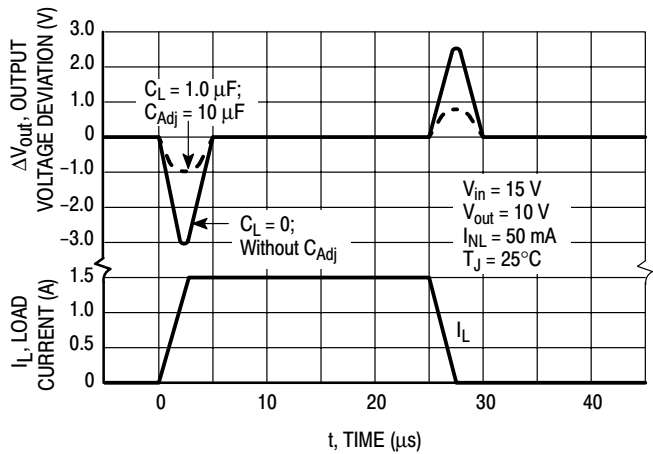Figure 15. Line Transient Response

Figure 16. Load Transient Response

LM317

APPLICATIONS INFORMATION

Basic Circuit Operation

The LM317 is a 3–terminal floating regulator. In operation, the LM317 develops and maintains a nominal 1.25 V reference (V_{ref}) between its output and adjustment terminals. This reference voltage is converted to a programming current (I_{PROG}) by R_1 (see Figure 17), and this constant current flows through R_2 to ground.

The regulated output voltage is given by:

$$V_{out} = V_{ref}\left(1 + \frac{R_2}{R_1}\right) + I_{Adj}R_2$$

Since the current from the adjustment terminal (I_{Adj}) represents an error term in the equation, the LM317 was designed to control I_{Adj} to less than 100 μA and keep it constant. To do this, all quiescent operating current is returned to the output terminal. This imposes the requirement for a minimum load current. If the load current is less than this minimum, the output voltage will rise.

Since the LM317 is a floating regulator, it is only the voltage differential across the circuit which is important to performance, and operation at high voltages with respect to ground is possible.
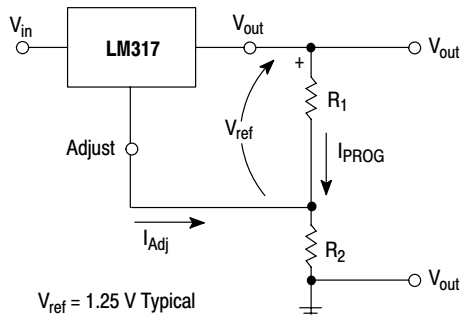

Figure 17. Basic Circuit Configuration

Load Regulation

The LM317 is capable of providing extremely good load regulation, but a few precautions are needed to obtain maximum performance. For best performance, the programming resistor (R_1) should be connected as close to the regulator as possible to minimize line drops which effectively appear in series with the reference, thereby degrading regulation. The ground end of R_2 can be returned near the load ground to provide remote ground sensing and improve load regulation.

External Capacitors

A 0.1 μF disc or 1.0 μF tantalum input bypass capacitor (C_{in}) is recommended to reduce the sensitivity to input line impedance.

The adjustment terminal may be bypassed to ground to improve ripple rejection. This capacitor (C_{Adj}) prevents ripple from being amplified as the output voltage is increased. A 10 μF capacitor should improve ripple rejection about 15 dB at 120 Hz in a 10 V application.

Although the LM317 is stable with no output capacitance, like any feedback circuit, certain values of external capacitance can cause excessive ringing. An output capacitance (C_O) in the form of a 1.0 μF tantalum or 25 μF aluminum electrolytic capacitor on the output swamps this effect and insures stability.

Protection Diodes

When external capacitors are used with any IC regulator it is sometimes necessary to add protection diodes to prevent the capacitors from discharging through low current points into the regulator.

Figure 18 shows the LM317 with the recommended protection diodes for output voltages in excess of 25 V or high capacitance values ($C_O > 25$ μF, $C_{Adj} > 10$ μF). Diode D_1 prevents C_O from discharging thru the IC during an input short circuit. Diode D_2 protects against capacitor C_{Adj} discharging through the IC during an output short circuit. The combination of diodes D_1 and D_2 prevents C_{Adj} from discharging through the IC during an input short circuit.
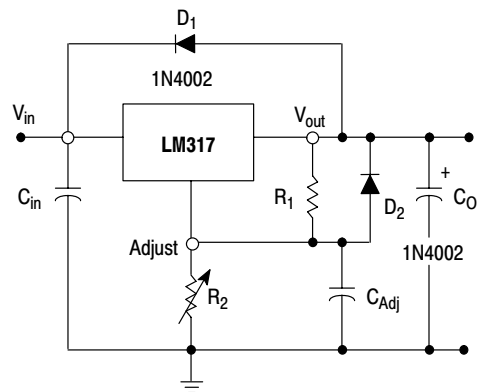
Figure 18. Voltage Regulator with Protection Diodes

LM317
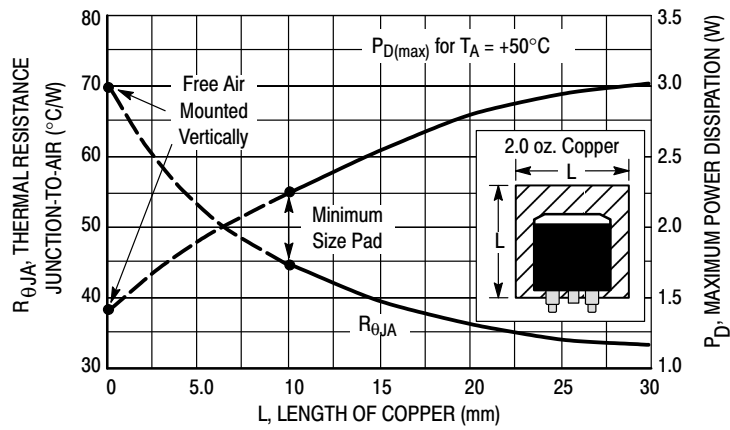
Figure 19. D²PAK Thermal Resistance and Maximum Power Dissipation versus P.C.B. Copper Length
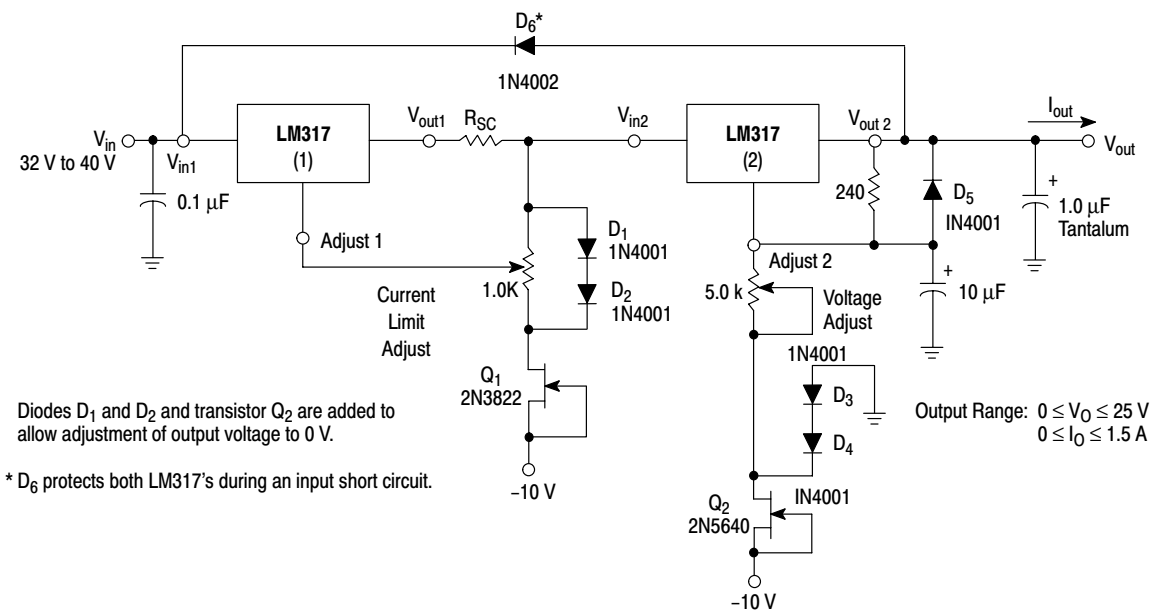
Diodes D_1 and D_2 and transistor Q_2 are added to allow adjustment of output voltage to 0 V.

* D_6 protects both LM317's during an input short circuit.

Output Range: $0 \leq V_O \leq 25$ V
$0 \leq I_O \leq 1.5$ A

Figure 20. "Laboratory" Power Supply with Adjustable Current Limit and Output Voltage

LM317

* To provide current limiting of I_O to the system ground, the source of the FET must be tied to a negative voltage below – 1.25 V.

$$R_1 = \frac{V_{ref}}{I_{Omax} + I_{DSS}} \qquad R_2 \leq \frac{V_{ref}}{I_{DDS}}$$

$V_O < BV_{DSS} + 1.25\ V + V_{SS}$,
$I_{Lmin} - I_{DSS} < I_O < 1.5\ A$.
As shown $0 < I_O < 1.0\ A$.
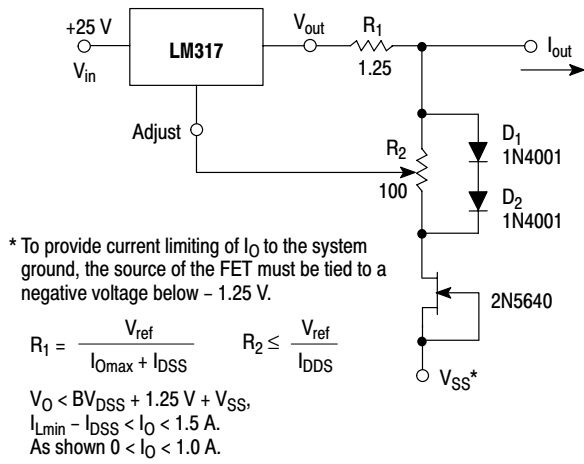
Figure 21. Adjustable Current Limiter

* D_1 protects the device during an input short circuit.

Minimum $V_{out} = 1.25\ V$

Figure 22. 5.0 V Electronic Shutdown Regulator

Figure 23. Slow Turn–On Regulator

$$I_{out} = \left(\frac{V_{ref}}{R_1}\right) + I_{Adj}$$

$$= \frac{1.25\ V}{R_1}$$

$10\ mA \leq I_{out} \leq 1.5\ A$

Figure 24. Current Regulator

LM317

PACKAGE DIMENSIONS

T SUFFIX
PLASTIC PACKAGE
CASE 221A–09
ISSUE AA

NOTES:
1. DIMENSIONING AND TOLERANCING PER ANSI Y14.5M, 1982.
2. CONTROLLING DIMENSION: INCH.
3. DIMENSION Z DEFINES A ZONE WHERE ALL BODY AND LEAD IRREGULARITIES ARE ALLOWED.

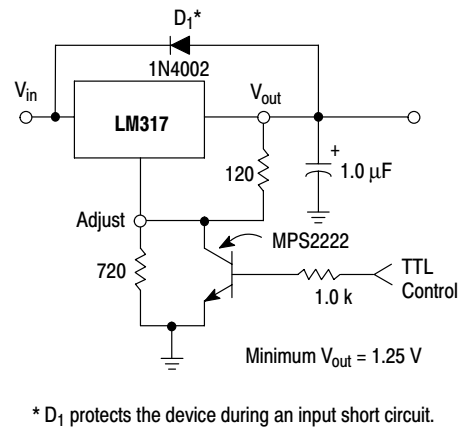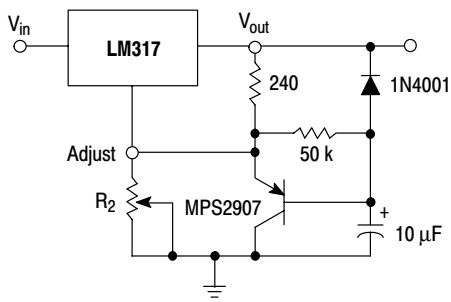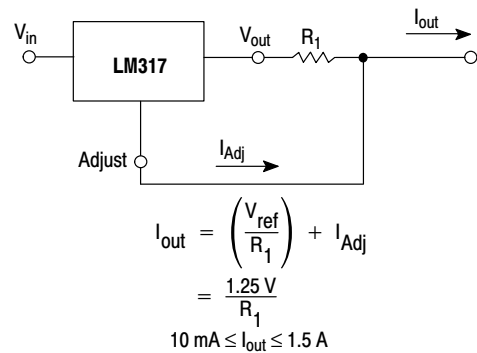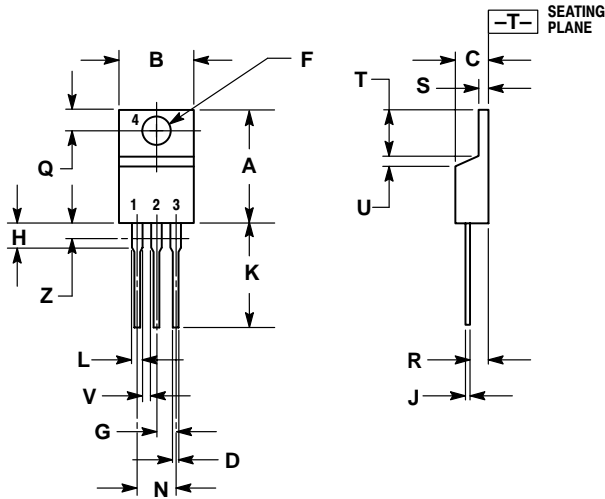| DIM	INCHES		MILLIMETERS	
	MIN	MAX	MIN	MAX
A	0.570	0.620	14.48	15.75
B	0.380	0.405	9.66	10.28
C	0.160	0.190	4.07	4.82
D	0.025	0.035	0.64	0.88
F	0.142	0.147	3.61	3.73
G	0.095	0.105	2.42	2.66
H	0.110	0.155	2.80	3.93
J	0.018	0.025	0.46	0.64
K	0.500	0.562	12.70	14.27
L	0.045	0.060	1.15	1.52
N	0.190	0.210	4.83	5.33
Q	0.100	0.120	2.54	3.04
R	0.080	0.110	2.04	2.79
S	0.045	0.055	1.15	1.39
T	0.235	0.255	5.97	6.47
U	0.000	0.050	0.00	1.27
V	0.045	---	1.15	---
Z	---	0.080	---	2.04

D2T SUFFIX
PLASTIC PACKAGE
CASE 936–03
(D^{2}PAK)
ISSUE B
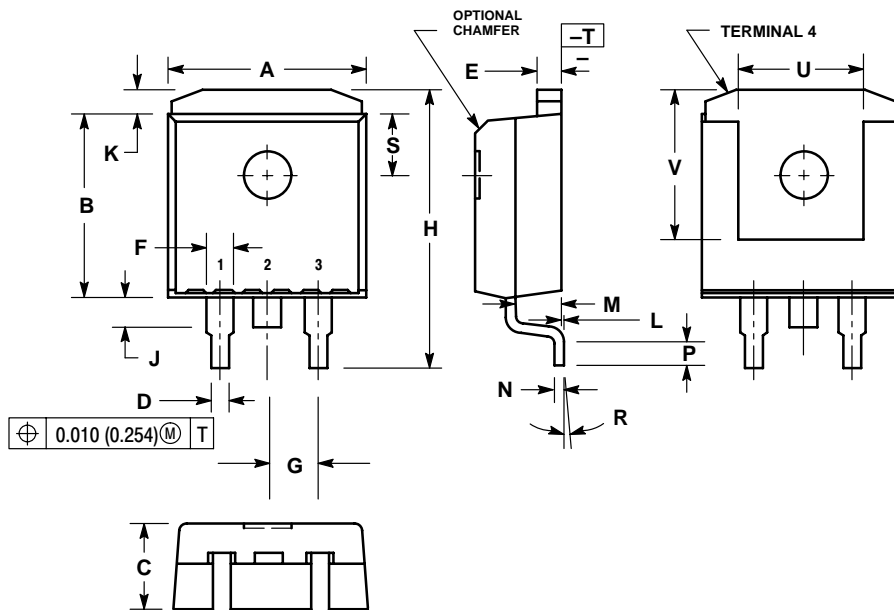
NOTES:
1. DIMENSIONING AND TOLERANCING PER ANSI Y14.5M, 1982.
2. CONTROLLING DIMENSION: INCH.
3. TAB CONTOUR OPTIONAL WITHIN DIMENSIONS A AND K.
4. DIMENSIONS U AND V ESTABLISH A MINIMUM MOUNTING SURFACE FOR TERMINAL 4.
5. DIMENSIONS A AND B DO NOT INCLUDE MOLD FLASH OR GATE PROTRUSIONS. MOLD FLASH AND GATE PROTRUSIONS NOT TO EXCEED 0.025 (0.635) MAXIMUM.

DIM	INCHES		MILLIMETERS	
	MIN	MAX	MIN	MAX
A	0.386	0.403	9.804	10.236
B	0.356	0.368	9.042	9.347
C	0.170	0.180	4.318	4.572
D	0.026	0.036	0.660	0.914
E	0.045	0.055	1.143	1.397
F	0.051 REF		1.295 REF	
G	0.100 BSC		2.540 BSC	
H	0.539	0.579	13.691	14.707
J	0.125 MAX		3.175 MAX	
K	0.050 REF		1.270 REF	
L	0.000	0.010	0.000	0.254
M	0.088	0.102	2.235	2.591
N	0.018	0.026	0.457	0.660
P	0.058	0.078	1.473	1.981
R	5° REF		5° REF	
S	0.116 REF		2.946 REF	
U	0.200 MIN		5.080 MIN	
V	0.250 MIN		6.350 MIN	

[Appendix-H]

Arduino UNO Code

```cpp
#include <LiquidCrystal_I2C.h>
#include <Wire.h>
#include <Adafruit_MLX90614.h>
#include <Ph_Sh.h>
Adafruit_MLX90614 mlx = Adafruit_MLX90614();
// set the LCD address to 0x27 for a 16 chars and 2 line display
LiquidCrystal_I2C lcd(0x27,20,4);
Ph_Sh(redac,irac);

int s1 =0;int s2 =1;
double T1 =0;double T2 =0;
double redac ;
double reddc ;
double irac ;
double irdc ;
float r1 ;
float r2 ;
double spo21 ;
double spo22 ;
double sum1 =0;
double sum2 =0;


void setup() {

Serial.begin(9600);
// initialize the lcd
lcd.init();
// Print a message to the LCD.
lcd.backlight();
lcd.setCursor(3,0);
lcd.print(" Ahmed^2");
lcd.setCursor(2,1);
lcd.print("Grad Project");
delay(5000);
lcd.clear();

mlx.begin();
//s1
pinMode(2, OUTPUT);
pinMode(4, INPUT);
digitalWrite(2, HIGH);

//s2
pinMode(A2, OUTPUT);
pinMode(A3, INPUT);
digitalWrite(A2, HIGH);

// IR TRANSISTOR ON/OFF
pinMode(8, OUTPUT);
// RED TRANSISTOR ON/OFF
pinMode(10, OUTPUT);
// dc part
```

```
pinMode(7, INPUT);
// ac part
pinMode(A0, INPUT);
}

void loop() {

lcd.setCursor(0,0);
lcd.print("Press S1 for T1 ");
delay(1000);
while(s1==0)
{ s1 = digitalRead(4);};

//buttonWait(4); t1 print
while (s1 == HIGH){
lcd.clear();
lcd.setCursor(0,0);
lcd.print("Temp1 = ");
lcd.setCursor(8,0);
lcd.print(mlx.readObjectTempC());
T1=mlx.readObjectTempC();
lcd.setCursor(14,0);
lcd.print("*C");
delay(5000);
lcd.clear();
s1=0;}

lcd.setCursor(0,0);
lcd.print("Press S1 for T2 ");
delay(1000);
while(s1==0)
{s1 = digitalRead(4);};

//buttonWait(4); t2 print
while (s1 == HIGH){
lcd.clear();
lcd.setCursor(0,0);
lcd.print("Temp2 = ");
lcd.setCursor(8,0);
lcd.print(mlx.readObjectTempC());
T2=mlx.readObjectTempC();
lcd.setCursor(14,0);
lcd.print("*C");
delay(5000);
lcd.clear();
s1=0;}

lcd.setCursor(0,0);
lcd.print("Press S2 for O1");
delay(1000);]
while(s2==0)
{ s2 = digitalRead(A3);};

//buttonWait(A3); spo2 numper 1 value
```

```
while (s2 == HIGH){
sum1 =0 ;
for(int i=1 ; i<=10 ; i++){
// RED COMPONENTS
digitalWrite(10,HIGH);
delay(20);
redac =analogRead(A0)+1;
reddc =analogRead(7)+1;
delay(60);
digitalWrite(10,LOW);

// IR COMPONENTS
digitalWrite(8,HIGH);
delay(20);
irac =analogRead(A0)+1;
irdc =analogRead(7)+1;
delay(60);
digitalWrite(8,LOW);

r1 = (redac/reddc)/(irac/irdc);
spo21 = 110 - 15*r1;
sum1 = sum1 +spo21;}
spo21 = sum1 /10;

lcd.clear();
lcd.setCursor(0,0);
lcd.print("SPO2 1 = ");
lcd.setCursor(8,0);
lcd.print(spo21);
lcd.setCursor(15,0);
lcd.print("%");
delay(5000);
lcd.clear();
s2=0;}

lcd.setCursor(0,0);
lcd.print("Press S2 for O2");
delay(1000);//
while(s2==0)
{ s2 = digitalRead(A3);}};

//buttonWait(A3); spo2 numper 2 value
while (s2 == HIGH){
sum2 =0 ;
for(int i=1 ; i<=10 ; i++){
// RED COMPONENTS
digitalWrite(10,HIGH);
delay(20);
redac =analogRead(A0)+1;
reddc =analogRead(7)+1;
delay(60);
digitalWrite(10,LOW);

// IR COMPONENTS
```

```arduino
digitalWrite(8,HIGH);
delay(20);
irac =analogRead(A0)+1;
irdc =analogRead(7)+1;
delay(60);
digitalWrite(8,LOW);

r2 = (redac/reddc)/(irac/irdc);
spo22 = 110 - 15*r2;

sum2 = sum2 +spo22;}
spo22 = sum2 / 10;

lcd.clear();
lcd.setCursor(0,0);
lcd.print("SPO2 2 = ");
lcd.setCursor(8,0);
lcd.print(spo22);
lcd.setCursor(15,0);
lcd.print("%");
delay(5000);
lcd.clear();
s2=0;}


// print the 2 values of temp

lcd.clear();
lcd.setCursor(0,0);
lcd.print("T1= ");
lcd.setCursor(3,0);
lcd.print(T1);
lcd.setCursor(0,1);
lcd.print("T2= ");
lcd.setCursor(3,1);
lcd.print(T2);


 // print the 2 values of SP02


lcd.setCursor(9,0);
lcd.print("O1= ");
lcd.setCursor(12,0);
lcd.print(spo21);
lcd.setCursor(14,0);
lcd.print("% ");
lcd.setCursor(9,1);
lcd.print("O2= ");
lcd.setCursor(12,1);
lcd.print(spo22);
lcd.setCursor(14,1);
lcd.print("% ");
delay(20000);
```

```
lcd.clear();

if ((abs(T1-T2)>1)&&(abs(spo21-spo22)>1)){
lcd.setCursor(0,0);
lcd.print("    Result :");
lcd.setCursor(0,1);
lcd.print("   malignant");
delay(20000);
lcd.clear();}
else {
lcd.setCursor(0,0);
lcd.print("    Result :");
lcd.setCursor(0,1);
lcd.print("    benign ");
delay(20000);
lcd.clear();}

}
```

VCC
7V
R2
290Ω
Arduino
R1
550Ω
Q1
2N3904
IR_LED1

VCC
C9
7V
100nF

C3
4.7μF

VCC
7V
U2A
AD822AN
AD822
VEE
-7V

VCC
7V
U3A
AD822AN
AD822
VEE
-7V

PHOTO_TRANSISTOR_RATED
U1B
AD822AN
AD822
VEE
-7V
Phototransistor
R15
7kΩ
R16
1kΩ

Vo1
R7
3.825kΩ
R6
6.410kΩ
C4
2.2μF

Vo2
C5
47μF
Vo3
R8
6.775kΩ

AC Arduino
R10
9kΩ
R5
1kΩ

C7
47nF

VCC
7V
U2B
AD822AN
AD822
VEE
-7V

VCC
7V
U3B
AD822AN
AD822
VEE
-7V

Vo1
R12
7.650kΩ
R11
12.821kΩ
C8
22nF

Vo4
R14
6kΩ
DC Arduino
R9
1kΩ

VCC
7V
R4
265Ω
Arduino
R3
550Ω
Q2
2N3904
Red_LED1